$R_2Fe_{14}B$ materials: Intrinsic properties and technological aspects

J. F. Herbst

Physics Department, General Motors Research Laboratories, Warren, Michigan 48090-9055

Magnetic materials research has entered a new and exciting period with the advent of the ternary rare-earth–iron-boron compounds, $R_2Fe_{14}B$. From the fundamental physics perspective the $R_2Fe_{14}B$ series and its isostructural relatives comprise a rich, fascinating area for the investigation of many intrinsic properties, including magnetic structures, magnetocrystalline anisotropy, and rare-earth–transition-metal exchange interactions. Intense interest in the technological aspects of these compounds has been ignited by the fact that energy products eclipsing all previous values have been realized in practical magnets based on $Nd_2Fe_{14}B$, the prototypical representative; these magnets also feature economic advantages over the earlier samarium-cobalt materials. Both facets of the $R_2Fe_{14}B$ systems are considered in this review.

CONTENTS

I. Introduction 819
II. Historical Perspective 820
III. Crystal Structure 822
  A. $Nd_2Fe_{14}B$ crystallography 822
  B. Other structural comparisons 825
  C. Isomorphs 826
IV. Magnetic Properties of the $R_2Fe_{14}B$ Compounds 827
  A. Systematics 827
    1. R and Fe magnetic moments and their couplings 827
    2. Curie temperatures 830
    3. Easy directions and sublattice anisotropies 831
  B. Temperature dependence of the magnetization and mean-field models 833
    1. Molecular-field model 834
    2. Heisenberg model and exchange energies 835
    3. Systematics of j_{RF} 836
  C. Fe sublattice anisotropy 837
  D. Rare-earth anisotropy and magnetic structure 838
    1. Crystal-field Hamiltonian 839
    2. R-Fe exchange 841
    3. Model calculations and analyses 841
  E. Information from Mössbauer studies 843
    1. Rare-earth nuclei 844
    2. ^{57}Fe investigations 845
V. Electronic Structure 847
VI. Isostructural Materials and their Properties 849
  A. Rare-earth replacements 849
  B. Replacements for iron 851
  C. $R_2Co_{14}B$ compounds and pseudoternary derivatives 859
  D. Partial boron replacement 861
  E. $R_2Fe_{14}C$ and related compounds 861
  F. Multiple substitutions 862
  G. Hydrides 863
VII. Technology: Practical Permanent Magnets 864
  A. Melt-spun magnets 865
    1. Nd-Fe-B 865
      a. Ribbon characteristics 865
      b. Consolidation techniques 866
      c. Elemental additives 868
    2. Cobalt-containing alloys 868
    3. Other $R_2Fe_{14}B$-based materials 869
  B. Sintered magnets 870
    1. Nd-Fe-B 870
    2. Compositionally modified materials 872
  C. Magnetization reversal and coercivity mechanisms 874
    1. Sintered magnets 875
    2. Melt-spun materials 877
      a. Ribbons 878
      b. Hot-pressed and die-upset magnets 878
    3. Interaction effects 879
  D. Other preparation methods 880
  E. Thin films 881
VIII. Concluding Remarks 882
Acknowledgments 882
Appendix: A Note on Units 882
References 882

I. INTRODUCTION

Research in magnetism has long included, as a vital component, the discovery and development of ever more powerful permanent-magnet materials. From the basic physics perspective this activity is motivated by the long-standing challenge of progressively enhancing properties such as the magnetization and magnetocrystalline anisotropy and of understanding the fundamental mechanisms controlling those properties. On the technological side, a potent stimulus is furnished by the growing number and diversity of applications for hard magnets. The novel class of $R_2Fe_{14}B$ materials, in which R is a rare-earth element, has recently propelled permanent-magnet research and technology into a new and exciting era. Energy products significantly exceeding all previous values have been attained in magnets based on the prototypical compound $Nd_2Fe_{14}B$. That fact, coupled with economic advantages over the earlier samarium-cobalt materials, has spurred considerable technological interest, and the new systems have also created an extraordinarily fertile area for basic scientific investigation.

This review aims to describe the intrinsic properties and physics of the $R_2Fe_{14}B$ compounds and to discuss the technological aspects of practical magnets prepared from them. It is organized in the following way. In Sec. II the new materials are placed in the historical context of permanent-magnet development; this century has witnessed an enormous increase in the energy product, the most widely used general measure of hard-magnet performance. The intricate tetragonal crystal structure of the $R_2Fe_{14}B$ phases and their relationships with other structures are considered in Sec. III. Section IV is devoted to the intrinsic magnetic properties of the stoichiometric compounds, including the magnetic moment arrangements, spin-reorientation phenomena, and the molecular-field and crystal-field–exchange models employed in analyzing the experimental information. Although the unit $R_2Fe_{14}B$ cell contains a large number of atoms, sixty-eight, progress is being made in elucidating the electronic structure, as discussed in Sec. V. The ternary nature of the compounds immediately affords a rich spectrum of possibilities for forming isostructural materials by substituting other elements; such systems and their properties are the subject of Sec. VI. Practical permanent magnets are discussed in Sec. VII. Two distinct preparation methods, the rapid-solidification technique of melt spinning and the traditional powder-metallurgy approach, are already in commercial use. Section VIII contains a few concluding remarks, and the Appendix is a note on units.

II. HISTORICAL PERSPECTIVE

Reported by the ancients and long applied in navigational compasses, lodestone was the first permanent magnet known to history. Lodestone is principally comprised of the ore magnetite (Fe_3O_4), found originally in the eponymous Greek province of Magnesia in Thessaly, from which the entire science of magnetism derives its name. The greatest strides in magnet development, however, have occurred in the last hundred years and have been invariably connected with the discovery of new classes of materials characterized by ever more desirable properties (a point emphasized by many authors, including Enz, 1982; Wallace, 1985; White, 1985; Buschow, 1986a; and Coey, 1987). Each such discovery has stimulated a period of intense technological activity, with the next cycle initiated by the advent of another genre of material.

This evolution has been monitored generally by one figure of merit for a permanent magnet, the maximum energy product $(BH)_{\max}$, which is the maximum product of magnetic induction B and applied field H in the second quadrant of the $B(H)$ hysteresis curve. $(BH)_{\max}$ provides a measure of the field that can be produced outside a unit volume of magnet material. In broad terms, the larger $(BH)_{\max}$, the greater the potential for reducing the size and weight of a device by replacing either electromagnets or permanent magnets having a lower energy product; the precise extent of such reduction depends upon the specific application. The so-called theoretical maximum energy product, the largest value realizable in principle, is an intrinsic quantity defined by

$$(BH)^*_{\max} = (4\pi M_s)^2/4 , \tag{1}$$

where M_s is the saturation magnetization. This can be achieved only if the magnet retains M_s in a reverse field at least as large as $(4\pi M_s)/2$. A thorough discussion of the physical and practical significance of $(BH)_{\max}$ has been given by Zijlstra (1982).

Figure 1 is a semilogarithmic plot of the highest $(BH)_{\max}$ values versus time during the past century for the five classes of technologically important permanent-magnet materials. The straight line drawn between the earliest magnet steels and the Nd-Fe-B magnets underscores the fact that $(BH)_{\max}$ has increased exponentially in this period. The steels have carbon, chromium, tungsten, or cobalt as the principal additives. They are characterized by rather high remanence B_r, on the order of 10 kG, but the coercivities are no larger than a few hundred oersted and severely limit $(BH)_{\max}$. These alloy systems essentially exploit the magnetic properties of elemental iron, for which $4\pi M_s = 21.5$ kG implies an enormous $(BH)^*_{\max}$ of 115 MGOe. The anisotropy field H_a (the external field required to rotate the magnetization from the easy to a hard direction) is only ~500 Oe for iron, however, and $(BH)^*_{\max}$ cannot be realized. The additives to the steels simply serve to translate the meager anisotropy field of iron into useful coercivity.

Alnicos were the next class of materials to advance the energy product. Mishima (1932) discovered the initial members of the series, thermally treated aluminum-nickel-iron alloys featuring coercivities more than a factor of 2 larger than those of the best cobalt steels. Present commercial alnicos generally contain iron, cobalt, nickel, and aluminum with minor additions of copper and titanium. As Enz (1982) observes, alnicos were the first magnets to be aptly designated permanent because of their resistance to stray magnetic fields, mechanical shock, and elevated temperatures. The mechanical and magnetic properties are linked strongly

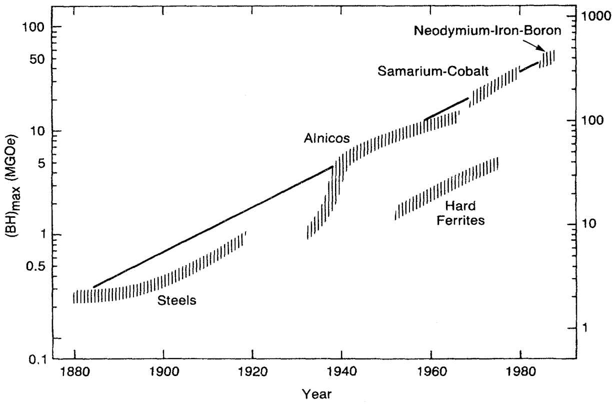

FIG. 1. Chronological trend of the maximum energy product $(BH)_{\max}$ achieved in various permanent-magnet materials.

to the microstructure, which is characterized typically by finely dispersed, oriented, elongated, single-domain particles precipitated by appropriate thermal treatment in a field. The shape anisotropy of the particles is responsible for the coercivity. In his comprehensive review of the alnico alloys, McCurrie (1982) reports that the highest energy product achieved is ~13 MGOe.

Although they do not lie on the increasing $(BH)_{\max}$ trend line of Fig 1, the hard ferrites are included because of their commercial importance. These materials are based on the hexagonal oxides $BaFe_{12}O_{19}$, $SrFe_{12}O_{19}$, and their solid solutions. The coercivity of ferrite magnets derives from the uniaxial magnetocrystalline anisotropy, rather than the shape anisotropy, of single-domain particles and can be substantially larger than that of the alnicos. The remanent magnetization is relatively low, however, and $(BH)_{\max}$ is no larger than 5 MGOe. Per unit energy product, the hexagonal ferrites are the least expensive hard magnets, and their high electrical resistivity ($\sim 10-10^5\ \Omega$ cm; all other materials in Fig. 1 are metallic) has made them useful in a variety of high-frequency applications. Kojima (1982) and Sugimoto (1982) have reviewed the fundamental properties of the ferrites, and the technological issues have been discussed in detail by Stäblein (1982).

Over the past three decades the energy product has been increased by rare-earth–transition-metal (R-TM) materials in which the R component provides most of the magnetocrystalline anisotropy intrinsically responsible for the coercivity in a practical magnet, while the magnetization arises principally from the TM sublattice. Investigation of such systems began with magnetization measurements on the RCo_5 compounds having the hexagonal $CaCu_5$ crystal structure (e.g., Nesbitt *et al.*, 1959, 1961, 1962; Hubbard *et al.*, 1960). Determinations of the anisotropy made it apparent to Strnat and co-workers in particular that the RCo_5 compounds were promising candidates for permanent-magnet development (Hoffer and Strnat, 1966; Strnat *et al.*, 1967). $SmCo_5$ became the focus of technological efforts, and energy products in the 16–28-MGOe range have been obtained by sintering (Strnat, 1987). For the compounds in which the $4f$ shell has a nonzero orbital magnetic moment, theoretical analyses demonstrated that the behavior of the R ion under the combined influence of the exchange and crystalline electric field controls the easy magnetization direction and accounts for much of the large uniaxial anisotropy (see, for example, Greedan and Rao, 1973; Buschow *et al.*, 1974).

In view of their richer cobalt content and, hence, higher magnetization and larger $(BH)^*_{\max}$ values, the R_2Co_{17} compounds were also heavily investigated as hard-magnet materials. The light-rare-earth members of the series have the rhombohedral Th_2Zn_{17} structure, which is closely related to the $CaCu_5$ structure. In contrast to the RCo_5 series, the cobalt sublattice in the R_2Co_{17} phases is characterized by basal-plane rather than uniaxial anisotropy, and the total anisotropy is unfortunately lower (Menth *et al.*, 1978). Nevertheless, the R_2Co_{17} magnetization and the RCo_5 anisotropy have been exploited via the technique of precipitation hardening. Energy products as large as 33 MGOe have been obtained in samarium-cobalt–based alloys featuring a two-component cellular microstructure in which a Sm_2Co_{17}-type phase is surrounded by a $SmCo_5$-type boundary phase (Mishra *et al.*, 1981). The development of both R_2TM_{17} and R-TM_5 permanent magnets has been reviewed extensively by Kumar (1988) and by Strnat (1988).

The samarium-cobalt materials are attractive replacements for electromagnets in many applications, but their use has been limited by economic constraints. Samarium is the least abundant, and hence most expensive, of the light rare earths (i.e., La, Ce, Pr, Nd, Sm); La, Ce, Pr, and Nd account for over 95% of the rare-earth content in a typical ore body. Exacerbating this unfavorable circumstance is the fact that the price and availability of cobalt are subject to gross, unpredictable excursions. The bulk of the world's cobalt is mined in Zaire, and in particular the 1978 civil war there diminished supplies, radically increased prices, and, perhaps in retrospect most importantly, helped spur searches for alternative R-TM systems having economically preferable elemental constituents (see G. Y. Chin *et al.*, 1979).

Iron-based materials having the characteristics of samarium-cobalt had long been desired; however, no suitable compounds were known in 1978. R-Fe phases with the $CaCu_5$ structure do not exist, and the R_2Fe_{17} compounds in which R is a light rare earth have unacceptably low Curie temperatures. Despite the apparent absence of appropriate compounds, two lines of research led, by the time of the 1983 Conference on Magnetism and Magnetic Materials in Pittsburgh, to the preparation of iron-based rare-earth hard magnets. One approach relied on the rapid solidification, by melt spinning, of rare-earth–iron–metalloid alloys (Croat *et al.*, 1984b; Koon and Das, 1984; Hadjipanayis *et al.*, 1984; Sellmyer *et al.*, 1984; Becker, 1984), and the other involved traditional powder-metallurgy (sintering) techniques (Sagawa, Fujimura, *et al.*, 1984a).

Croat *et al.* (1984a, 1984b) reported energy products as large as 14 MGOe in melt-spun ribbons of $Nd_{0.135}Fe_{0.817}B_{0.048}$, work that evolved from earlier studies (Croat, 1980, 1981a, 1981b, 1981c, 1982a, 1982b, 1982c; Croat and Herbst, 1982a, 1982b) of rapidly solidified R-Fe binary alloys. Extending previous investigations (Koon and Das, 1981; Koon *et al.*, 1982; Das and Koon, 1983) of crystallized amorphous $La_{0.05}Tb_{0.05}Fe_{0.74}B_{0.16}$ materials, Koon and Das (1984) found $(BH)_{\max} \simeq 13$ MGOe in annealed melt-spun $La_{0.020}Nd_{0.130}Fe_{0.783}B_{0.067}$ and $La_{0.005}Pr_{0.145}Fe_{0.783}B_{0.067}$. Hadjipanayis *et al.*, (1983, 1984) explored a variety of rapidly quenched rare-earth–iron–metalloid systems and observed an energy product of 13 MGOe in heat-treated $Pr_{0.16}Fe_{0.76}Si_{0.03}B_{0.05}$ (see also Hazelton *et al.*, 1984). These series of inquiries were encouraged in part by the seminal finding of Clark (1973) that amorphous

$Tb_{0.33}Fe_{0.67}$ developed a coercive force of ~3 kOe after annealing. Clark's result motivated examination of amorphous or metastable precursors, preparation of which necessitates rapid-cooling methods, as a possible route toward a high-energy-product iron-based magnet. With the working assumption that binary alloys were not promising, Sagawa, Fujimura, *et al.* (1984a) applied conventional sintering methods to ternary light-rare-earth–iron systems and obtained $(BH)_{\max} \simeq 36$ MGOe for $Nd_{0.15}Fe_{0.77}B_{0.08}$. All of these high-$(BH)_{\max}$ materials, rapidly solidified as well as sintered, contained a novel ternary crystalline compound. Although its chemical formula was tentatively and variously identified as $R_3Fe_{21}B$ (Stadelmaier *et al.*, 1983; Hadjipanayis *et al.*, 1984), $R_3Fe_{20}B$ (Hadjipanayis *et al.*, 1983), $R_3Fe_{20}B_2$ (Spada *et al.*, 1984), $R_5Fe_{25}B_3$ (Deryagin *et al.*, 1984), and as $R_3Fe_{16}B$ in an earlier crystallographic study of R-Fe-B systems by Chaban *et al.* (1979), the correct stoichiometry, $R_2Fe_{14}B$, and detailed crystal structure were soon determined (Givord, Li, and Moreau, 1984; Herbst *et al.*, 1984, 1985; Shoemaker *et al.*, 1984). The larger energy product reported by Sagawa, Fujimura, *et al.* (1984a) arose from the crystallite orientation afforded by the powder-metallurgy procedure.

Considerable technological interest has centered on $Nd_2Fe_{14}B$ because of its excellent intrinsic properties [$(BH)^*_{\max} \sim 64$ MGOe, $H_a \sim 73$ kOe] and economic advantages over samarium-cobalt materials. Practical magnets with energy products in the 40–50-MGOe range, values significantly larger than any previously attained (see Fig. 1), have been prepared from melt-spun (Lee, 1985; Croat, 1989a) and sintered (e.g., Sagawa, Hirosawa, *et al.*, 1987d) alloys, and large-scale production programs employing both approaches have been implemented (technological aspects are the subject of Sec. VII). The spectrum of applications for Nd-Fe-B magnets continues to expand. On the scientific side, the existence of an entire $R_2Fe_{14}B$ series has stimulated a great deal of research on their properties and the physics underlying those properties (see Secs. III–VI).

III. CRYSTAL STRUCTURE

$Nd_2Fe_{14}B$ emerged as the prototypical $R_2Fe_{14}B$ compound because magnets having the largest energy products contain it as the principal constituent. Roughly comparable hard-magnetic properties can be realized with $Pr_2Fe_{14}B$, but the Nd phase has received more attention as a magnet material because it has somewhat higher magnetization (see Table IV in Sec. IV) and neodymium is more abundant than praseodymium. The exact stoichiometry and crystal structure of $Nd_2Fe_{14}B$ were first established by neutron powder-diffraction analysis (Herbst *et al.*, 1984, 1985) and confirmed by two independent single-crystal x-ray investigations (Shoemaker *et al.*, 1984; Givord, Li, and Moreau, 1984). Buschow and colleagues (Buschow, de Mooij, and Van Noort, 1985; Buschow, de Mooij, *et al.*, 1986) have shown that $Nd_2Fe_{14}B$ is essentially a line compound with a homogeneity range considerably narrower than that characterizing $SmCo_5$.

A. $Nd_2Fe_{14}B$ crystallography

Figure 2 displays the $Nd_2Fe_{14}B$ unit cell. The lattice symmetry is tetragonal (space group $P4_2/mnm$), and each unit cell contains four formula units, or 68 atoms. There are six crystallographically distinct iron sites, two different rare-earth positions, and one boron site. Table I lists the nuclear positions from the work of Herbst *et al.* (1985), and Table II contains interatomic distances computed from them. Figure 3 is the Cu-K_α x-ray powder-diffraction diagram calculated for $Nd_2Fe_{14}B$ using the parameters in Table I. The coordinate systems differ among the structure determinations such that equivalent atomic positions are related by

$$(x,y,z)_{\text{Herbst } et\ al.} \leftrightarrow \begin{cases} (x,-y,z)_{\text{Shoemaker } et\ al.} \\ (x,y,z+\frac{1}{2})_{\text{Givord } et\ al.} \end{cases} .$$

The site designations, which differ as well, are included in Table I. There is no question, however, that the overall

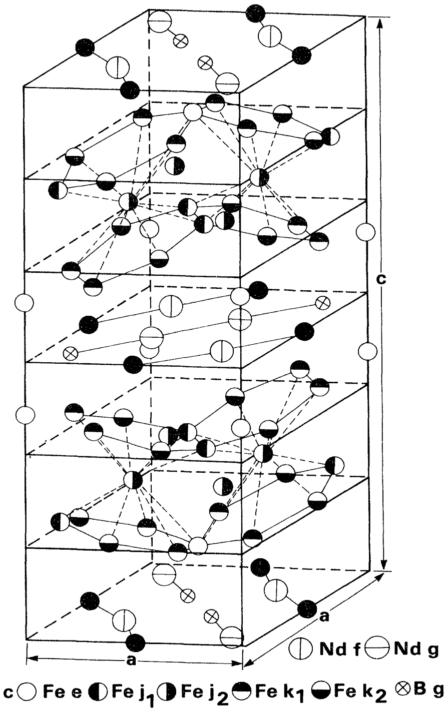

FIG. 2. Tetragonal unit cell of $Nd_2Fe_{14}B$, the prototypical structure of the $R_2Fe_{14}B$ compounds. The c/a ratio in the figure is exaggerated to emphasize the puckering of the hexagonal iron nets.

TABLE I. Atomic sites (number of positions and Wyckoff notation) and nuclear coordinates x,y,z (in units of the lattice constants $a=8.80$ Å, $c=12.20$ Å) for $Nd_2Fe_{14}B$ at 295 K from Herbst *et al.* (1985). The final two columns give the corresponding site designations of Shoemaker *et al.* (1984) and Givord, Li, and Moreau (1984). The space group is $P4_2/mnm$, No. 136 in the tables of Henry and Lonsdale (1952).

				Other site designations	
Atom	x	y	z	Shoemaker	Givord
Nd(4f)	0.268	0.268	0	Nd(2) 4g	Nd_2 4g
Nd(4g)	0.140	−0.140	0	Nd(1) 4f	Nd_1 4f
Fe(16k_1)	0.223	0.567	0.127	Fe(2) 16k	Fe_5 16k
Fe(16k_2)	0.037	0.360	0.176	Fe(3) 16k	Fe_6 16k
Fe(8j_1)	0.098	0.098	0.204	Fe(5) 8j	Fe_3 8j
Fe(8j_2)	0.317	0.317	0.246	Fe(4) 8j	Fe_4 8j
Fe(4e)	0.5	0.5	0.114	Fe(6) 4e	Fe_1 4e
Fe(4c)	0	0.5	0	Fe(1) 4c	Fe_2 4c
B(4g)	0.371	−0.371	0	*B* 4f	*B* 4f

$Nd_2Fe_{14}B$ structure is definitively established, and the atomic coordinates obtained in the three determinations agree very well. The Fe and Nd parameters differ by no more than 0.001 and 0.002, respectively, between the neutron and x-ray results, while the boron position shows the greatest disparity, 0.006 (0.08 Å). Since the boron cross section is comparable to the Nd and Fe cross sections for neutrons but much smaller for x rays, the boron position is likely better established by neutron scattering.

From Fig. 2 it can be seen that each $Nd_2Fe_{14}B$ unit cell consists of an eight-layer repeat structure perpendicular to the c axis. Spatial relationships among several of the layers are illustrated in Fig. 4. All the Nd and B atoms, but only the four Fe(c) atoms out of the total iron number of 56, reside in the $z=0$ and $z=\frac{1}{2}$ mirror planes [Fig. 2, Fig. 4(a)]; the planes are connected by 4_2 tetragonal screw axes passing through the 4c sites. Between these planes the other Fe atoms form three puckered nets. The Fe(k_1), Fe(k_2), Fe(j_1), and Fe(e) sites comprise two slightly distorted hexagonal arrays rotated by ~30° with respect to one another; they enclose a net of Fe(j_2) sites

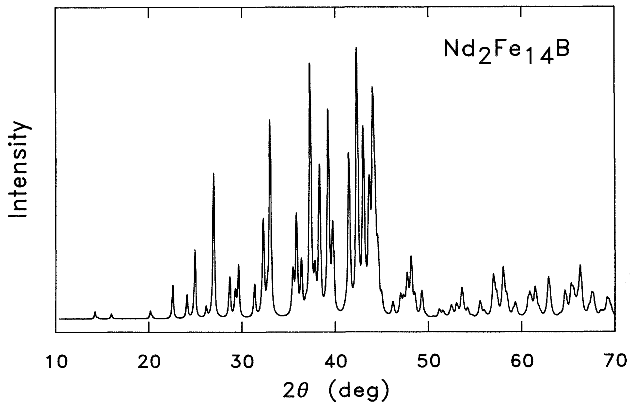

FIG. 3. Calculated Cu-K_α x-ray powder-diffraction pattern for $Nd_2Fe_{14}B$.

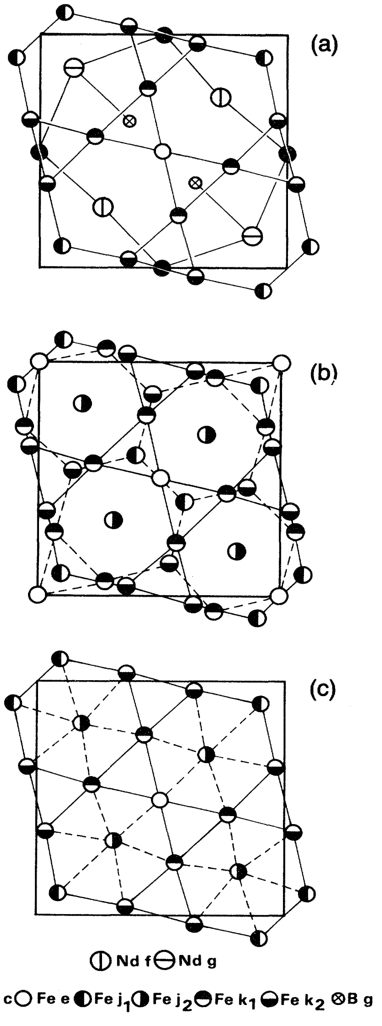

FIG. 4. (a) Projection of the basal plane and the first Fe layer ($z\sim1/6$) in $Nd_2Fe_{14}B$. (b) Projection of the three Fe layers between the basal and $z=\frac{1}{2}$ planes. (c) Projection of the first Fe layer and the neighboring layer of Fe(j_2) atoms ($z\sim\frac{1}{4}$).

located above or below the centers of the hexagons in the neighboring layers [Fig. 4(b)]. Many authors (e.g., Shoemaker *et al.*, 1984; Sagawa, Fujimura, *et al.*, 1984b; Boller and Oesterreicher, 1984; H. Oesterreicher *et al.*, 1984; Abache and Oesterreicher, 1985; Givord and Li, 1985) have discussed the close similarity of the iron layers in Fig. 4(b) to nets in the σ phase found in the Fe-Cr, Fe-Mo, and other systems (Bergman and Shoemaker, 1954). Figure 4(c) makes clear the essentially perfect triangular coordination of the Fe(j_2) atoms and each of the hexagonal layers. Although the j_2-site z coordinate is not fixed by the space group, it is very near $z=\frac{1}{4}$ (cf. Table I), so that the layers of Fe(j_2) atoms are almost precisely midway between the planes containing Nd and B.

The boron coordination in $Nd_2Fe_{14}B$ is simple and elegant. Each boron occupies the center of a trigonal prism (Fig. 5) formed by the three nearest iron atoms above and the three below the basal (or $z=\frac{1}{2}$) plane. Figure 4(a) shows that the triangular prism faces participate in completing the hexagonal Fe nets over the square basal-plane units. The prisms pucker the Fe nets because

TABLE II. Interatomic distances (Å) in $Nd_2Fe_{14}B$ from the coordinates of Table I. All pairs of atoms separated by less than 4 Å are included.

Atom	Neighbors and distances	
Nd(f)	4 Fe(k_2)	3.06
	2 Fe(j_2)	3.07
	4 Fe(k_1)	3.08
	2 Fe(c)	3.12
	2 Fe(e)	3.21
	2 Fe(j_1)	3.27
	2 B	3.30
	2 Nd(g)	3.76
Nd(g)	1 B	2.87
	4 Fe(k_1)	3.09
	2 Fe(j_2)	3.14
	4 Fe(j_1)	3.28
	4 Fe(k_2)	3.28
	2 Fe(c)	3.40
	1 Nd(g)	3.49
	2 Nd(f)	3.76
Fe(k_1)	1 B	2.10
	1 Fe(k_2)	2.46
	1 Fe(e)	2.51
	2 Fe(k_2)	2.52
	1 Fe(c)	2.57
	1 Fe(j_1)	2.60
	1 Fe(k_1)	2.60
	1 Fe(j_2)	2.70
	1 Fe(j_2)	2.76
	1 Nd(f)	3.08
	1 Nd(g)	3.09
	1 Fe(k_1)	3.11
	1 Fe(e)	3.86
Fe(k_2)	1 Fe(j_1)	2.39
	1 Fe(k_1)	2.46
	1 Fe(c)	2.50
	2 Fe(k_1)	2.52
	3 Fe(k_2)	2.56
	1 Fe(j_2)	2.63
	1 Fe(j_2)	2.66
	1 Nd(f)	3.06
	1 Nd(g)	3.28
Fe(j_1)	2 Fe(k_2)	2.39
	1 Fe(j_1)	2.44
	1 Fe(e)	2.53
	2 Fe(k_1)	2.60
	2 Fe(j_2)	2.65
	1 Fe(j_2)	2.77
	1 Nd(f)	3.27
	2 Nd(g)	3.28
	1 B	3.62
Fe(j_2)	2 Fe(k_2)	2.63
	2 Fe(j_1)	2.65
	2 Fe(k_2)	2.66
	2 Fe(k_1)	2.70
	2 Fe(k_1)	2.76
	1 Fe(j_1)	2.77
	1 Fe(e)	2.80
	1 Nd(f)	3.07
	1 Nd(g)	3.14
	1 B	3.88
Fe(e)	2 B	2.12
	4 Fe(k_1)	2.51
	2 Fe(j_1)	2.53
	1 Fe(e)	2.78
	2 Fe(j_2)	2.80
	2 Nd(f)	3.21
	4 Fe(k_1)	3.86
Fe(c)	4 Fe(k_2)	2.50
	4 Fe(k_1)	2.57
	2 Nd(f)	3.12
	2 Nd(g)	3.40
	2 B	3.46
B	4 Fe(k_1)	2.10
	2 Fe(e)	2.12
	1 Nd(g)	2.87
	1 B	3.21
	2 Nd(f)	3.30
	2 Fe(c)	3.46
	2 Fe(j_1)	3.62
	2 Fe(j_2)	3.88

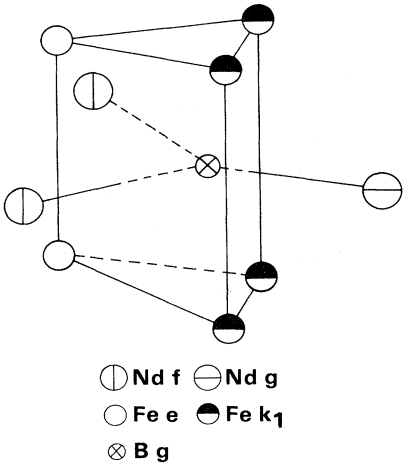

FIG. 5. Trigonal prism containing a boron atom in the $Nd_2Fe_{14}B$ structure.

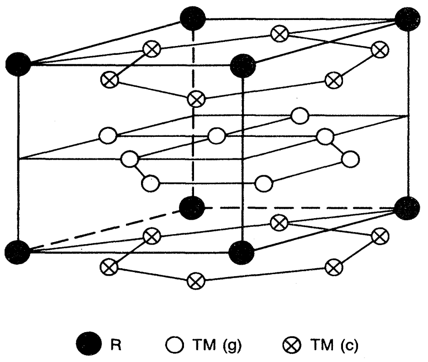

FIG. 6. Unit cell of the hexagonal R-TM_5 structure ($CaCu_5$-type; *P6/mmm*) formed by $SmCo_5$ and other R-TM compounds (adapted from Wernick and Geller, 1959).

the Fe(e) and Fe(k_1) atoms in them are displaced significantly toward the B-containing planes compared with the other Fe atoms in the nets; the B-Fe(k_1) and B-Fe(e) distances are the shortest in the structure (cf. Table II). Linking the Fe layers above and below the planes containing Nd and B, the prisms evidently contribute to the stability of the structure. Three rare-earth atoms are bonded to each boron through the rectangular prism faces. The prisms appear in pairs having a common Fe(e)-Fe(e) edge, and they share two rare-earth atoms. Such trigonal prisms are fundamental to the structure of many transition-metal–metalloid systems, both crystalline (e.g., FeB, Fe_3C, Fe_3P) and amorphous (Gaskell, 1981; Parthé *et al.*, 1983).

B. Other structural comparisons

In addition to the similarities with simpler TM-metalloid materials, many structural parallels exist between $Nd_2Fe_{14}B$ and other R-TM systems. Givord, Li, and Moreau (1984) have pointed out that the boron atoms in $R_2Fe_{14}B$ and those in the hexagonal RCo_3B_2 and related compounds occupy the same position inside a rhombus of R atoms. Reporting the formation of isomorphous $La_2Fe_{14}C$, Marusin *et al.* (1985) noted that the $R_2Fe_{14}B$ structure can be related to the cubic Th_6Mn_{23} structure, formed by many R-Fe and R-Mn compounds, via a tetragonal deformation ($a/\sqrt{2} \rightarrow c$) of the latter. Analogies with the hexagonal $CaCu_5$ structure characterizing the permanent-magnet compound $SmCo_5$ and a variety of other R-TM phases include the following, as comparison of Fig. 2 and Fig. 4 with Fig. 6 shows. Both structures can be viewed as stacks of triangular and hexagonal layers. The hexagonal arrays of Fe(k_1), Fe(k_2), Fe(j_1), and Fe(e) atoms in $R_2Fe_{14}B$ are the cognates of the TM(g) arrays in R-TM_5; both form hexagonal prisms enclosing the R atoms. Furthermore, as emphasized by Givord, Li, and Moreau (1984), the B and Fe(j_2) sites of $R_2Fe_{14}B$ correspond to the TM(c) and R sites, respectively, in R-TM_5.

Several other R-TM lattices can be derived from R-TM_5 by judicious replacement of R and TM atoms (see, for example, Buschow, 1971; Pearson, 1972). These include the R-TM_2 (cubic Laves phase; $MgCu_2$-type) structure formed by the extremely magnetostrictive compounds $TbFe_2$ and $SmFe_2$ (reviewed by Clark, 1980), the R-TM_3 (rhombohedral; $PuNi_3$-type) structure, the R-TM_{12} (tetragonal; $ThMn_{12}$-type) structure characterizing a class of magnetically anisotropic materials such as $RFe_{10}TM_2$, whose investigation has begun only recently (see de Boer *et al.*, 1987; de Mooij and Buschow, 1988a), and, of most interest here, the R_2TM_{17} (rhombohedral; Th_2Zn_{17}-type) structure. Representatives of the rhombohedral R_2TM_{17} class include the hard-magnet compound Sm_2Co_{17}; the recently discovered interstitial nitride $Sm_2Fe_{17}N_{2.3}$, which has some promise as a permanent-magnet material in view of its high Curie temperature ($T_c \simeq 749$ K), large room-temperature magnetization ($4\pi M_s \simeq 15$ kG), and uniaxial anisotropy (Coey and Sun, 1990; Coey *et al.*, 1990; H. Sun *et al.*, 1990); and Nd_2Fe_{17}, the binary intermetallic closest in stoichiometry to $Nd_2Fe_{14}B$. In discussing the crystallography of the R_2Co_{17} phases, Ostertag and Strnat (1966) noted that appropriate replacement of every third R atom by a pair of Co atoms in R-TM_5 generates the R_2TM_{17} lattice illustrated in Fig. 7.

Given the similarities of R-TM_5 and $Nd_2Fe_{14}B$ on the one hand and of R-TM_5 and R_2TM_{17} on the other, it is not surprising that many parallels exist between $Nd_2Fe_{14}B$ and R_2TM_{17}. The layered arrangement and the presence of hexagonal TM nets surrounding R atoms in each structure are apparent from Figs. 2 and 7.

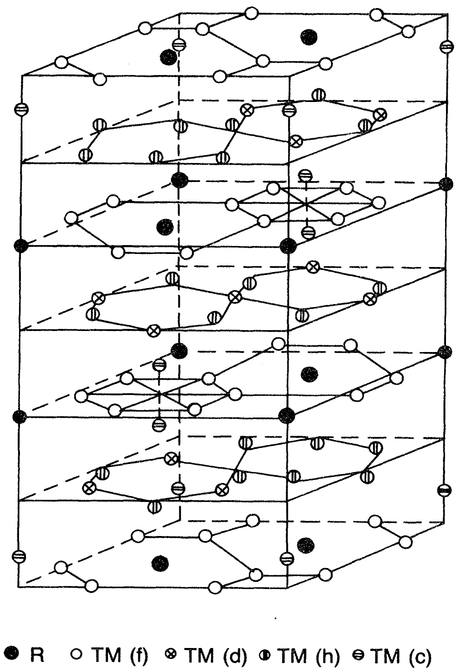

FIG. 7. Hexagonal unit cell of the rhombohedral R_2TM_{17} (Th_2Zn_{17}-type; $R\bar{3}m$) structure, whose representatives include Sm_2Co_{17} and Nd_2Fe_{17} (after Streever, 1979).

Despite the different symmetries, the lattice parameters of $Nd_2Fe_{14}B$ ($a=8.80$ Å, $c=12.20$ Å) approach those of its nearest R_2TM_{17} relative, Nd_2Fe_{17} ($a=8.57$ Å, $c=12.44$ Å). Perhaps the most significant correlation, however, is the fact that the Fe(j_2) atoms in $Nd_2Fe_{14}B$ and the Fe(c) atoms in Nd_2Fe_{17} are cognate magnetically as well as crystallographically (Herbst *et al.*, 1985, 1986). Residing above and below the centers of hexagons, each site has the largest number of near-neighbor Fe atoms and the largest magnetic moment in its structure. The Fe-Fe(j_2) bond lengths extend from 2.63 Å to 2.80 Å in $Nd_2Fe_{14}B$ (cf. Table II), and the Fe-Fe(c) bonds in Nd_2Fe_{17} span an almost identical interval, 2.62–2.74 Å. Moreover, neutron-diffraction studies of the $Nd_2Fe_{17-x}Co_x$ (Herbst *et al.*, 1982) and $Nd_2Fe_{14-x}Co_xB$ (Herbst and Yelon, 1986a) pseudoternary compounds demonstrate that these similarities persist for the Co-substituted systems, with the additional parallel that the c sites in the former and the j_2 sites in the latter are both preferentially occupied by Fe. A number of ^{57}Fe Mössbauer-effect studies also indicate that the j_2 site has a strong preference for Fe (see Sec. VI.B).

A very interesting further perspective on the analogy between the j_2 sites in $Nd_2Fe_{14}B$ and the c sites in Nd_2Fe_{17} has been provided by Bennett, Watson, and coworkers in studies of the topology of local atomic environments and its implications for magnetism and superconductivity. Those authors observe that the j_2 and c sites are the only TM sites in their respective structures having major ligand lines, i.e., lines connecting sixfold faces of Wigner-Seitz polyhedra constructed about the lattice sites, and they suggest that the occurrence of such lines generally encourages large moments (Bennett *et al.*, 1986; Bennett and Watson, 1987; Watson *et al.*, 1987). The orientation of the major ligand lines has also been related to the magnetocrystalline anisotropy in a number of R-TM materials (Melamud *et al.*, 1987; Watson *et al.*, 1988).

C. Isomorphs

The $R_2Fe_{14}B$ structure has been found to form with yttrium, thorium, and all the rare-earth elements except europium and radioactive promethium. Lattice constants and densities for these compounds are given in Table III. The effect of the lanthanide contraction, the decrease in the radii of the trivalent lanthanide ions with increasing atomic number Z, is apparent in the decrease of the c lattice parameter through the rare-earth (La-Lu) series. As Z increases, the addition of another electron to the $4f$ shell does not completely screen the larger nuclear charge, and the radius of the rare-earth ion contracts. $Ce_2Fe_{14}B$ clearly deviates from the trend. Its smaller lattice constants (and magnetization—see Table IV in Sec. IV) imply that Ce is essentially tetravalent with no $4f$ magnetic moment in the structure; neutron-diffraction measurements (Herbst and Yelon, 1986b; Dalmas de Réotier *et al.*, 1987) confirm this inference. All the other rare-earth constituents, including ytterbium, are evidently trivalent (Y and Th are almost certainly trivalent and tetravalent, respectively). The a lattice parameter declines much more slowly with Z, suggesting that the basal-plane dimension is influenced more by the particularly stable trigonal Fe-B prisms than by the size of the R ions. The crystallographic work on $Nd_2Fe_{14}B$ and neutron studies of the Ce, Lu (Herbst and Yelon, 1986b), Pr, Dy (Herbst and Yelon, 1985), Ho (Wolfers *et al.*, 1990), Er (Yelon and Herbst, 1986), Tm (Davis *et al.*, 1985), and Y, Ce, Er compounds (Dalmas de Réotier *et al.*, 1987) indicate that the nuclear position parameters (in units of the lattice constants) change minimally through the series.

Only two families of $Nd_2Fe_{14}B$-type compounds are known in which Fe or B is totally replaced by another element, namely, $R_2Co_{14}B$ and $R_2Fe_{14}C$. Partial substitution of R, Fe, or B with maintenance of the $R_2Fe_{14}B$ structure is possible with many other elements, and $R_2Fe_{14}BH_x$ and $R_2Co_{14}BH_x$ interstitial hydride series exist. These isostructural materials are the subject of Sec. VI.

TABLE III. Room-temperature lattice constants a,c and densities ρ computed from them for the tetragonal $R_2Fe_{14}B$ compounds.

Compound	a (Å)	c (Å)	ρ (g/cm^3)	References
$La_2Fe_{14}B$	8.82	12.34	7.40	a,b
$Ce_2Fe_{14}B$	8.76	12.11	7.67	c–g
$Pr_2Fe_{14}B$	8.80	12.23	7.54	e,g,h
$Nd_2Fe_{14}B$	8.80	12.20	7.60	d,f,g,i–k
$Sm_2Fe_{14}B$	8.80	12.15	7.72	e,l
$Gd_2Fe_{14}B$	8.79	12.09	7.87	a,e–g,l
$Tb_2Fe_{14}B$	8.77	12.05	7.96	a,d–g,l
$Dy_2Fe_{14}B$	8.76	12.01	8.05	a,d,e,g,h,l
$Ho_2Fe_{14}B$	8.75	11.99	8.12	a,d–g,l
$Er_2Fe_{14}B$	8.73	11.95	8.22	a,e–g,l,m
$Tm_2Fe_{14}B$	8.73	11.93	8.26	a,e,g
$Yb_2Fe_{14}B$	8.71	11.92	8.36	n
$Lu_2Fe_{14}B$	8.70	11.85	8.47	c
$Y_2Fe_{14}B$	8.76	12.00	7.00	a,d,f
$Th_2Fe_{14}B$	8.80	12.17	8.86	o,p

[a] Sinema *et al.* (1984).
[b] Stadelmaier, Liu, and ElMasry (1985).
[c] Herbst and Yelon (1986b).
[d] Hirosawa, Matsuura, *et al.* (1986).
[e] Sagawa, Fujimura, *et al.* (1984b).
[f] Abache and Oesterreicher (1986b).
[g] R. Fruchart *et al.* (1987).
[h] Herbst and Yelon (1985).
[i] Herbst *et al.* (1984, 1985).
[j] Shoemaker *et al.* (1984).
[k] Givord, Li, and Moreau (1984).
[l] Yamamoto *et al.* (1984).
[m] Yelon and Herbst (1986).
[n] Burlet *et al.* (1986).
[o] Pedziwiatr, Wallace, and Burzo (1986c).
[p] Andreev and Bartashevich (1990b).

IV. MAGNETIC PROPERTIES OF THE $R_2Fe_{14}B$ COMPOUNDS

A. Systematics

A sequence of homologous compounds, especially one formed by the rare earths, affords the opportunity to obtain valuable systematic information on which more detailed work can build. This opportunity has been well exploited with regard to the magnetic properties of the $R_2Fe_{14}B$ series. Saturation magnetizations M_s, anisotropy fields H_a, and Curie temperatures T_c of the $R_2Fe_{14}B$ phases are given in Table IV. The entries are a selected subset of the published results, one source of whose variation is the fact that preparation of single-phase samples is a nontrivial task; as a representative example, $Nd_2Fe_{14}B$ melts incongruently and forms by peritectic reaction of the liquid and Fe (for phase diagram information see, for example Matsuura *et al.*, 1985b; Schneider *et al.*, 1986). Single-crystal measurements are cited for most of the compounds; of particular note in this respect is the work of Hirosawa, Matsuura, *et al.* (1986), who prepared single crystals of eleven members of the series. In Table IV, H_a denotes the external magnetic field required to rotate the magnetization from an easy into a hard direction. The values of H_a were determined either from magnetization curves for the field parallel and normal to an easy direction (e.g., Sinnema *et al.*, 1984; Hirosawa, Matsuura, *et al.*, 1986) or by the singular-point detection method (e.g., Grössinger, Sun, *et al.*, 1985, 1986; Grössinger, Kirchmayr, and Buschow, 1988). The latter technique was pioneered by Asti and Rinaldi (1974) and is specifically applicable to polycrystalline samples; for a uniaxial material, H_a is identified as the field H for which the second derivative d^2H/dM^2 of the magnetization M exhibits a singularity when H is applied in a hard direction.

1. R and Fe magnetic moments and their couplings

An estimate of $2.1\mu_B$ for the average moment per Fe atom in the series is given by the 4 K magnetizations of the R=La, Ce, Lu, Y, and Th compounds in Table IV because those materials can be regarded as magnetically blank with respect to the rare-earth component. (The mean Fe moment in the tetravalent Ce and Th compounds, $2.06\mu_B$, is slightly lower than the $2.15\mu_B$ average for the trivalent La, Lu, and Y compounds, indicating the impact of additional charge transfer from the R component to the conduction bands.) This value closely approximates the $2.2\mu_B$ moment of elemental α-Fe, a remarkable fact considering that α-Fe is body-centered cubic with but one symmetry site, whereas $R_2Fe_{14}B$ is tetragonal with six crystallographically distinct Fe sites. The magnitude of the mean Fe moment suggests that the six iron sublattices in the $R_2Fe_{14}B$ structure are ferromagnetically coupled and collinear; no evidence to the contrary has emerged from neutron-diffraction, Mössbauer-effect, or other experiments. For the compounds in which the rare earth supports a moment, the average R moment μ_R can be estimated by subtracting M_s (4 K) for $Y_2Fe_{14}B$ from the other low-temperature magnetizations in Table IV. Values of μ_R generated in this way are given in Table V, and two inferences can be educed from them.

First, the sign of μ_R implies that the rare-earth and iron moments are coupled ferromagnetically (antiferromagnetically) for the light (heavy) rare earths, an observation which applies to a large number of crystalline as well as amorphous R-TM systems spanning a broad range of structures, compositions, and conduction-electron concentrations (see, for example, Buschow, 1971, 1977, 1980; Kirchmayr and Poldy, 1979). Now in first approximation it can be assumed that the rare-earth moment derives solely from the $4f$ electrons and that the ground state of the $4f$ shell is specified by Hund's rules (with the likely exception of Sm^{3+}, which features a low-lying excited multiplet). The total angular momentum J in the Hund's-rule state of the $4f$ shell is $J=L-S$ for the light lanthanides and $J=L+S$ for the heavy lanthanides (see Table V); i.e., the total R moment and the R spin moment are antiparallel for the light-rare-earth ions and parallel for the heavy-rare-earth ions. The above inference regarding the R-Fe moment coupling is thus equivalent to the statement that the rare-earth $4f$ and iron $3d$ spin moments are always antiparallel, that is, *the 3d-4f exchange interaction is invariably antiferromagnetic.* Understanding of this widely observed characteristic is far from complete. Wallace (1968) and Buschow (1971) proposed that the $3d$-$4f$ coupling occurs indirectly via polarization of the s conduction electrons by an interaction of the Ruderman-Kittel-Kasuya-Yosida (RKKY) type. The interaction Hamiltonian is then of the form (Buschow, 1971)

$$\mathcal{H}_{\text{R-TM}} \propto j_{sf} j_{sd} \sum_{i \neq j} F(2k_F R_{ij}) \mathbf{S}_i^{\text{R}} \cdot \mathbf{S}_j^{\text{TM}} , \tag{2}$$

where j_{sf} and j_{sd} are effective $4f$-s and $3d$-s exchange integrals, $\mathbf{S}_i^{\text{R}}$ and $\mathbf{S}_j^{\text{TM}}$ are the spin operators for local rare-earth $4f$ and TM $3d$ spins at lattice sites i and j separated by $\mathbf{R}_{ij}$, k_F is the Fermi wave vector, and

$$F(x) \equiv (x \cos x - \sin x)/x^4 \tag{3}$$

is the usual RKKY function. This mechanism, however,

TABLE IV. Saturation magnetizations M_s, anisotropy fields H_a, and Curie temperatures T_c of the $R_2Fe_{14}B$ compounds.

	4 K			295 K			
Compound	M_s (μ_B/f.u.)	$4\pi M_s$ (kG)	H_a (kOe)	M_s (μ_B/f.u.)	$4\pi M_s$ (kG)	H_a (kOe)	T_c (K)
$La_2Fe_{14}B$	30.6^{a}	14.8^{a}	12^{b-d}	$28.4^{c,d}$	$13.8^{c,d}$	20^{b-d}	$530^{a,d}$
$Ce_2Fe_{14}B$	29.4^{e}	14.7^{e}	$26^{b,c,e}$	$23.9^{e,f}$	$11.7^{e,f}$	$26^{b,c,e}$	$424^{a,e,g-j}$
$Pr_2Fe_{14}B$	37.6^{e}	18.4^{e}	$\sim 200^{b,c,f}$	31.9^{e}	15.6^{e}	$75^{b,c,f}$	$565^{a,e-l}$
$Nd_2Fe_{14}B$	$37.7^{e,m-p}$	$18.5^{e,m-p}$	$\sim 170^{b,c}$	$32.5^{e,m,n,q,r}$	$16.0^{e,m,n,q,r}$	73^{s}	$585^{a,e-h,}_{j,r,t,u}$
$Sm_2Fe_{14}B$	$33.3^{e,v}$	$16.7^{e,v}$	$>200^{v}$	$30.2^{e,m,v}$	$15.2^{e,m,v}$	$>150^{e,m,v}$	$616^{a,e,g-j}$
$Gd_2Fe_{14}B$	$17.9^{a,e}$	$9.2^{a,e}$	$19^{b,c,e}$	$17.5^{e-h,r}$	$8.9^{e-h,r}$	$24^{b,c,e,r}$	$661^{e-k,r}$
$Tb_2Fe_{14}B$	$13.2^{a,e}$	$6.6^{a,e}$	$\sim 300^{e}$	14.0^{e}	7.0^{e}	$\sim 220^{e}$	$620^{a,e,i,j}$
$Dy_2Fe_{14}B$	$11.3^{a,e,f}$	$5.7^{a,e,f}$	$\sim 170^{a,e}$	$14.0^{e,f}$	$7.1^{e,f}$	$\sim 150^{e,f}$	598^{e-j}
$Ho_2Fe_{14}B$	$11.2^{a,e}$	$5.7^{a,e}$	$>100^{b,c}$	15.9^{e}	8.1^{e}	$75^{e,k}$	$573^{a,e,g-j}$
$Er_2Fe_{14}B$	12.9^{e}	6.6^{e}	$\sim 260^{a}$	$17.7^{e,g,h,w}$	$9.0^{e,g,h,w}$	8^{w}	$554^{a,e-j,}_{l,u,x}$
$Tm_2Fe_{14}B$	$18.1^{a,e}$	$9.2^{a,e}$	$\sim 170^{a}$	$22.6^{a,e}$	$11.5^{a,e}$	8^{w}	$541^{a,e,g-j}$
$Yb_2Fe_{14}B$	$\sim 23^{y}$	$\sim 12^{y}$		$\sim 23^{y}$	$\sim 12^{y}$		524^{z}
$Lu_2Fe_{14}B$	28.2^{a}	14.7^{a}	$20^{b,c}$	22.5^{c}	11.7^{c}	$26^{b,c,k}$	$535^{a,i,j}$
$Y_2Fe_{14}B$	$31.4^{e,f,p}$	$15.9^{e,f,p}$	$18^{b,c,n}$	27.8^{e-g}	14.1^{e-g}	$26^{f,m,n,q,r}$	$565^{a,e-h,j,r}$
$Th_2Fe_{14}B$	28.4^{α}	12.2^{α}	$\sim 20^{c}$	24.7^{α}	14.1^{α}	$26^{\alpha,\beta}$	$481^{\alpha,\beta,\gamma,\delta}$

[a] Sinnema *et al.* (1984).
[b] Grössinger, Sun, *et al.* (1985).
[c] Grössinger, Sun, *et al.* (1986).
[d] Grössinger, Kirchmayr, and Buschow (1988).
[e] Hirosawa, Matsuura, *et al.* (1986).
[f] Boltich *et al.* (1985).
[g] Yamamoto *et al.* (1984).
[h] Sagawa, Fujimura, *et al.* (1984b).
[i] Belorizky *et al.* (1987).
[j] R. Fruchart *et al.* (1987).
[k] Abache and Oesterreicher (1985).
[l] Burzo, Oswald, *et al.* (1985).
[m] Sagawa, Fujimura, *et al.* (1985a).
[n] Givord, Li, and Perrier de la Bâthie (1984).
[o] Givord, Li, and Tasset (1985).
[p] Tokuhara *et al.* (1985).
[q] Koon *et al.* (1985).
[r] M. Q. Huang *et al.* (1985).
[s] Grössinger, Krewenka, *et al.* (1986).
[t] Fuerst *et al.* (1986).
[u] Pedziwiatr and Wallace (1987a).
[v] Hiroyoshi *et al.* (1985).
[w] Hirosawa and Sagawa (1985).
[x] Fuerst, Meisner, and Pinkerton (1987).
[y] Coey (1986).
[z] Burlet *et al.* (1986).
[α] Pedziwiatr and Wallace (1986a).
[β] Buschow, van Noort, and de Mooij (1985).
[γ] Bolzoni, Gavigan, *et al.* (1987).
[δ] Andreev and Bartashevich (1990b).

TABLE V. Estimates μ_R of the average magnetic moment per R atom in $R_2Fe_{14}B$ compounds from the 4 K magnetization data in Table IV, and magnetic moments gJ, ground levels, J, L, S quantum numbers, Landé g factors, and de Gennes factors $G \equiv (g-1)^2 J(J+1)$ for the corresponding trivalent rare-earth ions.

Compound	μ_R (μ_B)	gJ	Ground level	J	L	S	g	G
$Pr_2Fe_{14}B$	3.1	3.2	$4f^2\ {}^3H_4$	4	5	1	4/5	4/5
$Nd_2Fe_{14}B$	3.2	3.3	$4f^3\ {}^4I_{9/2}$	9/2	6	3/2	8/11	81/44
$Sm_2Fe_{14}B$	1.0	0.7	$4f^5\ {}^6H_{5/2}$	5/2	5	5/2	2/7	125/28
$Gd_2Fe_{14}B$	−6.8	7	$4f^7\ {}^8S_{7/2}$	7/2	0	7/2	2	63/4
$Tb_2Fe_{14}B$	−9.1	9	$4f^8\ {}^7F_6$	6	3	3	3/2	21/2
$Dy_2Fe_{14}B$	−10.1	10	$4f^9\ {}^6H_{15/2}$	15/2	5	5/2	4/3	255/36
$Ho_2Fe_{14}B$	−10.1	10	$4f^{10}\ {}^5I_8$	8	6	2	5/4	9/2
$Er_2Fe_{14}B$	−9.3	9	$4f^{11}\ {}^4I_{15/2}$	15/2	6	3/2	6/5	51/20
$Tm_2Fe_{14}B$	−6.7	7	$4f^{12}\ {}^3H_6$	6	5	1	7/6	7/6
$Yb_2Fe_{14}B$	−4.2	4	$4f^{13}\ {}^2F_{7/2}$	7/2	3	1/2	8/7	9/28

is incapable of accounting for the extensive experimental information. One defect of Eq. (2) is the explicit exclusion of on-site terms which can be expected to be significant. Furthermore, the lattice sum in Eq. (2) may well vary in sign for different structures, and nuclear-magnetic-resonance studies on many materials have shown that the 3*d*-*s* interaction does not always lead to the same sign of the *s*-electron polarization (Buschow, 1980). It is thus very unlikely that the 3*d*-4*f* interaction occurs via polarization of the *s*-like conduction electrons.

A more realistic coupling scheme has been proposed by Campbell (1972) and explicated by Buschow (1977, 1980). Emphasizing the importance of the rare-earth 5*d* electrons, Campbell suggests that the 4*f* spins induce a positive, local 5*d* moment via atomic, ferromagnetic 4*f*-5*d* exchange; 3*d*-5*d* exchange then generates the indirect 3*d*-4*f* interaction. Since all the rare-earth elements can be considered to reside at the beginning of a transition-metal series with respect to their 5*d* character (a trivalent rare-earth atom can contribute at most three electrons to the conduction bands), while iron, cobalt, and nickel are in the second half of the 3*d* series, Campbell argues that the 3*d*-5*d* interaction can be expected to be negative, yielding generally antiferromagnetic 3*d*-4*f* coupling. This qualitative model is very appealing, and evidence for its validity has come from quantitative theoretical work. An indication that the *d*-like conduction states are crucial was furnished by the calculations of Szpunar and Kozarzewski (1977), who considered the interaction of local 4*f* spins with narrow bands formed by the rare-earth 5*d* and TM 3*d* electrons within a coherent potential approximation; for the Gd compounds investigated, antiferromagnetic coupling of the R and TM spin moments emerged. In self-consistent, spin-polarized electronic structure calculations for $Y_2Fe_{14}B$ and $Nd_2Fe_{14}B$, Jaswal (1990) found antiparallel Fe and non-4*f* rare-earth spin moments and emphasized that the result supports the idea of negative 3*d*-5*d* interaction in a mixture of early and late transition metals. The same feature characterizes the band-structure results of Coehoorn (1991) for $Y_2Fe_{14}B$ and $Y_2Co_{14}B$, and of Gu and Ching (1987a) for $Y_2Fe_{14}B$. Experiments such as spin-polarized photoemission might be helpful in examining the role of the 5*d* electrons. For example, measurement of the spin-dependent energy distributions at two photon energies, one near the Cooper minimum for 5*d* emission, may enable determination of the individual 3*d* and 5*d* polarizations.

Comparison of the μ_R values with the 4*f*-shell moments gJ of the corresponding free rare-earth ions in Table V yields the second inference, namely, the R moments in the compounds are quite near their free-ion counterparts. The fact that $\mu_R \simeq gJ$ may initially appear surprising, since an R ion having orbital angular momentum $L \neq 0$ contributes greatly to the magnetocrystalline anisotropy, suggesting significant crystal-field splitting and a ground-state moment reduced from the free-ion value. As Sinnema *et al.* (1984) remark, however, observation of essentially the full free-ion moment should rather be interpreted as an indication that the influence of the exchange field acting on the 4*f* moments is stronger than that of the crystal field, even though the latter still controls the direction of the 4*f* moments.

Since M_s and μ_R are measured along an easy direction, a corollary is that the total R and total Fe sublattices can be considered collinear, at least in first approximation. Neutron powder-diffraction work on $Nd_2Fe_{14}B$ (Herbst *et al.*, 1984, 1985), $Pr_2Fe_{14}B$, $Dy_2Fe_{14}B$ (Herbst and Yelon, 1985), $Er_2Fe_{14}B$ (Yelon and Herbst, 1986), and $Tm_2Fe_{14}B$ (Davis *et al*, 1985) supports this inference. For the Nd, Ho, Er, and Tm compounds, which exhibit a change in easy direction as a function of temperature (see Sec. IV.A.3), there is evidence, however, that the total R moment or components of it deviate from collinearity in the low-temperature regime, where higher-order terms in the crystalline electric field acting on the R ions (see Sec. IV.D) become more important. M. Yamada *et al.* (1985) have proposed a noncollinear, five-sublattice model for $Tm_2Fe_{14}B$ based in part on single-crystal neutron measurements; the model contains two planar pairs of individual R sublattices with each pair canted symmetrically away from the direction antiparallel to the total Fe moment. Polarized neutron (Givord, Li, and Tasset, 1985) and ^{57}Fe Mössbauer measurements (Onodera, Yamauchi *et al.*, 1987) on $Nd_2Fe_{14}B$ have been interpreted in terms of noncollinear Nd and Fe moments, and the ^{145}Nd Mössbauer investigation of Nowik *et al.* (1990) strongly indicates that the Nd and Fe moments are not collinear below the temperature $T_s \simeq 135$ K, at which the total magnetization begins to cant away from the c axis. In $Er_2Fe_{14}B$, reflections forbidden by the $P4_2/mnm$ space group have been observed by Fuerst, Meisner, *et al.* (1988). The noncollinear magnetic structure of $Ho_2Fe_{14}B$ at low temperature has been established by very careful neutron diffraction on a single crystal (Wolfers *et al.*, 1990). Even with the powerful technique of neutron diffraction, the precise determination of skewed moment arrangements in these systems is a challenging enterprise; only two of the sixteen magnetic atoms per $R_2Fe_{14}B$ unit are rare earths, and the magnetic contribution is only a fraction of the total scattered intensity.

2. Curie temperatures

Measured values of the Curie temperatures T_c for the $R_2Fe_{14}B$ series are listed in the final column of Table IV. Despite the proximity of the average Fe moment in the compounds ($\sim 2.1\mu_B$)and that of elemental Fe ($2.2\mu_B$), $T_c(\mathrm{Fe}) = 1043$ K is substantially larger than any of the T_c entries in Table IV. This property is shared by all the known R-Fe binary compounds, whose Curie temperatures are displayed together with $T_c(R_2Fe_{14}B)$ in Fig. 8. A remarkable feature of Fig. 8 is the overall *decrease* of T_c as the TM:R ratio r *increases*; the progression is reversed in the R-Co and most of the R-Ni compounds (see, for example, Kirchmayr and Poldy, 1979; Buschow, 1980; Gavigan, Givord, *et al.*, 1988). The $R_2Fe_{14}B$ materials deviate somewhat from the trend of the binaries in Fig. 8 insofar as their T_c values reside roughly between $T_c(RFe_3)$ and $T_c(R_6Fe_{23})$, whereas an $r=7$ binary series might be expected to have ordering temperatures between those of the R_6Fe_{23} and R_2Fe_{17} series.

There is no detailed, quantitative understanding of the T_c vs r trends in R-TM systems. Qualitative interpretations have appealed to the more localized character of Fe moments as compared to Co and Ni moments and the particular sensitivity of Fe-Fe exchange interactions to the Fe-Fe separation. Buschow (1971) has identified the ratio of the wavelength λ of the principal Friedel oscillation about a localized moment to the distance d between moments as an important parameter in this regard. He argues that the interaction will be strongly ferromagnetic if $\lambda/d > 1$, that it will weaken as the ratio diminishes, and that in broad terms λ/d declines progressively from nickel to cobalt to iron compounds, raising the possibility of significant antiferromagnetic contributions to the Fe-Fe exchange interactions. Many authors simply assert that Fe-Fe separations smaller than about 2.5 Å (the nearest-neighbor distance in α-Fe) favor antiferromagnetic exchange and hence are responsible for lower Curie temperatures in the iron-based systems. Such shorter distances do occur in R-Fe compounds (see Table II for $R_2Fe_{14}B$), and a variety of other experimental results, such as the pressure dependence of the magnetization in Fe-Ni alloys (Kouvel and Wilson, 1961) and the magnetic ordering in γ-Fe films and precipitates (see Kümmerle and Gradmann, 1977), do intimate strong distance dependence of the Fe-Fe exchange energy. On the theoretical side, justification for the assertion is apparently based on very early ideas of Sommerfeld and Bethe (1933), Slater (1930), Néel (1936), and in particular on the Bethe-Slater curve (Sommerfeld and Bethe, 1933), which suggests antiferromagnetic exchange for small $3d$-$3d$ separations; however, in a discussion of this issue Goodenough (1963) has emphasized that the validity of the Bethe-Slater curve has been seriously called into question and that the curve is considered to be incorrect. Attributing T_c behavior solely to distance-dependent exchange is undoubtedly an oversimplification in many cases. Gavigan, Givord, *et al.* (1988) discussed the decline of T_c with increasing r

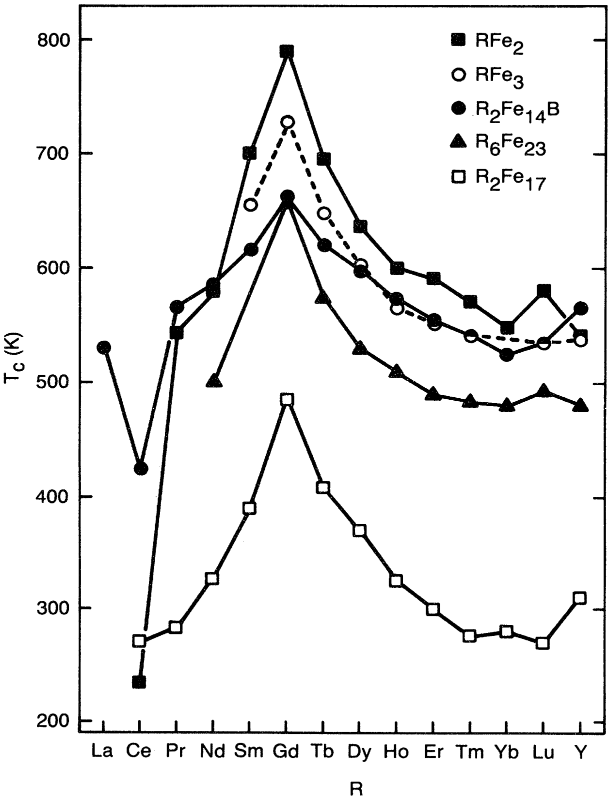

FIG. 8. Curie temperatures T_c of the RFe_2, RFe_3, $R_2Fe_{14}B$, R_6Fe_{23}, and R_2Fe_{17} intermetallic compounds. Table IV lists $T_c(R_2Fe_{14}B)$; values for the other compounds have been assembled from Kirchmayr and Poldy (1979), Buschow (1980), Meyer *et al.* (1980), and Herbst and Croat (1982, 1984).

in R-Fe systems in terms of a diminishing Fe-Fe molecular-field coefficient n_{FF} that describes the Fe-Fe exchange interactions and concluded that the behavior of n_{FF} is most strongly influenced by local environmental effects, especially the mean local Fe coordination number, rather than by the variation of Fe-Fe interatomic distances. Mohn and Wohlfarth (1987) have stressed the importance of long-wavelength (i.e., longer than any interatomic separations) spin fluctuations on the Curie temperature in itinerant electron systems; in calculations for elemental Fe, Co, Ni, and their compounds with Y, those authors found good agreement with experiment, including the disparate trends of T_c vs r in the Y-TM materials.

Figure 9 displays $T_c(R_2Fe_{14}B)$ as a function of $\sqrt{G}$, where $G \equiv (g-1)^2 J(J+1)$ is the de Gennes factor for the rare-earth ion, and $\sqrt{G}$ is the effective R spin (G factors for the trivalent rare-earth ions are listed in Table V). The values of T_c for the La, Ce, Lu, Y, and Th compounds, in which there is no R moment, show that the scale of T_c for the series is set by the exchange interactions among the iron spins. The substantial excursion from $T_c(Ce_2Fe_{14}B)=424$ K to $T_c(Y_2Fe_{14}B)=565$ K in these members of the series underscores the sensitivity of the electronic structure to the nature of the R ion and the lattice constants. Bolzoni, Gavigan, *et al.* (1987) discuss this variation in terms of local environmental factors and speculate that the high Curie temperature of $Y_2Fe_{14}B$ arises from magnetic interactions enhanced by the transfer of more localized $4d$ electrons to the band structure.

For the compounds with an R moment, the T_c data in Fig. 9 divide naturally into two categories depending on the character of the R-Fe moment coupling. T_c is one smooth function of $\sqrt{G}$ for the ferromagnetic (light-R) materials and another smooth function of $\sqrt{G}$ for the ferrimagnetic (heavy-R) phases. The simple relationships imply that the T_c variation through the series is most likely controlled by the R-Fe exchange, which is evidently somewhat smaller but of the same order as the Fe-Fe interactions (the T_c behavior is discussed further in Sec. IV.B). Wallace (1985) has suggested that the lower T_c values for the heavy-rare-earth systems are linked to the shorter Fe-Fe distances accompanying the smaller lattice constants. In any sequence of R-TM compounds the Gd member, whose R spin is the largest among the rare earths (see Table V), invariably exhibits the highest Curie temperature; the $R_2Fe_{14}B$ series is no exception.

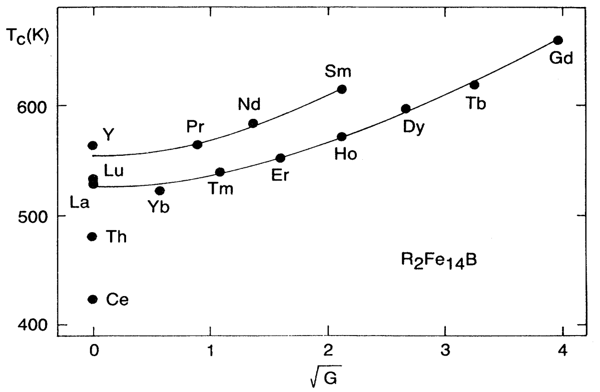

FIG. 9. Curie temperatures T_c of the $R_2Fe_{14}B$ compounds as a function of $\sqrt{G}$, where $G \equiv (g-1)^2 J(J+1)$ is the de Gennes factor of the rare-earth ion (see Table V). The curves are specified by Eq. (19) with the parameters given in the text.

Under pressure $T_c(R_2Fe_{14}B)$ is reduced substantially. Kamarad *et al.* (1987) reported a linear decrease specified by $dT_c/dP \simeq -27$ K/GPa in $Nd_2Fe_{14}B$ as measured by an initial susceptibility technique to a pressure of 4 GPa. Using a resistance method, Nagata *et al.* (1987) found pressure-dependent values of dT_c/dP for the Ce, Nd, and Y compounds ranging from -34 to -100 K/GPa over the 0–6 GPa interval; interestingly, $T_c(Ce_2Fe_{14}B)$ was observed to increase by ~ 60 K after heating under pressure, an effect Nagata *et al.* speculated to be indicative of anomalous Ce $4f$ electron behavior. Gavigan, Givord, *et al.* (1988) demonstrated, at least for the specific case of $Y_2Fe_{14}B$, that $T_c(P)$ is principally controlled by the pressure dependence of the magnetization, the Fe moment decreasing with decreasing atomic volume.

3. Easy directions and sublattice anisotropies

Table VI summarizes the easy directions of magnetization for the $R_2Fe_{14}B$ materials. Since there is no R moment in the La, Ce, Lu, Y, and Th representatives, it is clear from Table VI that the iron sublattice anisotropy in the $R_2Fe_{14}B$ structure favors the c axis as the easy direction. Moreover, the magnitude of the Fe anisotropy is extremely large, as the H_a entries for these compounds in Table IV indicate. The 20 kOe value for $La_2Fe_{14}B$ at 295 K is forty times greater than the anisotropy field of elemental Fe (500 Oe at room temperature). This fact implies that the Fe orbital moment is incompletely quenched in the $R_2Fe_{14}B$ lattice, an unusual characteristic; the crystal-field splitting of Fe, Co, and Ni levels most often dwarfs the spin-orbit spitting, leading to very small orbital moments and, hence, very small associated magnetocrystalline anisotropy. Neutron-scattering investigations have revealed relatively large moments on the j_2 site, and it is likely that a small but appreciable orbital component of the Fe(j_2) moment is mainly responsible for the Fe sublattice anisotropy (Herbst and Yelon, 1986a, 1986b; Herbst *et al.*, 1986; Szpunar *et al.*, 1987; Zhong and Ching, 1990; also see Sec. V).

Throughout the magnetically ordered temperature regime (Curie temperatures T_c are listed in Table IV) $Pr_2Fe_{14}B$, $Gd_2Fe_{14}B$, $Tb_2Fe_{14}B$, and $Dy_2Fe_{14}B$ are also uniaxial, while $Sm_2Fe_{14}B$ features basal-plane magnetization. The Nd, Ho, Er, Tm, and Yb compounds exhibit changes in the easy direction at a temperature T_s, commonly designated as the spin-reorientation temperature and given in the second column of Table VI. In $Er_2Fe_{14}B$, $Tm_2Fe_{14}B$, and $Yb_2Fe_{14}B$ the easy direction is a $\langle 100\rangle$ basal-plane direction below T_s and a $\langle 001\rangle$ direction above T_s. For these three compounds T_s is an increasing function of the de Gennes factor G, with T_s and G (see Table V) conspicuously lowest for the Yb member; however, the functional dependence departs from the $\sim G^{1/2}$ variation characterizing the Curie temperatures. $Nd_2Fe_{14}B$ and $Ho_2Fe_{14}B$ exhibit more complex behavior. Above T_s both compounds are uniaxial, but magnetization and Mössbauer-effect measurements show that below T_s the net magnetization cants away from the c axis toward the [110] direction by an angle that increases with decreasing temperature to ~30° at 4 K in $Nd_2Fe_{14}B$ (Givord, Li, and Perrier de la Bâthie, 1984; Deryagin *et al.*, 1984; Onodera *et al.*, 1984; Koon *et al.*, 1985; Sagawa, Fujimura, *et al.*, 1985a; Tokuhara *et al.*, 1985; Hirosawa, Matsuura, *et al.*, 1986; Koon, Abe, *et al.* 1986; O. Yamada *et al.*, 1986; R. Fruchart *et al.*, 1987; Onodera, Yamauchi, *et al.*, 1987; Cadogan *et al.*, 1988; Verhoef *et al.*, 1988; see also Nowik *et al.*, 1990). The same canting of the magnetization occurs to ~20° at 4 K in $Ho_2Fe_{14}B$ (Hirosawa, Matsuura, *et al.*, 1986; Yamauchi *et al.*, 1986; R. Fruchart *et al.*, 1987; Fujita *et al.*, 1987; Hiroyoshi, Yamada, *et al.*, 1987; Givord, Li, *et al.*, 1988; Maruyama *et al.*, 1988; see also the neutron-diffraction determination by Wolfers *et al.*, 1990).

It has been demonstrated that T_s and the character (e.g., axial→planar) of the spin reorientation can be identified by inflection points in low-field magnetization versus temperature curves (Boltich *et al.*, 1987b; Pedziwiatr and Wallace, 1987a; Christodoulou, Boltich, and Massalski, 1989). The transition temperature can also be determined by differential scanning calorimetry (Fuerst *et al.*, 1986), heat capacity (Fujii, Nagata, *et al.*, 1987; Lazaro *et al.*, 1990), and magnetic susceptibility measurements (Grössinger, Sun, *et al.*, 1986; Ling *et al.*, 1986; Lazaro *et al.*, 1990; single-crystal work on $Ho_2Fe_{14}B$ was reported by Rillo *et al.*, 1988). Anomalies

TABLE VI. Easy directions of magnetization for the $R_2Fe_{14}B$ compounds. T_s denotes the temperature at which a change in the easy direction, or spin reorientation, occurs. α_J represents the second-order Stevens coefficient (Stevens, 1952) corresponding to the rare-earth ion in the compound.

Compound	T_s (K)	Easy direction ($T<T_s \rightarrow T>T_s$)	α_J
$La_2Fe_{14}B$		$\langle 001\rangle$	0
$Ce_2Fe_{14}B$		$\langle 001\rangle$	0
$Pr_2Fe_{14}B$		$\langle 001\rangle$	$-52/2475=-0.021$
$Nd_2Fe_{14}B$	135[a-l]	canted→$\langle 001\rangle$	$-7/1089=-0.006$
$Sm_2Fe_{14}B$		$\langle 100\rangle$[k,m]	$+13/315=+0.041$
$Gd_2Fe_{14}B$		$\langle 001\rangle$	0
$Tb_2Fe_{14}B$		$\langle 001\rangle$	$-1/99=-0.010$
$Dy_2Fe_{14}B$		$\langle 001\rangle$	$-2/315=-0.006$
$Ho_2Fe_{14}B$	58[l,n-r]	canted→$\langle 001\rangle$	$-1/450=-0.002$
$Er_2Fe_{14}B$	325[f,i,l,n,p,s-z]	$\langle 100\rangle\rightarrow\langle 001\rangle$	$+4/1575=+0.003$
$Tm_2Fe_{14}B$	313[f,n,p,s,u,α,β,γ]	$\langle 100\rangle\rightarrow\langle 001\rangle$	$+1/99=+0.010$
$Yb_2Fe_{14}B$	115[δ]	$\langle 100\rangle\rightarrow\langle 001\rangle$	$+2/63=+0.032$
$Lu_2Fe_{14}B$		$\langle 001\rangle$	0
$Y_2Fe_{14}B$		$\langle 001\rangle$	0
$Th_2Fe_{14}B$		$\langle 001\rangle$	0

[a] Grössinger, Sun, *et al.* (1985).
[b] Grössinger, Sun, *et al.* (1986).
[c] Givord, Li, and Perrier de la Bâthie (1984).
[d] Givord, Li, *et al.* (1985).
[e] Tokuhara *et al.* (1985).
[f] Fuerst *et al.* (1986).
[g] O. Yamada *et al.* (1986, 1987).
[h] Koon, Abe, *et al.* (1986).
[i] Pedziwiatr and Wallace (1987a).
[j] Cadogan *et al.* (1988).
[k] Andreev *et al.* (1985).
[l] Abache and Oesterreicher (1986b).
[m] Hiroyoshi *et al.* (1985).
[n] Hirosawa, Matsuura, *et al.* (1986).
[o] R. Fruchart *et al.* (1987).
[p] Givord, Li, *et al.* (1988).
[q] Fujita *et al.* (1987).
[r] Rillo *et al.* (1988).
[s] Hirosawa and Sagawa (1985).
[t] Fuerst, Meisner, and Pinkerton (1987); Fuerst, Meisner, *et al.* (1988).
[u] Yelon and Herbst (1986).
[v] Vasquez *et al.* (1985).
[w] Gavigan *et al.* (1987).
[x] Niarchos and Simopoulos (1986).
[y] Boltich, Pedziwiatr, and Wallace (1987a).
[z] Vasquez and Sanchez (1987).
[α] M. Yamada *et al.* (1985).
[β] Davis *et al.* (1985).
[γ] Price *et al.* (1986).
[δ] Burlet *et al.* (1986).

serving as signatures of spin reorientation appear as well in the temperature dependence of other properties, including the lattice constants and thermal expansion (Andrev *et al.*, 1985; Fujii, Nagata, *et al.*, 1987), elastic moduli (Dadon *et al.*, 1986), muon spin rotation frequency (Yaouanc *et al.*, 1987), electrical resistivity of polycrystalline bulk (Lazaro *et al.*, 1990) and thin-film samples (Zasadzinski *et al.*, 1987a, 1987b), magnetostriction (measured on a single crystal of $Nd_2Fe_{14}B$ by Algarabel *et al.*, 1990), and the nuclear magnetic resonance of the rare-earth component (Shah *et al.*, 1987).

Discontinuities in magnetization versus applied field curves along hard directions have been observed in $Pr_2Fe_{14}B$ (Pareti, Szymczak, and Lachowicz, 1985; Hiroyoshi, Kato, *et al.*, 1987; Verhoef *et al.*, 1988) and $Nd_2Fe_{14}B$ (Pareti, Bolzoni, and Moze, 1985; Grössinger, Sun, *et al.*, 1985; Bolzoni, Moze, and Pareti, 1987; Kajiwara *et al.*, 1987; Kido *et al.*, 1987; Cadogan *et al.*, 1988; Verhoef *et al.*, 1988). Such field-induced, first-order magnetization processes (FOMPs) are analogous to the temperature-induced spin reorientations (i.e., a spin reorientation at T_s can be considered a zero-field FOMP). In $Nd_2Fe_{14}B$, a FOMP begins to appear as the temperature decreases below 200 K (Pareti, Bolzoni, and Moze, 1985), significantly higher than $T_s \simeq 135$ K; it occurs in the [100] direction in a field of ~ 170 kOe at or below 77 K (Bolzoni, Moze, and Pareti, 1987; Kajiwara *et al.*, 1987; Kido *et al.*, 1987; Cadogan *et al.*, 1988; Verhoef *et al.*, 1988). At temperatures above 1.5 K, $Pr_2Fe_{14}B$ features no spin reorientation, but Hiroyoshi, Kato, *et al.* (1987) and Verhoef *et al.* (1988) observed FOMPs, of a kind different from that of the Nd compound, in the [100] and [110] magnetization curves at 4 K in fields of ~ 130 kOe and ~ 160 kOe, respectively. Measurements on $Er_2Fe_{14}B$ and $Tm_2Fe_{14}B$ in fields as high as 550 kOe by Kido *et al.* (1987) have revealed the onset of another type of field-dependent process, the transition from ferrimagnetism to ferromagnetism.

Although the iron sublattice anisotropy is significant, the total magnetocrystalline anisotropy in much of the ordered regime, especially from low to moderate temperatures, is dominated by the rare-earth contribution produced by the crystal-field splitting of the $4f$ shell. This statement applies to the $R_2Fe_{14}B$ systems in which the R constituent has nonzero orbital moment L (see Table V) and, hence, a nonzero crystal-field splitting in lowest approximation. The H_a values in Table IV convey the magnitudes of the R and Fe anisotropy components; for example, at room temperature, $H_a(Nd_2Fe_{14}B) \simeq 73$ kOe is a factor of 3–4 greater than the anisotropy field of $La_2Fe_{14}B$ or $Lu_2Fe_{14}B$, and the factor is much larger at 4 K. The crystal-field Hamiltonian for the rare-earth ions contains second-, fourth-, and sixth-order terms, but the overall magnetic behavior is often controlled by the second-order terms alone (see Sec. IV.D.1). In particular, the sign of those terms is set by the sign of the Stevens coefficient α_J, a quantity dependent only on the quantum numbers of the rare-earth $4f$ shell. Table VI shows that for the Pr, Sm, Tb, Dy, Er, Tm, and Yb members of the series there is perfect correspondence between the sign of α_J and the low-temperature easy direction; that is, the c axis is easy if $\alpha_J < 0$, and the magnetization resides in the basal plane if $\alpha_J > 0$. Analogous correlations obtain in many other R-TM systems (see, for examples, Buschow, 1977; Kirchmayr and Poldy, 1979). The correlation is blurred in $Nd_2Fe_{14}B$ and $Ho_2Fe_{14}B$ by the moment canting below T_s, but it correctly specifies the c axis as easy above T_s. In $Er_2Fe_{14}B$, $Tm_2Fe_{14}B$, and $Yb_2Fe_{14}B$ the change of easy direction arises from competition between the R and Fe sublattice anisotropies; the rare-earth component dictates basal-plane moments below T_s, while above T_s the iron component, which decreases less rapidly with temperature, becomes the controlling factor, and the c axis becomes easy. Such competition also occurs in $Sm_2Fe_{14}B$ because $\alpha_J(\mathrm{Sm}) > 0$, but the R anisotropy is large enough [the magnitude of α_J (Sm) is larger than for any other α_J entry in Table VI] to prevent a change of easy direction (see Cadogan *et al.*, 1987).

B. Temperature dependence of the magnetization and mean-field models

Figure 10 displays the single-crystal measurements by Hirosawa, Matsuura, *et al.* (1986) of the temperature dependence of the saturation magnetization M_s for eleven $R_2Fe_{14}B$ compounds. The samples were allowed to rotate freely in an applied field of 10 kOe, so that the magnetization along an easy direction was measured in each case. The contrast between the ferromagnetic coupling of the R and Fe moments in the light-rare-earth members of the series and the antiferromagnetic (or, equivalently, ferrimagnetic) coupling for the heavy-rare-earth compounds is apparent from the monotonic decline of M_s with increasing T for the former [Fig. 10(a)] versus the positive temperature derivative of M_s characterizing the latter over limited ranges of T [Fig. 10(b)]. Since the Fe sublattice magnetization always exceeds the R sublattice magnetization, there is no temperature at which the total magnetization vanishes for any of the ferrimagnetic materials. Such *compensation points* do occur in many other R-TM systems; Er_6Fe_{23} is a specific example (see Kirchmayr and Poldy, 1979; Herbst and Croat, 1984). In Fig. 10 the anomalous increase of M_s below ~ 150 K for $Nd_2Fe_{14}B$ and the discontinuities near 300 K for $Er_2Fe_{14}B$ and $Tm_2Fe_{14}B$ are related to the spin reorientations in those compounds.

Ignoring site dependences, three types of generic exchange interactions among the R and Fe moments are possible: R-R, R-Fe, and Fe-Fe. The T_c behavior (see Sec. IV.A.2) suggests this as the hierarchy of increasing interaction strengths in the $R_2Fe_{14}B$ materials, and the order is a general characteristic of rare-earth–transition metal intermetallics (see Kirchmayr and Poldy, 1979). The strong Fe-Fe interactions proceed from direct exchange resulting from $3d$ wave-function overlap, while the R-Fe exchange is indirect and likely mediated for the most part by the rare-earth $5d$ states as discussed in Sec. IV.A.1. Atomic calculations (e.g., Herbst and Wilkins, 1979) show that the $4f$ radial matrix elements $\langle r \rangle_{4f}$ are less than 1 Å, quite small compared to the R-R separations in $R_2Fe_{14}B$ (> 3 Å in Table II). Hence direct exchange between R spins is negligible, and the R-R exchange can be expected to be significantly weaker than the Fe-Fe and R-Fe interactions. This point has been emphasized by many authors, including Buschow (1986a), Radwański (1986a), Belorizky *et al.* (1987), and Radwański and Franse (1987). Belorizky *et al.* (1988) have estimated the R-R interaction for several rare-earth intermetallic series from data in both the ordered state and the paramagnetic regime and concluded that the indirect R-R exchange is also very likely mediated by the rare-earth $5d$ electrons.

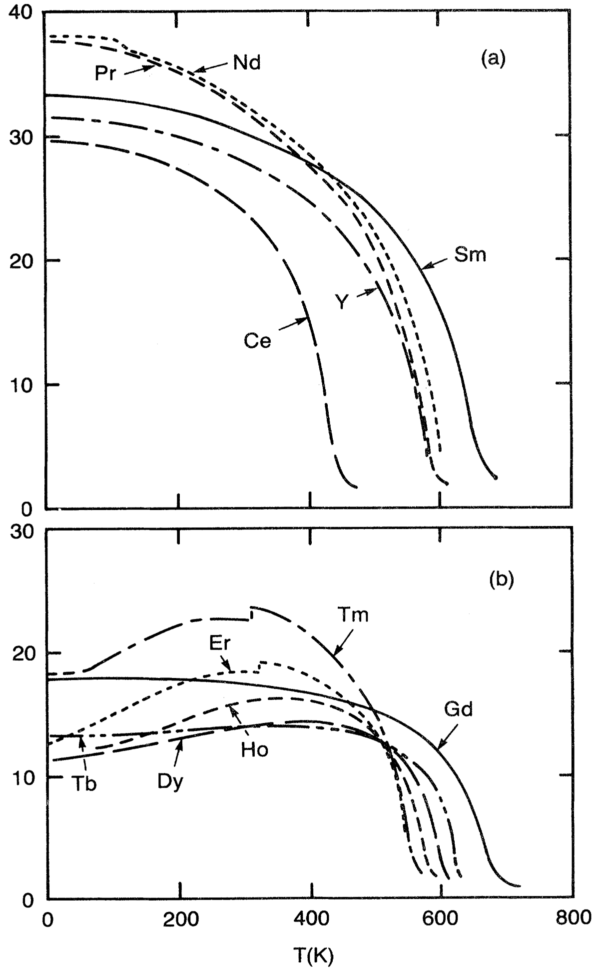

FIG. 10. Saturation magnetization M_s vs temperature T for $R_2Fe_{14}B$ compounds (adapted from Hirosawa, Matsuura, *et al.*, 1986). (a) Light rare earths (R and Fe magnetic moments ferromagnetically coupled). (b) Heavy rare earths (antiferromagnetic R-Fe coupling).

1. Molecular-field model

More specific information can be obtained by analyzing the temperature dependence of the magnetization with a phenomenological molecular-field model. In the form employed by Fuerst *et al.* (1986) and H.-S. Li, Zhang, and Dang (1988), separate molecular fields for the R and Fe components are written as

$$\mathbf{H}_R(T)=\mathbf{H}+d[2n_{RR}\mu_R(T)+14n_{RF}\mu_F(T)] , \qquad (4)$$

$$\mathbf{H}_F(T)=\mathbf{H}+d[14n_{FF}\mu_F(T)+2n_{RF}\mu_R(T)] . \qquad (5)$$

$\mathbf{H}$ is the applied field, μ_R and μ_F are the R and Fe ionic moments, and $d \equiv N_A \mu_B \rho / A$ with N_A Avogadro's number, ρ the density, and A the $R_2Fe_{14}B$ formula weight (d converts the moment per $R_2Fe_{14}B$ unit in μ_B to gauss). The molecular-field coefficients n_{RR}, n_{RF}, and n_{FF} (dimensionless as defined here) describe the R-R, R-Fe, and Fe-Fe magnetic interactions, respectively. A Brillouin function is assumed to govern the temperature dependence of each moment:

$$\mu_R(T)=\mu_R(0)B_J[\mu_B\mu_R(0)\cdot\mathbf{H}_R(T)/k_BT] , \qquad (6)$$

$$\mu_F(T)=\mu_F(0)B_{S_F}[\mu_B\mu_F(0)\cdot\mathbf{H}_F(T)/k_BT] . \qquad (7)$$

$\mu_R(0)$ and $\mu_F(0)$ are the zero-temperature moments, J is the total angular momentum of the R $4f$ shell, and S_F the Fe spin. The free-ion moment can be used for $\mu_R(0)$ ($=gJ$ in Table V), and $\mu_F(0) \equiv g_F S_F$ can be inferred from the measured low-temperature magnetization. A reasonable assumption for S_F is $S_F=1$ since $\mu_F(0) \sim 2$; moreover, available spin-resonance studies on crystalline YFe_2 and Y-Fe amorphous alloys (Bhagat *et al.*, 1979; Lloyd *et al.*, 1979) find iron gyromagnetic ratios very close to 2. $B_J(x)$ is defined in the standard way:

$$B_J(x)=\frac{2J+1}{2J}\coth\left[\frac{(2J+1)x}{2J}\right]-\frac{1}{2J}\coth\left[\frac{x}{2J}\right] , \qquad (8)$$

and the physical demand that $\mu_R(T)$ and $\mu_F(T)$ separately vanish as $T \to T_c$ leads to a relation between T_c and the molecular-field coefficients n_{AB}:

$$T_c=\tfrac{1}{2}\{\alpha n_{FF}+\beta n_{RR}+[(\alpha n_{FF}-\beta n_{RR})^2+4\alpha\beta n_{RF}^2]^{1/2}\} , \qquad (9)$$

where

$$\alpha \equiv 14\mu_F^2(0)\left[\frac{d\mu_B}{k_B}\right]\left[\frac{S_F+1}{3S_F}\right] \qquad (10)$$

and

$$\beta \equiv 2\mu_R^2(0)\left[\frac{d\mu_B}{k_B}\right]\left[\frac{J+1}{3J}\right] . \qquad (11)$$

The n_{AB} are determined by numerically solving Eqs.

(6) and (7) subject to the condition that the calculated magnetization

$$\mathbf{M}(T)=d\,[2\boldsymbol{\mu}_{\rm R}(T)+14\boldsymbol{\mu}_{\rm F}(T)] \tag{12}$$

corresponds best with experiment. For $Nd_2Fe_{14}B$, Fuerst *et al.* (1986) found good correspondence with the measured magnetization using $n_{\rm FF}\simeq 5.9\times 10^3$, $n_{\rm RF}\simeq 2.2\times 10^3$, and $n_{\rm RR}\simeq 3.3\times 10^2$, values conforming to the usual hierarchy; their results are shown in Fig. 11. The result for $n_{\rm FF}$ is basically identical to $n_{\rm FF}\simeq 6.0\times 10^3$ for elemental iron obtained from Eq. (9) in the form $T_c=\alpha n_{\rm FF}$ for one sublattice with $T_c(\mathrm{Fe})=1043$ K. H.-S. Li, Zhang, and Dang (1988) performed similar analyses for nine members of the series; although $n_{\rm FF}$ was always determined to be the largest coefficient and essentially independent of the R component, they somewhat surprisingly found $n_{\rm RR}$ and $n_{\rm RF}$ to be of the same order for the heavy-rare-earth compounds, which would suggest that R-R interactions are not negligible for those materials. In contrast, Radwański and Franse (1987) have estimated that the R contribution to the rare-earth molecular field is small compared to the iron component [i.e., $n_{\rm RR}\ll n_{\rm RF}$ in Eq. (4)], and Belorizky *et al.* (1988) have noted that in several other series $n_{\rm RR}$ declines by almost an order of magnitude from the light-R to the heavy-R compounds.

Given the proximity of the R moments to their free-ion values, use of a Brillouin function as in Eq. (6) to model $\mu_{\rm R}(T)$ is not unreasonable, even though it is rigorously justified only in the noninteracting limit. Support exists for this description in addition to the adequacy of molecular-field theory in analyzing the total moment. Bogé *et al.* (1985) isolated $\mu_{\rm Gd}(T)$ in $Gd_2Fe_{14}B$ from an appropriate difference of the $Gd_2Fe_{14}B$ and $Y_2Fe_{14}B$ magnetizations and showed that $\mu_{\rm Gd}(T)/\mu_{\rm Gd}(0)$ is well represented by $B_{7/2}[2S\mu_B H_{\rm ex}(T)/k_B T]$, where $S=\frac{7}{2}$ is the Gd spin and $H_{\rm ex}(T)$ is proportional to the non-4f component of the $Gd_2Fe_{14}B$ magnetization. Similar analyses of $\mu_{\rm R}(T)$ were conducted by Hirosawa, Matsuura, *et al.* (1986) on seven of the compounds. Berthier *et al.* (1986) extracted the temperature variation of the Dy moment in $Dy_2Fe_{14}B$ from the measured Dy hyperfine field and found it accurately described by a Brillouin form.

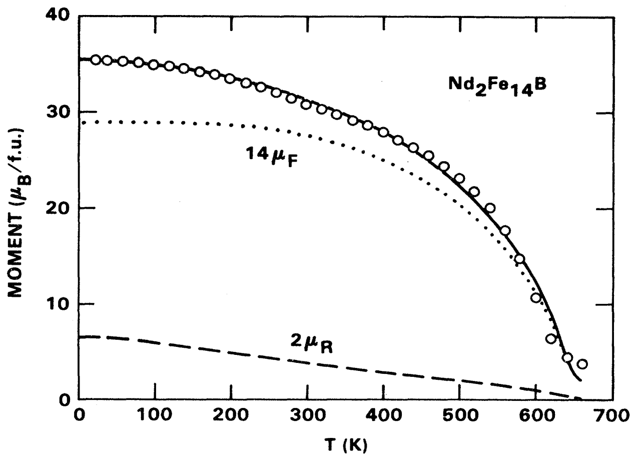

FIG. 11. Molecular-field analysis for $Nd_2Fe_{14}B$ (Fuerst *et al.*, 1986). Open circles denote the measured moment per formula unit. The solid line is the calculated total moment, which is the sum of the iron (dotted line) and neodymium (dashed line) contributions.

2. Heisenberg model and exchange energies

Exchange interaction energies j_{AB} among the R and Fe spins can be related to the molecular-field coefficients n_{AB} by exploiting the equivalence of the molecular-field model and the two-sublattice Heisenberg model in the nearest-neighbor self-consistent-field (or mean-field) approximation. In zero field the Hamiltonian for the latter can be written as

$$\mathcal{H}\equiv -2j_{\rm FF}\sum_{i<j}\mathbf{S}_{\rm F}^i\cdot\mathbf{S}_{\rm F}^j-2j_{\rm RR}\sum_{i<j}\mathbf{S}_{\rm R}^i\cdot\mathbf{S}_{\rm R}^j-2j_{\rm RF}\sum_{i<j}\mathbf{S}_{\rm R}^i\cdot\mathbf{S}_{\rm F}^j \tag{13a}$$

$$\sim -2j_{\rm FF}\sum_{i<j}\mathbf{S}_{\rm F}^i\cdot\langle\mathbf{S}_{\rm F}^j\rangle-2j_{\rm RR}\sum_{i<j}\mathbf{S}_{\rm R}^i\cdot\langle\mathbf{S}_{\rm R}^j\rangle-j_{\rm RF}\left[\sum_{i<j}\mathbf{S}_{\rm R}^i\cdot\langle\mathbf{S}_{\rm F}^j\rangle+\sum_{i<j}\mathbf{S}_{\rm F}^j\cdot\langle\mathbf{S}_{\rm R}^i\rangle\right] \tag{13b}$$

$$\sim -\sum_i\boldsymbol{\mu}_{\rm F}^i(0)\cdot\left[2\left[\frac{1}{g_{\rm F}}\right]^2 j_{\rm FF}Z_{\rm FF}\boldsymbol{\mu}_{\rm F}(T)+\frac{1}{g_{\rm F}}\left[\frac{g-1}{g}\right]j_{\rm RF}Z_{\rm FR}\boldsymbol{\mu}_{\rm R}(T)\right]$$
$$-\sum_i\boldsymbol{\mu}_{\rm R}^i(0)\cdot\left[2\left[\frac{g-1}{g}\right]^2 j_{\rm RR}Z_{\rm RR}\boldsymbol{\mu}_{\rm R}(T)+\frac{1}{g_{\rm F}}\left[\frac{g-1}{g}\right]j_{\rm RF}Z_{\rm RF}\boldsymbol{\mu}_{\rm F}(T)\right], \tag{13c}$$

where the identifications $\langle\mathbf{S}_{\rm F}^i\rangle\rightarrow-\boldsymbol{\mu}_{\rm F}(T)/g_{\rm F}$ [so that $g_{\rm F}\rightarrow\mu_{\rm F}(0)$ since $S_{\rm F}=1$ is assumed] and

$$\langle\mathbf{S}_{\rm R}^i\rangle\rightarrow\langle(g-1)\mathbf{J}\rangle=-\left[\frac{g-1}{g}\right]\boldsymbol{\mu}_{\rm R}(T)$$

have been used, and Z_{AB} is the number of B atom neighbors of atom A. Comparing Eq. (13c) to the energy

$$-\mu_B\sum_i[\boldsymbol{\mu}_{\rm F}^i(0)\cdot\mathbf{H}_{\rm F}(T)+\boldsymbol{\mu}_{\rm R}^i(0)\cdot\mathbf{H}_{\rm R}(T)]$$

in the molecular-field model yields (noting that $Z_{\mathrm{FR}}=Z_{\mathrm{RF}}/7$ is imposed by the stoichiometry)

$$j_{\mathrm{FF}}=(7d\mu_B/Z_{\mathrm{FF}})g_{\mathrm{F}}^2 n_{\mathrm{FF}} \ , \tag{14a}$$

$$j_{\mathrm{RF}}=(14d\mu_B/Z_{\mathrm{RF}})g_{\mathrm{F}}\left[\frac{g}{g-1}\right]n_{\mathrm{RF}} \ , \tag{14b}$$

$$j_{\mathrm{RR}}=(d\mu_{\mathrm{B}}/Z_{\mathrm{RR}})\left[\frac{g}{g-1}\right]^2 n_{\mathrm{RR}} \ . \tag{14c}$$

Near-neighbor counts derived from weighted averages of the entries in Table II are $Z_{\mathrm{FF}}=10.5$, $Z_{\mathrm{RF}}=16$, and $Z_{\mathrm{RR}}=2.5$.

With Eqs. (14a)–(14c), the n_{AB} estimated by Fuerst *et al.* (1986) lead to $j_{\mathrm{FF}}\sim 3.8$ meV, $j_{\mathrm{RF}}\sim -2.4$ meV, and $j_{\mathrm{RR}}\sim 0.2$ meV for $Nd_2Fe_{14}B$. The negativity of j_{RF}, which can be expected to persist throughout the series, reflects the antiferromagnetic coupling of the R and Fe *spins*; on the other hand, $n_{\mathrm{RF}}>0$ (<0) for the light- (heavy-) R compounds (cf. H.-S. Li, Zhang, and Dang, 1988). Comparable values of j_{FF} were found by H.-S. Li, Zhang, and Dang (1988). In a molecular-field analysis for $Ho_2Fe_{14}B$ neglecting j_{RR}, Fujita *et al.* (1987) obtained $j_{\mathrm{FF}}\sim 3.1$ meV and [using Eq. (14b)] $j_{\mathrm{RF}}\sim -1.8$ meV. [An effort has been made here to base j_{AB} estimates on the same Heisenberg Hamiltonian, Eq. (13), in part to avoid double-counting difficulties; the definition of j_{AB} is often unclear in the literature.]

It is also possible to extract j_{RF} estimates from Mössbauer-effect measurements on the R component. The temperature dependence of the hyperfine field at an R site may be analyzed to obtain an effective rare-earth molecular field H_m or exchange field H_{ex} from which j_{RF} can be inferred. Gubbens *et al.* (1985, 1986) reported $H_m\sim 184$ T in the zero-temperature limit for $Dy_2Fe_{14}B$; identifying $\mu_B g\mathbf{J}\cdot\mathbf{H}_m$ with the last term in Eq. (13c) leads to

$$j_{\mathrm{RF}}\sim\frac{-g\mu_B H_m}{(g-1)Z_{\mathrm{RF}}S_{\mathrm{F}}}=-2.7\text{ meV} \ , \tag{15}$$

with $Z_{\mathrm{RF}}=16$ and $S_F=1$. In analogous studies of the same compound Berthier *et al.* (1986) found $2\mu_B H_{\mathrm{ex}}/k_B\sim 385$ K; equating

$$2\mu_B\mathbf{S}\cdot\mathbf{H}_{\mathrm{ex}}=2(g-1)\mu_B\mathbf{J}\cdot\mathbf{H}_{\mathrm{ex}}$$

with the final term in Eq. (13c) yields

$$j_{\mathrm{RF}}\sim\frac{-2\mu_B H_{\mathrm{ex}}}{Z_{\mathrm{RF}}S_{\mathrm{F}}}=-2.1\text{ meV} \ . \tag{16}$$

While in fair agreement with the result [Eq. (15)] from the work of Gubbens *et al.* (1985, 1986), this value compares very well with $j_{\mathrm{RF}}\sim -2.0$ meV derived from $2\mu_B H_{\mathrm{ex}}/k_B\sim 370$ K obtained by Bogé *et al.* (1985) from magnetization measurements on $Gd_2Fe_{14}B$. Preliminary ^{174}Yb Mössbauer results on $Yb_2Fe_{14}B$ from Meyer *et al.* (1989) yield an average exchange field $\mu_B H_{\mathrm{ex}}/k_B=115$ K at the 4*f* and 4*g* Yb sites, which corresponds to $j_{\mathrm{RF}}\sim -1.2$ meV.

3. Systematics of j_{RF}

In terms of the j_{AB} the molecular-field expression for the Curie temperature, Eq. (9), becomes

$$\begin{aligned}3k_B T_c=&Z_{\mathrm{FF}}S_{\mathrm{F}}(S_{\mathrm{F}}+1)j_{\mathrm{FF}}+Z_{\mathrm{RR}}Gj_{\mathrm{RR}}\\&+\{[Z_{\mathrm{FF}}S_{\mathrm{F}}(S_{\mathrm{F}}+1)j_{\mathrm{FF}}-Z_{\mathrm{RR}}Gj_{\mathrm{RR}}]^2\\&+\tfrac{1}{7}Z_{\mathrm{RF}}^2 S_{\mathrm{F}}(S_{\mathrm{F}}+1)Gj_{\mathrm{RF}}^2\}^{1/2} \ ,\end{aligned} \tag{17}$$

where $G\equiv(g-1)^2J(J+1)$ is the de Gennes factor. This relation can be used to obtain alternative estimates of j_{FF} and j_{RF} from the measured T_c values, as Sinnema *et al.* (1984) and others have emphasized. In the absence of an R moment Eq. (17) reduces to

$$j_{\mathrm{FF}}=\frac{3k_B T_c}{2Z_{\mathrm{FF}}S_{\mathrm{F}}(S_{\mathrm{F}}+1)} \ . \tag{18}$$

With T_c(Fe)=1043 K and $T_c(La_2Fe_{14}B)=530$ K Eq. (18) yields $j_{\mathrm{FF}}(\mathrm{Fe})\sim 8.4$ meV ($Z_{\mathrm{FF}}=8$) and $j_{\mathrm{FF}}(La_2Fe_{14}B)\sim 3.2$ meV ($Z_{\mathrm{FF}}=10.5$).

If R-R interactions are neglected, Eq. (17) can be written as

$$3k_B T_c=Z_{\mathrm{FF}}S_{\mathrm{F}}(S_{\mathrm{F}}+1)j_{\mathrm{FF}}\left\{1+\left[1+\frac{1}{7}\frac{1}{S_{\mathrm{F}}(S_{\mathrm{F}}+1)}\left[\frac{Z_{\mathrm{RF}}j_{\mathrm{RF}}}{Z_{\mathrm{FF}}j_{\mathrm{FF}}}\right]^2 G\right]^{1/2}\right\} . \tag{19}$$

This equation affords some insight into possible systematic behavior of j_{RF} through the series; although the estimates obtained in Sec. IV.B.2 are broadly consistent, uncertainties in the measurements as well as the approximations used in deriving the estimates cause variances that might obscure trends. The $\sim G^{1/2}$ dependence of T_c in Eq. (19) agrees qualitatively with the T_c data displayed in Fig. 9, and the existence of two distinct curves for the light- and heavy-R compounds in Fig. 9 suggests a different j_{RF} value for each (controverting the not infrequent assertion in the literature that j_{RF} is roughly constant throughout a given series). In fact, with j_{FF} fixed at $j_{\mathrm{FF}}(La_2Fe_{14}B)\sim 3.2$ meV, least-squares fits to the T_c data based on Eq. (19) yield $j_{\mathrm{RF}}\sim -3.5$ meV for the Pr, Nd, and Sm compounds with a 2.1% average discrepancy between the observed and calculated T_c values and $j_{\mathrm{RF}}\sim -2.2$ meV for the Gd-Yb compounds with an average departure of only 0.4%. If j_{FF} is allowed to vary also, T_c of the Pr-Sm materials is fit to 0.3% using $j_{\mathrm{FF}}\sim 3.4$ meV, $j_{\mathrm{RF}}\sim -2.8$ meV; for the Gd-Yb compounds $j_{\mathrm{FF}}\sim 3.2$ meV and $j_{\mathrm{RF}}\sim -2.3$ meV lead to an average difference of 0.5% between the measured and calculated Curie temperatures. The curves in Fig. 9 represent Eq. (19) for these two sets of parameters.

This suggestion of larger j_{RF} values for the light-R versus the heavy-R compounds is consonant with results from a variety of sources. Sinnema *et al.* (1984) found the T_c data for the R=Pr, Nd, and Sm compounds to be substantially underestimated with j_{RF} held at a value providing good correspondence with the Curie temperatures of the heavy-R members of the series. In investigations of $R_2Fe_{14}B$ magnetic properties using an exchange-plus-crystal-field model (see Sec. IV.D) M. Yamada *et al.* (1988) and Zhu *et al.* (1989) needed an R-Fe exchange field a factor of approximately two larger for the light-R than for the heavy-R materials in order to accommodate experiment. F. T. Parker (1987) noted a similar contrast in estimates of the R-Fe exchange field for several members of the series, and Z. W. Zhang *et al.* (1989) found analogous differences in H_{ex} values for $Nd_2Fe_{14}B$ and $Ho_2Fe_{14}B$ needed to describe spin reorientations in their crystal-field analyses. The analyses of $\mu_R(T)$ by Hirosawa, Matsuura, *et al.* (1986) yielded n_{RF} values closely linear in $(g-1)/g$ for the heavy-R compounds, implying [according to Eq. (14b)] a single $j_{RF} \sim -2.0$ meV for them (in excellent accord with several of the estimates in Sec. IV.B.2), while their result for $Pr_2Fe_{14}B$ corresponds to $j_{RF} \sim -4.8$ meV. Using a new approach to determine crystal-field and exchange parameters, Cadogan *et al.* (1988) obtained $H_{ex}=466$ T for $Nd_2Fe_{14}B$ [corresponding to $j_{RF} \sim -3.4$ meV via Eq. (16)]; in contrast, Gavigan *et al.* (1987) and Givord, Li, *et al.* (1988) found values approximately half as large for the Tb, Dy, Ho, Er, and Tm compounds employing the same method. [H. S. Li, Gavigan, *et al.* (1988) actually specify $H_{ex}=466$ T. Both H. S. Li, Gavigan, *et al.* (1988) and Cadogan *et al.* (1988) report a molecular-field coefficient $n_{RM}=307\mu_0$ for $Nd_2Fe_{14}B$; from the definition of the exchange energy in the former reference n_{RM} is related to n_{RF} used here by $n_{RF}=4\pi[2(g-1)/g]n_{RM}/\mu_0$.] By analyzing T_c data for the $R_2Fe_{14}B$ and other series on the basis of an equation for $T_c(n_{AB})$ derived in the paramagnetic state, Belorizky *et al.* (1987) concluded that the molecular-field coefficient n_{RF} is not constant through a given series but decreases by a factor of about two from the light-R to the heavy-R compounds. The decrease is attributed to weakening of the 4*f*-5*d* exchange as the R atomic number increases, an explanation providing further support for the suggestion (Campbell, 1972) that R 5*d* states are key to the magnetic interactions involving R ions. Radwański *et al.* (1990a) reported a finding similar to that of Belorizky *et al.* (1987) for the exchange fields estimated for a number of R-TM systems from magnetization, inelastic neutron scattering, specific heat, and T_c measurements.

There is also evidence that the behavior of j_{RR} may be linked to that of j_{RF}. Cross-comparing available estimates of n_{RR} for the RAl_2 and RNi_5 materials with n_{RF} values for the RCo_2 and $R_2Fe_{14}B$ compounds, Belorizky *et al.* (1988) reach the interesting conclusion that n_{RR}/n_{RF}^2 is roughly constant through a given R-TM series. This implies via Eqs. (14b) and (14c) that j_{RR}/j_{RF}^2 is insensitive to the rare-earth component and that any variation of j_{RR} is much stronger than that of j_{RF}.

C. Fe sublattice anisotropy

For the $R_2Fe_{14}B$ phases with R=La, Ce, Lu, Y, Th (no R moment) and R=Gd (*S*-state ion having zero crystal-field splitting to first order), the magnetocrystalline anisotropy is generated by the Fe sublattice alone and selects the *c* axis as the easy direction of magnetization (Table VI). Because the magnetization curves measured along a hard direction in these $L=0$ materials are linear in the applied field (see Givord, Li, and Perrier de la Bâthie, 1984; Hirosawa, Matsuura, *et al.*, 1986), the anisotropy energy E_a may be expressed appropriately as

$$E_a=K_1\sin^2\theta , \qquad (20)$$

where θ is the angle between the magnetization vector $\mathbf{M}$ and the *c* axis. Minimization of the total magnetic energy $E=E_a-\mathbf{M}\cdot\mathbf{H}$ with respect to θ yields the following relation among K_1, the anisotropy field H_a, and the saturation magnetization M_s:

$$K_1=H_aM_s/2 . \qquad (21)$$

Estimates of K_1 at 4 K derived via Eq. (21) from the data in Table IV are listed in Table VII. The values are large relative to that of elemental Fe [cubic $K_1 \sim 0.06$ MJ/m^3 at 4 K (Bozorth, 1951)], but Givord and Li (1985) note they are not record values in comparison with cognate R-TM systems; hexagonal YCo_5, for example, features $K_1 \sim 7.4$ MJ/m^3 at low temperatures (Alameda *et al.*, 1981).

The temperature dependence of H_a and K_1 is anomalous in the $L=0$ compounds. Figure 12 displays $H_a(T)$ from the work of Grössinger, Sun, *et al.* (1986). It is evident that the anisotropy field of the Fe sublattice *maximizes* in the vicinity of $T/T_c \sim 0.6$ and so *decreases* from that point with decreasing temperature; on the other hand, M_s rises monotonically as T declines (Fig. 10).

TABLE VII. Magnetocrystalline anisotropy constant K_1 at 4 K estimated for $R_2Fe_{14}B$ compounds characterized by Fe-only anisotropy.

Compound	K_1 (MJ/m^3)
$La_2Fe_{14}B$	0.7
$Ce_2Fe_{14}B$	1.5
$Gd_2Fe_{14}B$	0.7
$Lu_2Fe_{14}B$	1.2
$Y_2Fe_{14}B$	1.1
$Th_2Fe_{14}B$	1.0

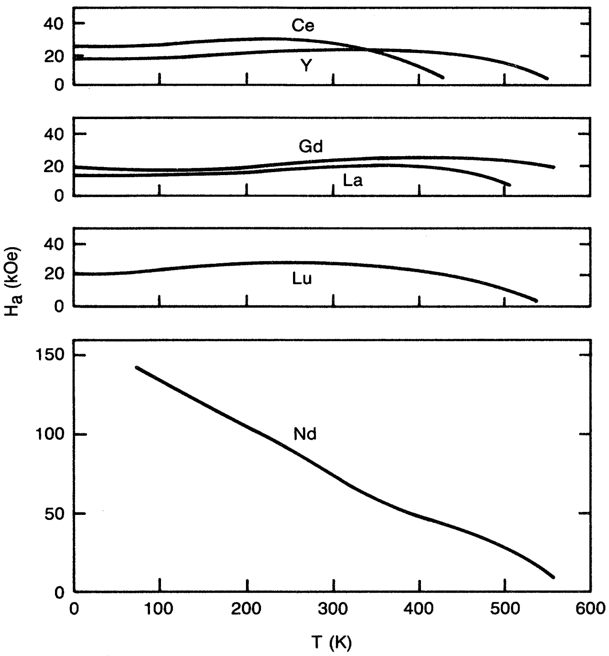

FIG. 12. Anisotropy field H_a vs temperature T in $R_2Fe_{14}B$ materials with $L=0$ (R=Ce,Y,Gd,La,Lu) and $L\neq0$ (R=Nd); after Grössinger, Sun, *et al.* (1986).

Comparison with H_a of $Nd_2Fe_{14}B$, also shown in Fig. 12, illustrates that, in contrast, the anisotropy of an $L\neq0$ rare-earth ion increases with decreasing temperature and dominates the total anisotropy at low T. Measurements of $K_1(T)$ by Givord, Li, and Perrier de la Bâthie (1984) for $Y_2Fe_{14}B$, by Bogé *et al.* (1985) for $Gd_2Fe_{14}B$, and by Hirosawa, Matsuura, *et al.* (1985, 1986) for the R=Y, Ce, and Gd compounds exhibit maxima corresponding to those in Fig. 12.

Qualitative explanations of the Fe sublattice anisotropy behavior have been proposed (cf. Givord, Li, and Perrier de la Bâthie, 1984; Hirosawa, Matsuura, *et al.*, 1985; Coey, 1986; Grössinger, Sun, *et al.*, 1986; Bolzoni, Gavigan, *et al.*, 1987). In a localized moment picture, competition among anisotropy contributions from the six crystallographically distinct Fe sites is likely. R. Fruchart *et al.* (1987) have observed anisotropy of the Fe hyperfine field in Mössbauer measurements on oriented $Y_2Fe_{14}B$ powders in a field, suggesting a small orbital component ($\lesssim 0.1\mu_B$) of the average Fe moment having opposite sign on the $k_{1,2}$ and j_2 sites. Moreover, their work on all the members of the series except $Yb_2Fe_{14}B$ indicates that the temperature variation of the k_2-site hyperfine field is more rapid than that of the k_1 and j_2 sites. Bolzoni, Gavigan, *et al.* (1987) have suggested a parallel between the $K_1(T)$ behavior and the large thermal expansion anomalies observed in these and other $R_2Fe_{14}B$ systems (Grössinger *et al.*, 1984; Andreev *et al.*, 1985; Givord, Li, *et al.*, 1985, 1986; Buschow, 1986b; Buschow and Grössinger, 1987; Cheng *et al.*, 1987; Fujii, Nagata, *et al.*, 1987; Ibarra *et al.*, 1987); the anomalies stem from magnetostrictive deformations that accompany magnetic ordering. Exploring the possibility of relating the anisotropy behavior to the magnetovolume anomaly via a single-ion crystal-field-type description [analogous to the effort of Szpunar and Lindgård (1979) on the $3d$ anisotropy in R-Co systems], Bolzoni, Gavigan, *et al.* (1987) note that the maximum in $K_1(T)$ for $Y_2Fe_{14}B$ can be simulated roughly by the temperature dependence of $M_s^3[1-\alpha(c/a)^2]$ with $\alpha=0.52$. From an extended-state viewpoint the Fe anisotropy might be attributed to band-structure effects associated with the presence of a $3d$ orbital moment and spin-orbit coupling; it would be sensitive to the Fermi-level position and its temperature variation linked to $3d$ band splitting.

Detailed quantitative understanding of the TM anisotropy in R-TM materials continues to pose a formidable challenge to theory. In addition to the subtleties of the $R_2Fe_{14}B$ compounds, many examples exist of complex variation underscoring the sensitivity to crystal and electronic structure; among them are the following. $La_2Co_{14}B$ and $Y_2Co_{14}B$ form the $R_2Fe_{14}B$ structure but show basal-plane anisotropy. $LaCo_5$ and YCo_5 are uniaxial (hexagonal c-axis easy), but the structurally related Y_2Fe_{17} and Y_2Co_{17} compounds are planar; to complicate matters further, the $Y_2(Co_xFe_{1-x})_{17}$ pseudobinary systems are uniaxial in certain ranges of Co concentration as well as temperature (Perkins and Nagel, 1975).

D. Rare-earth anisotropy and magnetic structure

It was emphasized in Sec. IV.A.3 that the magnetocrystalline anisotropy of the $R_2Fe_{14}B$ compounds whose R component has nonzero orbital moment (R=Pr, Nd, Sm, Tb, Dy, Ho, Er, Tm, Yb) is dominated by the rare-earth contribution (the Fe sublattice providing, in contrast, most of the magnetization). Considerable progress toward a detailed understanding of the anisotropy and magnetic structure has been afforded by models that treat the crystal-field splitting of the R ions together with a mean-field description of the R-Fe exchange. The underlying physics is conceptually straightforward. If $L\neq0$, the $4f$ charge distribution is aspherical [graphs of the $4f$ density in the Hund's-rule ground states have been calculated by Sievers (1982)] and thus interacts nontrivially with the crystalline electric field (CEF). Directional preferences emerge which also influence the R moment alignment because the $4f$ spin-orbit coupling is strong (leading to a well defined total angular momentum **J** and associated magnetic moment $-g\mathbf{J}$ in the ground state). On the other hand, the large Fe-Fe exchange interactions couple the six distinct Fe moments to form a single overall Fe magnetization, and Eq. (20) adequately represents the Fe anisotropy. Insofar as R-R exchange can be neglected, a simplification that appears quite reasonable, it can thus be expected that the magnetic behavior of the $R_2Fe_{14}B$ systems arises primarily from the interplay of the rare-earth CEF and the R-Fe exchange interactions, which, at least in first approximation, can be described by an effective R-Fe exchange field of the kind discussed in Sec. IV.B.1. A useful heuristic discussion of the origin of the rare-earth anisotropy in $Nd_2Fe_{14}B$ has been given by Gavigan and Givord (1990) in terms of energy-level diagrams for the Nd ions interacting with crystal and exchange fields. Exchange-plus-CEF models have been of considerable value in elucidating anisotropy and magnetization phenomena in many other R-TM materials; examples are RCo_5 (Greedan and Rao, 1973; Buschow *et al.*, 1974; Sankar *et al.*, 1975; Radwański, 1986b), RFe_2 (van Diepen *et al.*, 1973; Atzmony and Dariel, 1976; Shimotomai *et al.*, 1980), and $Sm_2(Co_{1-x}M_x)_{17}$ with M=Fe,Mn,Cr (Perkins and Strässler, 1977a, 1977b).

1. Crystal-field Hamiltonian

Although two crystallographically inequivalent R sites (f,g) exist in the tetragonal $R_2Fe_{14}B$ structure, the CEF acting on each R ion has orthorhombic (mm) point symmetry and differs for ions residing on the basal $(z=0)$ or midplanes $(z=\frac{1}{2})$ of Fig. 2. Consequently, four R sites must be considered in constructing the CEF Hamiltonian (cf. Honma *et al.*, 1985; Adam *et al.*, 1986; Cadogan *et al.*, 1988; Radwański and Franse, 1988; M. Yamada *et al.*, 1988). Using the coordinate system $x\|[100]$, $y\|[010]$, $z\|[001]\|c$ and notation of M. Yamada *et al.* (1988), in which $i=1,2,3,4$ denotes f_1, f_2, g_1, g_2, respectively [the subscript 1 (2) pertaining to the $z=0$ $(z=\frac{1}{2})$ plane], we find that the CEF Hamiltonian of each R ion within the lowest J multiplet has the form

$$\begin{aligned}\mathcal{H}_{\mathrm{CEF}}(i)=&\sum_{n,m} B_n^m(i)O_n^m\\ =&B_2^0(i)O_2^0+B_2^{-2}(i)O_2^{-2}\\ &+B_4^0(i)O_4^0+B_4^{-2}(i)O_4^{-2}+B_4^4(i)O_4^4\\ &+B_6^0(i)O_6^0+B_6^{-2}(i)O_6^{-2}+B_6^4(i)O_6^4\\ &+B_6^{-6}(i)O_6^{-6}\ .\end{aligned} \tag{22}$$

Here the B_n^m are given by

$$B_n^m=\theta_J^n\langle r^n\rangle A_n^m\ , \tag{23}$$

where θ_J^n is the Stevens factor (α_J, β_J, γ_J for $n=2,4,6$, respectively), $\langle r^n\rangle$ is the r^n radial matrix element for the $4f$ shell, and the A_n^m are coefficients of the spherical harmonics of the CEF. The O_n^m are operator equivalents (see, for example, Stevens, 1952; Hutchings, 1964): $O_2^0\equiv 3J_z^2-J(J+1)$, $O_2^{-2}\equiv J_xJ_y+J_yJ_x$, and so on. The crystal symmetry imposes the following relations between coefficients:

$$B_n^{4k}(i+1)=B_n^{4k}(i)\quad (k=0,1;\ i=1,3)\ , \tag{24a}$$

$$B_n^{-2k}(i+1)=-B_n^{-2k}(i)\quad (k=1,3;\ i=1,3)\ , \tag{24b}$$

so that the total CEF Hamiltonian

$$\mathcal{H}_{\mathrm{CEF}}=\sum_{i=1}^{4}\mathcal{H}_{\mathrm{CEF}}(i) \tag{25}$$

contains different parameters (18 in all) only for one f and one g site. With the quantization axis along a direction specified by (θ,ϕ), the anisotropy energy per ion is identified as a diagonal matrix element of $\mathcal{H}_{\mathrm{CEF}}$ (M. Yamada *et al.*, 1988):

$$E_a(\theta,\phi)=\langle JM=\mp J|\mathcal{H}_{\mathrm{CEF}}|JM=\mp J\rangle/4-\text{const} \tag{26a}$$

$$\begin{aligned}&=K_1\sin^2\theta+K_2\sin^4\theta+K_3\sin^4\theta\cos4\phi\\ &\quad+K_4\sin^6\theta+K_5\sin^6\theta\cos4\phi\ .\end{aligned} \tag{26b}$$

In this expression + applies to a heavy and − to a light rare earth,

$$K_1=-3f_2\bar{B}_2^0-40f_4\bar{B}_4^0-168f_6\bar{B}_6^0\ , \tag{27a}$$

$$K_2=35f_4\bar{B}_4^0+378f_6\bar{B}_6^0\ , \tag{27b}$$

$$K_3=f_4\bar{B}_4^4+10f_6\bar{B}_6^4\ , \tag{27c}$$

$$K_4=-231f_6\bar{B}_6^0\ , \tag{27d}$$

$$K_5=-11f_6\bar{B}_6^4\ ; \tag{27e}$$

$$f_2=J(J-\tfrac{1}{2})\ , \tag{28a}$$

$$f_4=f_2(J-1)(J-\tfrac{3}{2})\ , \tag{28b}$$

$$f_6=f_4(J-2)(J-\tfrac{5}{2})\ ; \tag{28c}$$

and

$$\bar{B}_n^m\equiv\tfrac{1}{2}[B_n^m(f)+B_n^m(g)]\ . \tag{29}$$

Equation (26b) is frequently employed to analyze measurements; its terms correspond to the phenomenological expansion for the anisotropy energy of a rigidly collinear moment in a tetragonal crystal. Note that the $B_n^{-|m|}$ coefficients cancel pairwise in $E_a(\theta,\phi)$ owing to Eqs. (24), *but their absence and the validity of Eq. (26b) are assured only in the strong exchange limit when all R and Fe moments are collinear* (see Sec. IV.D.2).

Estimates of the CEF parameters have been obtained within the point-charge model, in which the A_n^m of Eq. (23) are given by lattice sums over a distribution of point charges on neighboring sites. Calculations of this kind have been performed by a number of authors, including Cadogan and Coey (1984), Givord, Li, and Perrier de la Bâthie (1984), Honma *et al.* (1985), H. Oesterreicher (1985a), H. Szymczak (1985), M. Yamada *et al.* (1985, 1988), Abache and Oesterreicher (1986b), Adam *et al.* (1986), Buschow (1986a), Friedt *et al.* (1986), Cadogan *et al.* (1988), and Zhong and Ching (1988, 1989). The point-charge model is afflicted with shortcomings in principle, such as ambiguity in the choice of charges and difficulty in describing conduction-electron contributions [see Schmitt (1979a, 1979b) and references therein for a discussion of the latter], as well as in practice, such as uncertainties in the convergence of the lattice sums [especially for the $n=6$ terms, as Zhong and Ching (1989) indicate]. With the usual assumption of a set of charges external to the R site in question, therefore, quantitatively accurate results cannot be anticipated, but the point-charge model has provided useful qualitative information. In particular, it demonstrates that among the B_n^m the $n=2$ terms are largest. This means that B_2^0 controls the sign of K_1 [see Eq. (27a)], which often determines the anisotropy preference (easy *c* axis or basal plane). Positive charges on the R neighbors alone lead to $A_2^0(f)$, $A_2^0(g)>0$, implying $K_1>0$ (<0) if $\theta_J^2 \equiv \alpha_J <0$ (>0) [cf. Eqs. (23), (26b), (27a)]. That is, based on the R anisotropy originating from the crystal-field splitting of the 4*f* shell, the $R_2Fe_{14}B$ compounds having an oblate 4*f* charge distribution (R = Pr, Nd, Tb, Dy, Ho) are predicted to be *c*-axis easy, while those having prolate 4*f* charge (R = Sm, Er, Tm, Yb) should exhibit basal-plane anisotropy. This is in overall accord with experiment (above T_s for $Nd_2Fe_{14}B$, $Ho_2Fe_{14}B$ and below T_s for $Er_2Fe_{14}B$, $Tm_2Fe_{14}B$, $Yb_2Fe_{14}B$, as described in Sec. IV.A.3). Givord, Li, and Perrier de la Bâthie (1984) have shown that analogous considerations for the RCo_5 series yield signs of A_2^0 opposite to those in $R_2Fe_{14}B$, also in agreement with the observed anisotropy behavior.

More realistic calculation of CEF parameters must be based on electronic structure work, and progress in this regard is being made (see also Sec. V). Zhong and Ching (1988, 1989) have computed the B_n^m for $Nd_2Fe_{14}B$ by explicitly treating the intrasite environmental charge penetration neglected in the conventional point-charge model. The point-charge model is employed for intersite contributions, but with effective charges derived from a band calculation. The charges depart substantially from the choices made by others in applying the point-charge

TABLE VIII. Crystal-field and exchange parameters for $Nd_2Fe_{14}B$. All entries in K.

		Reference						
		a	b	c	d	e	f	g
B_2^0	*f*	-3.77	-1.90	-2.2	-1.93	-1.6	-2.36	-4.94
	g	-2.85	-1.90	-2.2	-1.93	-1.6	-2.36	-4.87
B_2^{-2}	*f*	-1.45	2.92	4.3			4.53	9.70
	g	1.26	2.92	1.4			-1.46	3.21
B_4^0	*f*	0.0215	0.00860	0.0107	0.025	0.011	0.0135	
	g	0.0181	0.00860	0.0123	0.025	0.011	0.0135	
B_4^{-2}	*f*	0.0504						
	g	0.0631						
B_4^4	*f*	0.0140		0.0344			-0.0033	
	g	-0.0192		-0.0367			-0.0033	
B_6^0	*f*	-0.0176	0.000866	0.00125		0.0012	0.00166	
	g	-0.00250	0.000866	0.00125		0.0012	0.00166	
B_6^{-2}	*f*	0.315	-0.00461					
	g	0.0866	-0.00461					
B_6^4	*f*	-0.0234	0.00749	0.00722			0.0069	
	g	-0.0700	0.00749	0.0189			0.0069	
B_6^{-6}	*f*	-0.0206						
	g	-0.242						
$\mu_B H_{ex}(T=0)/k_B$			350	313^h	323	310	313	

[a] Zhong and Ching (1989).
[b] M. Yamada *et al.* (1988).
[c] Cadogan *et al.* (1988).
[d] F. T. Parker (1987).
[e] Zhao and Jin (1987).
[f] Radwański and Franse (1989).
[g] Bogé *et al.* (1985, 1986) as cited by Cadogan *et al.* (1988).
[h] H. S. Li, Gavigan, *et al.* (1988).

model; interestingly, the boron charge, most often assumed positive elsewhere, is found to be negative, in agreement with a suggestion made by Buschow (1986a) based on electronegativity arguments. Compared to point-charge results the calculated CEF parameters are in much better accord with values inferred from experiments (cf. Table VIII). Coehoorn (1991) has obtained the major, valence charge component of A_2^0 from self-consistent electronic structure calculations for $Gd_2Fe_{14}B$.

2. R-Fe exchange

With the assumption that R-Fe exchange interactions can be subsumed into an effective exchange field $\mathbf{H}_{\mathrm{ex}}$ acting on the rare-earth spins, the Hamiltonian for an R ion in an applied field $\mathbf{H}$ becomes

$$\mathcal{H}_{\mathrm{R}}(i)=\mathcal{H}_{\mathrm{CEF}}(i)+2(g-1)\mathbf{J}\cdot\mathbf{H}_{\mathrm{ex}}+g\mathbf{J}\cdot\mathbf{H} \ . \tag{30}$$

Written this way, $\mathbf{H}_{\mathrm{ex}}$ is taken to be parallel to the Fe spin, i.e., antiparallel to the Fe moment. In zero field and in the limit of strong exchange, $H_{\mathrm{ex}}\rightarrow\infty$, it is clear that all R and Fe moments will be collinear. Equation (26b) then applies, and the anisotropy parameters K_i can be expressed analytically in terms of the B_n^m [Eqs. (27)] and are dependent only on the temperature through thermal averages $\langle O_n^m \rangle$ of the operator equivalents. At low temperatures $\langle O_n^m \rangle$ varies as the $n(n+1)/2$ power of the R sublattice magnetization (Callen and Callen, 1966); consequently, the importance of higher-order CEF terms to the anisotropy increases with decreasing temperature, as Givord and Li (1985) and Coey (1986, 1987) have emphasized.

Although the exchange energy is larger than the crystal-field energy in the $R_2Fe_{14}B$ compounds (the exchange is evidently great enough to ensure that the R moments are near their free-ion values), the two are of the same order of magnitude. In considering the R anisotropy Radwański and Franse (1987, 1988) assessed the relative importance of the two contributions for each member of the series by comparing estimates of the overall crystal-field splitting $\Delta E_{\mathrm{CF}} \sim 3|B_2^0|J^2$ and the total exchange splitting $\Delta E_{\mathrm{EF}} \sim 4|g-1|JH_{\mathrm{ex}}$; they found each to be of order $\sim 10^2$ K and $\Delta E_{\mathrm{CF}}/\Delta E_{\mathrm{EF}} \sim 0.1-1$. This fact has important physical consequences (see Asti *et al.*, 1987; Coey, 1987; Fujita *et al.*, 1987; Sagawa, Hirosawa, *et al.*, 1987d; M. Yamada *et al.*, 1988). The CEF can admix other $|JM\rangle$ eigenfunctions into the ground state, noncollinear R and Fe moment arrangements can develop, and the saturation magnetization may be anisotropic (Figure 10 shows this to be the case for $Er_2Fe_{14}B$ and $Tm_2Fe_{14}B$ as the easy direction changes through T_s). If $\alpha_J > 0$ and the $n=2$ terms dominate the CEF, for example, the four R moments can be expected to form a fan structure with each having a [110] or [110] component via matrix elements of $B_2^{-2}(i)$ but with the total magnetization in the [100] direction (see M. Yamada *et al.*, 1988). Moreover, the K_i can no longer be specified analytically as functions of the B_n^m and can acquire substantial field dependence. Such field sensitivity is evident in the K_i determined by O. Yamada *et al.* (1987) and Ono *et al.* (1986, 1987) from torque measurements on $Nd_2Fe_{14}B$ using Eq. (26b), while Bolzoni, Moze, and Pareti (1987) experienced difficulty in choosing K_i to reproduce $Nd_2Fe_{14}B$ magnetization curves in the canted-moment regime (see also Nakagawa *et al.*, 1989). Caution must therefore be exercised in interpreting anisotropy "constants" obtained from conventional analyses of magnetization data when noncollinear moment configurations are possible [see also Asti *et al.* (1987), Radwański and Franse (1987, 1988), Radwański *et al.* (1987), and Zhao *et al.* (1990) with regard to this issue for $R_2Fe_{14}B$ and other R-TM materials], and the B_n^m are more properly regarded as the intrinsic quantities governing the rare-earth anisotropy in the $L\neq0$ $R_2Fe_{14}B$ systems.

3. Model calculations and analyses

Various forms of the crystal-field-plus-exchange model have been applied to the $R_2Fe_{14}B$ compounds by many investigators (e.g., Boltich and Wallace, 1985; Honma *et al.*, 1985; M. Yamada *et al.*, 1985, 1987, 1988; Sankar and Narasimhan, 1986; Boltich *et al.*, 1987a; Cadogan, 1987, 1988; Cadogan *et al.*, 1987, 1988; Gavigan *et al.*, 1987; Hiroyoshi, Kato, *et al.*, 1987; F. T. Parker, 1987; Radwański and Franse, 1987, 1988, 1989; Vasquez and Sanchez, 1987; Zhao and Jin, 1987; Boltich, 1988a, 1988b; Gavigan, Li, *et al.*, 1988a; Givord, Li, *et al.*, 1988; Takano *et al.*, 1988; Zhao *et al.*, 1988, 1989, 1990; Luong *et al.*, 1989; Z. W. Zhang *et al.*, 1989, 1990; Zhu *et al.*, 1989; Deruelle *et al.*, 1990; Kou *et al.*, 1990b; H.-S. Li *et al.*, 1990; Nakagawa *et al.*, 1990; Radwański *et al.*, 1990b). These efforts, phenomenological in the sense that their aim is to determine the parameters in Eq. (30) capable of explaining experimental results, collectively demonstrate that the model contains most of the basic physics responsible for the rare-earth anisotropy and magnetic structure of the $R_2Fe_{14}B$ systems.

Treating only the B_2^0 and B_4^0 terms in Eq. (30), Boltich and Wallace (1985) found that the existence of a spin reorientation in $Nd_2Fe_{14}B$ and the absence of such a transition in $Pr_2Fe_{14}B$ could be explained with reasonable parameter ranges. Their work showed that $n>2$ CEF terms, rather than anisotropy competition between f and g sites, control the moment canting. The result is qualitatively consistent with the fact that $|\alpha_J|$ for Nd^{3+} is smallest among the values for the light rare earths (as is the case for $|\alpha_J|$ of Ho^{3+} among the heavy-R ions), enabling higher-order CEF terms to have more impact on the anisotropy (see also H. Oesterreicher, 1985a; Abache and Oesterreicher, 1986b; R. Fruchart *et al.*, 1987; Onodera, Yamauchi, *et al.*, 1987). F. T. Parker (1987) in fact demonstrated that the temperature dependence of the canting angle Θ in $Nd_2Fe_{14}B$ can be approximated very well as a function of the ratio $B_4^0\langle O_4^0\rangle/B_2^0\langle O_2^0\rangle$; Zhao and Jin (1987) calculated $\Theta(T)$ using B_6^0 as well as B_2^0 and B_4^0 terms. Sousa *et al.* (1990) measured the electrical resistivity $\rho(T)$ of an $Nd_2Fe_{14}B$ single crystal and found that the peak observed in $d\rho/dT$ at 75 K could be reproduced by a two-level crystal-field expression with a splitting $\Delta=210$ K between the lowest Nd levels, in satisfactory agreement with the exchange splitting $\Delta\sim290$ K from the theoretical work of Boltich and Wallace (1985), F. T. Parker (1987), and Z. W. Zhang *et al.* (1989).

Unquestionably the most comprehensive investigation of all nine $L\neq0$ $R_2Fe_{14}B$ compounds within the CEF-plus-exchange framework has been that of M. Yamada *et al.* (1988), who used the system Hamiltonian

$$\mathcal{H}=\sum_{i=1}^{4}\mathcal{H}_R(i)+28K_1^{Fe}(T)\sin^2\theta-28\mu_F(T)\cdot\mathbf{H}\qquad(31)$$

with $\mathcal{H}_R(i)$ specified by Eq. (30) to calculate magnetization curves and derive magnetic structures. The Fe anisotropy constant $K_1^{Fe}(T)$ and moment $\mu_F(T)$ were taken to have the same temperature dependence (scaled to T_c) as in $Y_2Fe_{14}B$. M. Yamada *et al.* (1988) found good accommodation of experiment for the heavy-R materials by analyzing $\mathcal{H}_R(i)$ within the ground-state J multiplet. Except for $Ho_2Fe_{14}B$ the results could be reproduced well with only the B_2^0 and B_2^{-2} CEF parameters. The spin-reorientation temperatures calculated for $Ho_2Fe_{14}B$ and $Er_2Fe_{14}B$ are in excellent agreement with measured values, while those for $Tm_2Fe_{14}B$ and especially $Yb_2Fe_{14}B$ exceed experiment. Fascinating [100] and [110] FOMPs associated with an abrupt transition from ferrimagnetic to ferromagnetic order are predicted for $Tm_2Fe_{14}B$; incipient stages of such a transition have been observed by Hiroyoshi *et al.* (1986) and Kido *et al.* (1987). Excited multiplets were discovered to have appreciable impact on the results for the light-R compounds, for which the generalization

$$\mathcal{H}_R(i)=\lambda\mathbf{L}\cdot\mathbf{S}+\mathcal{H}_{CEF}(i)+2\mathbf{S}\cdot\mathbf{H}_{ex}+(\mathbf{L}+2\mathbf{S})\cdot\mathbf{H}\qquad(32)$$

of Eq. (30) with λ the R spin-orbit coupling constant was also employed. When $J=\frac{7}{2}$ and $J=\frac{9}{2}$ states are considered in addition to the $J=\frac{5}{2}$ Hund's-rule ground state, a ferro-ferrimagnetic transition in $Sm_2Fe_{14}B$ is predicted to occur with increasing temperature. Comparisons made by M. Yamada *et al.* (1988) of theoretical and experimental magnetization curves at 4 K and 290 K for $Pr_2Fe_{14}B$ and $Nd_2Fe_{14}B$ are shown in Fig. 13. Solid lines represent calculations in which the $J=4$ ($J=\frac{9}{2}$) ground and $J=5$ ($J=\frac{11}{2}$) excited multiplets are included for the Pr (Nd) compound; dashed lines correspond to the ground multiplet alone. The effect of the excited state is particularly apparent in the 4-K $Pr_2Fe_{14}B$ results in fields where FOMPs are observed by Hiroyoshi, Kato, *et al.* (1987) and Verhoef *et al.* (1988). The calculated $Nd_2Fe_{14}B$ equilibrium spin structure below $T_s^{calc}=130$ K ($T_s^{expt}=135$ K in Table VI) is slightly noncollinear with all moments in the $(1\bar{1}0)$ plane.

Cadogan *et al.* (1988) developed a new method for determining CEF and exchange parameters, which was applied initially to $Nd_2Fe_{14}B$ and subsequently to the Tb, Dy, Ho, Er, Tm compounds (Gavigan *et al.*, 1987; Givord, Li, *et al.*, 1988) and to the Pr and Yb members of the series (Gavigan, Li, *et al.*, 1988a). Principally designed to reduce the amount of iterative computing, the technique relies on comparison of calculated anisotropy constants with those deduced from experimental magnetization curves. Each compound is described by two coupled equations:

$$\mathcal{H}_R(i)=\mathcal{H}_{CEF}(i)-\boldsymbol{\mu}_R(T)\cdot[n_{RF}\boldsymbol{\mu}_F(T)+\mathbf{H}]\ ,\qquad(33a)$$

$$E_{Fe}=K_1^{Fe}(T)\sin^2\theta-\boldsymbol{\mu}_F(T)\cdot[n_{RF}\boldsymbol{\mu}_R(T)+\mathbf{H}]\ .\qquad(33b)$$

$K_1^{Fe}(T)$ and $\mu_F(T)$ are specified by measurements on $Y_2Fe_{14}B$, the molecular-field coefficient n_{RF} is derived by fitting the observed spontaneous magnetization, and different f- and g-site CEF parameters are allowed (a distinction often neglected in other investigations). A basic contrast with the work of M. Yamada *et al.* (1985, 1987, 1988) is the inclusion of the $n_{RF}\boldsymbol{\mu}_R(T)\cdot\boldsymbol{\mu}_F(T)$ term in Eq. (33b), which does not appear in Eq. (31); the effect of that

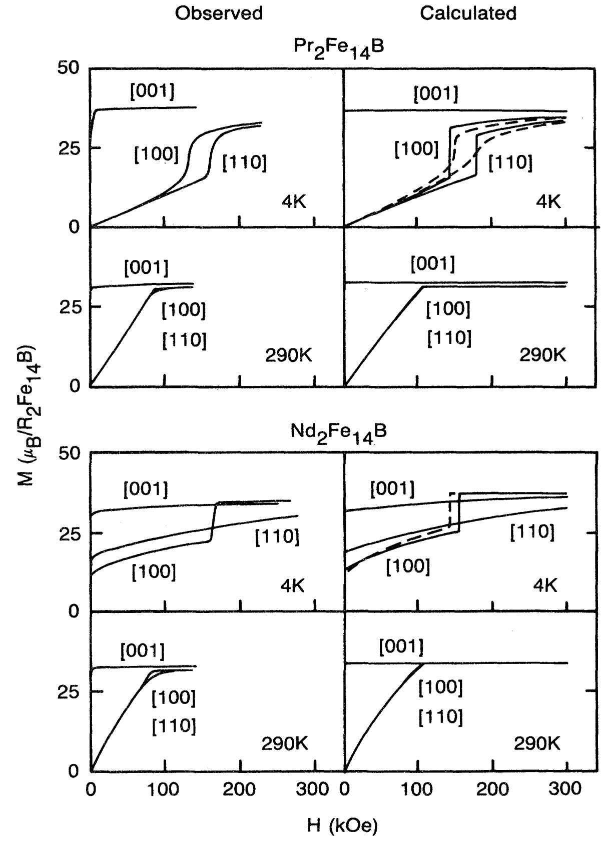

FIG. 13. Observed and calculated 4 K and 290 K magnetization curves for $Pr_2Fe_{14}B$ and $Nd_2Fe_{14}B$ adapted from M. Yamada *et al.* (1988).

term on the B_n^m values has been examined by Cadogan (1987) in a treatment of the noncollinear magnetic structure of $Tm_2Fe_{14}B$ observed and analyzed via Eq. (31) by M. Yamada *et al.* (1985). Overall, the new approach successfully describes the compounds to which it has been applied. In the case of $Nd_2Fe_{14}B$, for example, Cadogan *et al.* (1988) found the FOMP to be reproduced well and $T_s^{\rm calc}=138$ K. The calculated 4-K moment arrangement, shown in Fig. 14, is similar to that derived by M. Yamada *et al.* (1988). Each Nd moment in Fig. 14 deviates by at most 3° from the Fe magnetization; on the basis of more recent ^{145}Nd Mössbauer-effect measurements Nowik *et al.* (1990) have concluded that the total Nd moment is canted by an angle $\sim 7°$ larger than that of the Fe moment at 4 K. Imperfections of the method have been noted by its practitioners. An *ad hoc* 15% reduction of the $Nd_2Fe_{14}B$ parameters, determined in the low-temperature regime, was necessary to improve agreement with experiment above 150 K (Cadogan *et al.*, 1988), and the prediction of the 4-K easy direction in $Er_2Fe_{14}B$ is apparently incorrect (Gavigan *et al.*, 1987). Part of the difficulty may originate in the use of Eq. (26b) to obtain anisotropy parameters during the course of the procedures.

In applying the method to $Pr_2Fe_{14}B$ and $Yb_2Fe_{14}B$, Gavigan, Li, *et al.* (1988a) found second-order CEF terms $\sim 50\%$ smaller than those for the other compounds and attributed the reduction to incipient valence instability of the Pr and Yb ions. This attribution, as well as a related suggestion regarding anomalous Pr valence behavior in the $Pr_2Fe_{14-x}Co_xB$ system (Gavigan, Li, *et al.*, 1988b), points to a need for measurements such as R core-level x-ray absorption or photoemission to determine if $4f$ configurations other than the trivalent $4f^2$ (Pr) and $4f^{13}$ (Yb) are present in these materials.

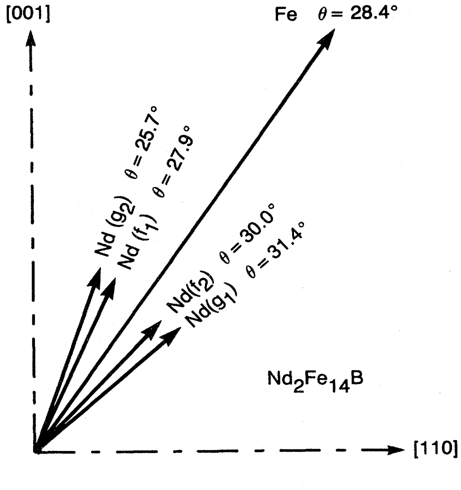

FIG. 14. Schematic diagram of calculated $Nd_2Fe_{14}B$ magnetic structure at 4 K after Cadogan *et al.* (1988). All moments reside in the $(1\bar{1}0)$ plane. Subscript 1 (2) designates the $z=0$ $(z=\frac{1}{2})$ plane.

Given the parameter freedom afforded by a crystal-field–exchange model, it is not surprising that application under various simplifying conditions (neglect of f-g site dependences and/or excited multiplets, restriction of the number of B_n^m terms in the CEF, constraint of certain ratios to point-charge results, etc.) leads to differences in the parameters emerging from the analyses despite, in many instances, comparable success in simulating magnetization data. This point is illustrated by Table VIII, which lists CEF and exchange parameters for $Nd_2Fe_{14}B$ from several investigations already mentioned in this section (a comparison of parameters determined by three groups for the $R_2Fe_{14}B$ (and $R_2Co_{14}B$) series has been made by Nakagawa *et al.*, 1990). Also included in Table VIII are the *ab initio* B_n^m calculated by Zhong and Ching (1988) as well as experimental values scaled (without a screening correction) by Cadogan *et al.* (1988) from the $Gd_2Fe_{14}B$ Mössbauer work of Bogé *et al.* (1985, 1986); $\langle r^n \rangle$ from Freeman and Watson (1962) were used to convert the A_n^m reported by M. Yamada *et al.* (1988) to B_n^m in the table. Deviations among sets of results are obvious. The situation might be ameliorated somewhat by careful investigation of systematics; Zhao *et al.* (1989, 1990) and Givord, Li, *et al.* (1988), using the methods of M. Yamada *et al.* (1988) and Cadogan *et al.* (1988), respectively, have discussed variation of the A_n^m with rare-earth constituent for the heavy-R compounds. More definitive parameter evaluation, however, must await accurate interpretation of microscopic measurements, especially inelastic neutron diffraction. Loewenhaupt *et al.* (1988, 1990) have made initial efforts in this direction, observing magnetic excitation spectra in polycrystalline samples of nine $R_2Fe_{14}B$ compounds. Reasonable agreement of measured splittings with calculated values based on CEF-exchange model results was obtained, but significant departures regarding details of the spectra were noted.

E. Information from Mössbauer studies

While bulk measurements furnish site-averaged magnetic properties, Mössbauer spectroscopy can provide local, site-dependent information regarding magnetic moments, crystal-field parameters, and magnetic structure (particularly spin reorientations). As discussed in Sec. IV.B.2, the temperature dependence of rare-earth hyperfine fields has also yielded indirect assessments of R-Fe exchange interaction parameters. Furthermore, the contrasting signatures of different materials have made Mössbauer spectroscopy useful in phase analysis of ingot and technological R-Fe-B samples (see, for example, Friedt *et al.*, 1985, 1986; Grössinger, Hilscher, *et al.*, 1985; Kostikas *et al.*, 1985; Rotenberg *et al.*, 1985; Rosenberg, Deppe, and Stadelmaier, 1986; R. Fruchart *et al.*, 1987). Numerous Mössbauer investigations of both the R and the Fe nuclei in $R_2Fe_{14}B$ compounds have been reported. The existence of several nuclear energy levels and the presence of the two R and, especially, the six Fe sites in the $R_2Fe_{14}B$ structure complicates the analyses significantly, however, so that the results can depend sensitively on the procedures used to extract them.

1. Rare-earth nuclei

Mössbauer spectroscopy studies have been conducted with the following rare-earth isotopes: ^{145}Nd (Nowik *et al.*, 1990), ^{155}Gd (Bogé *et al.*, 1985, 1986; Buschow, de Vries, and Thiel, 1985a, 1985b; Czjzek *et al.*, 1989), ^{161}Dy (Ferreira *et al.*, 1985; Friedt *et al.*, 1985, 1986; Gubbens *et al.*, 1985, 1986; Vasquez *et al.*, 1985; Berthier *et al.*, 1986; R. Fruchart *et al.*, 1987), ^{166}Er (J. P. Sanchez *et al.*, 1986; R. Fruchart *et al.*, 1987), ^{169}Tm (Gubbens *et al.*, 1987), and ^{174}Yb (Meyer *et al.*, 1989). The opportunity for such research depends, of course, on the availability of relevant source isotopes; in particular, investigation of the Nd nuclei in $Nd_2Fe_{14}B$ by means of the ^{145}Nd resonance has been impeded by the difficulty of obtaining the ^{145}Pm source.

The magnetic hyperfine field acting on a rare-earth nucleus can be written (Buschow, 1986a; Friedt *et al.*, 1986) as

$$H_{\rm hf}(T)=H_{\rm ion}\langle\langle\Gamma_i|J_z|\Gamma_i\rangle\rangle/J+H_{\rm cep}\ , \tag{34}$$

where $H_{\rm ion}$ is a constant, free-ion value for each isotope, the outer angular brackets denote the thermal average over the exchange- and crystal-field-split states $|\Gamma_i\rangle$ of the $4f$ shell, and $H_{\rm cep}$ represents a relatively small contribution from conduction-electron polarization. $H_{\rm cep}$ can be estimated from the hyperfine fields observed in the compounds having S-state rare-earth ions. Equation (34) indicates that determination of $H_{\rm hf}(T)$ can provide information on each R moment $[\mu_R(T)\propto\langle\langle\Gamma_i|J_z|\Gamma_i\rangle\rangle]$, and $T\rightarrow 0$ results can elucidate the character of the ground state. In this way, nearly pure $J_z=J$ ground states for both R sites have been identified from Mössbauer spectra on $Dy_2Fe_{14}B$ (Friedt *et al.*, 1985, 1986; Gubbens *et al.*, 1985, 1986; Berthier *et al.*, 1986), $Er_2Fe_{14}B$ (J. P. Sanchez *et al.*, 1986), and $Tm_2Fe_{14}B$ (Gubbens *et al.*, 1987). Figure 15 displays a ^{161}Dy spectrum for $Dy_2Fe_{14}B$ from the work of Friedt *et al.* (1986). These results imply that each R moment deviates by no more than several percent from its free-ion value, amplifying the second inference made from magnetization measurements in Sec. IV.A.1.

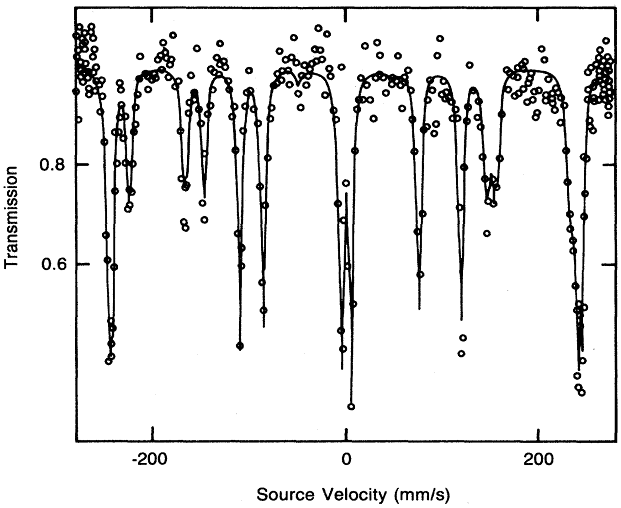

FIG. 15. ^{161}Dy Mössbauer spectrum of $Dy_2Fe_{14}B$ at 4 K; the solid line is a calculated fit to the data (adapted from Friedt *et al.*, 1986).

Interaction of the rare-earth nuclear quadrupole moment Q_R with the electric-field gradient (EFG) at the nucleus produces the quadrupole splittings observed in Mössbauer spectroscopy. The EFG is specified by a tensor, $V_{\alpha\beta}\equiv\partial^2V/\partial x_\alpha\partial x_\beta$, with V the potential at the nucleus, and the overall splitting is often expressed as $\frac{1}{2}eQ_R V_{\alpha\alpha}$, where $V_{\alpha\alpha}$ is the principal-axis component of the EFG. $V_{\alpha\alpha}$ is comprised of on-site $4f$ and surrounding lattice contributions and can be approximated (Buschow, 1986a; Friedt *et al.*, 1986) as

$$V_{\alpha\alpha}=V_{\alpha\alpha}^{4f}\frac{\langle\langle\Gamma_i|O_2^0|\Gamma_i\rangle\rangle}{J(2J-1)} +\tfrac{1}{2}V_{\alpha\alpha}^{\rm latt}(3\cos^2\xi-1+\eta_{\rm latt}\sin^2\xi\cos2\zeta)\ . \tag{35}$$

Here $V_{\alpha\alpha}^{4f}$ is a free-ion constant, $\eta_{\rm latt}=(V_{\alpha\alpha}^{\rm latt}-V_{\beta\beta}^{\rm latt})/V_{\gamma\gamma}^{\rm latt}$ is the asymmetry parameter of the lattice EFG, and ξ,ζ are the polar angles of the easy magnetization direction relative to the principal EFG axis. If $V_{\alpha\alpha}^{\rm latt}$ and $\eta_{\rm latt}$ can be obtained from fits to the Mössbauer spectra, estimates of the second-order crystal-field parameters A_2^m can be inferred from them:

$$^*A_2^0=-\frac{V_{\alpha\alpha}^{\rm latt}(1-\sigma_2)}{4(1-\gamma_\infty)}\ , \tag{36}$$

$$|^*A_2^{-2}|=\eta_{\rm latt}|^*A_2^0|\ ; \tag{37}$$

σ_2 and γ_∞ are (somewhat uncertain) atomic screening and Sternheimer antishielding factors, respectively, and the asterisk signifies that the coordinate system is that of the lattice EFG terms (Friedt *et al.*, 1986). With the use of such relations it has been established that both R ions have the same (positive) sign of A_2^0, referred to conventional crystal axes ($c\|z$), in $Gd_2Fe_{14}B$ (Bogé *et al.*, 1985, 1986), $Dy_2Fe_{14}B$ (Friedt *et al.*, 1986), and $Yb_2Fe_{14}B$ (Meyer *et al.*, 1989), a result very likely applicable to the other compounds as well. To lowest order, then, each $L\neq 0$ R ion contributes in the same manner to the R sublattice anisotropy that principally determines c-axis or basal-plane total moment orientation in the corresponding $R_2Fe_{14}B$ compound [cf. Sec. IV.D.1, especially Eqs. (23), (26b), and (27a)]. Suggestions that $B_2^0(f)$ and $B_2^0(g)$

are of opposite sign and hence contribute competitively to the magnetocrystalline anisotropy (Buschow, de Vries, and Thiel, 1985a, 1985b; Ferreira *et al.*, 1985; Gubbens *et al.*, 1987) apparently arise from ambiguity in the reference coordinates (see also Buschow, 1986a, 1988a; Price *et al.*, 1986; Rani and Kamal, 1986; Smit *et al.*, 1987).

2. ^{57}Fe investigations

Comprised of overlapping components from each of the six Fe sites, the complex ^{57}Fe Mössbauer spectra of the $R_2Fe_{14}B$ compounds have been explored by a great many investigators, including Onodera *et al.* (1984), Pinkerton and Dunham (1984, 1985), Buschow, van Noort, and de Mooij (1985), Coey *et al.* (1985), Dalmas de Réotier *et al.* (1985a), Ferreira *et al.* (1985), Friedt *et al.* (1985, 1986), Kamal and Andersson (1985), Kostikas *et al.* (1985), Rosenberg *et al.* (1985), van Noort *et al.* (1985, 1986), Vasquez *et al.* (1985), Bolzoni *et al.* (1986), Burlet *et al.* (1986), Cadogan and Coey (1986), Koon, Abe, *et al.* (1986), Ling *et al.* (1986), Price *et al.* (1986), Rani *et al.* (1986), Rani and Kamal (1986), Bocelli *et al.* (1987), Deppe *et al.* (1987), Erdmann *et al.* (1987), R. Fruchart *et al.* (1987), Fujita *et al.* (1987), Matsui *et al.* (1987), Onodera, Fujita, *et al.* (1987), Onodera, Yamauchi *et al.* (1987), Rosenberg, Deppe, *et al.* (1986), Rosenberg, Deppe, and Stadelmaier (1986), Tharp *et al.* (1987, 1988), Vasquez and Sanchez (1987), Y-C. Yang *et al.* (1987), Zeng and Yu (1987), Bara *et al.* (1988), Dai *et al.* (1988), Grandjean *et al.* (1988, 1990), Pringle, Long, *et al.* (1988), Pringle, Marasinghe, *et al.* (1988), Sano *et al.* (1989), Shi *et al.* (1989), Leccabue *et al.* (1990), and Long and Grandjean (1991). The spectra exhibit broad similarity to that for α-Fe (see Coey *et al.*, 1985) and closer resemblance to that for Nd_2Fe_{17} (Onodera *et al.*, 1984); in the easy-*c*-axis regime the shape changes little with rare-earth component (see, for example, Pinkerton and Dunham, 1985; van Noort *et al.*, 1986; R. Fruchart *et al.*, 1987). A representative example, that for $Nd_2Fe_{14}B$, is shown in Fig. 16.

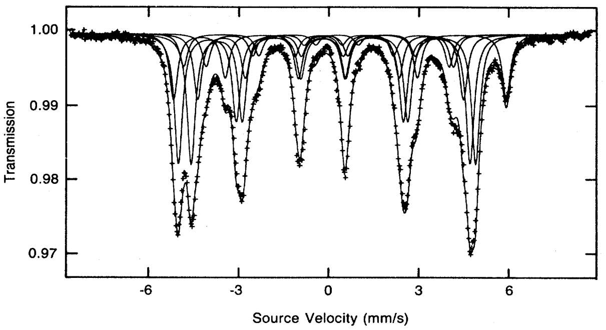

FIG. 16. Room-temperature ^{57}Fe Mössbauer spectrum of $Nd_2Fe_{14}B$ and calculated six-subspectrum fit (Grandjean *et al.*, 1988).

Unfortunately there is no unique decomposition of an observed spectrum into individual subspectra for the six iron sites, each with its own hyperfine field, quadrupole splitting, and isomer shift. To distinguish among sets of subspectra affording equally good fits to the data, most authors proceed by first imposing the reasonable condition that the intensities obey the 16:16:8:8:4:4 ratio hierarchy corresponding to the crystallographic multiplicities (Table I). It is then often assumed that, for each pair of equal-intensity subspectra, the subspectrum with the larger hyperfine field belongs to the site having the larger number of Fe nearest neighbors (R. Fruchart *et al.*, 1987). Additional constraints regarding parameters such as linewidths, EFG principal-axis directions, and isomer shifts differ in various analyses (see, for example, van Noort *et al.*, 1985, 1986; Onodera, Fujita, *et al.*, 1987; Onodera, Yamauchi, *et al.*, 1987; Grandjean *et al.*, 1988, 1990). A magnetic moment for each site can be estimated from its hyperfine field using the crucial *assumption*, based on previous observations for iron intermetallics (Buschow, 1986a), whose reliability for $R_2Fe_{14}B$ demands further scrutiny, that the two quantities are related by a single, site-independent conversion factor, $\simeq 150$ kOe/μ_B. Site moments determined by several groups for $Y_2Fe_{14}B$ and $Nd_2Fe_{14}B$ at low temperatures are listed in Table IX, which also includes results from polarized-neutron work (Givord, Li, and Tasset, 1985) and electronic structure studies (Inoue and Shimizu, 1986a; Gu and Ching, 1987a; Itoh *et al.*, 1987; Szpunar *et al.*, 1987; Jaswal, 1990; Zhong and Ching, 1990; Coehoorn, 1991). R. Fruchart *et al.* (1987) have tabulated similar comparisons for several other $R_2Fe_{14}B$ compounds as well. Since moment canting can lead to the magnetic inequivalence of crystallographically equivalent sites, Onodera, Yamauchi, *et al.* (1987) obtained the 4 K ($< T_s \simeq 135$ K) $Nd_2Fe_{14}B$ results given in Table IX by using twelve, rather than six, subspectra in analyzing their Mössbauer data; Shi *et al.* (1989) have argued that eighteen subspectra should be employed below T_s.

Table IX reflects the almost universal agreement in the literature that the $8j_2$ site, characterized by the largest number of nearest-neighbor iron atoms, carries the largest moment, and either the 4*c* or 4*e* moment is usually found to be smallest. Friedt *et al.* (1986) note that the Fe 4*f* site in Dy_2Fe_{17} (hexagonal Th_2Ni_{17} structure; $P6_3/mmc$), whose Fe coordination is similar to that of the $8j_2$ site in $Nd_2Fe_{14}B$, has also been found to feature the largest hyperfine field among the iron sites in that compound by Bara *et al.* (1982). Studies of the temperature dependence of the site-decomposed hyperfine fields in the Y, Pr, and Gd compounds (Grandjean *et al.*, 1990), above T_s in $Nd_2Fe_{14}B$ (Onodera, Yamauchi, *et al.*, 1987; Grandjean *et al.*, 1988), and throughout the magnetically ordered regime for $Ho_2Fe_{14}B$ (Fujita *et al.*, 1987) indicate that each site moment decreases uniformly with increasing temperature. Also consistent with bulk magnetization measurements is the observation, made by

Pinkerton and Dunham (1985) in work on the R=Y, Ce, Pr, Nd, Gd, Dy, and Ho compounds, that the site-averaged hyperfine fields at 295 K scale with the Curie temperature.

Mössbauer spectroscopy is well suited for identifying spin reorientations, and ^{57}Fe Mössbauer work has served usefully in confirming the results of magnetization and neutron-diffraction measurements on $Er_2Fe_{14}B$, $Tm_2Fe_{14}B$, $Yb_2Fe_{14}B$, featuring plane-to-axis transitions, and $Nd_2Fe_{14}B$, $Ho_2Fe_{14}B$, characterized by moments canting away from the c direction (see also Sec. IV.A.3). In random powder samples the variation of the spectral shape and the hyperfine parameters (especially the quadrupole splittings, which depend on the orientation of the EFG, dictated by the lattice, relative to the magnetization direction) can be monitored. Van Noort *et al.* (1986) noted qualitative changes in $Er_2Fe_{14}B$ spectra near $T_s \simeq 325$ K, and through $T_s \simeq 313$ K in $Tm_2Fe_{14}B$ Price *et al.* (1986) observed variations in the shape of the spectra and sign changes in most of the quadrupole splittings. For $Yb_2Fe_{14}B$ Burlet *et al.* (1986) reported a change in sign of the $8j_2$-site quadrupole shift and an increase in the average hyperfine field, implying some degree of magnetization anisotropy, as the temperature decreased below $T_s \simeq 115$ K. Resolving the spectrum with six subspectra above and twelve below $T_s \simeq 58$ K in $Ho_2Fe_{14}B$, Fujita *et al.* (1987) found significant changes in the quadrupole splittings and, comparing the canting angles obtained from the Mössbauer spectroscopy analyses with magnetization measurements on a single crystal, concluded that the spin reorientation proceeds via coherent rotation of antiparallel Fe and Ho moments. From their single-crystal neutron work Wolfers *et al.* (1990) have also concluded that the total Ho and Fe moments remain antiparallel below T_s, but the individual Ho moments form a complex noncollinear structure. Below T_s in $Nd_2Fe_{14}B$ Onodera, Yamauchi, *et al.* (1987) noted anomalies in the isomer shifts as well as the quadrupole splittings. A large deviation of the Nd and Fe moments from collinearity was considered responsible for differences between the canting angles determined by the Mössbauer spectroscopy work for the Fe spins and by single-crystal magnetization measurements of the total moment; noncollinearity of the Nd and Fe moments has been confirmed by the ^{145}Nd Mössbauer investigation of Nowik *et al.* (1990).

Striking changes in the spectra of single crystals or magnetically aligned powder specimens can be observed in the spin-reorientation regime by exploiting the polarization properties of the gamma radiation (cf. Vasquez *et al.*, 1985; Koon, Abe, *et al.*, 1986). The probabilities for $\Delta m=0$ and $\Delta m=\pm 1$ nuclear transitions are to first

TABLE IX. Low-temperature Fe site moments in $Y_2Fe_{14}B$ and $Nd_2Fe_{14}B$.

Compound	Fe site moment (μ_B)							
	$16k_1$	$16k_2$	$8j_1$	$8j_2$	$4e$	$4c$	T (K)	Reference
					Experiment			
$Y_2Fe_{14}B$	2.07	2.23	2.31	2.43	2.28	1.90	4	R. Fruchart *et al.* (1987)
	2.25	2.32	2.15	2.59	2.10	2.25	4	Onodera, Yamauchi, *et al.* (1987)
	2.17	2.29	2.14	2.54	2.13	2.16	4	Friedt *et al.* (1986)
	2.22	2.32	2.10	2.57	2.03	1.24	25	Van Noort *et al.* (1986)
	2.25	2.25	2.40	2.80	2.15	1.95	4	Givord, Li, and Tasset (1985)
					Theory			
	2.08	2.15	2.07	2.74	2.06	2.53	0	Jaswal (1990)
	2.11	2.31	2.22	2.51	2.40	2.10	0	Coehoorn (1991); Coehoorn *et al.* (1991)
	2.16	2.47	2.50	3.08	1.80	1.60	0	Gu and Ching (1987a)
	2.41	2.11	2.16	2.74	2.32	2.28	0	Inoue and Shimizu (1986a)
	2.36	2.62	2.35	2.61	2.11	2.31	0	Itoh *et al.* (1987)
					Experiment			
$Nd_2Fe_{14}B$	2.08	2.16	2.06	2.43	2.28	1.97	4	R. Fruchart *et al.* (1987)
	2.24	2.30	2.21	2.55	2.00	2.17	4	Onodera, Yamauchi, *et al.* (1987)
	2.27	2.41	2.19	2.70	2.20	2.10	25	Van Noort *et al.* (1986)
	2.60	2.60	2.30	2.85	2.10	2.75	4	Givord, Li, and Tasset (1985)
					Theory			
	2.15	2.18	2.12	2.74	2.13	2.59	0	Jaswal (1990)
	2.18	2.34	2.39	3.35	2.34	3.11	0	Zhong and Ching (1990) (orbital contribution included)
	2.45	2.43	2.33	2.72	2.44	2.51	0	Szpunar *et al.* (1987) (orbital contribution included)
	2.46	2.67	2.50	2.80	2.28	2.31	0	Itoh *et al.* (1987)

order proportional to $\sin^2\omega$ and $(1+\cos^2\omega)$, respectively, and the intensities of various subspectra depend differently on the angle ω between the gamma-ray wave vector and the quantization (i.e., magnetization) axis. In work on a single crystal of $Nd_2Fe_{14}B$, Koon, Abe, *et al.* (1986) demonstrated that two of the lines (the second and fifth major structures in Fig. 16), which are clearly evident below $T_s \simeq 135$ K, diminish to negligible intensity in the $\omega=0$ geometry at 300 K; the canting angles of the Fe moment determined as ω increased with decreasing $T < T_s$ were found to track the results of single-crystal magnetization experiments. Similar intensity variations have been observed on oriented powder samples of $Nd_2Fe_{14}B$ (Onodera *et al.*, 1984), $Er_2Fe_{14}B$ (Vasquez *et al.*, 1985; Friedt *et al.*, 1986), and $Ho_2Fe_{14}B$ (R. Fruchart *et al.*, 1987).

V. ELECTRONIC STRUCTURE

Several theoretical efforts probing the electronic structure of $R_2Fe_{14}B$ have been reported, the rather daunting complexity of the $Nd_2Fe_{14}B$ crystal structure (Fig. 2) notwithstanding. Calculated iron site moments in $Y_2Fe_{14}B$ and $Nd_2Fe_{14}B$ from the work of the six different groups discussed below are included in Table IX. Some experimental information on electronic structure is available as well.

Semiempirical analyses have been conducted by three sets of authors. Itoh *et al.* (1987) cursorily described a highly simplified treatment of the d bands and anisotropy contributions in $Y_2Fe_{14}B$ and $Nd_2Fe_{14}B$ using various input parameters; the results are suspect because, as Buschow (1988a) remarks, a negative K_1 for $Y_2Fe_{14}B$ is calculated, whereas the experimental value is positive (Table VII). Extending earlier studies (Szpunar and Szpunar, 1985; Szpunar, 1986, 1987), Szpunar *et al.* (1987) employed the recursion (continued-fraction) method with a number of input quantities, such as atomic energy levels and hopping integrals, to obtain approximate d bands and local densities of states (DOS) in $Nd_2Fe_{14}B$. Each iron site DOS was decomposed into spin and orbital components. The $8j_2$ site was found to have both the largest spin and the largest orbital moment, $\sim 0.1\mu_B - 0.2\mu_B$, depending on the spin-orbit splitting assumed. This value is comparable to that estimated in Mössbauer spectroscopy work on $Y_2Fe_{14}B$ (R. Fruchart *et al.*, 1987) and at the same time quite similar to the $0.09\mu_B$ orbital moment in Fe metal (Reck and Fry, 1969). The similarity of the orbital moments indicates that the huge difference in anisotropy between α-Fe and the Fe sublattice in $R_2Fe_{14}B$ arises mainly from the lower symmetry of the tetragonal as compared to the cubic structure, the latter having no second-order crystal-field terms [i.e., $B_2^m \equiv 0$ in expressions such as Eq. (22)]. Szpunar *et al.* (1987) investigated Y_2Fe_{17} (Th_2Ni_{17} structure) as well and determined that the $4f$ site, the $8j_2$ cognate, has the largest spin and orbital moments. Inoue and Shimizu (1986a) also employed tight-binding d bands and the recursion method to calculate local densities of states in $Y_2Fe_{14}B$; rigid splitting of the bands was chosen so as to reproduce the measured average Fe moment. A strong field dependence of the $4c$-site moment was predicted, and the temperature-dependent magnetic susceptibility and the high-field, zero-temperature susceptibility were estimated. The total DOS resembles that obtained in analogous work on Y_2Fe_{17} (Inoue and Shimizu, 1985); the $4f$ and $8j_2$ moments are again found to be the largest in their respective structures.

In a series of papers Ching and co-workers (Gu and Ching, 1986a, 1986b; 1987a, 1987b; Ching and Gu, 1987, 1988; Zhong and Ching, 1990) have reported the application of a first-principles technique, the orthogonalized linear combination of atomic orbitals (OLCAO) method, to the $R_2Fe_{14}B$ compounds. Their paramagnetic calculation for $Y_2Fe_{14}B$ (Gu and Ching, 1986a) was a groundbreaking investigation for these materials. Spin-polarized studies on $Y_2Fe_{14}B$ and $Nd_2Fe_{14}B$ were thereafter conducted (Gu and Ching, 1987a), $Gd_2Fe_{14}B$ was also investigated (Ching and Gu, 1988), and Fe orbital moments in $Nd_2Fe_{14}B$ ($\lesssim 0.1\ \mu_B$ and largest at the j_2 sites) were computed (Zhong and Ching, 1990). An important shortcoming of the method is that self-consistent iteration is not performed, even though R and Fe potentials are constructed so that the quality of the band structure and DOS calculated in the same way for each *elemental* metal is comparable to other self-consistent work for that metal. The results include contour maps of the charge and spin distributions in various planes in addition to total, site-, spin-, and angular momentum-projected densities of states. Figure 17 displays the calculated charge and positive spin density in the (110) plane of $Nd_2Fe_{14}B$. The $4f$ electrons are included in the charge density [Fig. 17(b)] but not in the spin-density map [Fig. 17(c)], which corresponds to the Fe sublattice alone and from which it is clear that the Fe(j_1), Fe(j_2), and Fe(e) sites constitute a strong magnetic network. With regard to the role of the trigonal prisms in stabilizing the structure, Gu and Ching (1987a) find that each boron atom forms strong multicenter bonds with the six Fe atoms comprising a prism and emphasize that the special function of the Fe(e) sites in connecting the hexagonal Fe networks across the $z=0$ and $z=\frac{1}{2}$ planes [cf. Figs. 2 and 17] is facilitated by the presence of the boron. An effective valence charge for each atom is estimated, and the $Y_2Fe_{14}B$ and $Nd_2Fe_{14}B$ results indicate charge transfer from the Fe sites into the R d bands. The extent of the transfer, as much as five (eight) electrons for Fe(Y), is unphysically large and likely symptomatic of the lack of self-consistency; its direction, however, is compatible with soft x-ray appearance potential measurements on $Nd_2Fe_{14}B$ by Chourasia and Chopra (1989), who ascribe the observed chemical shifts of the Nd M_V and Fe L_{III} levels and the increased Fe L_{III} linewidth (relative to elemental iron) to charge transfer from Fe to Nd. The total moments calculated by Gu and Ching (1987a) for $Y_2Fe_{14}B$ and $Nd_2Fe_{14}B$ (with the use of the Nd free-ion $4f$ moment in conjunction with computed polarization contributions from the bands) and that for $Gd_2Fe_{14}B$ (Ching and Gu, 1988) agree well with experiment.

Using the linear muffin-tin orbital (LMTO) method in the local-density and semirelativistic approximations, Sellmyer *et al.* (1988) and Jaswal (1990) conducted the first self-consistent spin-polarized electronic structure calculations for $Y_2Fe_{14}B$ and $Nd_2Fe_{14}B$. The exchange splitting of the Fe d bands is ~ 2.1 eV, a value comparable to results from both calculations (e.g., Calloway and Wang, 1977) and spin-polarized, angle-resolved photoemission measurements (Kisker *et al.*, 1985) on Fe metal. The computed charge transfers, <0.5 (1.5) for Fe (Nd, Y) sites, are substantially smaller than those determined by Gu and Ching (1987a). The work of Sellmyer *et al.* (1988) is also distinguished as the only published photoemission study of $R_2Fe_{14}B$ electronic structure; spectra at various photon energies on the Y, Nd, and Gd members of the series were reported. Their calculated DOS for $Y_2Fe_{14}B$ is in good overall accord with the measured spectra, which, aside from $4f$ features, are essentially independent of the rare-earth constituent.

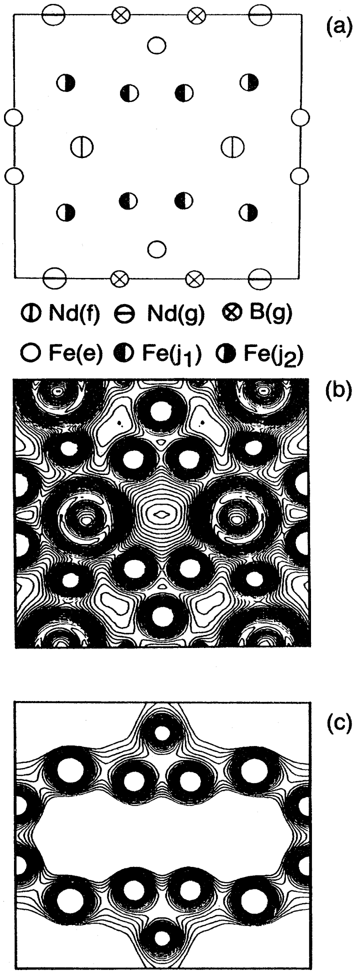

FIG. 17. Atomic sites in the (110) plane of the $Nd_2Fe_{14}B$ structure (a); calculated charge (b) and spin (c) densities in that plane for $Nd_2Fe_{14}B$ (Gu and Ching, 1987a).

The $4f$ electron binding energies measured by Sellmyer *et al.* (1988), 5.4 eV in $Nd_2Fe_{14}B$ and 8.9 eV in $Gd_2Fe_{14}B$, closely approach those calculated and observed in the corresponding elemental rare-earth metals and measured in other materials containing Nd or Gd (see Herbst and Wilkins, 1987). A relative shift of Nd and Sm $4f$ levels in $Nd_2Fe_{14}B$ and $SmCo_5$ was inferred by Cheung *et al.* (1987) from the $5s$-$4f$ transitions observed in their electron-energy-loss experiments on thin films, but such changes almost certainly arise from contrast in electronic structure rather than from the differing anisotropy fields of the two compounds as the authors speculate.

Self-consistent band-structure calculations employing the augmented spherical wave method within the local-spin-density-functional approximation have been performed for $Y_2Fe_{14}B$ and $Gd_2Fe_{14}B$ by Coehoorn (1991). In the case of $Y_2Fe_{14}B$, the densities of states and Fe site moments are in good accord with the LMTO work of Jaswal (1990); the calculated total moments are in excellent agreement with each other and with experiment. Coehoorn (1991) has also calculated (i) the site-dependent Fermi contact contribution to the hyperfine fields in $Y_2Fe_{14}B$, finding evidence for significant deviation from simple proportionality between local Fe moments and the corresponding hyperfine fields (see also Coehoorn *et al.*, 1991); (ii) the principal (valence charge) component of the second-order crystal-field parameter A_2^0 in $Gd_2Fe_{14}B$, concluding, as did Zhong and Ching (1989), that the asphericity of the valence electron density, and *not* the charge density on neighboring atoms, chiefly determines A_2^0; and (iii) the valence charge contribution to the $V_{\alpha\alpha}$ component of the electric-field gradient at the rare-earth nucleus in $Gd_2Fe_{14}B$, enabling assessment of the validity of relations such as Eq. (36) between $V_{\alpha\alpha}$ and A_2^0 (see also Coehoorn and Buschow, 1991).

Fujii, Nagata, *et al.* (1987) measured the specific heat C (and thermal expansion) of the R=Y, Nd, and Tm compounds. The low-temperature data on $Y_2Fe_{14}B$ was fit with the expression

$$C(T)=\gamma T+\beta T^3 , \tag{38}$$

and the coefficient $\gamma=86$ mJ/K^2 mol f.u. of the electronic contribution was deduced (a possible $T^{3/2}$ spin-wave contribution was neglected). The density of states at the Fermi level $N(\epsilon_F)$ follows from the standard relation

$$\gamma=\frac{\pi^2}{3}k_B^2 N(\epsilon_F) \tag{39}$$

and can be compared with the available theoretical re-

TABLE X. Calculated and experimental total densities of states at the Fermi energy, $N(\epsilon_F)$, for $Y_2Fe_{14}B$ and Fe metal.

	$N(\epsilon_F)$ (states/eV-atom)	Reference
$Y_2Fe_{14}B$		
Theory	0.86	Jaswal (1990)
	~0.8	Coehoorn (1991)
	1.88	Gu and Ching (1987a)
	1.96	Inoue and Shimizu (1986a)
Experiment	2.1	Fujii, Nagata, *et al.* (1987)
Fe		
Theory	1.1	Callaway and Wang (1977)
Experiment	2.011	Dixon *et al.* (1965)

sults. Values for $Y_2Fe_{14}B$ as well as elemental Fe are presented in Table X, from which it is clear that the experimental $N(\epsilon_F)$ of the two materials are almost identical. For $Y_2Fe_{14}B$ the $N(\epsilon_F)$ calculated by Inoue and Shimizu (1986a) and Gu and Ching (1987a) agree well with the measurements of Fujii, Nagata, *et al.* (1987), but the agreement is fortuitous. This is because the entries for Fe in Table X strongly suggest (see also Wohlfarth, 1980) that a large electron-phonon (and perhaps electron-magnon) enhancement, *not included in any of the calculations,* is also to be expected in $Y_2Fe_{14}B$. Such an enhancement would move $N(\epsilon_F)$ obtained by Jaswal (1990) and Coehoorn (1991) toward experiment and have the reverse effect on the other theoretical results.

Mohn and Wohlfarth (1987) used the $N(\epsilon_F)$ obtained by Inoue and Shimizu (1986a) for $Y_2Fe_{14}B$ to derive a theoretical estimate of the Curie temperature, $T_c(\text{calc})=575$ K, which compares exceedingly well with $T_c(\text{expt})\simeq 565$ K in Table IV, while the smaller $N(\epsilon_F)$ of Jaswal (1990) yields a T_c(calc) about twice as large (Jaswal *et al.*, 1988). The theory and the estimate of Mohn and Wohlfarth (1987) embrace a number of approximations, however, including the assumption of a Stoner exchange parameter and a Fermi degeneracy temperature for elemental iron, so that the comparison of T_c(calc) with experiment may not serve as a basis for definitively distinguishing $N(\epsilon_F)$ values from electronic structure calculations.

VI. ISOSTRUCTURAL MATERIALS AND THEIR PROPERTIES

Many other elements can replace the rare-earth, iron, or boron constituent of an $R_2Fe_{14}B$ compound without altering the $Nd_2Fe_{14}B$ structure type. This section surveys the vigorous work on such isostructural materials. In general these efforts serve the dual purpose of broadening our understanding of the properties of the $R_2Fe_{14}B$ systems and identifying substitutions that enhance intrinsic characteristics important to permanent-magnet applications. Separate subsections are devoted to the $R_2Co_{14}B$ and $R_2Fe_{14}C$ compounds, the only two series known in which either Fe or B is totally replaced by another element.

A. Rare-earth replacements

Table XI summarizes research on $R_{2-x}R'_xFe_{14}B$ materials in which the rare-earth component is replaced by another element. The studies all involve replacement by another rare earth or Y, with the exceptions of Sc substitution, which degrades both H_a and T_c (S. K. Chen *et al.*, 1988b), Zr substitution, which increases the anisotropy field H_a while reducing T_c (Jurczyk and Wallace, 1986a; since the magnetization is observed to decline in both light- and heavy-R compounds, however, Zr could be replacing Fe), and Th substitution, as a result of which there is evidence for intriguing two-stage spin reorientation in $Er_{2-x}Th_xFe_{14}B$ (Pedziwiatr and Wallace, 1986a; Pedziwiatr, Wallace, and Burzo, 1986c). X-ray (Abache and Oesterreicher, 1986b) and neutron-diffraction work (Yelon *et al.*, 1986; Moze *et al.*, 1989) indicates that an R′ substituent having a radius less than that of the R ion preferentially enters the 4*f* site, a result in accord with simple steric considerations, since the volume associated with the 4*f* site is somewhat smaller than that of the 4*g* site. Wigner-Seitz volumes of sites in various $R_2Fe_{14}B$ compounds have been computed and tabulated by Fuerst, Meisner, Pinkerton, and Yelon (1987), Pringle *et al.* (1989), and Grandjean *et al.* (1990). As Tables IV and VI suggest, Tb or Dy substitution can markedly enhance the uniaxial anisotropy of $Nd_2Fe_{14}B$, although at the expense of the saturation magnetization, because heavy-R and Fe moments are antiparallel; Pareti, Bolzoni, *et al.* (1987) have investigated the $Nd_{2-x}Tb_xFe_{14}B$ system in detail.

Much of the research catalogued in Table XI is concerned with the behavior and character of the spin reorientations, especially for those systems in which R and R′ have Stevens factors α_J of opposite sign and contribute competitively to the anisotropy (e.g., Sm, Er, or Tm replaced by Pr, Nd, Tb, or Dy). In addition to expected axial and planar configurations, canted-moment arrangements in certain concentration ranges have been identified in $Er_{2-x}Dy_xFe_{14}B$ (Ibarra, Algarabel, *et al.*, 1989), $Tm_{2-x}Dy_xFe_{14}B$ (Pourarian, Jiang, Zhang, *et al.*, 1988), $Er_{2-x}Pr_xFe_{14}B$ (Boltich *et al.*, 1987a; Boltich, 1988a, 1988b), and $Pr_{2-x}Sm_xFe_{14}B$ (C. Lin and Liu, 1986). The critical behavior in the vicinity of spin reorientations in $Er_{2-x}Dy_xFe_{14}B$ and $Er_{2-x}Nd_xFe_{14}B$ has been investigated extensively by del Moral *et al.* (1989, 1990), who have determined critical exponents with the use of a scaling model developed for the low-field ac susceptibility χ. Crystal-field-plus-exchange analyses have been performed for several systems, as Table XI documents; the basic model appears capable in principle of describing the phenomena, although specifics vary with the extent to which a particular pseudoternary compound has been probed. In the case of $Tm_{2-x}Dy_xFe_{14}B$,

TABLE XI. Summary of research on $R_{2-x}R'_xFe_{14}B$ compounds. (CFA≡crystal-field–exchange analysis; FOMP≡first-order magnetization process; MBS≡Mössbauer spectroscopy; MCA≡magnetocrystalline anisotropy; MFA≡molecular-field analysis; MPD≡magnetic phase diagram; ND≡neutron diffraction; SP≡site preference; SR≡spin reorientation; χ≡magnetic susceptibility.)

R	R′	x	Properties; methods	References
Ce	$\sim La_{0.6}Pr_{0.1}ND_{0.3}$ (mischmetal)	0.94	M, T_c, H_a,χ	Hien *et al.* (1987)
Ce, Pr, Gd, Y, Th	Er	0–2	T_s	Pedziwiatr and Wallace (1986a)
Ce, Pr, Nd, Gd, Dy, Y	Zr	0.1	a, c, M, T_c, H_a	Jurczyk and Wallace (1986a)
Pr	La, Y	0.4, 0.6	H_a, MCA, SP; ND	Moze *et al.* (1989)
Pr, Sm	Nd	0–2	M, T_s, MCA, SR	Y-C. Yang, James, *et al.* (1986a)
Pr	Nd	0–2	a, c, M, MCA, FOMP, SR	Y.-K. Huang *et al.* (1987)
Pr	Nd	0–2	MCA, SP; CFA	Z-D. Zhang, Sun, *et al.* (1991)
Pr	Nd, Sm, Gd, Er	0–2	M, T_s, MCA, FOMP	Z-D. Zhang, Huang, *et al.* (1989a)
Pr	Nd,Gd	0–2	MCA, SP; CFA	Z-D. Zhang, Sun, *et al.* (1990b)
Nd	Gd			
Pr	Sm	0–2	M, MCA	C. Lin and Liu (1986)
Pr	Sm, Er	0–2	M, MCA, FOMP, SR	F-M. Yang, Zhao, *et al.* (1988)
			FOMP, SR, MPD; CFA	F-M. Yang, Li, *et al.* (1988)
Pr	Gd	0–2	M, T_c, MCA, FOMP	Z-D. Zhang, Sun, *et al.* (1988)
Pr, Nd, Er	Gd, Ho, Y	0–2	MPD; CFA	Zhu *et al.* (1989)
Pr, Y	Er	0–2	a, c, M, T_c, T_s, SR; CFA	Boltich, Pedziwiatr, and Wallace (1987a)
Pr	Er	0–2	SR, MPD; CFA	Boltich (1988a, 1988b)
Pr, Tb, Dy	Er, Tm	0–2	SR, MPD; CFA	Boltich, Pourarian, *et al.* (1988)
Pr	Y	0–2	M, MCA, FOMP, SP	Z-D. Zhang, Sun, *et al.* (1990d)
Nd	Ce, Gd, Tb, Dy, Ho, Er, Y	0.4–1.8	a, c, M, T_c, T_s, H_a, SR	Abache and Oesterreicher (1985, 1986b)
Nd	Sm	0–2	M; CFA	Nakagawa *et al.* (1990)
Nd	Gd, Y	0–2	M, T_c, T_s, MCA, FOMP, SR	Z-D. Zhang, Huang, *et al.* (1989b)
Nd	Tb	0–2	T_c, H_a	Pareti, Bolzoni *et al.* (1987)
Nd	Dy	1	a, c, T_c, T_s, SP; ND	Yelon *et al.* (1986)
Nd	Dy	0.66, 0.94	M	Nakagawa, Hiroyoshi, *et al.* (1987)
Nd	Dy	0–1.2	M, H_a	Sagawa, Hirosawa, *et al.* (1987b)
Nd	Er	0–2	M, T_s, χ, SR	Ibarra *et al.* (1988)
Nd, Dy	Er	0–2	T_s, χ, MPD, critical SR behavior	Del Moral *et al.* (1989, 1990); Ibarra, Marquina, *et al.* (1989)
Nd	Er	0–2	T_s, H_a, MCA, FOMP, SR	Marusi *et al.* (1990)
Nd	Tm	0–1	T_s	Buschow (1987)
Nd	Y	0–2	T_c	Leccabue *et al.* (1985)
Nd	Y	0–2	M, T_c, H_a, FOMP, SR; MBS	Bolzoni *et al.* (1986)
Nd	Y	0–2	MCA; CFA	Kapusta *et al.* (1990)
Nd, Dy, Er, Lu, Y	Sc	0–0.4	a, c, M, T_c, H_a	S. K. Chen *et al.* (1988b)
Gd	Er	0–2	T_s; MBS, CFA	Vasquez and Sanchez (1987)
Gd	Y	0–2	M	Burzo, Boltich, *et al.* (1985)

TABLE XI. (*Continued*).

R	R'	x	Properties; methods	References
Dy	Er	0–2	a, c, T_s; MBS	Niarchos and Simopoulos (1986)
Dy	Er	0–2	M, H_a, χ, SR, MPD; CFA	Ibarra, Algarabel, *et al.* (1989)
Dy	Tm	0–2	a, c, M, T_c, T_s, H_a, MPD	Pourarian, Jiang, Sankar, and Wallace (1987); Pourarian, Jiang, Zhang, *et al.* (1988)
Dy, Er, Y	Th	0–2	a, c, M, T_c, T_s, H_a	Pedziwiatr *et al.* (1986c); Pedziwiatr and Wallace (1986a)
Dy, Er	Th	0–1.5	M; MFA	Pedziwiatr (1988)
Er	Sm	0–0.3	T_s	Coey *et al.* (1989)
	Tb	0–0.6		
Er	Dy	0–1	H_a, SR	Algarabel *et al.* (1989)
Er	Dy	0.2–1.6	a, c, T_c, SR; MBS, CFA	Rechenberg *et al.* (1987)
Er	Ho	0.8	M, χ, SR	Marquina *et al.* (1989)
Y	Nd	0.1,0.2	MCA, SR; CFA	Williams *et al.* (1988)
Y	Sm	0–0.2	M, T_s, MCA	C. Lin *et al.* (1988)
Y	Tb, Er	0.2	M, SR	Koon, Das, and Williams (1986)
Y	Er	0.2	SR; MBS	Abe *et al.* (1987)
Y	Er	0.2	MCA, SR; CFA	Williams *et al.* (1987)

for example, the magnetic phase diagram determined by Pourarian, Jiang, Zhang, *et al.* (1988) is in good agreement with that predicted by Boltich *et al.* (1988) using only $n=2$ terms in the CEF (see Fig. 18). On the other hand, Ibarra, Algarabel, *et al.* (1989) found it necessary to include fourth-order CEF terms to model adequately the magnetic phase diagram, and the temperature and concentration dependence of the canting angle in the canted-moment regime, of $Er_{2-x}Dy_xFe_{14}B$. Williams *et al.* (1987) employed CEF terms to the sixth order in accurately fitting detailed torque magnetometry measurements on $Y_{1.8}Er_{0.2}Fe_{14}B$.

B. Replacements for iron

In view of the substantially lower Curie temperatures of the $R_2Fe_{14}B$ phases relative to the ~1000 K value for either α-Fe or $SmCo_5$ (see Table IV), one primary object of substitutional investigations is the identification of replacements that enhance T_c, particularly for $Nd_2Fe_{14}B$. Since the magnetism of the Fe sublattice sets the scale for T_c, it is not surprising that the majority of such work has been aimed at Fe replacements. Table XII summarizes the voluminous research on the $R_2Fe_{14-x}T_xB$ systems. Most efforts cited in the table have included x-ray analysis to establish that the samples are single phase and of the $Nd_2Fe_{14}B$ structure type, but in a few instances some uncertainty exists regarding integration of the substituent into the $R_2Fe_{14}B$ compound. For example, Allibert (1989) concluded from microstructural studies that niobium does not dissolve in $Nd_2Fe_{14}B$ but forms Nb-Fe-B precipitates (see also Schrey, 1988), and Lovleen

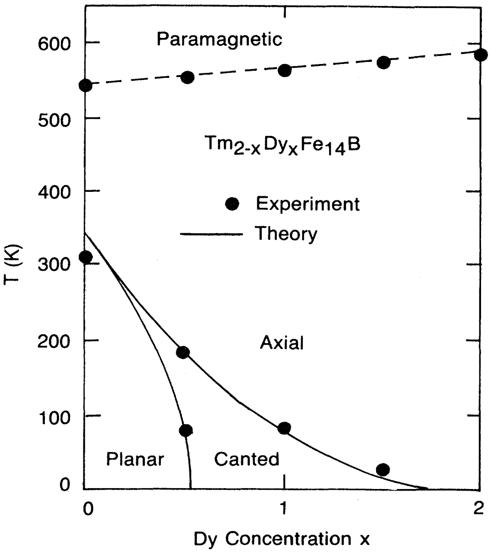

FIG. 18. Magnetic phase diagram for the pseudoternary compound $Tm_{2-x}Dy_xFe_{14}B$ (adapted from Pourarian, Jiang, Zhang, *et al.*, 1988).

TABLE XII. Summary of research on $R_2Fe_{14-x}T_xB$ compounds. (DS≡domain structure; NMR≡nuclear magnetic resonance; R_e≡resistance; σ_W≡domain-wall energy density; other abbreviations as in Table XI.)

R	T	x	Properties; methods	References
La	Co	0–14	M	Buschow, de Vries, and Thiel (1985b)
La	Co	0–14	a, c, M, T_c, H_a, MCA	Grössinger, Kirchmayr and Buschow (1988)
La, Nd	Co	0–14	a, c, T_c; MFA	Villas-Boas *et al.* (1988)
	Mn	0–1.4		
Ce, Pr, Nd, Gd, Dy, Y	Si	0–1.4	M, T_c, H_a	Xing and Ho (1988)
Pr	Co	0–14	a, c, M, T_c, T_s, H_a	Pedziwiatr, Jiang, and Wallace (1986); Pedziwiatr and Wallace (1986a)
Pr	Co	0–14	a, c, M, T_c, H_a, SP; MBS	Bolzoni, Coey, *et al.* (1987)
Pr	Co	0–14	a, c, M, T_c, H_a, MCA, FOMP	Grössinger, Krewenka, *et al.* (1987b)
Pr, Nd	Co	0–14	M, T_c, T_s, MPD	Pedziwiatr and Wallace (1987a)
Er		2,4,5		
Pr, Nd, Gd, Tb, Y	Co	0–14	MPD	Pedziwiatr and Wallace (1987c)
Er		0–5		
Tm		0–4		
Pr	Co	0–14	M, T_c	Shimao *et al.* (1987)
Pr, Nd, Gd, Tb, Y	Co	0–14	M, H_a, MPD	Wallace and Pedziwiatr (1987)
Dy		0–8		
Er		0–5		
Tm		0–4		
Pr	Co	0–14	T_c, T_s, H_a, FOMP	Gavigan, Li, *et al.* (1988b)
Pr	Cr	0,1,2,3	a, c, M, T_c, H_a	Kowalczyk (1989)
	Cu	0.5,1		
	Ga	1		
	Si	1,2		
Pr, Nd	Ga	0,1	a, c, M, T_c, T_s, H_a, SR	Pedziwiatr *et al.* (1988)
Pr, Nd, Gd, Y	Mn	0–2	a, c, M, T_c, T_s, H_a	M. Q. Huang *et al.* (1986a)
Pr	Mn	0–4.9	SP; MBS, ND	Pringle *et al.* (1990)
Pr, Nd, Y	Mn	1.4–5.6	a, c, M, T_c, H_{ci}	Y-C. Yang and Zhang (1990)
Pr, Nd, Er, Y	Si	0–2	M, T_c, T_s, H_a	Pedziwiatr and Wallace (1986a)
Pr, Nd, Er	Si	0–2	a, c, M, T_c, T_s, H_a; MFA	Pedziwiatr, Wallace, and Burzo (1987)
Pr, Nd, Er	Si	0–2	M, T_c, H_a; MFA	Wallace, Pedziwiatr, *et al.* (1987)
Nd	Al	2	a, c, M, T_c, H_a	Abache and Oesterreicher (1985)
	Co	0–14		
Nd, Y	Al	2,3	a, c, M, T_c, H_a, SP, SR	Abache and Oestereicher (1986a)
	Co	0–14		
	Cr, Mn, Ni	2		
Nd	Al, Si	4.7	T_c, SP; MBS	Kamal *et al.* (1986)
Nd	Al	0–1.1	$a(T)$, $c(T)$	Cheng *et al.* (1987)
	Co	0–2.8		

TABLE XII. (*Continued*).

R	T	x	Properties; methods	References
Nd	Al	0.4–1.5	M, T_c, T_s, H_a, SP; ND	Hirosawa, Yamaguchi, *et al.* (1987)
	Co	0–14		
	Cr, Mn	0.7		
Nd	Al	0, 0.28	M, T_c, MCA	Hock and Kronmüller (1987)
Nd	Al, Co, Ga, Ni, Si	0,1	T_s, H_a, SP; MBS	Grössinger, Chou, *et al.* (1988); Grössinger, Heiss, *et al.* (1989); Wiesinger *et al.* (1989)
Nd	Al	0.2–0.8	SP; MBS	Hauet, Lemarchand, and Teillet (1988)
Nd	Al, Ga, Si	1	a, c, M, T_c, T_s, H_a; CFA	Kou *et al.* (1989c)
Nd	Al, Co, Cr, Mn, Ni, Si	0.7, 1.4	M, T_c, T_s, MCA; CFA	C. Lin *et al.* (1989)
	Cu, Ti	0.7		
Nd	Al	0.56–1.46	M, T_s, H_a, FOMP, SR, χ; CFA	Deruelle *et al.* (1990)
	Mn	0.7		
Nd	Co	0–7	T_c	Buschow, van Noort, and de Mooij (1985)
Nd, Y	Co, Mn	0–3	T_c	Leccabue *et al.* (1985)
Nd	Co	0–14	a, c, M, T_c, MCA	Matsuura *et al.* (1985a)
Nd	Co	13.7	SP; MBS	Van Noort and Buschow (1985)
Nd	Co	0–14	SR; CFA	Boltich and Wallace (1986)
	Ga	1		
	Mn, Si, Ru	1,2		
Nd	Co	0–14	M, T_c; MFA	Fuerst *et al.* (1986)
Nd	Co	0–14	T_c, T_s, H_a, χ, MPD	Grössinger, Krewenka, *et al.* (1986)
Nd	Co	0–14	a, c, SP; ND	Herbst and Yelon (1986a); Yelon (1988)
Nd, Gd, Y	Co	0–14	a, c, M, T_c, T_s, H_a	M. Q. Huang *et al.* (1986b)
Nd	Co	0–14	T_c, T_s	Pedziwiatr and Wallace (1986a)
Nd, Y	Co	0–14	a, c, M, T_c, T_s, H_a, MCA, FOMP, SP; MBS	Bolzoni, Leccabue, *et al.* (1987b)
Nd	Co	0–12	SP; MBS	Deppe *et al.* (1987)
Nd	Co	0–14	H_a	Hirosawa, Tokuhara, Yamamoto, *et al.* (1987)
Nd	Co	0–14	SP; MBS	Honma and Ino (1987)
Nd	Co, Cr, Mn, Ni, Sc, Ti, V	1.4	a, c, M, T_c, H_a	Ku and Yen (1987)
Nd, Y	Co	0–12.6	M, T_c, T_s, MCA	C. Lin, Liu, and Xu (1987)
Nd	Co	0–5.6	M, SP; MBS	Matsui *et al.* (1987)
Nd	Co	1.8	M, T_c, SP; MBS	Rani and Kamal (1987a)
Nd	Co	3.5	T_c, SP; MBS	Rani and Kamal (1987b)
Nd	Co	0–4.1	M, H_a	Sagawa, Hirosawa, *et al.* (1987b)
Nd	Co	0–4.2	SP; MBS	Tharp *et al.* (1987)
Y		0–5.6		
Nd	Co, Ni, Ru	1.4	a, c, M, T_c, T_s, SR, R_e	Yen *et al.* (1987)
Nd	Co	0–2.0	SP; NMR	Y. D. Zhang *et al.* (1987, 1988)
Nd	Co	0–14	T_c; MFA	Gavigan, Givord, *et al.* (1988)
Nd	Co	1.7–14	SP; NMR	Jedryka *et al.* (1988)
Nd	Co	0–14	SP, SR	H. S. Li, Gavigan, *et al.* (1988)

TABLE XII. (*Continued*).

R	T	x	Properties; methods	References
Nd	Co	0–2.2	SP; MBS	Ge *et al.* (1989)
Nd	Co	2.1,5.3	M, FOMP	Nakagawa *et al.* (1989)
Nd	Co	$\sim 10^{-6}$	SP; MBS source technique	Ryan *et al.* (1989, 1990)
Nd	Co	1.7–14	NMR	Wojcik *et al.* (1989)
Nd	Co, Ni, Ru	0,1.4	SR; CFA	Z. W. Zhang *et al.* (1989)
Nd	Co	0–14	a, c, T_c, SP; ND	Girgis *et al.* (1990)
Nd	Co	12.6–13.99	SR; NMR	Jedryka *et al.* (1990)
Nd, Gd, Y	Co	2	a, c, T_c, T_s, H_a; CFA	Kou *et al.* (1990b)
Nd, Gd, Y	Cr	0–3	a, c, M, T_c, T_s, H_a	Kowalczyk and Wrzeciono (1988a)
Nd	Cr	0–3	M, T_c, T_s, MPD	Kowalczyk, Stefanski, Szlafarek, and Wrzeciono (1990)
	Cu	0.5–1.5		
	Si	1–2		
Nd	Cu	0–0.7	a, c, M, T_c, T_s, MPD	S. K. Chen *et al.* (1988a)
Nd, Gd, Y	Cu	0–1.5	a, c, M, T_c, T_s, H_a	Kowalczyk and Wrzeciono (1988b)
Nd, Er	Cu	0–1.5	a, c, M, T_c, T_s, H_a	Burzo and Plugaru (1990)
Nd	Ga	1	M, T_c, T_s, H_a	Pedziwiatr and Wallace (1986a)
	Ru	1,2		
Nd	Ga	0–2.1	T_c, T_s, H_a	Hu *et al.* (1988)
	Mo, Nb	0–1.4		
Nd	Ga	0–1.5	M, T_c, H_a, MCA	Xie *et al.* (1988b, 1990c)
Nd	Ga	0–2.1	a, c, M, T_c, T_s, H_a, SP	Quan *et al.* (1989)
			SP; MBS, ND	Quan *et al.* (1990)
Nd	Ge	0–0.5	a, c, M, T_c, T_s, H_a	Kowalczyk and Ivanov (1990)
Nd	Mg	0,0.7,1.1	M, T_c, H_a	C. H. Lin *et al.* (1988)
Nd	Mn, Ni	1,2,3	a, c, M, T_c, T_s, H_a	Bolzoni, Leccabue, *et al.* (1987a)
Nd	Mn	0–5.6	$a(T)$, $c(T)$, M, T_c	Cheng *et al.* (1988)
Nd, Er	Mn	0–3.0	M, SR, Kerr effect	Iida *et al.* (1990)
Nd	Ni	0–2.8	a, c, M, T_c	Chuang, Wu, and Xie (1987, 1988)
Nd	Ni	0–2.8	SP; MBS	Dai *et al.* (1988)
Nd	Ru	1.4,2.8	a, c, M, T_c, MCA	Ku *et al.* (1986)
Nd	Ru	0,1,2	a, c, M, T_c, T_s, H_a	Pedziwiatr *et al.* (1986b)
Nd	Si	0,1,2	M, T_c	Van Mens (1986)
Nd	Si	2	M, SR	Boltich *et al.* (1987b)
Nd	Si	0–1.5	a, c, M, T_c, H_a	Jurczyk *et al.* (1987a)
Nd, Y	Si	0–2	a, c, M, T_c, H_a	Jurczyk *et al.* (1987b)
Nd, Y	Si	0–2.1	M, T_c, H_a, SR	Xing and Ho (1987)
Nd, Y	Si	0–2.0	MBS	Pringle *et al.* (1989)
Nd	Si	0.5–2.0	a, c, SP; ND	Pringle *et al.* (1991)
Y		0.2–1.7		
Nd	Si	0,1.5	SP; MBS	Z. W. Li *et al.* (1990)
Nd	V	1.4	T_c, SP; MBS	Kamal and Lovleen (1989)

TABLE XII. (*Continued*).

R	T	x	Properties; methods	References
Gd	Al	0–6	M, T_c, χ	Burzo, Lupsa, and Pedziwiatr (1986)
Gd, Y	Al, Ga, Si	1	a, c, M, T_c, H_a	X. K. Sun *et al.* (1989b)
Gd, Y	Al, Ga, Si	0,1	H_a, SP; MBS	Kou, Wiesinger, and Grössinger (1990)
Gd	Co	0–14	a, c, M, T_c	L'Héritier and Fruchart (1985)
Gd	Co	0–14	M, H_a	Z-D. Zhang, Sun, *et al.* (1990a)
Gd, Y	Cr	0–3	M, T_c, H_a	Kowalczyk and Wrzeciono (1988c)
	Cu	0–1.5		
	Si	0–2		
Gd, Tb, Dy, Ho, Er, Tm	Mn	0–4	M; MFA	Verhoef, Quang, *et al.* (1990a, 1990b)
Tb	Co	0–14	a, c, M, T_c, T_s, H_a, MPD	Pedziwiatr, Chen, and Wallace (1987)
Dy	Co	0–8	a, c, M, T_c, T_s, H_a	Pedziwiatr and Wallace (1987b)
Er		2,4,5		
Er	Al	0–5	T_c, T_s; MFA	Quang *et al.* (1987)
Er	Co	0–5	a, c	Meisner and Fuerst (1986)
	Mn	1–9		
Er	Mn	0–9	a, c, M, T_c, T_s, MPD	Fuerst, Meisner, and Pinkerton (1987)
Er	Mn	2–9	a, c, SP; ND	Fuerst, Meisner, Pinkerton, and Yelon (1987)
Er	Mn	0–8.8	M; MFA	Pinkerton *et al.* (1987)
Er	Mn	0–9	M, T_c, T_s, MPD, SP; ND	Fuerst, Meisner, Pinkerton, and Yelon (1988)
Er	Mn	0–3	M, $T_s(H)$, MCA, SR	Pinkerton *et al.* (1988a)
Er	Mn	2.0,2.5	$M(H,T)$	Pinkerton *et al.* (1988b)
Er	Mn	0–8	magnetic structure; ND	Yelon (1989); Yelon *et al.* (1989)
Er	Mn	0–3	a, c, M; MFA	Verhoef, Radwański, and Franse (1990)
Tm	Co	0,2,4	T_c, T_s, MPD	Pourarian, Jiang, Sankar, and Wallace (1987)
Tm	Co	0,2,4	a, c, M, T_c, T_s	Pourarian, Jiang, Zhang, *et al.* (1988)
Y	Al	0–4	M, T_c, H_a	Burzo, Plugaru, *et al.* (1986)
	Co, Ni	1–5		
Y	Al	0–1.1	M, T_c, H_a, MCA, SP	Y-C. Yang, James, *et al.* (1986b)
Y	Al	0–1.4	a, c, M, T_c, MCA	C. Lin, Lan, and Xu (1987)
	Cr, Ni	0.4–2.1		
	Mn	0.4–3.5		
	Ti	0.4, 0.7		
Y	Al	0–1.1	SP; MBS	Y-C. Yang, Tharp, *et al.* (1987)
Y	Al	0–1.1	MBS	Tharp *et al.* (1988)
Y	Al	0–1.7	a, c, M, T_c, H_a, MCA	Wu *et al.* (1990)
Y	Co, Ni	0–7	M, T_c	Burzo, Stanciu, and Wallace (1985); Burzo, Boltich, *et al.* (1985)

TABLE XII. (*Continued*).

R	T	x	Properties; methods	References
Y	Co	0–14	electronic structure; site moments	Gu and Ching (1987b)
Y	Co	0–14	M, T_c, H_a, MCA	Pareti, Solzi, *et al.* (1987)
	Cr, Mn	1–4		
	Ni	1–5		
Y	Co, Mn, Ni	1.3,3.1	SP; MBS	Bara *et al.* (1988)
Y	Co	0–14	M, MCA	Thuy *et al.* (1988)
			a, c, M, T_c, MCA, SP	Hong *et al.*(1989)
Y	Co	0–12	a, c, M, T_c, SP; MBS, MFA	Sano *et al.* (1989)
	Mn	1–5		
Y	Co	0–4.2	$a(T)$, $c(T)$	Andreev and Bartashevich (1990a)
Y	Cr	1	a, c, H_a, SP; ND	Moze *et al.* (1988)
	Mn	1,3		
Y	Cr, Si	0,1,2	M, H_a	Kowalczyk, Stefanski, and Wrzeciono (1990)
	Cu	1,1.5		
Y	Cu	0–1.5	a, c, M, T_c, H_a, χ	Pedziwiatr, Wallace, Burzo, and Pop (1987)
	Si	1,2		
Y	Mn	0–5.6	SP; MBS, ND	Pringle, Marasinghe, *et al.* (1988)
Y	Mn	1,3	DS, σ_W	Wyslocki and Bolzoni (1990)
Y	Nb	0–0.5	a, c, M, T_c, H_a	Jurczyk *et al.* (1989)
Y	Re	0–0.5	a, c, M, T_c, H_a	Jurczyk and Chistyakov (1989b)
Y	Si	0–2.1	a, c, M, T_c, H_a, SP; ND	Y-C. Yang *et al.* (1988)

and Kamal (1988b) reported a similar finding for titanium.

Only cobalt has been found capable of replacing iron over the whole concentration range (and only in the La, Pr, Nd, Sm, Gd, Tb, and Y compounds), and it produces the largest T_c enhancement. Figure 19(a) shows $T_c(x)$ for $Nd_2Fe_{14-x}Co_xB$, which is representative of the other R systems as well; the increase is most rapid at the lowest Co concentrations, and T_c $(Nd_2Co_{14}B) \simeq 1000$ K is nearly twice the 585 K value for $Nd_2Fe_{14}B$. At most, partial substitution of other elements for Fe in $R_2Fe_{14}B$ has been demonstrated. Of the replacements in $Nd_2Fe_{14}B$ listed in Table XII, Ga, Ni, Sc, and Si enhance T_c somewhat, while Al, Cr, Ru, and V degrade it severely, but for each of the former the improvement in T_c is accompanied unfortunately by depression of the saturation magnetization.

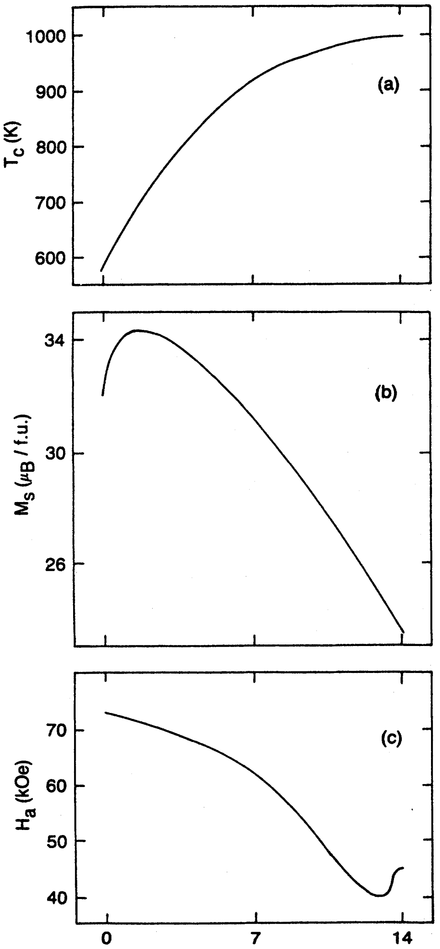

FIG. 19. Magnetic characteristics of $Nd_2Fe_{14-x}Co_xB$ pseudoternary compounds as functions of cobalt concentration x: (a) Curie temperature T_c and (b) saturation magnetization M_s at 295 K (Fuerst *et al.*, 1986); (c) room-temperature anisotropy field (after Grössinger, Krewenka, *et al.*, 1986).

Whereas the Fe sublattice is characterized by c-axis moment alignment ($K_1 > 0$ in Table VII), Co substitution generates a progression toward basal-plane anisotropy, which is responsible for spin reorientations as functions of temperature and/or concentration. The easy direction in $Y_2Fe_{14-x}Co_xB$ and $Gd_2Fe_{14-x}Co_xB$ changes from the c direction to the basal plane for $x \gtrsim 9$ and in the pseudoternary La compound for $x \gtrsim 12$ with no temperature-induced transitions; in certain concentration ranges the Pr, Nd, and Tb systems do exhibit such changes with temperature, a low-temperature, canted-moment regime occurring in $Nd_2Fe_{14-x}Co_xB$ for all x (cf. Pedziwiatr and Wallace, 1987c; Grössinger, Krewenka, *et al.*, 1986).

The room-temperature saturation magnetization of the $R_2Fe_{14-x}Co_xB$ materials features a modest maximum in the vicinity of $x=2$, as Fig. 19(b) indicates for the Nd system (the maximum becomes less pronounced at lower T). This property, qualitatively similar to that displayed by the moment of Fe-Co alloys in the Slater-Pauling curve, offers the prospect of improving the energy product of practical magnets. There is, however, a disadvantageous aspect to Co replacement of Fe. The room-temperature anisotropy field declines with x for $x \lesssim 13$ in $Nd_2Fe_{14-x}Co_xB$ [see Fig. 19(c)] and for $x \lesssim 10$ in $Pr_2Fe_{14-x}Co_xB$ (cf. Grössinger, Krewenka, *et al.*, 1987b), prompting in part a number of studies on $R_2Fe_{14-y-z}Co_yT'_zB$ systems, surveyed in Table XIII, in which replacements T′ are sought to preserve the M_s and T_c increases afforded by Co substitution while offsetting the decline in H_a. Aluminum, gallium, and silicon appear promising in this regard. Xie *et al.* (1988a) have elaborated on the theme by examining triply substituted $Nd_2Fe_{11.5-y-z}Co_{2.5}Ga_yNb_zB$ materials; H_a(295 K) is observed to increase slightly with y, developing a maximum in the $y \sim 0.15$, $0.1 \leq z \leq 0.2$ region.

Site preferences of the replacement atoms are linked undoubtedly to the magnetic properties of the substituted compounds and have been explored by neutron diffraction, Mössbauer spectroscopy, and nuclear magnetic resonance (NMR) in several cases. Aluminum, chromium, and manganese favor occupation of the $8j_2$ site (Fuerst, Meisner, Pinkerton, and Yelon, 1987; Hirosawa, Yamaguchi, *et al.*, 1987; Y-C. Yang *et al.*, 1987; Hauet, Lemarchand, and Teillet, 1988; Moze *et al.*, 1988; Pringle, Marasinghe, *et al.*, 1988; Pringle, Fu, *et al.* 1990), silicon preferentially enters the $4c$ site (Pringle, Marasinghe, *et al.*, 1991), and nickel evidently prefers the $16k_2$ and $8j_2$ sites (Dai *et al.*, 1988). In general the site preferences do not correlate with simple atomic size considerations (Wiesinger *et al.*, 1989; Kou, Wiesinger, and Grössinger, 1990).

Regarding cobalt substitution there is almost unanimous agreement among the studies conducted that Fe maintains a strong preference for the $8j_2$ site; van Noort and Buschow (1985) have made an attractive argument for this preference in $Nd_2Fe_{14-x}Co_xB$ by considering the

TABLE XIII. Summary of research on $R_2Fe_{14-y-z}Co_yT'_zB$ compounds. (Abbreviations as in Tables XI and XII.)

R	T′	y	z	Properties; methods	References
Pr, Nd	Al	0–7	0–0.7	M, T_c, H_a	Burzo, Plugaru, and Pop (1987)
Pr	Cr	0–3	0–1	M, T_c, H_a	Kowalczyk *et al.* (1988)
Pr, Nd, Gd	Mn	2	0–1	a, c, M, T_c, H_a	Jurczyk and Wallace (1986b)
Pr	Nb	0,1	0–0.2	a, c, M, T_c, H_a	Jurczyk and Chistjakov (1989a)
Nd	Al	0–3	0–1	M, T_c, H_a	Burzo, Pedziwiatr, and Wallace (1987)
Nd	Al, Ta, W	2	0–0.5	a, c, M, T_c, H_a	Jurczyk (1987a)
	Mo		0.05–0.15		
Nd	Al	0–2	0–1	M, T_c, H_a, σ_W	R. Szymczak *et al.* (1987)
Nd	Al, Cr	2	0–1	a, c, M, T_c, H_a	Jurczyk (1988a)
	V		0.1–0.5		
Nd	Al	2	0–1.2	a, c, T_c, T_s; CFA	Kou *et al.* (1989b)
Nd	Ga	2.5	0.1–1.5	M, T_c, H_a, FOMP	Xie *et al.* (1989)
Nd	Ga	0,2.5	0.1–1.5	T_c, T_s, χ, FOMP, MPD	Xie *et al.* (1990a)
				SP;MBS	Xie *et al.* (1990b)
Nd	Mn	2	0–1	a, c, M, T_c, H_a	Jurczyk and Wallace (1986c)
Nd	Mn	1.4	1.4	M, T_c; MBS	Lovleen and Kamal (1988a)
Nd	Mo	1.4	1.4	M, T_c, SP; MBS	Lovleen and Kamal (1988c)
Nd	Nb	0,2	0–0.5	a, c, M, T_c, H_a	Kowalczyk *et al.* (1989)
Nd	Re	0,2	0–0.2	a, c, M, T_c, H_a	Jurczyk (1990a)
Nd	Si	2	0–0.6	a, c, M, T_c, H_a	Jurczyk and Kowalczyk (1987)
Nd	Si	0–4.2	0.8	M, T_c, H_a	Xing and Ho (1988)

numbers of Nd nearest neighbors and relative bond strengths inferred from heats of solution. Neutron powder diffraction reveals a weak preference of Co for the $4e$ site and near-random population of the $16k_1$, $16k_2$, $8j_1$, and $4c$ sites (Herbst and Yelon, 1986a), but Mössbauer spectroscopy and NMR efforts have produced the conflicting results that (i) Co favors the $16k_2$ site (van Noort and Buschow, 1985; Bolzoni, Leccabue, *et al.*, 1987b; Y. D. Zhang *et al.*, 1987, 1988; Bara *et al.*, 1988; Jedryka *et al.*, 1988; Ge *et al.*, 1989); (ii) Co avoids the $8j_2$ while populating the other five sites randomly (Ryan *et al.*, 1989, 1990); (iii) Co prefers the $16k_1$ and $16k_2$ and Fe the $8j_1$ and $8j_2$ sites (Honma and Ino, 1987); and (iv) no preferential occupancy occurs (Matsui *et al.*, 1987). At least partial resolution of the matter may be provided by research connecting the site populations to other properties. Hong *et al.* (1989) have analyzed the anomalous concentration dependence of the anisotropy energy in $Y_2Fe_{14-x}Co_xB$ using a model in which the transition-metal sites contribute individually to the anisotropy. The site occupancies are crucial inputs to the analysis, and Hong *et al.* (1989) find that the neutron-diffraction results for $Nd_2Fe_{14-x}Co_xB$ (Herbst and Yelon, 1986a) lead to an excellent description of the anisotropy data within their model while the occupancies determined via Mössbauer spectroscopy for $Y_2Fe_{14-x}Co_xB$ by Bolzoni, Leccabue, *et al.* (1987b) do not. Investigating differences in crystal-field parameters for $Nd_2Fe_{14}B$ and $Nd_2Co_{14}B$, H. S. Li, Gavigan, *et al.* (1988) have suggested that a correlation should exist between the concentration dependence of the low-T spin-reorientation temperature T_s and the Co occupancy $n_{Co}(4c)$ of the $4c$ site in $Nd_2Fe_{14-x}Co_xB$; their plots of T_s/T_c and the $n_{Co}(4c)$ from the neutron work versus x do indeed have very similar shapes.

Frequently it is asserted that site preference and the T_c behavior on substitution are related by the replacement of Fe atoms having ferromagnetic (positive) or antiferromagnetic (negative) exchange interactions with their neighbors, T_c rising if negative nearest-neighbor bonds (length $d \lesssim 2.5$ Å) are disrupted and decreasing if positive bonds ($d \gtrsim 2.5$ Å) are weakened. This notion (see also Sec. IV.A.2) is in accord with experiment for substituents such as Al and Mn, which degrade T_c and enter the $8j_2$ site ($d > 2.6$ Å in Table II), but its limited validity is underscored by Si substitution. Silicon increases T_c, and the negative-bond-breaking argument predicts that the Si atoms should preferentially occupy $8j_1$ and $16k_2$ sites (see Pedziwiatr and Wallace, 1986a). Neutron-diffraction work by Pringle *et al.* (1991), however, demonstrates conclusively that Si strongly prefers the $4c$ site in $Nd_2Fe_{14-x}Si_xB$ and $Y_2Fe_{14-x}Si_xB$; fluorescence extended x-ray absorption fine structure measurements on Si-substituted, melt-spun Nd-Fe-B ribbons by Brennan *et al.* (1989) also point to preferential Si occupation of the $4c$ site.

Verhoef, Quang, *et al.* (1990a, 1990b; see also Verhoef, Radwański, and Franse, 1990) have measured magnetization curves on Mn-substituted heavy-R compounds for which high but accessible fields can collapse the rare-earth and transition-metal moments, antiparallel in zero field, to a parallel configuration. In a model assuming one R and one TM sublattice, the slope of the $M(H)$ curve at intermediate fields is inversely proportional to the R-TM molecular-field coefficient n_{RT}, enabling a rather direct determination of that important parameter. Interestingly, n_{RT} is found to be nearly independent of Mn content. Although the model is somewhat oversimplified inasmuch as there are, at least in the $Er_2Fe_{14-x}Mn_xB$ system, several sublattices (Fuerst, Meisner, Pinkerton, and Yelon, 1988; Yelon *et al.*, 1989), the results provide valuable estimates of n_{RF} (and, hence, j_{RF}) for the unsubstituted materials which compare well with those derived by other methods (Verhoef, Quang, *et al.*, 1990b).

C. $R_2Co_{14}B$ compounds and pseudoternary derivatives

Early systematic work on the $R_2Co_{14}B$ series was done by Buschow, de Mooij, *et al.* (1985); Le Roux *et al.* (1985) performed a single-crystal x-ray structure determination of $Nd_2Co_{14}B$ confirming the $Nd_2Fe_{14}B$-type structure. Lattice parameters and a few magnetic characteristics of the seven $R_2Co_{14}B$ compounds known to form are presented in Table XIV. The low-temperature saturation magnetizations of the La and Y members indicate an average Co moment of $1.4\mu_B$, somewhat more removed from the $1.7\mu_B$ moment per atom in elemental cobalt metal than is the average Fe moment in $R_2Fe_{14}B$ ($2.1\mu_B$) from that of α-Fe ($2.2\mu_B$). As in $R_2Fe_{14}B$, the six Co sublattices can be expected to be ferromagnetically coupled and collinear [neutron diffraction shows this explicitly for $Nd_2Co_{14}B$ (Herbst and Yelon, 1986a)], and subtraction of the average Co sublattice magnetization from the $M_s(4\ \mathrm{K})$ data of the Pr, Nd, and Gd compounds suggests (i) R moments near their free-ion $gJ\mu_B$ values and (ii) antiferromagnetic coupling of the R and Co spin moments. $Sm_2Co_{14}B$ is exceptional insofar as $M_s(4\ \mathrm{K})$ is below that for either $La_2Co_{14}B$ or $Y_2Co_{14}B$, implying antiparallel arrangement of the Sm and Co sublattice moments even though Sm^{3+} is a light-rare-earth ion characterized by $J=L-S$ in the Hund's-rule ground state. Buschow, de Mooij, *et al.* (1985) point out that this behavior, which also occurs in $SmCo_5$, Sm_2Co_{17}, and $SmFe_2$ but not in $Sm_2Fe_{14}B$, may arise from an admixture of the low-lying excited Sm^{3+} multiplets by the combined action of the exchange and crystal fields.

It is evident from Tables IV and XIV that each $R_2Co_{14}B$ compound has a much higher Curie temperature than its $R_2Fe_{14}B$ counterpart, and the difference can be attributed via Eq. (18) for the La or Y members to stronger Co-Co than Fe-Fe exchange. Another significant contrast between the two series is the fact, apparent from comparison of the easy directions in the La, Gd, and Y compounds given in Tables VI and XIV, that the Co sublattice anisotropy favors magnetization in the tetragonal basal plane ($K_1<0$), whereas the Fe anisotropy prefers an easy axis parallel to the c direction ($K_1>0$ in Table VII).

In the $R_2Co_{14}B$ phases having $L\neq 0$ rare-earth ions

TABLE XIV. Lattice constants (a,c), saturation magnetizations (M_s) at 4 K, Curie temperatures (T_c), spin-reorientation temperatures (T_s), easy directions of magnetization, and room-temperature anisotropy fields of $R_2Co_{14}B$ compounds.

Compound	a (Å)	c (Å)	$M_s(4\ \mathrm{K})$ (μ_B/f.u.)	T_c (K)	T_s (K)	Easy direction ($T<T_s \rightarrow T>T_s$)	$H_a(295\ \mathrm{K})$ (kOe)
$La_2Co_{14}B$	8.67	12.01[a]	19.3[b,c]	955[a]		$\perp c$[a–d]	30[b]
$Pr_2Co_{14}B$	8.63	11.87[a,e]	24.8[a,e]	995[a,f,g]	664[h]	$\parallel c \rightarrow \perp c$[h]	100[g,i]
$Nd_2Co_{14}B$	8.64	11.86[j,k]	25.7[b,c,e]	1000[e,h,l,m]	37[b,n]	canted $\rightarrow \parallel c$[b,h]	45[b,n,o]
					543[h,j]	$\parallel c \rightarrow \perp c$[b,h,j]	
$Sm_2Co_{14}B$	8.61	11.79[a]	18.1[a]	1029[a]		$\perp c$[a,d]	–
$Gd_2Co_{14}B$	8.61	11.76[a]	5.4[b]	1050[a]		$\perp c$[a–c,h]	90[b]
$Tb_2Co_{14}B$	8.60	11.73[a,p]	–	1035[a,h,p]	795[h,p]	$\parallel c \rightarrow \perp c$[h,p]	140[p]
$Y_2Co_{14}B$	8.60	11.71[a]	19.8[j]	1015[a,e,q,m]		$\perp c$[a,d,h,j]	28[j]

[a] Buschow, de Mooij, Sinnema, *et al.* (1985).
[b] Hirosawa, Tokuhara, Yamamoto, *et al.* (1987).
[c] Yamauchi *et al.* (1987).
[d] Sinnema *et al.* (1985).
[e] Pedziwiatr and Wallace (1987d).
[f] Chuang, Wu, and Xie (1987, 1988).
[g] Chuang, Wu, Chang, *et al.* (1988).
[h] Pedziwiatr and Wallace (1986b, 1987c).
[i] Grössinger, Krewenka, *et al.* (1987b).
[j] Le Roux *et al.* (1985).
[k] Herbst and Yelon (1986a).
[l] Fuerst *et al.* (1986).
[m] M. Q. Huang *et al.* (1986b).
[n] Abache and Oesterreicher (1985).
[o] Grössinger, Krewenka, *et al.* (1986).
[p] Pedziwiatr, Chen, and Wallace (1987).
[q] Pareti, Solzi, *et al.* (1987).

(R = Pr, Nd, Sm, Tb), the room-temperature easy direction is again dictated by the single-ion anisotropy of the R sublattice and corresponds to the sign of the second-order Stevens coefficient α_J, but competition between the R and Co anisotropies generates axial→planar spin reorientations in $Pr_2Co_{14}B$, $Nd_2Co_{14}B$, and $Tb_2Co_{14}B$ ($\alpha_J < 0$) at higher temperatures (T_s) analogous to the transitions in $Er_2Fe_{14}B$, $Tm_2Fe_{14}B$, and $Yb_2Fe_{14}B$. $Nd_2Co_{14}B$ features in addition a low-temperature canting of the magnetization away from the c axis in the (110) plane; its onset is at ~ 37 K, and the canting angle reaches $\sim 13°$ at 4 K (Hirosawa, Tokuhara, *et al.*, 1987), while the values for the corresponding transition in $Nd_2Fe_{14}B$ are ~ 135 K and $\sim 30°$. Hiroyoshi, Yamada, *et al.* (1987) have observed a first-order magnetization process (FOMP) in $Nd_2Co_{14}B$ when a 210-kOe field is applied at 4 K in the hard [100] direction, which is qualitatively similar to the FOMP occurring in $Nd_2Fe_{14}B$ (see also Nakagawa, Kido, *et al.*, 1987; Kato *et al.*, 1988). Compared to $Nd_2Fe_{14}B$, $Nd_2Co_{14}B$ is a less desirable permanent-magnet material in view of its large cobalt content, lower saturation magnetization and anisotropy field (cf. Tables IV and XIV), and the fact that the spin-reorientation temperature $T_s \sim 543$ K, at which the easy direction changes from axial to planar, serves as the effective upper limit to practical magnetics rather than T_c. In contrast to $Pr_2Fe_{14}B$, no FOMPs have been observed in $Pr_2Co_{14}B$ (Kato *et al.*, 1988).

H. S. Li, Gavigan, *et al.* (1988) have analyzed the temperature dependence of the spontaneous magnetization in $Nd_2Co_{14}B$ and find that the Nd-Co molecular-field coefficient is essentially the same as its cognate in $Nd_2Fe_{14}B$; the exchange field acting on the Nd^{3+} ion in the former compound is substantially smaller than that in the latter simply because of the lower Co moment. Applying the crystal-field-plus-exchange model of Cadogan *et al.* (1988), these authors conclude that $T_s \sim 37$ K for the spin-canting transition in $Nd_2Co_{14}B$ cannot be explained solely by the reduced exchange field but requires fourth- and sixth-order CEF terms lower than those found for $Nd_2Fe_{14}B$. With such modifications H. S. Li, Gavigan, *et al.* (1988) obtain excellent agreement between calculated and experimental values of the axial→canted T_s, the canting angle, and the threshold field for the FOMP. Cadogan (1988) has investigated the relative strengths of the second-order CEF interactions in the $R_2Fe_{14}B$ and $R_2Co_{14}B$ systems with R = Pr, Nd on the basis of observed anisotropy fields; the analysis suggests that A_2^0 is enhanced in $Pr_2Co_{14}B$ relative to $Nd_2Co_{14}B$, whereas the reverse is true for the corresponding $R_2Fe_{14}B$ compounds. Kato *et al.* (1988) analyzed magnetization curves for $Pr_2Co_{14}B$ and $Nd_2Co_{14}B$ single crystals using the CEF-exchange model of M. Yamada *et al.* (1988); the calculated T_s of $Nd_2Co_{14}B$, 42 K, agrees satisfactorily with experiment, while the A_2^0 values for the two compounds are equal, contrary to the suggestion of Cadogan (1988). From ^{155}Gd Mössbauer-effect measurements on $Gd_2Co_{14}B$, Smit *et al.* (1987) have derived A_2^0 values that have the same (positive) sign at both rare-earth sites and that compare well with those for $Gd_2Fe_{14}B$ obtained by Bogé *et al.* (1986).

Electronic structure studies employing the methods outlined in Sec. V have been reported for $Y_2Co_{14}B$ (Inoue and Shimizu, 1986b; Gu and Ching, 1987a; Jaswal *et al.*, 1988; Coehoorn, 1991), $Nd_2Co_{14}B$ (Gu and Ching, 1987a), and $Gd_2Co_{14}B$ (Coehoorn, 1991; Coehoorn and Buschow, 1991). Considerable differences exist among the sets of (spin-only) Co site moments in the various calculations. The results of Jaswal *et al.* (1988) and Coehoorn (1991) for $Y_2Co_{14}B$ are in excellent accord with the Co site moments in $Nd_2Co_{14}B$ estimated from neutron powder-diffraction data (Herbst and Yelon, 1986a). In contrast to $R_2Fe_{14}B$, whose $8j_2$ site exhibits the largest Fe moment, the $4c$ site appears to support the largest Co moment in $R_2Co_{14}B$. Jaswal *et al.* (1988) also measured the 21-eV photoelectron spectrum of $Y_2Co_{14}B$ and found reasonable agreement with their calculated density of states.

NMR investigations of $R_2Co_{14}B$ compounds have been reported by a number of authors, including Kapusta *et al.* (1986), Erdmann *et al.* (1987, 1988), Figiel *et al.* (1987), Berthier *et al.* (1988), Wojcik *et al.* (1988, 1990), Erdmann and Rosenberg (1989), Nadolski *et al.* (1989), and Panissod *et al.* (1989). Berthier *et al.* (1988) estimated Co spin moments from the hyperfine fields in $Y_2Co_{14}B$ and found the $4c$ site moment to be largest, with the $4e$ site moment smallest, in accord with the electronic structure and neutron work cited above; from estimates of the orbital components it was concluded that the $8j_1$ and $8j_2$ sites contribute principally to the Co sublattice anisotropy. Pronounced changes in the ^{59}Co NMR spectrum through the low-temperature spin reorientation in $Nd_2Co_{14}B$ were observed by Panissod *et al.* (1989), who also found the greatest and least hyperfine fields at the $4c$ and $4e$ sites, respectively; evidence for conical domain walls (NMR signals are primarily generated in domain walls) was reported for $Nd_2Co_{14}B$ in the canted-moment regime by Wojcik *et al.* (1990). Nadolski *et al.* (1989) detected two components in the ^{145}Nd spectrum of $Nd_2Co_{14}B$ at 4 K (below $T_s \sim 37$ K) that were associated with the two inequivalent Nd sites having moments canted away from the c axis; similar doublet structures were observed in $Nd_2Fe_{14}B$, with line positions agreeing with those reported previously for that compound by Potenziani (1985) and Berthier *et al.* (1986).

A few substitutional investigations based on the $R_2Co_{14}B$ materials have been conducted. L'Héritier and Fruchart (1985) found that manganese depresses T_c by ~ 135 K per substituted Mn in $Gd_2Co_{14-x}Mn_xB$, which forms only for $x \le 4$. Pedziwiatr and Wallace (1987d) reported that the $Nd_2Fe_{14}B$-type structure is maintained in $Pr_2Co_{14-x}Si_xB$ and $Nd_2Co_{14-x}Si_xB$ for $x \le 2$ and in $Y_2Co_{14-x}Si_xB$ for $x \le 1.6$; in marked contrast to the effect of Si substitution in $R_2Fe_{14}B$, T_c *decreases* precipitously with increasing Si content. According to Chuang, Wu, and Xie (1987, 1988) $Pr_2Co_{14-x}Ni_xB$ forms for $x \leq 2.8$, with T_c and T_s both declining with x. In the $Nd_2Co_{14-x}T_xB$, T=Ni, Cu, Ga, Ge systems, S. K. Chen *et al.* (1989) observed solubility limits of 2.8 (Ni), 1.1 (Cu), and 1.4 (Ga, Ge) and found that each substituent degrades the magnetization and T_c. The contrasting behavior of the NMR hyperfine fields in $Nd_2Co_{14-x}T_xB$ with T=Fe, Mn was studied by Ichinose *et al.* (1988).

Pourarian, Sankar, *et al.* (1987) examined $Nd_{2-x}Pr_xCo_{14}B$ over the entire composition range; the low-temperature spin reorientation vanishes for $x \gtrsim 0.2$, and the higher T_s increases linearly with Pr concentration. The $Y_{2-x}Nd_xCo_{14}B$ system was explored by Kakol *et al.* (1987, 1988) and Kapusta and Figiel (1988); among other results, the room-temperature anisotropy was found to be planar for $x \lesssim 0.8$ and axial for greater Nd content. The effect of rare-earth substitution on crystallographic and magnetic properties with an emphasis on the behavior of spin reorientations has been explored in $Pr_{2-x}Y_xCo_{14}B$ and $Nd_{2-x}Y_xCo_{14}B$, for which complete magnetic phase diagrams have been constructed (Pedziwiatr, Chen, Wallace, and Malik, 1987); $Nd_{2-x}Tb_xCo_{14}B$ (Jiang, Pourarian, *et al.*, 1988); $R_{2-x}Pr_xCo_{14}B$ with R=Tb, Dy, Ho, and Tm (Jiang, Pourarian, *et al.*, 1987); and $Pr_{2-x}R_xCo_{14}B$ in which R=Dy and Er (Pourarian, Jiang, Sankar, and Wallace, 1988).

D. Partial boron replacement

Only carbon has been reported capable of replacing boron in $R_2Fe_{14}B$, and preparation of homogeneous materials is difficult. Partially substituted, single-phase samples of $Nd_2Fe_{14}B_{1-x}C_x$ with $x \leq 0.75$ were investigated by Leccabue *et al.* (1985) and Bolzoni *et al.* (1985); Sagawa, Hirosawa, *et al.* (1987d) explored the same system in the $x \leq 0.9$ regime. Kou *et al.* (1989a) examined $R_2Fe_{14}B_{0.5}C_{0.5}$ materials with R=Nd, Y. In each case the Curie temperature and saturation magnetization were observed to decrease with increasing carbon concentration, T_c declining by ~30 K at $x=0.5$. Results for the anisotropy field conflict. Bolzoni *et al.* (1985) reported H_a (295 K) to increase monotonically with carbon content, noting a 16% improvement at $x=0.75$. Kou *et al.* (1989a) observed a similar trend; however, H_a(295 K) measured by Sagawa, Hirosawa, *et al.* (1987d) decreases modestly with increasing carbon level.

E. $R_2Fe_{14}C$ and related compounds

Carbides having the $Nd_2Fe_{14}B$ structure form with most of the rare-earth elements as do the borides, but their intrinsic properties have not been studied as extensively. One reason for this is the difficulty of preparing single-phase materials, particularly for the light-rare-earth systems. The $R_2Fe_{14}C$ compounds do not crystallize from the melt and must be formed by a solid-solid transformation in an appropriate temperature range (see Gueramian *et al.*, 1987; Buschow, de Mooij, and Denissen, 1988a; de Mooij and Buschow, 1988b; van Mens *et al.*, 1988). Stadelmaier and Park (1981) early reported a tetragonal carbide with the approximate stoichiometry $Gd_3Fe_{20}C$, which was subsequently identified as $Gd_2Fe_{14}C$ (Stadelmaier and El-Masry, 1985). For some time $Nd_2Fe_{14}C$ was considered nonexistent, but Buschow, de Mooij, and Denissen (1988a) were able to isolate it by discovering a suitable annealing regimen. [Jang and Stadelmaier (1990) have found that the formation of $Pr_2Fe_{14}C$ and $Nd_2Fe_{14}C$ can be accelerated by the addition of 1–2 at. % Cu.] The $Nd_2Fe_{14}B$ structure type has been confirmed for $La_2Fe_{14}C$ in a single-crystal x-ray investigation (Marusin *et al.*, 1985), for $Lu_2Fe_{14}C$ by x-ray (Denissen *et al.*, 1988a) and neutron powder diffraction (Hellwig *et al.*, 1990), and for the Nd (Helmholdt and Buschow, 1988) and Dy, Er, Lu compounds (Yethiraj *et al.*, 1991) by neutron powder diffraction.

Table XV lists characteristics of the $R_2Fe_{14}C$ phases. There are no reports on formation of these compounds with Yb or Th, whose borides exist. In a study of the Y-Fe-C equilibrium phase diagram at 1073 K, El-Masry and Stadelmaier (1989) did not detect $Y_2Fe_{14}C$, but $Y_2Fe_{14}C$, $Ce_2Fe_{14}C$, and other $R_2Fe_{14}C$ phases were prepared subsequently by heat treatment of melt-spun precursors (Fuerst and Herbst, 1991). Relative to its $R_2Fe_{14}B$ companion, each $R_2Fe_{14}C$ compound has a comparable *a* but smaller *c* lattice constant (and, hence, contracted unit-cell volume; Yethiraj *et al.* (1991) demonstrated that most of the largest reductions of interatomic distances can be ascribed to the smaller trigonal prisms in the carbides); the $R_2Fe_{14}C$ compounds also have lower Curie temperatures (by ~50 K) and Fe moments reduced by ~3%, as indicated by comparison of M_s (4 K) for $Lu_2Fe_{14}B$ and $Lu_2Fe_{14}C$ in Tables IV and XV as well as by ^{57}Fe Mössbauer-effect studies on several of the carbides (Buschow, de Mooij, and Denissen, 1988a, 1988b; Denissen *et al.*, 1988a, 1988b; Deppe *et al.*, 1988; Burzo *et al.*, 1989; Erdmann *et al.*, 1989; J. L. Sanchez *et al.*, 1989a; Verhoef, de Boer *et al.*, 1989a; Long and Grandjean, 1991). The T_c and Fe moment reduction may stem from the contribution of more electrons to the minority 3*d* bands by carbon than by boron. Anisotropy field and magnetization measurements indicate that, despite the lower Fe moments, the Fe sublattice anisotropy energy is ~20% greater in the carbides than in the $R_2Fe_{14}B$ compounds (Grössinger *et al.*, 1990; Kou *et al.*, 1990a; Xing and Ho, 1990). Otherwise the properties of the $R_2Fe_{14}C$ series closely resemble those of the borides, including rare-earth moments near their free-ion values; antiparallel R and Fe spin moments; identical easy directions of magnetization; comparable spin-reorientation temperatures; crystal-field-induced, single-ion R sublattice anisot-

TABLE XV. Lattice constants (a,c), saturation magnetizations (M_s) at 4 K, Curie temperatures (T_c), and spin-reorientation temperatures (T_s) of $R_2Fe_{14}C$ compounds.

Compound	a (Å)	c (Å)	M_s(4 K) (μ_B/f.u.)	T_c (K)	T_s (K)
$La_2Fe_{14}C$	8.82	12.14[a]	–	–	
$Ce_2Fe_{14}C$	8.74	11.84[b,c]	23.9[b]	345[b,c]	
$Pr_2Fe_{14}C$	8.82	12.04[c–e]	33.7[e]	513[c,e]	
$Nd_2Fe_{14}C$	8.83	12.03[f,g]	31.4[g]	535[g,h]	140[i]
$Sm_2Fe_{14}C$	8.80	11.95[c,d,g]	30.2[g]	580[c,g]	
$Gd_2Fe_{14}C$	8.79	11.89[c,d,g,j]	18.1[d,g]	630[c,g]	
$Tb_2Fe_{14}C$	8.77	11.86[d,g]	12.0[g]	585[g]	
$Dy_2Fe_{14}C$	8.75	11.83[d,g,k,l]	10.5[g]	555[c,g,l]	
$Ho_2Fe_{14}C$	8.74	11.80[d,g,m,n]	10.9[d,g,n]	525[g,m]	35[n]
$Er_2Fe_{14}C$	8.74	11.79[d,g,l,o]	11.6[d,l,o]	505[c,d,g]	322[g,o]
$Tm_2Fe_{14}C$	8.72	11.75[d,g]	18.4[g]	500[c,d,g]	300[g]
$Lu_2Fe_{14}C$	8.71	11.71[d,g,p]	27.2[d,g]	495[d,g]	
$Y_2Fe_{14}C$	8.76	11.86[c]	–	520[c]	

[a] Marusin *et al.* (1985).
[b] Jacobs *et al.* (1989).
[c] Fuerst and Herbst (1991).
[d] Gueramian *et al.* (1987).
[e] Verhoef, de Boer, *et al.* (1989b).
[f] Helmholdt and Buschow (1988).
[g] De Boer, Huang, *et al.* (1988).
[h] Buschow, de Mooij, and Denissen (1988a).
[i] Denissen *et al.* (1988b).
[j] Abache and Oesterreicher (1985).
[k] N. C. Liu and Stadelmaier (1986).
[l] Pedziwiatr *et al.* (1986a).
[m] Verhoef, de Boer, *et al.* (1990).
[n] De Boer, Verhoef, *et al.* (1988).
[o] Verhoef, de Boer, *et al.* (1989a).
[p] Denissen *et al.* (1988a).

ropy (shown by ^{155}Gd Mössbauer-effect work on $Gd_2Fe_{14}C$ by Buschow, de Mooij, *et al.*, 1988); the largest Fe moment at the $8j_2$ site; and analogous thermal-expansion anomalies generated by the spontaneous volume magnetostriction of the iron sublattice (Buschow, 1988b). Using ^{161}Dy Mössbauer spectroscopy, Gubbens *et al.* (1988) estimated a coupling constant j_{RF} for $Dy_2Fe_{14}C$ which is the same as the corresponding value for $Dy_2Fe_{14}B$. Radwański *et al.* (1989) measured the high-field magnetization of polycrystalline samples of the Gd, Tb, Dy, Ho, Er, Tm, and Lu carbides and analyzed the results via the phenomenological free-energy expression of Radwański and Franse (1988).

Some research on replacements in $R_2Fe_{14}C$ compounds has been performed. De Boer, Verhoef, *et al.* (1988) investigated $Nd_{1.8}Lu_{0.2}Fe_{14}C$ and $Nd_{2-x}Dy_xFe_{14}C$ ($0 \leq x \leq 2$) systems; magnetization measurements on the latter indicate a FOMP in the Nd-rich regime similar to that characterizing $Nd_2Fe_{14}B$. Manganese substitution has been found to facilitate sample preparation, and its effect on various magnetic properties has been explored in the Ce (Jacobs *et al.*, 1989), Pr (Buschow, Denissen, *et al.*, 1988; Verhoef, de Boer, *et al.*, 1989b), Nd (Buschow, de Mooij, and Denissen, 1988b), Ho (Verhoef, de Boer, *et al.*, 1990), and Er (Verhoef, de Boer, *et al.*, 1989a) compounds. Verhoef, de Boer, *et al.* (1989b) report evidence for FOMPs in $Pr_2Fe_{14-x}Mn_xC$ for $x \leq 5$, and mean-field analyses of magnetization curves in $Ho_2Fe_{14-x}Mn_xC$ (Verhoef, de Boer *et al.*, 1990) and $Er_2Fe_{14-x}Mn_xC$ (Verhoef, de Boer, *et al.*, 1989a) have been employed to estimate the intersublattice molecular-field coefficient n_{RT} which, as in analogous work on Mn-substituted $R_2Fe_{14}B$ compounds (see Sec. VI.B), is virtually independent of Mn concentration. Cooling in an applied magnetic field generates pronounced changes in the low-temperature magnetization of $Pr_2Fe_{14-x}Mn_xC$ and $Ho_2Fe_{14-x}Mn_xC$; these magnetohistory effects have been attributed to the presence of narrow Bloch walls whose propagation can be thermally activated (Buschow, Denissen, *et al.*, 1988; Jacobs *et al.*, 1990). As in the boride systems, Co substitution for Fe enhances the Curie temperature (J. L. Sanchez *et al.*, 1989b).

F. Multiple substitutions

Studies involving replacement of two of the R, Fe, or B components in $R_2Fe_{14}B$ have been aimed mostly at improving the magnetic properties of Pr- and Nd-based systems and at optimizing the characteristics of materials in which the R constituent comprises mixtures of rare-earth elements more abundant than Nd or Pr alone. Enhancements of both H_a and T_c relative to their $R_2Fe_{14}B$ values have been observed for $R'_2Fe_{12-x}Co_2T_xB$ materials in which (i) R′=synthetic mischmetal (29 at. % La, 50 at. % Ce, 5 at. % Pr, 16 at. % Nd; approximately the abundances in ore bodies) or R′=didymium (5 at. % Ce, 15 at. % Pr, 80 at. % Nd) and T=Al or Mo (Jurczyk, 1988b) and (ii) R′=didymium and T=Cr, Si, Ta, V, or W (Jurczyk, 1988c). The didymium systems investigated are characterized by theoretical maximum energy products $(BH)^*_{\max}$ approaching the ~64 MGOe value for

$Nd_2Fe_{14}B$; mischmetal depresses $(BH)^*_{\max}$ substantially. Increases in H_a, but in most cases at the expense of saturation magnetization and $(BH)^*_{\max}$, have been reported for $R_{2-x}R'_xFe_{12}Co_2B$ with R=Pr, Nd and R'=Tb, Dy (Fujii *et al.*, 1986); $Pr_{1.9}Zr_{0.1}Fe_{12}Co_2B$ and $Nd_{1.9}Zr_{0.1}Fe_{12}Co_2B$ (Jurczyk and Wallace, 1986a); $Nd_{1.9}Ti_{0.1}Fe_{12}Co_2B$ and $Nd_{1.9}Hf_{0.1}Fe_{12}Co_2B$ (Jurczyk, 1987b); $Pr_{2-x-y}Nd_xR'_yFe_{11.6}Co_2Al_{0.4}B$ with R=Tb, Dy (Pourarian, Sankar, and Wallace, 1988); $Pr_{1.9}Dy_{0.1}Fe_{13-x}Co_1Nb_xB$ (Jurczyk and Chistjakov, 1989a); $Nd_2Fe_{13.8}Mo_{0.1}Nb_{0.1}B_{1-x}C_x$ (J. F. Liu and Luo, 1989); $Nd_2Fe_{14-x}Co_xB_{0.5}C_{0.5}$ (X. K. Sun *et al.*, 1989a); $Pr_2Fe_{14-x}Co_xB_{1-y}C_y$ (X. K. Sun *et al.*, 1990); $Pr_{2-x}Dy_xFe_{14-y-z}Re_yCo_zB$ (Jurczyk, 1990b); and $Nd_{2-x}R_xFe_{12-y}Re_yCo_2B$ with R=Tb, Dy (Jurczyk and Chistyakov, 1990). High-field magnetic properties and spin-reorientation phenomena in the $Nd_{2-x}Gd_xFe_{10}Co_4B$ compounds have been examined systematically by Z-D. Zhang, Sun, *et al.* (1990c).

Pourarian, Sankar, *et al.* (1987) noted a reduction in the anisotropy field of $Pr_{1.6}Nd_{0.4}Fe_3Co_{11}B$ compared to that for $Pr_{1.6}Nd_{0.4}Co_{14}B$. The decrease is consistent with measurements on $Pr_2Fe_{14-x}Co_xB$ in the same concentration regime (Pedziwiatr, Jiang, and Wallace, 1986; Bolzoni, Coey, *et al.*, 1987; Grössinger, Krewenka, *et al.*, 1987b). The H_a behavior of $Pr_2Fe_{14-x}Co_xB$, especially the rapid rise observed for $x \gtrsim 10$, is not fully understood. Bolzoni, Coey, *et al.* (1987) have extracted a suggestive correlation between the anomalous variations of the Pr anisotropy and the c/a ratio with x and have speculated that the concentration dependence of H_a can be attributed to changes in the Pr crystal fields associated with transition-metal site preferences, while Gavigan, Li *et al.* (1988b) have speculated that the Pr anisotropy variation is connected with valence instability of the Pr ion for $x \lesssim 10$ and normal Pr^{3+} behavior for higher Co content.

Malik *et al.* (1990) studied spin reorientation in $Nd_{0.5}Er_{1.5}Fe_{14-x}T_xB$ (T=Al, Co) systems via ac susceptibility measurements; Al levels $x=2,3$ were found to induce a second transition whose character remains to be clarified.

G. Hydrides

Many R-3*d* intermetallic compounds, of which $LaNi_5$ is perhaps the best known example, are capable of absorbing considerable amounts of hydrogen [for a review of hydrides based on binary intermetallics, see Buschow (1984)], and the $R_2Fe_{14}B$ materials do so as well. L'Héritier *et al.* (1984) first demonstrated that isostructural hydrides of the $R_2Fe_{14}B$ (and $R_2Co_{14}B$) series form, and from this and other early work (Oesterreicher and Oesterreicher, 1984; Abache and Oesterreicher, 1985; Coey *et al.*, 1985; Dalmas de Réotier *et al.*, 1985b; Ferreira *et al.*, 1985; Friedt *et al.*, 1985; D. Fruchart *et al.*, 1985; L'Héritier and Fruchart, 1985; H. Oesterreicher and Abache, 1985) it became clear that hydrogenation produces a number of significant changes in the physical properties. $R_2Fe_{14}BH_x$ systems form for $0 \leq x \lesssim 5$, are stable at room temperature, and, relative to the unhydrided parent compounds, feature (i) increased lattice parameters and unit-cell volumes ($\Delta V/V \sim 3-6\%$); (ii) enhanced Fe moments; (iii) higher Curie temperatures ($\Delta T_c \sim 50$ K); and (iv) markedly lower anisotropy fields.

D. Fruchart *et al.* (1985) developed a model for the hydrogen filling based on the occupation of four interstitial, tetrahedral sites having R_3Fe and R_2Fe_2 coordinations. The model predicts a maximum hydrogen content $x=5.5$, in good agreement with experiments, and it has been used successfully to interpret neutron-diffraction measurements on $Ce_2Fe_{14}BH_{3.7}$, $Ce_2Fe_{14}BD_{3.7}$, $Er_2Fe_{14}BD_{2.6}$, and $Y_2Fe_{14}BD_{3.6}$ (Dalmas de Réotier *et al.*, 1987). The cerium hydride (or deuteride) exhibits a fascinating valence change having a parallel in the α-γ transition in cerium metal; the Ce ions in $Ce_2Fe_{14}B$ are tetravalent (or nearly so), but, on hydriding, *one* of the Ce sites (the 4*f*) develops a magnetic moment equal, within experimental accuracy, to the $2.1\mu_B$ value for Ce^{3+} (Dalmas de Réotier *et al.*, 1987; D. Fruchart *et al.*, 1987).

Magnetization measurements on $Y_2Fe_{14}BH_x$ have established that the average Fe moment increases by a few percent on hydriding (Andreev *et al.*, 1986; Coey *et al.*, 1986; Pourarian *et al.*, 1986; Pareti *et al.*, 1988). The hyperfine fields determined via ^{57}Fe Mössbauer spectroscopy are also enhanced (e.g., Ferreira *et al.*, 1985; Cadogan and Coey, 1986; Coey *et al.*, 1986; Friedt *et al.*, 1985, 1986), but to a lesser extent, a circumstance that has led Coey *et al.* (1986) to conclude that the conversion factor ($\simeq 150$ kOe/μ_B) widely used to relate hyperfine fields to Fe moments in the parent compounds does not apply to the hydrides. The moment increase certainly indicates that hydrogen exerts an appreciable influence on the electronic structure; its origin is unclear, however, in the absence of any more direct information on the electronic properties. Possible mechanisms include the following: (i) hydrogen may create low-lying states that are filled from the 3*d* bands, leading to a lower Fermi energy, increased exchange splitting, and larger Fe moments (Andreev *et al.*, 1986; Wallace, Pourarian, *et al.*, 1987); (ii) narrowing of the 3*d* bands by the lattice expansion could produce greater 3*d* electron localization and concomitant moment enhancement (Ferreira *et al.*, 1985); and (iii) the overlap of Fe 3*d* and R (5*d*,6*s*) wave functions might be screened by hydrogen and thus increase the localization and magnitude of the Fe moments (Dalmas de Réotier *et al.*, 1987; D. Fruchart *et al.*, 1988). At least some of the T_c enhancement in the hydrides stems from the larger Fe magnetization, but the unit-cell expansion and an increase in the Fe-Fe exchange coupling constant j_{FF} likely play a role also (Andreev *et al.*, 1986; Friedt *et al.*, 1986).

With regard to spin-reorientation phenomena, the $R_2Fe_{14}BH_x$ systems offer even more complex and interesting behavior than their unhydrided antecedents. On hydrogenation the planar→axial spin-reorientation temperature T_s of $Er_2Fe_{14}B$ is raised by ~30 K (Dalmas de Réotier *et al.*, 1987; L. Y. Zhang *et al.*, 1988a), T_s for the canted→axial transition in $Nd_2Fe_{14}B$ is reduced by ~40 K (Pourarian *et al.*, 1986; Wiesinger *et al.*, 1987), but the temperature of the similar reorientation in $Ho_2Fe_{14}B$ increases by as much as 15 K at $x=4$ (Regnard *et al.*, 1987). The variation of T_s with x has been reported for a number of the hydrides by D. Fruchart *et al.* (1990). More profoundly, moment rearrangements have been observed in the hydrides of $R_2Fe_{14}B$ compounds that exhibit no such changes. In $Dy_2Fe_{14}BH_x$ Ferreira *et al.* (1985) and Coey *et al.* (1987) inferred noncollinear magnetic structures from magnetization measurements, D. Fruchart *et al.* (1988) reported a spin reorientation at $T_s \sim 100$ K, and L. Y. Zhang *et al.* (1988a) found $T_s \sim 45$ K for $x=4.2$. Axial→planar transitions as functions of hydrogen concentration and temperature have been reported in $Ce_2Fe_{14}BH_x$, $Pr_2Fe_{14}BH_x$, $Y_2Fe_{14}BH_x$ (Pourarian *et al.*, 1986) and $Gd_2Fe_{14}BH_x$ (L. Y. Zhang *et al.*, 1988a; Bartashevich and Andreev, 1990). Figure 20 displays the magnetic phase diagram determined by L. Y. Zhang *et al.* (1988a) for the Gd materials. Since the gadolinium ion can be plausibly assumed to remain trivalent in the hydrides, the results in Fig. 20 imply that the spin reorientation arises from the impact of hydrogen absorption on the Fe sublattice, rather than from exchange and crystal-field effects on the R ion (the case for the canted→axial transitions in $Nd_2Fe_{14}B$ and $Ho_2Fe_{14}B$) or from competition between R and Fe sublattice anisotropies (as for the planar→axial reorientations in $Er_2Fe_{14}B$, $Tm_2Fe_{14}B$, and $Yb_2Fe_{14}B$).

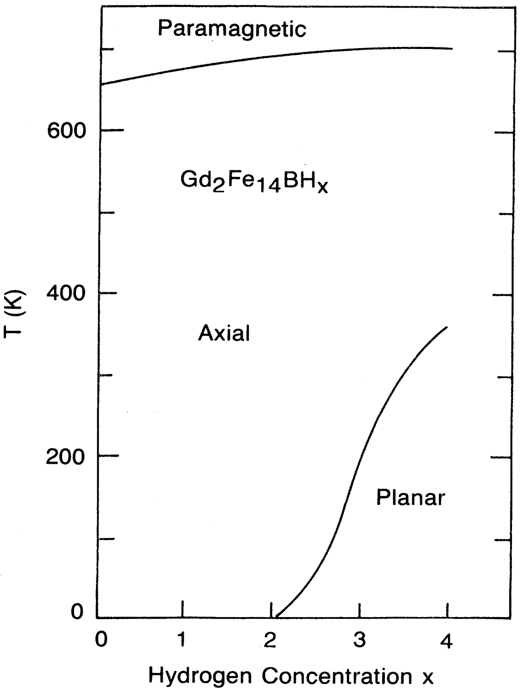

FIG. 20. Magnetic phase diagram for $Gd_2Fe_{14}BH_x$ (adapted from L. Y. Zhang *et al.*, 1988a).

Quite generally, hydrogen depresses both the rare-earth and the iron contributions to the magnetocrystalline anisotropy (cf. Friedt *et al.*, 1986; J. P. Sanchez *et al.*, 1986; Pareti, Bolzoni, *et al.*, 1987; Wiesinger *et al.*, 1987; Andreev and Bartashevich, 1990b), and this aspect makes the $R_2Fe_{14}B$ hydrides unsuitable as permanent-magnet materials. Absorption and subsequent desorption of hydrogen can, however, produce fine powders appropriate for the preparation of sintered magnets; hydrogen-decrepitated Nd-Fe-B magnet alloys have been the focus of a number of investigations, including those of Harris *et al.* (1985, 1987), McGuiness *et al.* (1986, 1989; McGuiness, Ahmed, *et al.*, 1990), Harris (1987), McGuiness and Harris (1988), Moosa and Nutting (1988), J. Chen and Kronmüller (1990), Harris and McGuiness (1990), N. C. Liu and Kim (1990), and Moosa *et al.* (1990a, 1990b).

Some results on cobalt-containing hydrides are available. L'Héritier *et al.* (1984) showed that the $Nd_2Fe_{14}B$ structure type is maintained by the $R_2Co_{14}BH_x$ series, with the unit-cell volume again expanded by hydrogen. L. Y. Zhang *et al.* (1988b) investigated $R_2Co_{14}BH_x$ systems with R = La, Pr, Nd, Sm, Gd, Tb, and Y; in contrast to the Fe-based materials, hydrogen decreases the Co sublattice magnetization, and it also reduces both spin-reorientation temperatures in $Nd_2Co_{14}B$. Structural and magnetic properties of the hydrides of $Pr_{2-x}Dy_xCo_{14}B$, $Pr_{2-x}Er_xCo_{14}B$ (Pourarian, Jiang, Sankar, and Wallace, 1988) and $Pr_2Fe_{14-x}Co_xB$ (Pourarian, Jiang, and Wallace, 1987) have been reported as well (see also Pourarian, 1990).

VII. TECHNOLOGY: PRACTICAL PERMANENT MAGNETS

In order to serve as a base for a viable permanent magnet, a stoichiometric compound must meet the three principal requirements of (i) a Curie temperature T_c significantly exceeding any magnet operating temperature, (ii) high spontaneous magnetization M_s, and (iii) a large magnetocrystalline anisotropy as measured, for instance, by the anisotropy field H_a necessary to divert the magnetization from an easy to a hard direction. The upper limit for the zero-field or remanent magnetization M_r ($\equiv B_r/4\pi$) of a practical magnet is set by M_s, and that for the intrinsic coercivity H_{ci} (the reverse field for which the magnetization M of a sample vanishes) is dictated by H_a.

Technologically important permanent-magnet compounds such as $SmCo_5$ and $Nd_2Fe_{14}B$ are characterized by large and uniaxial (two equivalent easy magnetization directions) anisotropy, but uniaxial anisotropy is not an indispensable attribute as sometimes asserted. In fact, if large enough anisotropy energy barriers were to separate the easy directions in a material having a greater number of equivalent easy directions, a magnet composed of an isotropic distribution of crystallites of that material could feature a ratio of remanent to saturation magnetization M_r/M_s greater than the 0.5 maximum value for a uniaxial system. This is of practical interest because a larger fraction of M_s could be realized as remanence without magnetic alignment of the crystallites. For example, an isotropic magnet based on a cubic compound with the eight $\langle 111 \rangle$ directions easy (e.g., $TbFe_2$) could have $M_r/M_s=\sqrt{3}/2=0.866$. Clark (1973) reported magnetic hardening [$H_{ci}\simeq 3.4$ kOe; $(BH)_{max}\simeq 7$ MGOe] of $TbFe_2$ via annealing of an amorphous precursor.

Fabrication of a practical magnet from a compound possessing suitable intrinsic properties demands a specific preparation method and an associated starting ingot composition. The technical magnetic characteristics B_r, H_{ci}, and energy product $(BH)_{max}$ are extrinsic inasmuch as they depend crucially on the microstructure of the material. The microstructure involves the size, shape, and orientation of the crystallites of the compound and also the nature and distribution of secondary phases, which usually control domain-wall formation and motion and hence determine the magnetization and demagnetization behavior. (In the opposite extreme of a single crystal, reversed domains can nucleate and grow very easily at room temperature; H_{ci} and the other technical properties are negligible, since there is no impediment to domain-wall motion.) Depending on the preparation technique and the secondary constituents, the starting composition yielding optimum magnetics can deviate appreciably from the stoichiometry of the major phase. Two quite distinct methods are in commercial use for producing Nd-Fe-B magnets: the rapid-solidification technique of melt spinning and the traditional powder-metallurgy (sintering) approach.

A. Melt-spun magnets

Melt spinning has been employed for some time in the production of soft (i.e., very-low-coercivity) amorphous magnetic alloys for such applications as transformer cores, but its use in hard-magnet technology represents a fundamental departure from conventional powder-metallurgy methods. The melt-spinning procedure involves ejection of molten starting alloy through a crucible orifice onto the surface of a substrate disc (generally copper because of its high thermal conductivity) rotating with surface velocity v_S. Because the rare earths are very reactive chemically, the process is carried out in an inert atmosphere, most often argon gas. The cooling or quench rate attainable by melt spinning can be as high as 10^6 K/s, and that rate can be varied by changing v_S, which in first approximation is directly proportional to the cooling rate. For R-Fe-B and related materials ribbons are produced that are typically 30–50 μm thick, 1–3 mm wide, and have lengths on the millimeter or centimeter scale depending on v_S. Ruhl (1967) has investigated cooling rates for such processes by numerically solving the one-dimensional heat-transfer equation, and an intuitively appealing discussion of the influence of melt-spinning process variables on ribbon thickness and width has been given by Liebermann and Graham (1976).

1. Nd-Fe-B

a. Ribbon characteristics

The microstructure and magnetic properties of melt-spun neodymium-iron-boron ribbons are sensitively dependent on the quench rate (i.e., on v_S), with H_{ci} and $(BH)_{max}$ each exhibiting a maximum as a function of v_S (see, for example, Croat *et al.*, 1984a, 1984b; Ogilvy *et al.*, 1985; Hilscher *et al.*, 1986; Wecker and Schultz, 1987a; Xu *et al.*, 1989; G. X. Huang *et al.*, 1990). This point is illustrated in Fig. 21, which displays demagnetization curves obtained by Croat *et al.* (1984b) for powdered and compacted $Nd_{0.135}Fe_{0.817}B_{0.048}$ ribbons melt spun at $v_S=14$, 19, and 35 m/s together with corresponding scanning electron micrographs of ribbon fracture surfaces. High quench rates ($v_S \gtrsim 30$ m/s) produce essentially amorphous, "overquenched" materials with negligible H_{ci} and $(BH)_{max}$; Xu *et al.* (1989) have identified the decrease of H_{ci} with increasing v_S in this quench-rate regime with the growth of the amorphous fraction. Quench rates near $v_S=19$ m/s in the example of Fig. 21 yield ribbons having the highest coercivities ($H_{ci}\sim 14$ kOe) and energy products [$(BH)_{max}\sim 14$ MGOe]. The scanning electron micrograph for $v_S=19$ m/s in Fig. 21 shows that these optimally quenched ribbons consist of spheroidal $Nd_2Fe_{14}B$ grains with an average diameter of ~ 300 Å. Comparable grain sizes have

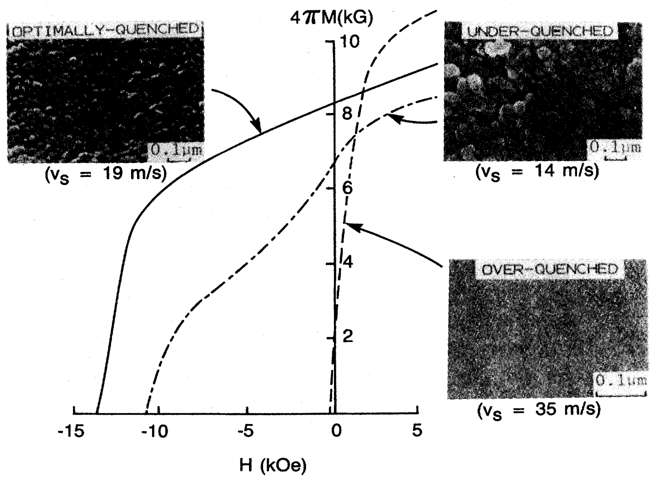

FIG. 21. Room-temperature demagnetization curves and corresponding scanning electron micrographs of melt-spun $Nd_{0.135}Fe_{0.817}B_{0.048}$ ribbon fracture surfaces.

been detected by scanning tunneling microscopy (Corb *et al.*, 1987), field-ion microscopy (Hütten and Haasen, 1987, 1991), and transmission electron microscopy studies (Y. L. Chen, 1985; Mishra, 1986, 1987a), which have revealed that the distribution of *c* axes is spatially, and hence magnetically, isotropic throughout most of the ribbon volume and that a very thin (~ 20 Å) Nd-rich, B-deficient amorphous phase of approximate composition $Nd_{0.7}Fe_{0.3}$ (close to the eutectic in the binary Nd-Fe phase diagram) is present in the intergranular regions (see Fig. 22). $Nd_2Fe_{14}B$ comprises about 95% of the volume. Some preferential orientation of the easy *c* axes normal to the ribbon plane has been produced by decreasing the quench rate (Dadon *et al.*, 1987; Coehoorn and Duchateau, 1988; Tu *et al.*, 1988) or by increasing the melt temperature (Yamasaki *et al.*, 1989), but at the expense of coercivity. As v_S is reduced below the value leading to optimum magnetics, ribbons comprised of progressively larger $Nd_2Fe_{14}B$ crystallites and characterized by decreasing H_{ci} and $(BH)_{max}$ are formed (cf. the $v_S = 14$ m/s results in Fig. 21).

Canting of the magnetization away from the *c* axis in $Nd_2Fe_{14}B$ below the spin-reorientation temperature $T_s \simeq 135$ K (see Sec. IV.A.3) leads to two-step demagnetization of melt-spun Nd-Fe-B ribbons: a substantial magnetization decrease at low reverse field is followed by a second sharp decline as H_{ci} is approached at higher reverse field. This effect can be understood in terms of the isotropic $Nd_2Fe_{14}B$ crystallite distribution characterizing the ribbons and the intrinsic easy-direction behavior; it has the concomitant deleterious consequence that the coercivity decreases with temperature below T_s (Hilscher *et al.*, 1986; Durst and Kronmüller, 1987; Durst *et al.*, 1987; Hadjipanayis and Kim, 1987; Heisz and Hilscher, 1987; Pinkerton, 1988b). Pinkerton (1988b) demonstrated that the temperature dependence of the effective remanence (extrapolated from the high-field magnetization) correlates well with that of the canting angle in $Nd_2Fe_{14}B$ and that the anomalies do not occur in melt-spun Pr-Fe-B whose principal constituent, $Pr_2Fe_{14}B$, does not exhibit spin reorientation.

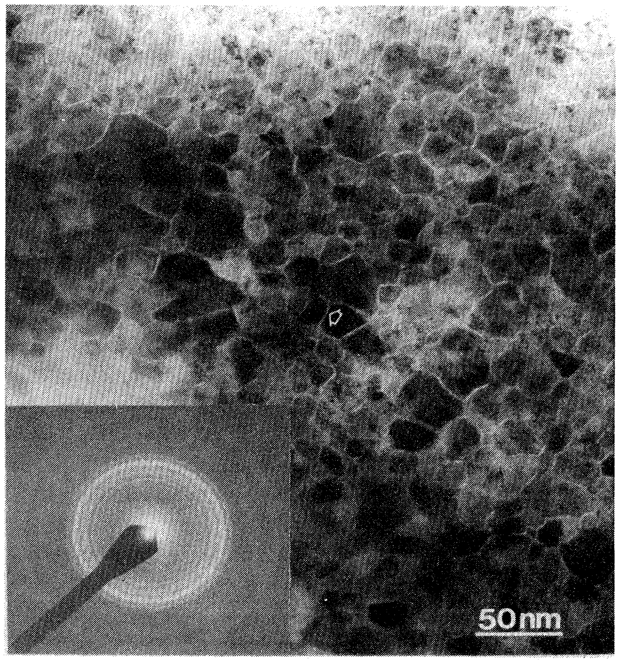

FIG. 22. Bright-field transmission electron micrograph of optimally quenched Nd-Fe-B ribbon (Mishra, 1986). The inset is a selected area diffraction pattern whose rings indicate random distribution of $Nd_2Fe_{14}B$ grains. Note the very thin intergranular phase indicated by the arrow.

From the technological perspective it is significant that largely amorphous, overquenched ribbons, melt spun at quench rates required only to exceed a minimum value rather than confined to a narrow interval, can be suitably annealed to nearly duplicate the properties of optimum direct-quenched materials (Croat *et al.*, 1984a). Devitrification of overquenched Nd-Fe-B ribbons has been investigated by a number of groups. The crystallization temperature is ~ 900 K and the activation energy for crystallization is $E_c \sim 3$ eV, both quantities somewhat dependent on starting composition (Wecker and Schultz, 1987a; Tu *et al.*, 1988; Jha *et al.*, 1989). Crystallization apparently occurs primarily via diffusion-controlled growth with a constant rate of nucleation (Tu *et al.*, 1988), but Mulyukov *et al.* (1989) report evidence for a second stage having a lower activation energy (~ 1 eV), which they ascribe to crystallite growth following the exhaustion of nucleation sites. Noting, among other indications, a large disparity between the measured E_c and that predicted using a model assuming homogeneous nucleation, Jha *et al.* (1989) concluded that crystallization in the Nd-Fe-B system is likely governed by heterogeneous nucleation. Carr *et al.* (1988) annealed overquenched ribbons to various crystallite sizes and observed optimum magnetic properties for grain diameters of 400–500 Å, consistent with direct-quench results. Muir *et al.* (1989) examined the impact of composition and annealing rate on the coercivity, finding that H_{ci} can be improved by crystallization at rapid rates.

b. Consolidation techniques

Fabrication of a bulk magnet necessitates consolidation of the brittle melt-spun ribbons into a dense form. Lee and co-workers have developed three means for accomplishing this (Lee, 1985; Lee *et al.*, 1985). The first and most straightforward procedure is to cold press coarsely ground, optimally quenched ribbons or annealed overquenched ribbons with a bonding medium such as epoxy. Due to the extremely fine particle size, no degradation of the properties accompanies pulverization, making melt-spun materials very desirable for bonded-magnet production. The flat geometry of the ribbon fragments (~ 0.5 mm$\times$0.5 mm$\times$40 μm) facilitates efficient packing so that densities of $\sim 85\%$ with respect to $Nd_2Fe_{14}B$ can be realized with modest pressures of 600–700 MPa. Like its constituent ribbons, the resulting bonded magnet is magnetically isotropic. The remanence is reduced from the optimally quenched ribbon value $B_r \sim 8$ kG (see Fig. 21) to ~ 7 kG, and the energy product is ~ 9 MGOe.

Complete densification of melt-spun ribbons is afforded by the second procedure, hot pressing. Requisite pressures P and temperatures T depend on the starting alloy composition, but for compositions near $Nd_{0.135}Fe_{0.817}B_{0.048}$ (as in Fig. 21), full density is achieved for $P \sim 100$ MPa and $T \sim 970$ K. The most desirable grain size is developed by hot pressing overquenched ribbons, and variation of the magnetics with pressing conditions has been investigated by Gwan *et al.* (1987) as well as by Lee (1985) and Lee *et al.* (1985). Energy products of the hot-pressed magnets are in the 10–20 MGOe range.

Uniaxial hot pressing introduces only a slight ($\sim 10\%$) crystallographic alignment of the easy c axes parallel to the press direction. Much greater alignment ($\sim 75\%$), and consequently much larger energy products, can be obtained by the third method, in which an initial hot press is followed by another in a die cavity of greater diameter. This second hot press in a larger die, designated die upsetting, produces bulk lateral plastic flow and an accompanying reduction in ribbon thickness. Nozawa *et al.* (1988) and Tokunaga *et al.* (1989b) have examined the dependence of the magnetics on composition and on process parameters such as strain rate, working temperature, and the extent of deformation; greatest magnetic alignment was achieved only if the original sample height was reduced by at least a factor of four during die upsetting. Xie and Graham (1990) have suggested that the deformation behavior is controlled by atomic diffusion in the grain boundary regions. Like their hot-pressed precursors, die-upset magnets are fully dense, and energy products as large as 45 MGOe have been attained (Croat, 1989a).

Figure 23 shows optical micrographs of these three forms of rapidly solidified Nd-Fe-B magnets and also representative room-temperature demagnetization curves measured with the applied field parallel to the press direction. It is clear that the hot-pressed ribbons deform plastically to fill the available volume without developing the cracks apparent in the bonded magnet. The diminished ribbon thickness resulting from the lateral plastic flow in the die-upset magnet is evident.

The optical micrographs of Fig. 23 convey the overall packing features of the ribbons comprising the magnets, but it is the microstructure on the dimensions of grains and intergranular regions *within* the ribbons that controls the macroscopic magnetic properties. The grain texture of a hot-pressed magnet, prepared from overquenched ribbons, is similar to that of optimally quenched ribbons in Fig. 21, although somewhat coarser (Mishra, 1987a, 1987b). Die upsetting, however, modifies the spheroidal grains in the hot-pressed ribbons to platelets ~ 3000 Å in diameter and ~ 600 Å thick (Mishra and Lee, 1986; Mishra, 1987a, 1987b), as shown in the transmission electron micrograph of Fig. 24. From measurements of the thermal and electrical conductivities of a die-upset magnet Morelli *et al.* (1990) inferred a crystallite dimension of ~ 1000 Å, which agrees well with the directly observed platelet thickness. The platelets are stacked transverse to the press direction with the easy c axis perpendicular to the face of each grain. A crystalline (fcc)

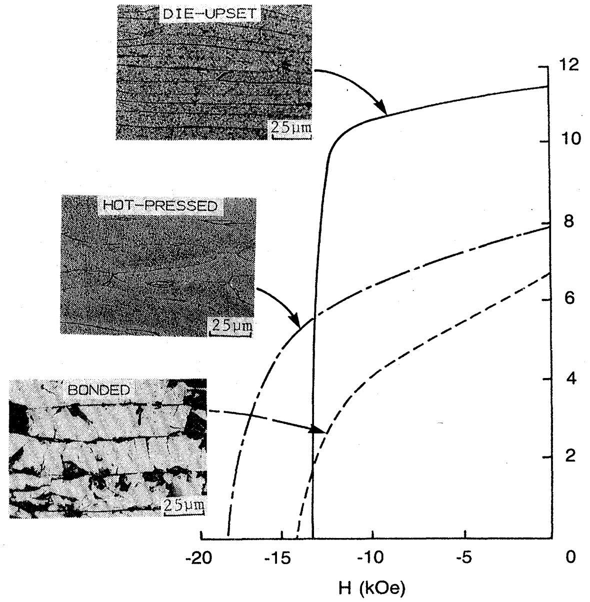

FIG. 23. Room-temperature demagnetization curves and optical micrographs of bonded, hot-pressed, and die-upset Nd-Fe-B magnets prepared from melt-spun ribbons.

FIG. 24. Transmission electron micrograph of a die-upset Nd-Fe-B magnet (courtesy R. K. Mishra).

phase, again near the $Nd_{0.7}Fe_{0.3}$ composition, forms in the intergranular regions (Mishra, 1987b). The growth and stacking of these platelet grains is responsible for the magnetic alignment and the increased energy product. Mishra (1987b), Mishra *et al.* (1988, 1990), and L. Li and Graham (1990) have demonstrated that the mechanism for grain alignment during die upsetting involves grain-boundary sliding and anisotropic grain growth. These findings agree qualitatively with the results of Tenaud *et al.* (1987), who demonstrated that the *a* axis is the easy growth direction of $Nd_2Fe_{14}B$ single crystals and inferred that, under an applied stress, only grains with *a* axes perpendicular to the press direction can be expected to grow. Powdered die-upset material has been employed to prepare anisotropic bonded magnets (Eshelman *et al.*, 1988; Nozawa *et al.*, 1988; Croat, 1989b; Tokunaga, Nozawa, *et al.*, 1989b).

c. Elemental additives

Compositional modification of technological magnet materials offers the prospect of altering both the intrinsic properties of the stoichiometric component and the nature of the secondary phases and their influence on the magnetic characteristics, particularly the coercivity. Improvements in the properties of melt-spun Nd-Fe-B ribbons and magnets prepared from them have been sought via introduction of low concentrations (< 5 at. %) of other elements. Doping with Nb or Zr has been reported to improve H_{ci} (Kohmoto *et al.*, 1987; S. F. H. Parker, Pollard, Lord, and Grundy, 1987; Yoneyama *et al.*, 1987, 1990; Pollard *et al.*, 1988; Yajima *et al.*, 1988; Wecker and Schultz, 1990; S.-X. Zhou *et al.*, 1990). Low-level Cu additions can increase the coercivity by as much as 30% over that of Cu-free materials; copper segregates preferentially to the intergranular regions (Herbst *et al.*, 1991). The addition of gallium to the starting ingots has been shown to enhance H_{ci} as well as improve the high-temperature behavior of die-upset Nd-Fe-B magnets (Nozawa *et al.*, 1988; Endoh *et al.*, 1989; Panchanathan and Croat, 1989; Tokunaga *et al.*, 1989a, 1989b; Akayama *et al.*, 1990; S.-X. Zhou *et al.*, 1990). By combining small amounts of fine elemental powders with Nd-Fe-B ribbons prior to hot deformation as a means to explore diffusion alloying of additives, Fuerst and Brewer (1990, 1991) found coercivities enhanced by 10–90% in hot-pressed and die-upset magnets containing Ag, Au, Cd, Cu, Ir, Mg, Ni, Pd, Pt, Ru, or Zn.

2. Cobalt-containing alloys

Efforts to magnetically harden cobalt-substituted (Pr,Nd)-Fe-B alloys underscore the importance of composition in producing magnets containing $R_2Fe_{14-x}Co_xB$ as the principal constituent and having the best technological properties. Such materials are of interest because Co substitution can elevate substantially the Curie temperature T_c of $R_2Fe_{14}B$ (cf. Sec. VI.B), and that enhancement may be desirable for some applications.

Initial investigations of Co-containing, melt-spun Nd-Fe-B were based on Fe-only compositions and include $Nd_{0.15}(Co_yFe_{1-y})_{0.77}B_{0.08}$ with $y \leq 0.60$ (Wecker and Schultz, 1987b) and $Nd_{0.135}(Co_yFe_{1-y})_{0.822}B_{0.043}$ with $y \leq 1$ (Fuerst and Herbst, 1988a). For $y \leq 0.35$, T_c is indeed enhanced in these materials, and the temperature stability of the remanence B_r is improved relative to $y=0$. In the $y \geq 0.40$ regime, however, H_{ci} and $(BH)_{max}$ deteriorate severely due to the formation of progressively larger amounts of $Nd_2Fe_{17-x}Co_x$, which is characterized by easy basal-plane magnetization, rather than $Nd_2Fe_{14-x}Co_xB$, which is uniaxial at room temperature for all Co levels.

Exploring the extremes of cobalt replacement, Fuerst and Herbst (1988b, 1988c) obtained energy products as large as ~5 MGOe in Nd-Co-B ribbons consisting chiefly of $Nd_2Co_{14}B$ but prepared from ingot formulations substantially richer in boron than those relevant to Nd-Fe-B. Hot-pressed magnets based on $Nd_2Co_{14}B$ have also been produced (Fuerst and Brewer, 1989). Knowledge of appropriate compositions for Nd-Fe-B and Nd-Co-B facilitated determination of the most suitable starting alloy formulations for Nd-(Fe,Co)-B, and ribbons composed primarily of $Nd_2Fe_{14-x}Co_xB$ and featuring optimum $(BH)_{max}$ were melt spun; the boron content δ of ingot compositions specified by $Nd_\eta(Fe_{1-y}Co_y)_{1-\eta-\delta}B_\delta$ was found to vary linearly with Co concentration y (Fuerst and Herbst, 1989a, 1989b). Figure 25 compares the room-temperature magnetics with the earlier results for fixed Nd:TM:B ratios, and the improvement arising from the compositional modification is evident. Although T_c increases monotonically with y, a uniaxial→basal-plane spin reorientation occurs at a temperature $T_s < T_c$ for $y \gtrsim 0.65$ as a consequence of the competition between the Fe and Co sublattice anisotropies. This intrinsic behavior limits the technological properties: H_{ci}, B_r, and $(BH)_{max}$ vanish as T approaches T_s rather than T_c in that Co concentration range.

Incorporating a plasma activation step to remove surface contaminants, Wada and Yamashita (1990) produced hot-pressed $Nd_{0.13}Fe_{0.65}Co_{0.16}B_{0.06}$ magnets having $(BH)_{max} \simeq 15$ MGOe and $H_{ci} \simeq 17$ kOe.

Melt spinning has also been used to magnetically harden $Pr_2Fe_{14-x}Co_xB$ materials. Overfelt and Becker (1984) early reported substantial improvement of T_c and temperature stability in melt-spun $Pr_{0.16}(Co_yFe_{1-y})_{0.76}B_{0.08}$ as the Co concentration was increased to $y=0.3$. Wecker and Schultz (1989) prepared ribbons composed mainly of $Nd_2Fe_{14}B$-type material over the entire Co substitution range using the $Pr_{0.15}(Co_yFe_{1-y})_{0.77}B_{0.08}$ starting ingot composition; in particular, an intrinsic coercivity of 19.1 kOe was observed for $y=1$. $Pr_2Co_{14}B$ is of interest because it features a room-temperature anisotropy field H_a of $\simeq 100$ kOe, more than a factor of two larger than $H_a(Nd_2Co_{14}B) \simeq 45$ kOe (see Table XIV). Ribbons consisting chiefly of $Pr_2Co_{14}B$ and having coercivities and energy products as large as 25.0 kOe and 5.5 MGOe, respectively, have been obtained through systematic compositional variation by Fuerst, Herbst, and Pinkerton (1988). The $Pr_{0.138}Co_{0.750}B_{0.112}$ formulation was found to maximize H_{ci}, while $Pr_{0.125}Co_{0.775}B_{0.100}$ generated the highest $(BH)_{max}$, illustrating that the most appropriate starting composition depends to some extent on the property to be optimized. Fuerst (1990) varied the TM:B ratio with Co content and prepared melt-spun materials having $Pr_2Fe_{14-x}Co_xB$ as the primary constituent and optimum $(BH)_{max}$.

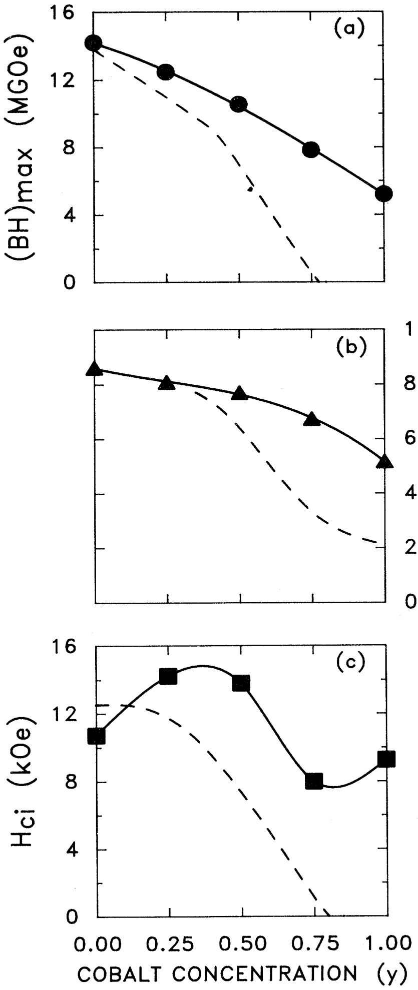

FIG. 25. Room-temperature (a) energy product $(BH)_{max}$, (b) remanence B_r, and (c) intrinsic coercivity H_{ci} vs cobalt concentration y for optimum melt-spun Nd-(Fe,Co)-B ribbons; the dashed lines denote results for $Nd_{0.135}(Fe_{1-y}Co_y)_{0.822}B_{0.043}$ alloys in which the Nd and B concentrations were held fixed as y was varied (Fuerst and Herbst, 1989a).

In melt-spun $Pr_2Fe_{14-x}Co_xB$ with $x \gtrsim 7$, T_c exceeds the crystallization temperature T_x. Otani, Sun, *et al.* (1990) explored the interesting possibility (also recognized by Hadjipanayis, 1986) of annealing such materials in an applied field at a temperature between T_x and T_c to produce crystallite alignment. Some texture was observed in Pr-Co-B heat treated in zero field, but only slight modification occurred in the presence of a 3-kOe field.

Yamamoto *et al.* (1989) systematically investigated a range of (Pr, Nd)-(Fe,Co)-B compositions and obtained $(BH)_{max} \simeq 21$ MGOe for melt-spun $(Nd_{0.5}Pr_{0.5})_{0.11}Fe_{0.72}Co_{0.08}B_{0.09}$. Bonded magnets featuring $H_{ci} \simeq 7.9$ kOe and $(BH)_{max} \simeq 11.1$ MGOe were produced by Yamamoto *et al.* (1990) from melt-spun didymium-(Fe,Co)-B alloys.

3. Other $R_2Fe_{14}B$-based materials

Early survey work by Croat *et al.* (1984b) and Hadjipanayis *et al.* (1984) indicated that melt-spun ribbons containing $R_2Fe_{14}B$ as the major component could be prepared with most of the rare earths and substitutions among them, and the crystallization behavior and magnetic properties of amorphous R-Fe-B materials were also studied (Tao and Hadjipanayis, 1985; Aly *et al.*, 1986). Subsequent efforts have focused on the magnetic hardening of specific $R_2Fe_{14}B$ systems. Yamasaki *et al.* (1986) prepared optimum-quenched mischmetal-Fe-B ribbons with $H_{ci}=9.4$ kOe and $(BH)_{max}=8.1$ MGOe; the material was used to form bonded magnets having corresponding properties of 7.6 kOe and 4.4 MGOe, values that compare very favorably with those for anisotropic ferrite magnets.

Coehoorn *et al.* (1989) successfully produced magnet materials primarily composed of $Nd_2Fe_{14}C$ by annealing melt-spun flakes having a starting composition in a narrow interval near $Nd_{0.135}Fe_{0.796}C_{0.069}$. As-quenched specimens consist mainly of $Nd_2Fe_{17}C_x$, α-Fe, and an amorphous phase, but heat treatment at 1000 K generates $Nd_2Fe_{14}C$. H_{ci} and B_r as large as 10 kOe and 7.2 kG, respectively, were observed in the annealed samples.

Pinkerton (1986a) reported $H_{ci} > 80$ kOe in melt-spun Tb-Fe-B and $H_{ci} > 60$ kOe in Dy-Fe-B at room temperature. These values are records for any magnet material and reflect the huge anisotropy fields of the corresponding $R_2Fe_{14}B$ compounds (Table IV); they imply that substitution by Tb or Dy can increase the coercivity of other R-Fe-B alloys. Ribbons based on $Er_2Fe_{14}B$ and characterized by $H_{ci} \sim 5$ kOe and $(BH)_{max} \sim 3$ MGOe were prepared by Meisner (1987). The theoretical maximum energy product for all three of these materials, however, is roughly a factor of four lower than that of $Nd_2Fe_{14}B$

because of the smaller saturation magnetizations stemming from antiparallel R and Fe moment coupling (see Sec. IV.A.1).

B. Sintered magnets

Powder-metallurgy processing, which involves a sequence of orient, press, and sinter operations on finely divided alloy powders, has long been employed in the commercial production of ferrite and samarium-cobalt magnets. Magnets prepared in this general way are most often simply designated as sintered. Sagawa, Fujimura, *et al.* (1984a) were the first to demonstrate that such methods can be applied to neodymium-iron-boron.

1. Nd-Fe-B

Compositional and processing details vary to some extent, but the canonical preparation procedure is that given by Sagawa, Fujimura, *et al.* (1984a). Induction-melted ingots having the composition $Nd_{0.15}Fe_{0.77}B_{0.08}$, substantially enriched in Nd and B relative both to stoichiometric $Nd_2Fe_{14}B$ ($\sim Nd_{0.12}Fe_{0.82}B_{0.06}$) and to the optimum melt spinning composition $\sim Nd_{0.13}Fe_{0.82}B_{0.05}$, are crushed, milled, and then pulverized to powder with a particle size of ~ 3 μm. The powder is aligned in a magnetic field (~ 10 kOe) and pressed ($P \sim 200$ MPa) perpendicular to the alignment direction. The resulting compact is sintered at ~ 1370 K in argon gas for one hour and cooled quickly. A postsinter anneal at ~ 900 K, again under Ar, improves the coercivity to its maximum value. Extensive discussions of the methodology can be found in the reviews by Ormerod (1985), Sagawa, Hirosawa, *et al.* (1987d), Buschow (1988a), Burzo and Kirchmayr (1989), and Cook and Rossiter (1989). Sagawa, Hirosawa *et al.* (1987d) emphasize that the success of powder-metallurgical fabrication of Nd-Fe-B magnets is due not only to the superior intrinsic properties of $Nd_2Fe_{14}B$ but also to several favorable metallurgical features, such as the fact that $Nd_2Fe_{14}B$, Nd, and the tetragonal compound $Nd_{1+\epsilon}Fe_4B_4$ form a ternary eutectic which makes liquid-phase sintering possible, enabling high densification without significant grain growth. The demagnetization curve of a representative sintered magnet, having an energy product of 36 MGOe, is shown in Fig. 26; it resembles that of the aligned, die-upset magnet in Fig. 23. As is the case for melt-spun Nd-Fe-B and other permanent-magnet materials, improvements in the remanence at the expense of coercivity and vice versa are possible by altering the composition and processing parameters. Narasimhan (1985) achieved an energy product of 45 MGOe using a composition near $Nd_{0.15}Fe_{0.80}B_{0.05}$, and Sagawa, Hirosawa *et al.* (1987d) have reported the record value $(BH)_{\max} \simeq 50.6$ MGOe for a sintered $Nd_{0.13}Fe_{0.81}B_{0.06}$ magnet; in both cases B_r and H_{ci} are respectively higher and lower than the corresponding values for the magnet of Fig. 26.

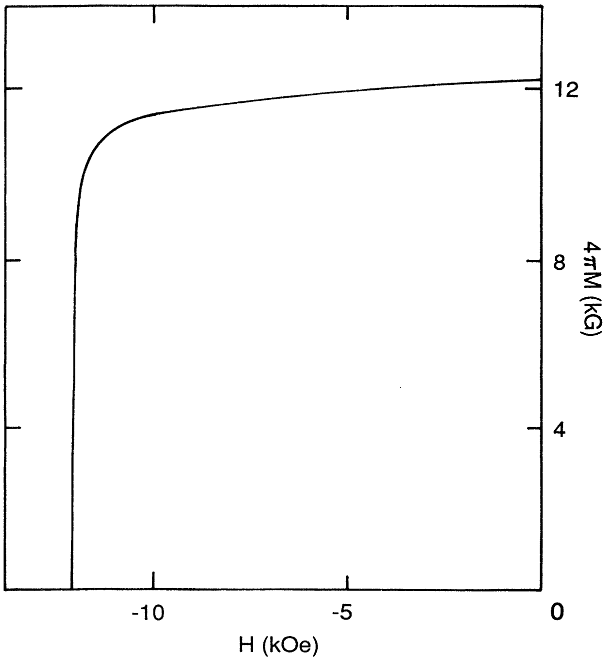

FIG. 26. Room-temperature demagnetization curve of a sintered $Nd_{0.15}Fe_{0.77}B_{0.08}$ magnet characterized by $(BH)_{\max} \simeq 36$ MGOe (after Sagawa, Fujimura, *et al.*, 1984a).

Sintered Nd-Fe-B magnets are relatively complex multiphase systems containing, in addition to $Nd_2Fe_{14}B$, all or most of the following: $Nd_{1+\epsilon}Fe_4B_4$, Nd-rich phases, α-Fe, Nd oxides, and pores. Figure 27 is a composition image of a representative $Nd_{0.15}Fe_{0.77}B_{0.08}$ magnet; the contrast with the simpler microstructure of melt-spun

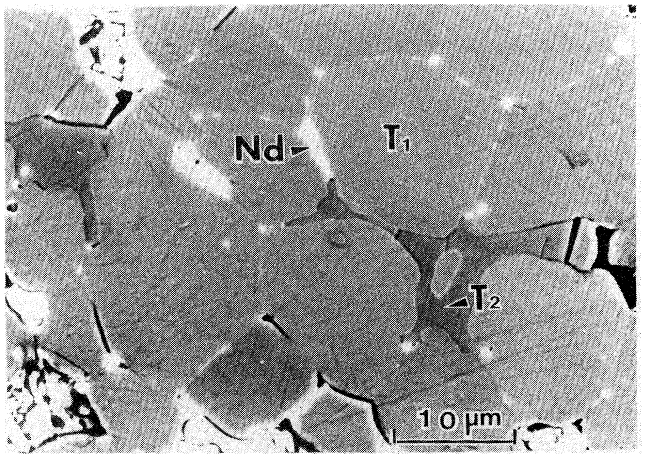

FIG. 27. X-ray composition micrograph of a sintered $Nd_{0.15}Fe_{0.77}B_{0.08}$ magnet; T_1, T_2, and Nd denote $Nd_2Fe_{14}B$, $Nd_{1+\epsilon}Fe_4B_4$, and a Nd-rich phase, respectively (Sagawa, Hirosawa, *et al.*, 1987d).

materials in Figs. 22 and 24 is clear. The major $Nd_2Fe_{14}B$ component occupies ~85% of the volume with an average grain size of ~10 μm (Sagawa, Fujimura, *et al.*, 1984a, 1984b; Sagawa, Hirosawa, *et al.*, 1987d; Durst and Kronmüller, 1985, 1986; Fidler and Knoch, 1989), approximately two orders of magnitude larger than that in optimum melt-spun ribbons. More boron-rich $Nd_{1+\epsilon}Fe_4B_4$, frequently identified in early papers as $Nd_2Fe_7B_6$, forms irregularly distributed, heavily faulted grains of roughly the same size as those of $Nd_2Fe_{14}B$ (Fidler and Yang, 1985; Hadjipanayis, Tao, and Lawless, 1985, 1986; Y.-J. Chang and Qian, 1986). The Curie temperature of $Nd_{1+\epsilon}Fe_4B_4$ ($\epsilon \simeq 0.1$) is ~10 K, and its very intricate crystal structure consists of interpenetrating Nd and Fe sublattices with incommensurate periods (Bezinge *et al.*, 1985, 1987; Buschow *et al.*, 1986; Givord, Moreau, and Tenaud, 1985). A neodymium-rich, *fcc* ($a \sim 5.2$ Å) phase of approximate composition $Nd_{0.95}Fe_{0.05}$ appears at grain-boundary junctions and in thin intergranular layers (see Fig. 27); it serves as a liquid-phase sintering aid in the powder-metallurgy process (Sagawa, Fujimura, *et al.*, 1984a, 1984b; Sagawa, Hirosawa, *et al.*, 1987d; Ramesh, Chen and Thomas, 1987; Fidler *et al.*, 1989). Estimates of the thickness of such intergranular layers range from ~50 Å, indicated by small-angle neutron scattering (Fujii, Saga, *et al.*, 1987) and Auger measurements (Elbicki *et al.*, 1988, 1989; Wallace *et al.*, 1989), to ~200 Å from transmission electron microscopy work (Mishra *et al.*, 1986; Ramesh, Chen, and Thomas, 1987). Other Nd-rich intergranular phases with different structures and compositions have been reported (Fidler, 1985, 1987a, 1987b), α-Fe precipitates have been observed (El-Masry and Stadelmaier, 1985; Hadjipanayis, Lawless, and Dickerson, 1985; Fidler and Tawara, 1988), and inclusions of Nd_2O_3 and other oxides occur (Lemarchand *et al.*, 1988; Fidler and Knoch, 1989). Transmission electron microscopy has been widely used in the microstructural studies, and, as Schrey (1986) and others have emphasized, artifacts can be generated by various means such as oxidation. A *bcc* intergranular phase was reported to have a strong association with the development of coercivity (Hiraga *et al.*, 1985a, 1985b, 1985c; Sagawa, Fujimura, *et al.*, 1985b; Sagawa, Hirosawa, *et al.*, 1986; Suzuki and Hiraga, 1986; Tokunaga *et al.*, 1986), but subsequent investigations (Mishra *et al.*, 1986; Schrey, 1986; Fidler, 1987a; Ramesh, Chen, and Thomas, 1987; Sagawa, Hirosawa, *et al.*, 1987c; Sagawa and Hirosawa, 1988a; Tsubokawa *et al.*, 1988) furnished cogent evidence that the *bcc* phase was an artifact of ion milling in transmission electron microscopy sample preparation. It now appears that smoothing of the intergranular layers is the principal microstructural effect accompanying the postsintering heat treatment which enhances the coercivity (Sagawa and Hirosawa, 1988a; Hirosawa and Tsubokawa, 1990; G. F. Zhou, Fu, *et al.*, 1990); the reduction of irregularities likely impedes reverse domain formation by diminishing the local demagnetization fields produced by sharp projections. Schneider *et al.* (1990) have suggested, however, that dissolution of a metastable ferromagnetic phase ($T_c \simeq 520$ K) in the intergranular regions is the major beneficial effect of the postsinter anneal, and Ramesh (1990) has concluded that anisotropy reduction in grain-boundary regions due to thermal expansion stresses plays a significant role.

Despite the complications introduced by the presence of other phases and the texture of the $Nd_2Fe_{14}B$ grains, Durst and Kronmüller (1986) successfully extracted intrinsic $Nd_2Fe_{14}B$ material parameters from measurements on $Nd_{0.15}Fe_{0.77}B_{0.08}$ magnets.

Large, discontinuous changes in the magnetization of sintered magnets for applied fields near the coercive field in magnitude have been observed by Otani *et al.* (1989; Otani, Coey, *et al.*, 1990) below ~10 K. Each of these Barkhausen jumps, illustrated in Fig. 28, corresponds to magnetization reversal in ~5% of the sample volume and is accompanied by a temperature spike as large as 5 K. Otani, Coey, *et al.* (1990) have interpreted the behavior on the basis of an appealing model in which the magnetization of a small volume V_a first abruptly reverses and then thermally induces domain-wall motion in a larger volume, ~100 V_a; the process is self-sustaining, with the magnetization jumps adiabatically generating the thermal pulses. V_a is identified as the activation volume derived from magnetic viscosity measurements, which indicate $V_a \sim \delta^3$, where $\delta \sim 25$ Å is the low-temperature domain-wall width (cf. Givord, Lienard, *et al.*, 1987; Givord, Tenaud, and Viadieu, 1988a); similar results for V_a have been obtained from measurements of the angular dependence of the coercivity, i.e., the variation of H_{ci} with the angle between the applied field and alignment direction (Otani, Miyajima, *et al.*, 1990). Barkhausen jumps have also been observed in low-

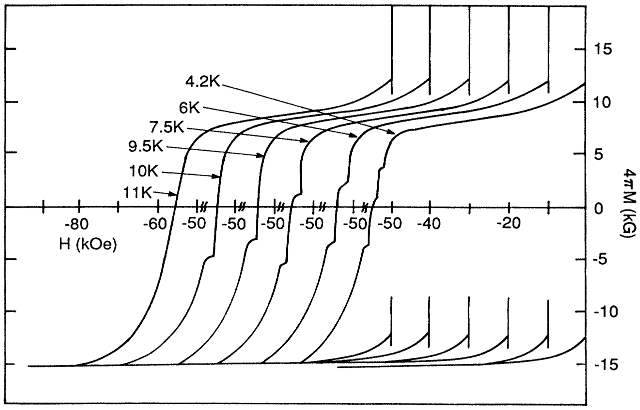

FIG. 28. Magnetization jumps in the second and third quadrants of low-temperature hysteresis loops for a sintered $Nd_{0.15}Fe_{0.77}B_{0.08}$ magnet (adapted from Otani, Coey *et al.*, 1990).

temperature magnetic viscosity data (Hadjipanayis, Lawless, and Dickerson, 1985) and room-temperature Hall voltage traces (Damento and Demer, 1987) of sintered Nd-Fe-B magnets as well as in the magnetization curve of a Dy-substituted sintered magnet at 4 K (Nakagawa, Hiroyoshi, *et al.*, 1987).

As in melt-spun materials, the spin reorientation in $Nd_2Fe_{14}B$ at $T_s \simeq 135$ K produces a shoulder in the magnetization curve of sintered magnets near remanence, which becomes more pronounced with decreasing temperature (Ho *et al.*, 1985; Kuntze *et al.*, 1985; Strnat *et al.*, 1985; Givord, Tenaud, and Viadieu 1986; Otani *et al.*, 1986, 1987; Heisz and Hilscher, 1987; Müller *et al.*, 1987; Ma *et al.*, 1989; Kawai *et al.*, 1990). Heisz and Hilscher (1987) have argued convincingly that, even though factors such as oxidation and the presence of soft-magnetic secondary phases (e.g., α-Fe) may contribute at all temperatures to indented hysteresis loops [as can low-coercivity grains at the surface of a magnet (Givord, Tenaud, and Viadieu, 1986; Hirosawa Tokuhara, and Sagawa, 1987; Fukuno and O'Handley, 1989) and a heterogeneous distribution of grain sizes (Ramesh *et al.*, 1988)], spin reorientation is the dominant influence below T_s. Together with the intrinsic anisotropy variation in $Nd_2Fe_{14}B$, the degree of $Nd_2Fe_{14}B$ crystallite alignment (i.e., texture) exerts crucial impact on the demagnetization behavior. In particular, if a $Nd_2Fe_{14}B$-based magnet produced by any means were perfectly aligned, no shoulder in $M(H)$ due to the moment canting would occur in a field applied parallel to the alignment direction, while the coercivity would vanish below T_s (assuming no in-plane anisotropy) in a perpendicular field (Heisz and Hilscher, 1987; Müller *et al.*, 1987; Ma *et al.*, 1989). The coercivity of well aligned sintered Nd-Fe-B magnets has indeed been observed to approach these limits (see, for example, Grössinger, Krewenka, *et al.*, 1985; Kuntze *et al.*, 1985; Heisz and Hilscher, 1987).

When measured along the alignment direction the coercivity of sintered Nd-Fe-B magnets increases with decreasing temperature below T_s (Durst and Kronmüller, 1985, 1987; Chikazumi, 1986; Hirosawa, Tokuhara, *et al.*, 1986; Durst *et al.*, 1987; Givord, Lienard, *et al.*, 1987; Givord, Tenaud, and Viadieu, 1988a; Grössinger, Krewenka, *et al.*, 1988), the reverse of the situation for isotropic melt-spun ribbons (see Sec. VII.A.1.a.). The deterioration of H_{ci} in the latter is due to the random distribution of the spin-reorienting $Nd_2Fe_{14}B$ crystallites; in aligned die-upset Nd-Fe-B magnets H_{ci} rises with diminishing T (Pinkerton and Fuerst, 1990a, 1990b) as in aligned sintered materials.

With increasing temperature in the $T > T_s$ regime the remanence and coercivity of Nd-Fe-B magnets decline simply because they are limited by the spontaneous magnetization and anisotropy of $Nd_2Fe_{14}B$, which decrease as $T \to T_c$. In some applications the temperature dependence of the technical properties is an important issue; various microwave devices, for example, require persistent flux output at high operating temperature (Potenziani *et al.*, 1985). The temperature behavior is gauged usually by a coefficient specifying the percentage rate of change of a given characteristic with T. For the remanence and coercivity the coefficients can be defined by

$$\alpha(T) \equiv -\frac{d \ln B_r(T)}{dT} \tag{40a}$$

and

$$\beta(T) \equiv -\frac{d \ln H_{ci}(T)}{dT} \tag{40b}$$

or by discrete versions of these. In the 300–400 K range

$$0.1 \lesssim \alpha \lesssim 0.2\ \%/\mathrm{K} \quad \text{and} \quad 0.4 \lesssim \beta \lesssim 0.7\ \%/\mathrm{K}$$

for both sintered and melt-spun Nd-Fe-B magnets (cf. Sagawa, Fujimura, *et al.*, 1984a, 1984b; Sagawa, Hirosawa, *et al.*, 1987d; D. Li *et al.*, 1985; Potenziani *et al.*, 1985; Ma and Narasimhan, 1986a). Compared with the coefficients for Sm-Co magnets, the β values can be twice as large while α is a factor ~3–5 greater; the primary cause is the lower Curie temperature of $Nd_2Fe_{14}B$. Sagawa, Hirosawa, *et al.* (1987d) and Hirosawa, Hanaki, *et al.* (1990) emphasize that a large β is a more serious technological concern, since it can be associated with irreversible loss of magnetic flux after high-temperature exposure. [The so-called irreversible loss actually consists of two components: (i) a fraction recoverable by remagnetizing, and (ii) a permanent, irrecoverable fraction caused by metallurgical degradation of the magnet at elevated temperature.]

2. Compositionally modified materials

Chief among the driving forces for the many investigations of substitutions and additions in sintered, as well as melt-spun, Nd-Fe-B magnets is extension of the useful operating temperature range via enhancement of the Curie temperature and coercivity, improvement (i.e., reduction) of the temperature coefficients α, β, and diminution of the irreversible losses. Sagawa, Fujimura, *et al.* (1984b) first demonstrated that Co substitution increases T_c and decreases α, observing $T_c = 740$ K and $\alpha = 0.07\ \%/\mathrm{K}$ for $x = 0.2$ in $Nd_{0.15}(Fe_{1-x}Co_x)_{0.77}B_{0.08}$ as compared with $T_c = 585$ K and $\alpha = 0.12\ \%/\mathrm{K}$ for $x = 0$. Arai and Shibata (1985) achieved $(BH)_{max} = 42$ MGOe and $\alpha = 0.02\ \%/\mathrm{K}$ over the 300–400 K range in $Nd_{0.16}Fe_{0.66}Co_{0.11}B_{0.07}$. Cobalt substitution introduces microstructural changes, including the formation of the soft-magnetic Laves phase $Nd(Fe,Co)_2$ (Fidler, 1985; Fidler and Yang, 1985; Yamamoto *et al.*, 1987). It is also accompanied by loss of coercivity (see, for example, Ma and Narasimhan, 1986a; Grössinger, Harada, *et al.*, 1987; Grössinger, Keresztes, *et al.*, 1987; Sagawa, Hirosawa, *et al.*, 1987b). Partial replacement of Nd by Dy substantially enhances H_{ci} and reduces β, chiefly by increasing the anisotropy field of $Nd_2Fe_{14}B$, although B_r is lowered somewhat (Sagawa, Fujimura, *et al.*, 1984b; Rodewald, 1985; Tokunaga *et al.*, 1985; Arai *et al.*, 1987; Grössinger, Harada, *et al.*, 1987; Grössinger, Keresztes, *et al.*, 1987; Nakagawa, Hiroyoshi, *et al.*, 1987; Ramesh, Thomas, and Ma, 1987; Handstein *et al.*, 1990). For the $(Nd_{0.53}Dy_{0.47})_{0.15}Fe_{0.77}B_{0.08}$ composition Sagawa, Hirosawa, *et al.* (1987b) achieved $(BH)_{max} \geq 20$ MGOe and $H_{ci} = 50$ kOe, the largest room-temperature coercivity ever observed in a neodymium-based sintered magnet (Sagawa and Hirosawa, 1987, 1988b). Ma and Krause (1987) observed that finer particle size improves coercivity and found that Dy substitution also provides desirable inhibition of grain growth during sintering. Combined Dy and Co substitution is effective in raising T_c and H_{ci} and in decreasing α and the irreversible losses (W. Li *et al.*, 1986; Tokunaga, Tobise, *et al.*, 1986; Tokunaga, Endoh, and Harada, 1987; Arai *et al.*, 1987; Gauder *et al.*, 1988). Using low-field ac thermomagnetic analysis, Strnat *et al.* (1988) found evidence for a thin ferromagnetic grain-boundary layer having T_c 50–80 K lower than that of the bulk in a (Nd,Dy)-(Fe,Co)-B magnet; pinning of residual domain walls in that layer was suggested as the mechanism for coercivity.

A fascinating example of opposing intrinsic and microstructural effects is provided by aluminum substitution. Despite the fact that it *degrades* the anisotropy field of $Nd_2Fe_{14}B$, aluminum can *enhance* H_{ci} of sintered Nd-Fe-B magnets by as much as a factor of two (M. Zhang *et al.*, 1985; Y-C. Yang, James, *et al.*, 1986b; Durst *et al.*, 1987; Handstein *et al.*, 1987; Rodewald, 1987; Grössinger, Haslinger, *et al.*, 1988; Leonowicz *et al.*, 1988; Rodewald and Fernengel, 1988; Hu *et al.*, 1989) and even has a similar influence on Dy-substituted magnets (Kim, 1988a; Strzeszewski, Hadjipanayis, and Kim, 1988; Grössinger, Heiss, *et al.*, 1989). Evidently the coercivity improvement is a consequence of changes in the microstructure introduced by aluminum, but the microstructural information on the role of Al is inconclusive. In addition to the presence of Al in the $Nd_2Fe_{14}B$ matrix, Al enrichment of the Nd-rich intergranular phase has been reported (Schrey, 1986; J. K. Chen and Thomas, 1987; Hauet, Lemarchand, Labulle, *et al.*, 1988), precipitates of an Al-rich phase have been observed among the Nd-rich grains and in the vicinity of pores (Leonowicz *et al.*, 1988), and crystallites of $Nd(Fe,Al)_2$ embedded in the intergranular phase have been detected (Grieb *et al.*, 1989); phase relations in the Nd-Fe-Al system have been studied by Grieb *et al.* (1990). While also observing $Nd(Fe,Al)_2$, Fidler *et al.* (1989), on the other hand, found no evidence for Al enrichment of the Nd-rich intergranular phase. Knoch *et al.* (1989; Knoch, Grieb, *et al.*, 1990; Knoch, Henig, and Fidler, 1990) and Schneider *et al.* (1990) have shown that Al substitution decreases the wetting angle between $Nd_2Fe_{14}B$ and the surrounding liquid during sintering and have made the quite plausible suggestion that the improved wettability affords more complete separation of $Nd_2Fe_{14}B$ grains and enhances H_{ci} by reducing exchange interactions among them. G. F. Zhou, Sun, *et al.* (1990) reached a similar conclusion regarding the role of Al in studies of (Nd,Dy)-(Fe,Co)-B magnets substituted with both Al and Nb. Maki *et al.* (1989) analyzed domain structures in an Al-substituted magnet and identified two regimes of distinct demagnetization behavior demarcated by a critical value of the applied magnetizing field.

Aside from the capability of greatly enhancing H_{ci}, aluminum substitution decreases the saturation magnetization and Curie temperature, but these effects can be overcome by partial replacement of Fe with Co. Simultaneous substitution of Co and Al in sintered Nd-Fe-B magnets has been explored by Ma and Narasimhan (1986b), Jiang, Chen, *et al.* (1988), and by Mizoguchi *et al.* (1986a), who achieved $B_r = 13.2$ kG, $H_{ci} = 11.0$ kOe, $(BH)_{max} = 41.0$ MGOe, $T_c = 770$ K, and $\alpha = 0.07\,\%/K$ (half the value for an unsubstituted reference magnet) for the $Nd_{0.15}Fe_{0.625}Co_{0.16}B_{0.055}Al_{0.01}$ composition. Mizoguchi *et al.* (1986b, 1987) have speculated that the occurrence of an Al-containing $Nd(Fe,Co)_2$ Laves phase is related intimately to the coercivity behavior of the substituted alloys. Kim (1988b) observed that Al substitution can improve α, β and substantially reduce irreversible losses in (Nd,Dy)-(Fe,Co)-B magnets.

Low levels of gallium and niobium can also benefit the coercivity and thermal stability of sintered magnets. In a survey of twenty elemental substituents in a Nd-(Fe,Co)-B alloy Endoh *et al.* (1987) found Ga to be most effective in enhancing H_{ci} and reported that the Ga-substituted magnets feature better magnetic properties and lower irreversible losses than those containing Al or Dy; Tsutai *et al.* (1987) reported $B_r = 13.1$ kG, $H_{ci} = 12.2$ kOe, $(BH)_{max} = 40$ MGOe, $\alpha = 0.08\,\%/K$, and $\beta = 0.5\,\%/K$ over the 300–450 K interval for $Nd_{0.145}Fe_{0.63}Co_{0.16}Ga_{0.01}B_{0.055}$. Knoch, Grieb, *et al.* (1990) have speculated that Ga acts similarly to Al by improving wettability of the matrix phase, and Endoh *et al.* (1990b) have suggested that the addition of Ga serves to smooth the grain boundaries as well as to enhance domain-wall pinning in those regions. The addition of niobium has been shown to increase H_{ci} in Nd-Fe-B (Hu *et al.*, 1988; Pan *et al.*, 1990), (Nd,Dy)-Fe-B (Parker, Grundy, and Fidler, 1987; Parker, Pollard, *et al.*, 1987) and (Nd,Dy)-(Fe,Co)-B (Xiao *et al.*, 1987) and to reduce irreversible losses in such alloys (Tokunaga, Harada, and Trout, 1987). Microstructural work has revealed that small (~ 500 Å), finely dispersed Nb-containing precipitates appear within the hard-magnetic grains and may be responsible for improving H_{ci} by serving as domain-wall pinning sites (Parker, Grundy, and Fidler, 1987; Parker, Pollard, *et al.*, 1987; Schrey, 1988; Ishikawa *et al.*, 1989; G. F. Zhou, Chuang, *et al.*, 1990). Rodewald and Wall (1989) also observed such precipitates, but, puzzlingly, found no appreciable improvement of properties with Nb substitution for Fe in the $Nd_{0.156}Fe_{0.769}B_{0.075}$ composition. Combined Nb and Ga substitution in (Nd,Dy)-(Fe,Co)-B magnets can be more effective in elevating H_{ci}

and decreasing irreversible losses than Nb admixture alone (Tokunaga, Endoh, and Harada, 1987; Tokunaga, Kogure, *et al.*, 1987; G. F. Zhou, Sun, *et al.*, 1988; G. F. Zhou, Zhong, *et al.*, 1990).

Among other substituents investigated, Mo (M. Zhang *et al.*, 1985; Shen *et al.*, 1987; Rodewald and Schrey, 1989; Hirosawa, Tomizawa, *et al.*, 1990), V (Hirosawa, Tomizawa, *et al.*, 1990; Sagawa, Tenaud, *et al.*, 1990), Cr (Rodewald and Fernengel, 1988; Leonowicz, 1990a, 1990b), Mg (C. H. Lin *et al.*, 1988), and W (Rodewald and Schrey, 1990) can enhance H_{ci}, but in most cases to a lesser extent than Dy, Al, Ga, or Nb, whereas Si (Fernengel, 1989) and Y (Fernengel, 1990) cause it to deteriorate. With the object of producing sintered magnets from more abundant rare-earth elements, Okada *et al.* (1985) and Okada and Homma (1985) examined alloys based on Ce, Pr, and Nd mixtures, achieving energy products as large as 40 MGOe. Anisotropic (Ce,Pr,Nd)-Fe-B bonded magnets with $H_{ci} \simeq 7.3$ kOe and $(BH)_{max} \simeq 7.7$ MGOe were prepared via a powder-metallurgy procedure by Paik *et al.* (1987). Jiang, Chen, *et al.* (1988) obtained $(BH)_{max} = 39.4$ MGOe, $B_r = 12.9$ kG, and $H_{ci} = 12.4$ kOe for the $Pr_{0.15}Fe_{0.79}B_{0.06}$ composition and also found that simultaneous Co and Al substitution improves T_c and reduces the temperature coefficients α and β. Coercivities exceeding 50 kOe have been observed by Endoh *et al.* (1990a) in sintered magnets based on $Tb_2Fe_{14}B$. Only one $R_2Co_{14}B$-based material has been magnetically hardened by powder-metallurgy methods: Christodoulou, Wallace, and Massalski (1989) reported $(BH)_{max} = 10.3$ MGOe and $H_{ci} = 5.2$ kOe for a Pr-Co-B magnet having $Pr_2Co_{14}B$ as the primary component.

C. Magnetization reversal and coercivity mechanisms

There is no question that the fundamental origin of the coercivity in Nd-Fe-B magnets is the large magnetocrystalline anisotropy of $Nd_2Fe_{14}B$. If magnetization reversal involved only coherent rotation, however, the intrinsic coercivity H_{ci} would equal the anisotropy field, $H_a \simeq 73$ kOe at room temperature (Table IV), and even with the inclusion of shape anisotropy the *lower* bound for the coercivity of an isolated, ellipsoidal particle is (Brown, 1945)

$$H_{ci} = H_a - N(4\pi M_s) , \tag{41}$$

where N is an appropriate demagnetization factor. With $N = \frac{1}{3}$ for a sphere, the right side of Eq. (41) is still ~ 70 kOe and at least a factor of three *greater* than the ~ 20 kOe maximum coercivity of an aligned $Nd_2Fe_{14}B$-based magnet. This disparity also characterizes other permanent-magnet materials and is known as Brown's paradox (see Aharoni, 1962; Kronmüller, 1987; Kronmüller, Durst, Hock, and Martinek, 1988; Kronmüller, Durst, and Sagawa, 1988). Its relevance should be assessed specifically for small, well separated $Nd_2Fe_{14}B$ particles, a challenging experimental task; Richter *et al.* (1989) have made preliminary efforts in this regard. Because actual Nd-Fe-B magnets are structurally complex systems whose $Nd_2Fe_{14}B$ grains are not simple ellipsoids and can interact, the discrepancy between the theoretical limit set by Eq. (41) and the observed H_{ci} values must arise from magnetization reversal via generation and growth of reverse domains and the attendant formation and/or motion of domain walls. [Fanning, curling, and buckling processes are only pertinent to systems governed by shape anisotropy (see Chikazumi, 1986).] Domains in Nd-Fe-B magnets have indeed been observed by many investigators using techniques such as the magneto-optical Kerr effect and Lorentz electron microscopy.

Most of the numerous efforts to understand the coercivity of Nd-Fe-B magnets rely on interpretations based on either the nucleation of reverse domains or the pinning of domain walls by inhomogeneities, the mechanisms earlier found pertinent to Sm-Co materials [a valuable discussion of the extremes of nucleation- and pinning-controlled coercivity in Cu-modified Sm-Co magnets was given by Becker (1976)]. Distinctions between these two possibilities have been drawn according to guidelines such as the initial susceptibility behavior, domain structure, microstructure, and the dependence of H_{ci} on magnetizing field, temperature, and the angle between the applied field and the alignment direction. The literature on this subject is often perplexing, and its terminology somewhat less than precise, in part because of the phenomenological and model-dependent nature of the criteria but also because the two mechanisms are not mutually exclusive. As Livingston (1985a, 1987) has emphasized, reverse-domain nucleation and domain-wall pinning occur in magnets of both designations. In nucleation-controlled systems pinning of domain walls is required to impede the propagation of magnetization reversal from grain to grain, since otherwise reversal in a single grain would precipitously reverse the entire magnet, and in the pinning-controlled case unpinning of a domain wall from a localized defect is virtually indistinguishable, at least by presently available techniques, from nucleation of a reverse domain (see also Hadjipanayis and Kim, 1988).

Three related parameters of relevance to the coercivity issue are the domain-wall width δ, the domain-wall energy density σ_W, and the critical single-domain particle diameter D_c. Estimates of σ_W have been extracted from measurements of δ or the domain width in Nd-Fe-B magnets and stoichiometric $Nd_2Fe_{14}B$ samples using Lorentz microscopy (Suzuki *et al.*, 1984; Mishra, 1986, 1987b; Mishra and Lee, 1986; Bras *et al.*, 1988), the Kerr effect (Durst and Kronmüller, 1985, 1986; Livingston, 1985b; Sagawa, Fujimura, *et al.*, 1985b; R. Szymczak *et al.*, 1985, 1987), or the Bitter pattern method (Plusa *et al.*, 1986, 1987). σ_W has also been obtained from coercivity data on sintered Nd-Fe-B magnets of varying grain size

(Fernengel, 1987). Representative values of these quantities at room temperature are $\delta \sim 50$ Å, $\sigma_W \sim 30$ mJ/m^2, and $D_c \sim 0.3$ μm. D_c is the diameter of an isolated sphere below which formation of a domain wall is energetically unfavorable and above which a multidomain configuration is stable (see Kittel and Galt, 1956). Although D_c is defined in the noninteracting limit, it nevertheless implies a sharp qualitative distinction between sintered Nd-Fe-B magnets, whose average grain diameter, $D_g \sim 10$ μm, is much larger than $D_c \sim 0.3$ μm, and melt-spun ribbons and hot-pressed magnets, for which $D_g \sim 300$ Å$=0.03$ μm$\ll D_c$. This contrast alone suggests that different reversal mechanisms may be operative in the two classes. For the die-upset magnets there is no clear distinction between grain size and D_c, since the diameter of the platelet grains is ~ 0.3 μm.

1. Sintered magnets

It is the prevailing view that sintered Nd-Fe-B magnets at room temperature are nucleation-dominated systems with domain-wall pinning relegated to a comparatively minor role. The results of a variety of experiments and analyses have been advanced as evidence for this interpretation. Domain observations show that in the thermally demagnetized state each $Nd_2Fe_{14}B$ grain has a multidomain structure (Hadjipanayis, Tao, and Lawless, 1985; Livingston, 1985b; Sagawa, Fujimura, *et al.*, 1985b), consistent with the property that $D_g \gg D_c$, and that the domain walls inside each grain move quite easily in small applied fields (Pastushenkov *et al.*, 1987). The latter characteristic is compatible with both the steep virgin magnetization curve (Sagawa, Fujimura, *et al.*, 1984a; Hadjipanayis and Tao, 1985; Handstein *et al.*, 1985; Heinecke *et al.*, 1985; D. Li and Strnat, 1985; Zhao *et al.*, 1986; Durst and Kronmüller, 1987; Heisz *et al.*, 1988; Eckert *et al.*, 1990) and with transmission electron spectroscopy studies indicating that the $Nd_2Fe_{14}B$ grains are mostly defect-free (Sagawa, Fujimura, *et al.*, 1984b; Fidler, 1985; Hadjipanayis, Lawless, and Dickerson, 1985; Hiraga *et al.*, 1985a; Y.-J. Chang and Qian, 1986; Hadjipanayis, Tao, and Lawless, 1986). Furthermore, measurements of minor hysteresis loops show that the coercivity saturates in magnetizing fields $H \geq H_{\mathrm{sat}}$ with $H_{\mathrm{sat}} < H_{\mathrm{ci}}$; Durst and Kronmüller (1985, 1987) have argued that H_{sat} may be considered the field associated with the pinning of domain walls at or near grain boundaries and that, because $H_{\mathrm{ci}} > H_{\mathrm{sat}}$, the coercivity must be controlled by the nucleation of reverse domains. From a study of minor loops for boron-rich Nd-Fe-B and Pr-Fe-B magnets Hirosawa and Sagawa (1987) concluded that local demagnetizing fields are the principal source of the dependence of H_{ci} and B_r on magnetizing field; in their view, domain walls experience an energy barrier near grain-boundary regions that originates from magnetostatic effects generated by sharp protrusions of $R_2Fe_{14}B$ grains rather than from inhomogeneity of the anisotropy energy as other authors assume (see below).

A rough estimate of H_{ci} for a nucleation mechanism was made by Livingston (1985a), who suggested that

$$H_{\mathrm{ci}} \sim \frac{\sigma_W}{M_s r_0} - N_{\mathrm{eff}}(4\pi M_s) \ . \tag{42}$$

The first term on the right represents the local internal field necessary to nucleate a reverse domain in a spherical defect region of radius r_0, and the second is an effective local demagnetization field that assists reversal. For $r_0 = 100$ Å and $N_{\mathrm{eff}} = 1$, this relation yields $H_{\mathrm{ci}} \sim 11$ kOe, on the order of the coercivities observed in sintered Nd-Fe-B magnets. Inasmuch as this model apparently requires a distribution of such small defects, however, it is not consistent with most of the microstructural studies. [The model is more germane to a pinning interpretation for the melt-spun ribbons and hot-pressed magnets, for which r_0 may be viewed quite reasonably as the $Nd_2Fe_{14}B$ grain radius and the first term on the right side of Eq. (42) describes the surface tension impeding expansion of a reverse domain.]

Building on earlier work (Durst and Kronmüller, 1985, 1987; Durst *et al.*, 1987; Kronmüller *et al.*, 1987; Kronmüller, Durst, Hock, and Martinek, 1988), Kronmüller, Durst, and Sagawa (1988) performed detailed analyses of the temperature dependence of H_{ci} which favor a nucleation-controlled coercivity mechanism for sintered Nd-Fe-B magnets. In their fullest treatment H_{ci} is written as

$$H_{\mathrm{ci}} = \frac{2K_1}{M_s}\alpha_K \alpha_\psi - N_{\mathrm{eff}}(4\pi M_s) \ , \tag{43}$$

where α_K describes inhomogeneity of the magnetocrystalline anisotropy in grain-boundary regions whose anisotropy is lower than that of the matrix phase and in which reverse-domain nucleation is supposed to occur, α_ψ accounts for misaligned grains, and N_{eff} is an average effective local demagnetization factor. Noting that empirical generalizations of Eq. (41) such as Eq. (43) enter nucleation as well as pinning models, Kronmüller, Durst, and Sagawa (1988) contrast predictions based on micromagnetic theory in both cases. Considering a planar inhomogeneity of thickness r_0 these authors obtain

$$\alpha_K^{\mathrm{pin}} = \begin{cases} \dfrac{1}{3\sqrt{3}}\dfrac{\pi r_0}{\delta}\left[\dfrac{A}{A'} - \dfrac{K_1'}{K_1}\right] \quad (r_0 < \delta) & \text{(44a)} \\[2ex] \dfrac{2\delta}{3\pi r_0} \quad (r_0 > \delta) & \text{(44b)} \end{cases}$$

for a pinning-controlled mechanism and

$$\alpha_K^{\mathrm{nuc}} = 1 - \frac{1}{4\pi^2}\frac{\delta^2}{r_0^2}\left[\left[1 + \frac{4\Delta K r_0^2}{A}\right]^{1/2} - 1\right]^2 \tag{45}$$

if nucleation dominates. δ is an approximate domain-wall width, A and K_1 are the exchange and anisotropy constants of the matrix phase, the primes in Eq. (44a) refer to the perturbed layer, and for $r_0 > \delta$ the anisotropy profile through the inhomogeneity is modeled by

$$K_1(z)=K_1-\frac{\Delta K}{\cosh^2(z/r_0)} . \tag{46}$$

In the $r_0 \ll \delta$ limit Eq. (45) differs substantially from Eq. (44a). The grain misalignment factors used in the two cases are

$$\alpha_\psi^{\text{pin}}=\frac{1}{\cos\psi} , \tag{47}$$

$$\alpha_\psi^{\text{nuc}}=\frac{1}{\cos\psi}\frac{1}{[1+\tan^{2/3}\psi]^{3/2}}\left[1+\frac{2K_2}{K_1}\frac{\tan^{2/3}\psi}{1+\tan^{2/3}\psi}\right] , \tag{48}$$

where ψ is the angle between the applied field and the alignment direction. While α_ψ^{pin} is an increasing function of ψ, α_ψ^{nuc} exhibits a minimum. Comparing $H_{\text{ci}}(T)$ data with the pinning description, Kronmüller, Durst, and Sagawa (1988) find (i) inconsistent results for the inferred values of r_0 and (ii) α_K^{pin} parameters exceeding the maximum of 0.3 expected from their model of the grain-boundary region. For the nucleation description, on the other hand, plots of H_{ci}/M_s vs $(2K_1/M_s^2)\alpha_K^{\text{nuc}}\alpha_\psi^{\text{nuc}}(\text{min})$, where $\alpha_\psi^{\text{nuc}}(\text{min})$ is chosen to yield a lower limit for H_{ci}, can be fit with a spectrum of r_0 values consistent with Eq. (45) and are linear over an extended temperature range for the three sintered magnets considered. Figure 29 shows results for a $Nd_{0.15}Fe_{0.77}B_{0.08}$ magnet; the two r_0 values are upper and lower bounds. Kronmüller, Durst, and Sagawa (1988) remark that the temperature dependence of $\alpha_\psi^{\text{nuc}}(\text{min})$ is important to the linearity of the plots below room temperature; the approximation for α_ψ^{nuc}, Eq. (48), contains the second anisotropy constant K_2, which becomes significant as T decreases in the vicinity of the spin reorientation. The departure of the curves in Fig. 29 from linearity for $T \gtrsim 450$ K indicates, according to Kronmüller, Durst, and Sagawa (1988), that domain-wall pinning governs the coercivity in that high-temperature range. Maki and Kronmüller (1990) have elaborated on the overriding importance of the grain alignment distribution, and Martinek and Kronmüller (1990) and Martinek *et al.* (1990) have amplified the point that the coercivity is limited by the minimum nucleation field for misaligned grains.

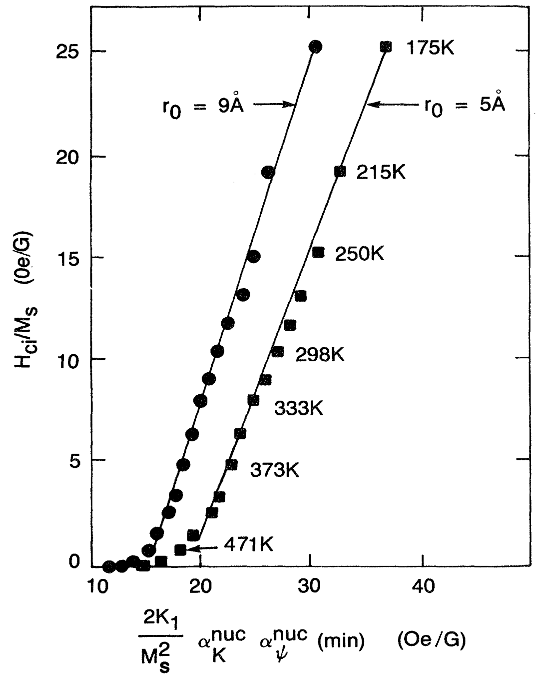

FIG. 29. H_{ci}/M_s vs $(2K_1/M_s^2)\alpha_K^{\text{nuc}}\alpha_\psi^{\text{nuc}}(\text{min})$ for a sintered $Nd_{0.15}Fe_{0.77}B_{0.08}$ magnet (after Kronmüller, Durst, and Sagawa, 1988).

A simpler version of Eq. (43) has been employed frequently to analyze the temperature dependence of H_{ci}:

$$H_{\text{ci}}=cH_a-N_{\text{eff}}(4\pi M_s) . \tag{49}$$

Again, the first term on the right is interpreted as the nucleation field of a reverse domain, the second describes average local demagnetizing effects, and accommodation of data by Eq. (49) is usually assumed to provide support for a nucleation-controlled coercivity mechanism. With $H_a=2K_1/M_s$ Eq. (49) is not obeyed in the case of sintered Nd-Fe-B magnets for temperatures approaching T_s from above (Durst and Kronmüller, 1985; Hirosawa, Tokuhara, *et al.*, 1986; Grössinger, Krewenka, *et al.*, 1987a; Sagawa and Hirosawa, 1987, 1988b; Sagawa, Hirosawa, *et al.*, 1987a, 1987c). The appropriate expression for H_a in relations such as Eqs. (41), (43), and (49) when K_2 is significant is uncertain, even with the tacit premise that the conventional expansion of the anisotropy energy, Eq. (26b), is correct; varying choices have been discussed by Kronmüller (1985), Herzer *et al.* (1986), Hirosawa, Tokuhara, *et al.* (1986), and Martinek and Kronmüller (1990). In part to circumvent difficulties associated with the inclusion of K_2, Hirosawa, Sagawa, and co-workers have extensively studied systems in which K_1 dominates over an extended temperature interval. It has been found that Eq. (49) adequately describes $H_{\text{ci}}(T)$ for Pr-Fe-B magnets of various compositions (Hirosawa, Tokuhara, *et al.*, 1986; Sagawa and Hirosawa, 1987, 1988a, 1988b; Sagawa, Hirosawa, *et al.*, 1987a, 1987c; Hirosawa and Sagawa, 1988; Hirosawa, 1989) and Co-substituted Nd-Fe-B materials (Sagawa, Hirosawa, *et al.*, 1987b). A linear relation between the temperature-independent constants c and N_{eff} as the elemental fractions are varied has been identified for some classes of materials (Tang *et al.*, 1988; Hirosawa and Tsubokawa, 1990). Ramesh (1990) has derived a relation similar to Eq. (49) via an energy minimization argument and has applied it successfully to Ce- and Dy-substituted Nd-Fe-B sintered magnets.

A somewhat different picture of nucleation-driven coercivity in sintered Nd-Fe-B magnets has emerged from the work of Givord and co-workers (Givord, Lienard, *et al.*, 1987; Givord, Tenaud, *et al.*, 1987; Givord, Heiden, *et al.*, 1988; Givord, Tenaud, and Viadieu, 1988a, 1988b) relying on measurements of the magnetic viscosity, the time development of the magnetization after the applied field has been changed suddenly [a useful introduction to the subject of magnetic viscosity can be found in Gaunt (1986)]. These authors consider that magnetization reversal is initiated (i.e., a domain wall is formed) in a volume equal to the activation volume V_a extracted from the observed magnetic viscosity. A model of the associated activation energy leads to the relation [recast from Eq. (11′) of Givord, Tenaud, and Viadieu, 1988a]

$$H_{\mathrm{ci}} \sim \frac{c\sigma_W}{V_a^{1/3} M_s} - N_{\mathrm{eff}}(4\pi M_s) \ . \tag{50}$$

Use of the measured temperature dependence of V_a in Eq. (50) enables a good fit to $H_{\mathrm{ci}}(T)$ data with appropriate choice of the constants c and N_{eff}. [Experimentally it is found that V_a is proportional to the cube of the domain-wall with δ (see also Singleton and Hadjipanayis, 1990), so that with the usual proportionalities $\delta \propto \sqrt{A/K_1}$ and $\sigma_W \propto \sqrt{AK_1}$ Eq. (50) has the same form as Eq. (49) for $H_a = 2K_1/M_s$.] Extension of the model to the angular dependence of H_{ci} (Givord, Tenaud, and Viadieu, 1988a, 1988b) also allows good agreement with experiment, and with the results of Kronmüller *et al.* (1987). The essential point stressed by Givord and collaborators is that a reasonable description of $H_{\mathrm{ci}}(T)$ and $H_{\mathrm{ci}}(\theta)$ measurements is afforded by their model without assuming that the anisotropy in the activation volume is strongly reduced with respect to the bulk, which differs from the view (e.g., Kronmüller, Durst, and Sagawa, 1988) that nucleation occurs in low-anisotropy regions of the magnet. From magnetic viscosity measurements on sintered Pr-Fe-B and Nd-Fe-B magnets Street *et al.* (1990) have suggested, however, that the model of Givord, Tenaud, and Viadieu (1988a, 1988b) requires modification with regard to the treatment of misaligned grains, while Jubb and McCurrie (1987) concluded from their minor loop and magnetic viscosity measurements that the hard-magnetic behavior of sintered magnets is determined chiefly by domain-wall pinning.

Demagnetization curves based on an inhomogeneous nucleation mechanism for sintered Nd-Fe-B magnets have been computed by Ramesh and Srikrishna (1988), Blank (1990), and Sakuma and Takeda (1990). A feature common to these otherwise quite distinct investigations is that reverse domains are assumed to be formed at the surfaces of grains where the anisotropy is reduced compared to the interior. Ramesh and Srikrishna (1988) employ a statistical approach to infer the distribution of nucleation fields from experimental hysteresis loops. Their findings predict that H_{ci} depends logarithmically on the average number of surface defects per grain and, hence, on the average grain size D_g (H_{ci} increasing with decreasing D_g). One perplexing aspect of their work is that hysteresis loops are computed for various prescribed grain-size distributions but not for the measured distribution of the magnet whose $M(H)$ curve was used to extract a nucleation field distribution. The simulation of Blank (1990) is carried out for a two-dimensional array of $(124)^2$ grains; local demagnetizing effects are included in a well defined way, and exchange coupling of adjacent grains is allowed. The model produces demagnetization curves whose shape favorably resembles measured curves, and the results suggest that the enhancement of coercivity by the postsinter anneal could arise from healing of defects at grain surfaces or from improved exchange decoupling of $Nd_2Fe_{14}B$ crystallites. Sakuma and Takeda (1990) find that the magnetic inhomogeneity lowers the nucleation field for reverse-domain formation while raising its angular profile, in qualitative agreement with the results of Kronmüller *et al.* (1987). Via numerical work Fukunaga and Fukuda (1990) examined the effect of reductions in both the anisotropy and the exchange interaction due to a magnetic inhomogeneity; decreased exchange was found to have negligible impact on the nucleation field. The simulated coercivity and its angular dependence could be roughly fit to experiment by assuming the anisotropy reduction to occur within 30–50 Å of the surface of $Nd_2Fe_{14}B$ grains.

An especially noteworthy aspect of the research on coercivity mechanisms is that it has produced valuable suggestions for improving sintered magnets, which can be summarized as follows. First, small $R_2Fe_{14}B$ grains are desirable for reducing the volume impacted by reverse-domain nucleation at a defect, and the grains should be smooth to limit the deleterious effect of local demagnetizing (stray) fields at sharp edges and protrusions (Sagawa and Hirosawa, 1987, 1988b; Sagawa, Hirosawa, *et al.*, 1987a; Kronmüller, Durst, and Sagawa, 1988; Ramesh *et al.*, 1988; Hirosawa, Hanaki, *et al.*, 1990). Second, a thin, smooth, defect-free grain-boundary layer serves to isolate the $R_2Fe_{14}B$ crystallites magnetically and provides a barrier to demagnetization of neighboring grains (Adler and Hamann, 1985; Sagawa and Hirosawa, 1988a; Hirosawa and Tsubokawa, 1990; Schneider *et al.*, 1990). Finally, it is helpful to minimize the amount of secondary phases such as $R_{1+\epsilon}Fe_4B_4$ and oxides, as well as pores, which can act as nucleation sites (Durst *et al.*, 1987; Schneider *et al.*, 1987).

2. Melt-spun materials

Research on the origin of coercivity in melt-spun systems, especially hot-pressed and die-upset magnets, is less extensive than that for sintered materials, and the spectrum of opinion is not as nearly unilateral as it is in the case of sintered magnets. Lorentz-microscopy investigations show that domain walls are pinned at grain boundaries in optimum ribbons (Hadjipanayis, Tao, and Lawless, 1985; Hadjipanayis, Dickenson, and Lawless, 1986; Mishra, 1986). The same statement applies to hot-pressed magnets, whose microstructure is essentially identical to that of the ribbons, and to die-upset magnets, in which the domain walls are parallel to the c axis (or, press direction) and can pass through many grains, unaffected if they intersect the faces of the platelets at right angles but pinned at grain edges (Mishra and Lee, 1986; Mishra, 1987b). Durst and Kronmüller (1987) caution, however, that such observations, made on thin samples in the demagnetized state, may not provide definitive evidence for a pinning mechanism.

a. Ribbons

In comparison with those of aligned sintered magnets, virgin magnetization curves of melt-spun Nd-Fe-B ribbons exhibit much lower initial susceptibility. Furthermore, the coercivity develops more slowly with applied field, attaining its maximum, high-field value $H_{\mathrm{ci}}=H_{\mathrm{ci}}(\infty)$ only for $H>H_{\mathrm{ci}}(\infty)$ (see Fig. 30). These characteristics argue in favor of a pinning-dominated mechanism (Hadjipanayis, Tao, and Lawless, 1985; Hadjipanayis, Dickenson, and Lawless, 1986; Hilscher *et al.*, 1986; Pinkerton and Van Wingerden, 1986; Heisz *et al.*, 1987; Hadjipanayis and Kim, 1988; Handstein *et al.*, 1988), as does the disparate behavior of the magnetic viscosity for ribbons and sintered magnets (Ferguson *et al.*, 1989). On the other hand, Durst *et al.* (1987) assert that minor loop measurements on isotropic systems such as the ribbons are not meaningful with regard to the magnetic hardening mechanism. To demonstrate the point those authors prepared an isotropic $Nd_{0.15}Fe_{0.77}B_{0.08}$ sintered magnet and found that $H_{\mathrm{ci}}(\infty)$ is reached only for $H \gg H_{\mathrm{ci}}(\infty)$, similar to the situation for ribbons but the reverse of the case for aligned sintered magnets; if the latter are nucleation-controlled, the implicit logic is that $H_{\mathrm{ci}}(H)$ data on isotropic systems, whether rapidly solidified or sintered, may not be inconsistent with a nucleation mechanism.

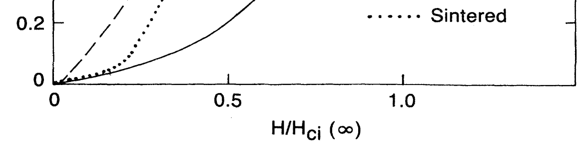

FIG. 30. Room-temperature intrinsic coercivity $H_{\mathrm{ci}}(H)$ vs magnetizing field H for Nd-Fe-B magnet materials; both quantities are normalized to the coercivity $H_{\mathrm{ci}}(\infty)$of a fully magnetized sample. [Adapted from Pinkerton and Van Wingerden (1986) and Durst and Kronmüller (1987).]

Conflicting inferences regarding the coercivity mechanism have been drawn from analyses of $H_{\mathrm{ci}}(T)$ for melt-spun Nd-Fe-B ribbons. Hadjipanayis, Lawless, and Dickerson (1985) reported good agreement of their measurements with the strong domain-wall pinning model of Gaunt (1983, 1987), in which H_{ci} is given by

$$(H_{\mathrm{ci}}/H_0)^{1/2}=1-[75k_B T/(4bf)]^{2/3}\,, \tag{51}$$

where H_0 is the critical field in the absence of thermal activation, $4b$ is the range of interaction between wall and pin, and f is the maximum restoring force per pin. Pinkerton and Fuerst (1990a) found, somewhat surprisingly, that $H_{\mathrm{ci}}(T)$ is very well described by Eq. (49) with $c=0.25$ and $N_{\mathrm{eff}}=0.26$ [for sintered Nd-Fe-B, $c\simeq0.37$ and $N_{\mathrm{eff}}\simeq1$ (Hirosawa, Tokuhara, *et al.*, 1986)]. Since the value of c is less than the $c\simeq0.3$ limit above which Kronmüller, Durst, and Sagawa (1988) expect that Eq. (49) cannot be valid for a pinning description (in which c is then interpreted as the pinning strength of an inhomogeneity such as a grain boundary), the results of Pinkerton and Fuerst (1990a) are at least not incompatible with pinning-dominated coercivity. In contrast, Durst and Kronmüller (1987) obtained good accommodation of their $H_{\mathrm{ci}}(T)$ data using Eq. (43) with $\alpha_\psi=1$, $\alpha_K=\delta/\pi r_0$ and inferred that melt-spun ribbons are nucleation-controlled systems for $T\lesssim520$ K; their result for the width of the soft magnetic inhomogeneity, $r_0\simeq21$ Å, is in excellent agreement with the grain-boundary thickness measured directly by Mishra (1986). From field-ion microscopy investigations of the microstructure of melt-spun Nd-Fe-B and Nd-(Fe,Co)-B materials Hütten and Haasen (1991) have also concluded that a nucleation model of coercivity is compatible with magnetic measurements.

b. Hot-pressed and die-upset magnets

As Fig. 30 shows, coercivity develops quickly with applied field for (isotropic) hot-pressed and (anisotropic) die-upset magnets but approaches saturation only in fields exceeding $H_{\mathrm{ci}}(\infty)$. Pinkerton and Van Wingerden (1986) ascribe the low-field behavior to domain propagation, with subsequent pinning in intergranular regions making further wall movement in larger magnetizing fields progressively more difficult. Magnetic viscosity measurements also indicate that the reversal mechanism for hot-pressed magnets is distinct from that of sintered materials (Givord, Tenaud, *et al.*, 1987; Givord, Heiden, *et al.*, 1988; Street *et al.*, 1988). In agreement with Pinkerton and Van Wingerden (1986), Givord, Heiden, *et al.*

(1988) conclude that the high-field part of the virgin magnetization curve of hot-pressed magnets is controlled by the same irreversible, pinning-dominated processes governing demagnetization on the hysteresis loop.

Pinkerton and Fuerst (1990a) analyzed $H_{ci}(T)$ for a die-upset Nd-Fe-B magnet and found that Eq. (49) approximately describes the data with $c=0.29$ and $N_{eff}=0.72$; however, a quantitatively improved fit was obtained using Eq. (51) for strong domain-wall pinning (Pinkerton and Fuerst, 1990b). Over a wide temperature range Eq. (51) also quite successfully models $H_{ci}(T)$ for die-upset Pr-Fe-B (Pinkerton and Fuerst, 1991).

3. Interaction effects

With the exception of the two-dimensional simulation of Blank (1990), the models discussed above incorporate possible interactions between $R_2Fe_{14}B$ grains only indirectly via parameters such as c and N_{eff} in Eq. (49). There is evidence, however, that intergranular interactions play a nontrivial role in both melt-spun and sintered R-Fe-B magnets, and further progress in understanding the magnetization reversal mechanisms will likely involve more explicit consideration of them.

Wohlfarth (1958) noted that the relation

$$B_d(H)=B_r(\infty)-2B_r(H) \tag{52}$$

holds for an assembly of noninteracting, uniaxial, single-domain particles, where $B_r(H)$ is the remanence after application and removal of a field H to an initially unmagnetized sample and $B_d(H)$ is the demagnetizing remanence that persists after removal of a reverse field having magnitude H applied to a sample previously exposed to a very large field in the opposite direction. McCurrie and Gaunt (1964) demonstrated that this remanence relationship is also valid for multidomain ferromagnets if the domain walls interact with the same density and distribution of pinning sites on both the initial and the demagnetization branches of the magnetization curve (see also Gaunt *et al.*, 1986). Hence, deviation from Eq. (52) can be construed as a signature of particle-interaction effects and/or different magnetizing and demagnetizing behavior. Quite substantial departures from Eq. (52) occur for sintered magnets and for all three forms of melt-spun Nd-Fe-B materials (Pinkerton, 1986b, 1987; Hadjipanayis and Kim, 1988; Handstein *et al.*, 1988); Figure 31 illustrates the point. For the melt-spun systems Pinkerton (1987) attributes the relative difficulty in demagnetizing a sample at low B_r (small H) to magnetic interactions between neighboring grains; as more crystallites reverse, those same interactions facilitate easier reversal of the remaining grains. The interactions are likely to be responsible for the "interaction domains," extended structures comprised of many grains, observed in melt-spun ribbons by Lorentz microscopy (Mishra, 1986; Hadjipanayis and Gong, 1987; Hadjipanayis and Kim, 1988; Bras *et al.*, 1990).

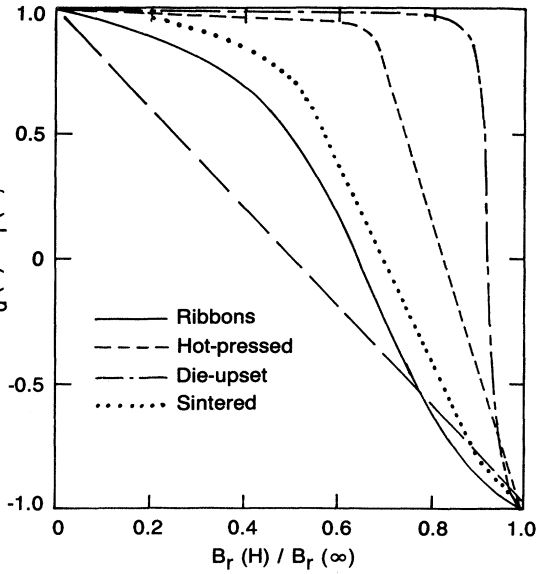

FIG. 31. Demagnetizing remanence $B_d(H)$ vs magnetizing remanence $B_r(H)$ for Nd-Fe-B magnet materials at room temperature; both quantities are normalized to the remanence $B_r(\infty)$ of a fully magnetized sample. The diagonal is the remanence relationship, Eq. (52), for noninteracting particles. [Adapted from Pinkerton (1987) and Hadjipanayis and Kim (1988).]

Additional indications of interaction effects in isotropic melt-spun ribbons have emerged from comparisons of magnetization data with the noninteracting, single-domain particle model of Stoner and Wohlfarth (1948), which predicts $H_{ci}\simeq 37$ kOe and $B_r=0.5(4\pi M_s)\simeq 8$ kG for $Nd_2Fe_{14}B$. Pinkerton (1988a) found significant quantitative disparities between the observed hysteresis loop of Nd-Fe-B ribbons and the model predictions, even after a modification to include approximately magnetization reversal by domain-wall motion. Several authors have also concluded that interaction effects are substantial from the large (>9 kG) remanent moments measured on fragments of $Nd_2Fe_{14}B$-based ribbons doped with Si and/or Al (Kadin *et al.*, 1987; McCallum *et al.*, 1987; Clemente *et al.*, 1988; Hadjipanayis and Gong, 1988; Matsumoto *et al.*, 1988). [To explain the large B_r values Hadjipanayis and Gong (1988) appealed to theoretical work by Callen *et al.* (1977) showing that $B_r/4\pi M_s$ can be enhanced over 0.5 if exchange coupling between particles is sufficiently strong. The random anisotropy model employed by Callen *et al.* (1977) is subject to difficulty in principle, however, since analytic renormalization-group calculations (Imry and Ma, 1975; Pelcovits *et al.*, 1978) have demonstrated that the ground state of the Hamiltonian for that model cannot be ferromagnetic in fewer than four dimensions.]

For sintered magnets the presence of interaction effects has been inferred from (i) disparities between measured remanence curves and those calculated in a noninteracting model (Heinecke *et al.*, 1985), (ii) the absence of a minimum in the experimental angular dependence of H_{ci} (Martinek and Kronmüller, 1990; see also Fukunaga and Fukuda, 1990; Sakuma *et al.*, 1990), and (iii) diminished coefficients relating H_{ci} to the nucleation field of isolated crystallites in analyses based on Eq. (49) (Tang *et al.*, 1988).

D. Other preparation methods

At present, sintering and the bonding, hot pressing, and die upsetting of melt-spun ribbons are the only commercialized processing techniques for Nd-Fe-B permanent magnets, but other preparation methods have been and continue to be explored.

With melt-spun starting material, magnets having energy products as large as 8 MGOe and 16 MGOe have been obtained by sintering (C. J. Yang *et al.*, 1988) and by hot extrusion (C. J. Yang and Ray, 1988), respectively. In the latter case the properties of the extruded bars are anisotropic, the largest energy products developing along directions transverse to the extrusion axis. Mukai *et al.* (1990) have prepared anisotropic Nd-Fe-B and Nd-Fe-B-Cu powders having energy products of 34–37 MGOe by hot rolling melt-spun ribbons; via an electrosintering technique the powders were consolidated into fully dense magnets featuring $H_{ci} \sim 11-16$ kOe and $(BH)_{max} \sim 24-27$ MGOe.

Magnets bonded with a soft metal such as aluminum and characterized by energy products in the 6–18 MGOe range and good machinability have been produced from isotropic melt-spun flakes and aligned anisotropic powder (derived from die-upset material) by rotary forging (Rowlinson *et al.*, 1989; Brett *et al.*, 1990). An extension of the process has afforded $(BH)_{max} \gtrsim 25$ MGOe in compacts formed from isotropic flakes only; some alignment evidently occurs in the axial forging direction (Rowlinson *et al.*, 1990).

Two other rapid-solidification techniques have been investigated. Twin-roller quenching, which may combine directional solidification and uniaxial deformation, has produced Nd-Fe-B flakes having $B_r \simeq 9.5$ kG and $(BH)_{max} \simeq 16$ MGOe along the surface normal (Kuji *et al.*, 1989; Harada *et al.*, 1990b) and has improved B_r and H_{ci} over single-wheel results for Pr-Fe-B (Paik *et al.*, 1990). A form of gas atomization, the liquid dynamic compaction process involves spray atomization of molten alloy onto a cooled substrate in a protective atmosphere (T. S. Chin *et al.*, 1986) and has yielded isotropic Nd-Fe-B deposits with $(BH)_{max} \simeq 10$ MGOe (Tanigawa *et al.*, 1986; Harada *et al.*, 1990a). Radially oriented Nd-Fe-B magnets with $H_{ci} \simeq 16.8$ kOe, $B_r \simeq 7.9$ kG, and $(BH)_{max} \simeq 13.8$ MGOe have been prepared from gas-atomized powder by hot extrusion (Ma *et al.*, 1987).

Stadelmaier, El-Masry, and Stallard (1985) demonstrated that sintered magnets can be produced via the heterogeneous diffusion of Nd, Fe, and Fe_2B powders, as opposed to the standard use of ternary Nd-Fe-B alloy. Reporting maximum coercivities of ~ 6 kOe, those authors noted that the technique does not allow particle alignment in a field because $Nd_2Fe_{14}B$ does not exist at the compaction stage, so that the attainable B_r and $(BH)_{max}$ are limited. Leonowicz (1990a) exploited this method as a rapid laboratory means for assessing the effect of elemental substitutions on the magnetic properties, especially H_{ci}.

In the mechanical alloying process, investigated extensively by Schultz and co-workers, elemental boron, rare-earth, and iron (or R-Fe master alloy) powders are combined and milled for times of order 10^1 h in a high-energy ball mill. With progressive milling, the powder particles are heavily deformed, cold welded, and reformed into layered particles; conversion to $R_2Fe_{14}B$ is accomplished by solid-state reaction, typically a ~ 0.5-h anneal at ~ 1000 K (Schultz *et al.*, 1987; Schultz and Wecker, 1987). Optimum Nd-Fe-B material features $B_r \sim 7$ kG, $H_{ci} \sim 15$ kOe, and an isotropic microstructure with an $Nd_2Fe_{14}B$ grain size of ~ 500 Å, approaching that of melt-spun ribbons (Schultz and Wecker, 1988; Schultz *et al.*, 1989). In addition to resin bonding, compacted magnets can be prepared, as for melt-spun alloys, by hot pressing and die upsetting (Heisz and Schultz, 1988); the die-upset magnets are characterized by $H_{ci} \sim 11$ kOe and $B_r \sim 9$ kG (Schultz *et al.*, 1988).

Powders obtained by grinding sintered Nd-Fe-B magnets lose coercivity quickly with diminishing particle size and are unsuitable for the preparation of bonded magnets (Stadelmaier and Liu, 1986). This circumstance, at least in part, motivated Takeshita, Nakayama, and colleagues to investigate further the hydrogenation and dehydrogenation of Nd-Fe-B ingots as an alternate processing approach to obtain fine-grained $Nd_2Fe_{14}B$ material having large H_{ci}. After heating under flowing hydrogen gas (a procedure that decrepitates the alloy, as indicated in Sec. VI.G), continued thermal treatment in vacuum was found to produce $Nd_2Fe_{14}B$ powder with an average grain diameter of $\sim 0.3\ \mu m \simeq D_c$, the critical single-domain size. Takeshita and Nakayama (1989) and Nakayama *et al.* (1990) achieved $H_{ci} \simeq 9.4$ kOe, $B_r \simeq 7.7$ kG, and $(BH)_{max} \simeq 12.2$ MGOe in the powders and energy products of ~ 8 MGOe in isotropic resin-bonded magnets produced from them; with additives such as Co, Ga, Hf, and Zr anisotropic bonded magnets having $(BH)_{max}$ as large as 18 MGOe have been prepared (Takeshita and Nakayama, 1990). McGuiness and co-workers (McGuiness, Zhang, Forsyth, and Harris, 1990; McGuiness, Zhang, Yin, and Harris, 1990) have termed this method the hydrogenation, disproportionation, desorption process; their detailed studies have shown that the initial alloy is first disproportionated into Fe, Fe_2B, and Nd hydride before recombining in the vacuum annealing step to yield the small-grained, coercive $Nd_2Fe_{14}B$ material. The possibility of hydrogen-induced decomposition of $Nd_2Fe_{14}B$ and its subsequent reformation in fine-particle form was adumbrated by H. Oesterreicher (1985b).

Technologically significant coercivities can be generated by heat treating R-Fe-C and doped R-Fe-B alloys, and this possibility has led to growing interest in the preparation of magnets from ingots without the need for such processing steps as powder metallurgy or melt spinning. Exploiting the fact that $R_2Fe_{14}C$ compounds generally do not crystallize from the melt but develop only with appropriate heat treatment, and thus offer a potential alternate route to a coercive microstructure, N. C. Liu and Stadelmaier (1986) early obtained $H_{ci} \sim 12$ kOe in annealed, as-cast Dy-Fe-C and (Nd,Dy)-Fe-(B,C) materials. The solid-state reaction produced by the anneal enables development of a cellular microstructure in which $R_2Fe_{14}C$ grains having diameters in the 1–10 μm range are surrounded by a thin intergranular layer (N. C. Liu *et al.*, 1987; Stadelmaier *et al.*, 1987; Stadelmaier and Jang, 1989). Also investigating annealed, as-cast Dy-Fe-C alloys, van Mens *et al.* (1988) and J. L. Sanchez *et al.* (1989a, 1989b) observed coercivities as large as 27.5 kOe and 17 kOe, respectively; Hadjipanayis *et al.* (1988) reported that H_{ci} can be improved by field cooling such materials.

Low-level elemental substitutions have afforded significant improvements in the magnetic properties of annealed Pr-Fe-B and Nd-Fe-B ingots. Shimoda *et al.* (1988a) obtained $H_{ci} \simeq 7.4$ kOe, $B_r \simeq 6.6$ kG, and $(BH)_{max} \simeq 8.8$ MGOe for the $Pr_{0.17}Fe_{0.765}B_{0.05}Cu_{0.015}$ composition, and in annealed, as-cast $Pr_{0.17}Fe_{0.765}B_{0.05}Al_{0.015}$ and $Nd_{0.19}Fe_{0.765}B_{0.03}Ag_{0.015}$ Hadjipanayis (1989) and Hadjipanayis *et al.* (1989) observed intrinsic coercivities of 7.2 kOe and 5.5 kOe, respectively. Of much greater significance from the energy-product standpoint, however, is the recognition that at least some degree of magnetic alignment can be introduced by hot deformation, as Lee (1985) discovered in his work on melt-spun ribbons. The first published results on hot deformation of ingots are those of Shimoda *et al.* (1988a), who reported $H_{ci} \simeq 10.0$ kOe and $(BH)_{max} \simeq 36.2$ MGOe for a die-upset Pr-Fe-B-Cu alloy. Among the effects of the copper substituent according to Shimoda *et al.* (1988a, 1988b) are smaller grain size and a lower melting point, which assists hot deformation by enhancing plasticity. It was shown subsequently that hot rolling Pr-Fe-B-Cu ingots can yield energy products in the 25–30 MGOe range (Mukai and Sakamoto, 1989; Ohki *et al.*, 1989; Shimoda *et al.*, 1989, 1990). W. C. Chang *et al.* (1990) achieved $H_{ci} \simeq 10.7$ kOe, $(BH)_{max} \simeq 18$ MGOe in hot-rolled Pr-Fe-B-Ga. Nozières *et al.* (1988, 1989) and Nozières and Perrier de la Bâthie (1989) have applied hot-working methods such as die upsetting and extrusion to Nd-Fe-B-based systems, claiming $(BH)_{max}$ as large as 20 MGOe for Nd-Fe-B-Al. Shimoda *et al.* (1990) have reported $B_r \simeq 11.5$ kG, $H_{ci} \simeq 11.5$ kOe, and $(BH)_{max} \simeq 31$ MGOe for hot-rolled Nd-Fe-B-Cu.

E. Thin films

In addition to their interest from the viewpoint of fundamental physics, thin films of $R_2Fe_{14}B$ compounds have potential utility in such applications as sensors, miniature motors (Carlisle, 1985), microwave magnetic devices (Stancil, 1987), and magnetic recording (H. Oesterreicher, 1985b). Prospects for magneto-optical information storage are encouraged by the large magnetocrystalline anisotropy, Curie temperatures in a reasonable range above room temperature, and a significant polar Kerr rotation, which measurements on bulk samples have demonstrated to be slightly enhanced relative to that in elemental iron (van Engelen and Buschow, 1987; Hirosawa, Sagawa, and Katayama, 1990). In comparison with the efforts on bulk materials, however, studies of thin films have been few.

Selectively thermalized rf sputtering was employed by Cadieu and co-workers to fabricate films (~ 1 μm) of $Nd_2Fe_{14}B$. The character of the films was found to be strongly dependent on the sputtering conditions. At deposition rates less than 1.8 Å/s films directly crystallized onto heated substrates exhibited perpendicular anisotropy (i.e., preferential *c*-axis texturing normal to the film plane) with B_r and H_{ci} as large as ~ 9 kG and ~ 14 kOe, respectively; higher deposition rates led to planar easy-axis orientation (Cadieu *et al.*, 1986a, 1986b; Cadieu, 1987). An alternate two-stage method, in which an amorphous deposit was first formed and then crystallized with an in-plane field of 2.5 kOe applied at each step, was also investigated (Cadieu *et al.*, 1987). As opposed to the directly crystallized samples, the films produced by this technique were highly dense, free of voids, and featured mirrorlike, specularly reflecting surfaces. With the measurement field in the direction of the field applied during sputtering and crystallization, an energy product of ~ 16 MGOe was obtained, despite the fact that only a small degree of in-plane alignment was achieved because the crystallization temperature (970 K) exceeded $T_c \simeq 585$ K. An average $Nd_2Fe_{14}B$ grain size of several hundred angstroms, well below $D_c \sim 0.3$ μm, characterized the high-coercivity films prepared by either means.

Films of substituted Nd-Fe-B materials crystallized from amorphous rf-sputtered deposits have been investigated by three groups. Strzeszewski, Nazareth, *et al.* (1988) reported in-plane texturing and $H_{ci} \sim 10$ kOe for an Nd-(Fe,Co)-B composition. Aylesworth *et al.* (1989) observed the anisotropy of Nd-(Fe,Co)-B films to be markedly influenced by the substrate material and its temperature. Amorphous deposits crystallized in the 770–970 K interval exhibited perpendicular anisotropy, coercivities of 5–10 kOe, and $B_r = 10$ kG; on mica substrates Fe buffer layers enhanced the perpendicular anisotropy. In contrast to the results of Cadieu *et al.* (1986b), Homburg *et al.* (1990) observed perpendicular anisotropy in (Nd,Dy)-Fe-B films sputtered at deposition rates of 15 Å/s or greater; $B_r \sim 6$ kOe and $H_{ci} > 18$ kOe were measured normal to the unsaturated films.

Zasadzinski *et al.* (1987a, 1987b) synthesized high-quality single-phase thin films (~ 4000 Å) of the Nd, Sm, and Er compounds by dc triode sputtering and also concluded that $Nd_2Fe_{14}B$ has promise as a perpendicular recording medium. Film structure and texture were found very sensitive to substrate temperature, nearly epitaxial films having crystallite *c* axes predominantly normal to the film plane developing for substrate temperatures near 870 K, while lower or higher temperatures, respectively, produced amorphous deposits or crystalline films showing no directional growth. Textured $Nd_2Fe_{14}B$ films featured $H_{ci} \sim 5$ kOe, a rather large value considering that the average lateral grain dimension was a few microns. Their results prompted Zasadzinski *et al.* (1987b) to suggest that single-crystal $R_2Fe_{14}B$ films might be grown through further optimization of the sputtering conditions.

VIII. CONCLUDING REMARKS

A new era in permanent-magnet technology has been initiated by the neodymium-iron-boron materials. Commercial production programs relying on both the melt-spinning and the powder-metallurgy approaches are in place, and Nd-Fe-B magnets can be found on products ranging from automotive cranking motors to computer disc drives and household appliances. The range and number of applications continue to enjoy expansion, driven by the economic advantages as well as the larger energy products of the new magnets relative to their predecessor samarium-cobalt materials.

Progress has been rapid, but many opportunities remain for research in the area of $R_2Fe_{14}B$ materials. On the technological side, the energy products thus far achieved are still substantially lower than the maximum limit, a circumstance which warrants continued investigation of coercivity-microstructure relationships, modified alloy compositions, and alternate preparation methods. From the perspective of fundamental research, our understanding of the intrinsic properties of these systems, and rare-earth–transition-metal materials in general, can be improved. Problems outstanding include the mechanism underlying the anisotropy of the transition-metal component and its variation with temperature and composition, accurate determination of crystal-field and exchange energies, site-dependent magnetic moments, hyperfine fields, and nuclear quadrupole splittings from both experiments and electronic structure calculations, more realistic inclusion of the localized $4f$ electrons in the latter, and the development of concepts and models for coercivity that go beyond the single-particle paradigm and more fully incorporate features of real interacting systems.

ACKNOWLEDGMENTS

It is a genuine pleasure to thank T. W. Capehart, J. J. Croat, C. D. Fuerst, S. S. Jaswal, R. W. Lee, R. K. Mishra, F. E. Pinkerton, and W. B. Yelon for stimulating discussions and perceptive comments. The assistance of D. J. Van Wingerden is keenly appreciated, as is the support of J. G. Larson. I am grateful to W. Y. Ching, G. J. Long, and M. Sagawa for kindly providing figures from their work.

APPENDIX: A NOTE ON UNITS

Gaussian units for magnetic field strength *H*, magnetization *M*, and energy product $(BH)_{\max}$ have been used in this review. These may be easily converted to SI units by the following relations:

$$H\ [\mathrm{Oe}] \times 10^3/4\pi \rightarrow H\ [\mathrm{A/m}]\ ,$$

$$4\pi M\ [G] \times 10^{-4} \rightarrow J\ [\mathrm{T}]\ ,$$

$$(BH)_{\max}\ [\mathrm{MGOe}] \times 10^2/4\pi \rightarrow (BH)_{\max}\ [\mathrm{kJ/m^3}]\ ,$$

where *J* is usually identified as the magnetic polarization in the SI system. A valuable discussion of units in magnetism has been given by Bennett *et al.* (1975).

REFERENCES

Abache, C., and H. Oesterreicher, 1985, J. Appl. Phys. **57**, 4112.
Abache, C., and H. Oesterreicher, 1986a, J. Appl. Phys. **60**, 1114.
Abache, C., and J. Oesterreicher, 1986b, J. Appl. Phys. **60**, 3671.
Abe, M., S. H. Liou, C. L. Chien, N. C. Koon, B. N. Das, and E. Callen, 1987, J. Appl. Phys. **61**, 3568.
Adam, S., Gh. Adam, and E. Burzo, 1986, J. Magn. Magn. Mater. **61**, 260.
Adler, E., and P. Hamann, 1985, in *Proceedings of the Fourth International Symposium on Magnetic Anisotropy and Coercivity in Rare Earth-Transition Metal Alloys,* edited by K. J. Strnat (University of Dayton, Dayton, Ohio), p. 747.
Aharoni, A., 1962, Rev. Mod. Phys. **34**, 227.
Akayama, M., S. Tanigawa, and M. Tokunaga, 1990, IEEE Trans. Magn. **26**, 1727.
Alameda, J. M., D. Givord, R. Lemaire, and Q. Lu, 1981, J. Appl. Phys. **52**, 2079.
Algarabel, P. A., M. R. Ibarra, C. Marquina, A. del Moral, and S. Zemirli, 1990, J. Magn. Magn. Mater. **84**, 109.
Algarabel, P. A., M. R. Ibarra, C. Marquina, G. Marusi, O. Moze, L. Pareti, M. Solzi, J. I. Arnaudas, and A. del Moral, 1989, Physica B **155**, 263.
Allibert, C. H., 1989, J. Less-Common Met. **152**, L1.
Aly, S. H., G. N. Nicolaides, Y. F. Tao, and G. C. Hadjipanayis, 1986, J. Phys. F **16**, L21.
Andreev, A. V., and M. I. Bartashevich, 1990a, J. Less-Common Met. **162**, 33.
Andreev, A. V., and M. I. Bartashevich, 1990b, J. Less-Common Met. **167**, 107.
Andreev, A. V., A. V. Deryagin, N. V. Kudrevatykh, N. V. Mushnikov, V. A. Reimer, and S. V. Terent'ev, 1986, Sov. Phys. JETP **63**, 608.
Andreev, A. V., A. V. Deryagin, S. M. Zadvorkin, and S. V. Terent'ev, 1985, Sov. Phys. Solid State **27**, 987.
Arai, S., and T. Shibata, 1985, IEEE Trans. Magn. **MAG-21**, 1952.
Arai, S., T. Shibata, N. Koshizuka, and M. Nagakura, 1987,

IEEE Trans. Magn. **MAG-23**, 2299.

Asti, G., F. Bolzoni, and L. Pareti, 1987, IEEE Trans. Magn. **MAG-23**, 2521.

Asti, G., and S. Rinaldi, 1974, J. Appl. Phys. **45**, 3600.

Atzmony, U., and M. P. Dariel, 1976, Phys. Rev. B **13**, 4006.

Aylesworth, K. D., Z. R. Zhao, D. J. Sellmyer, and G. C. Hadjipanayis, 1989, J. Magn. Magn. Mater. **82**, 48.

Bara, J. J., B. F. Bogacz, and A. Szytula, 1988, J. Magn. Magn. Mater. **75**, 293.

Bara, J. J., A. T. Pedziwiatr, and W. Zarek, 1982, J. Magn. Magn. Mater. **27**, 168.

Bartashevich, M. I., and A. V. Andreev, 1990, Physica B **162**, 52.

Becker, J. J., 1976, IEEE Trans. Magn. **MAG-12**, 965.

Becker, J. J., 1984, J. Appl. Phys. **55**, 2067.

Belorizky, E., M. A. Fremy, J. P. Gavigan, D. Givord, and H. S. Li, 1987, J. Appl. Phys. **61**, 3971.

Belorizky, E., J. P. Gavigan, D. Givord, and H. S. Li, 1988, Europhys. Lett. **5**, 349.

Bennett, L. H., C. H. Page, and L. J. Swartzendruber, 1975, in *Magnetism and Magnetic Materials—1975,* AIP Conference Proceedings No. 29, edited by J. J. Becker, G. H. Lander, and J. J. Rhyne (AIP, New York), p. xix.

Bennett, L. H., and R. E. Watson, 1987, Phys. Rev. B **35**, 845.

Bennett, L. H., R. E. Watson, and W. B. Pearson, 1986, J. Magn. Magn. Mater. **54-57**, 1537.

Bergman, G., and D. P. Shoemaker, 1954, Acta Crystallogr. **7**, 857.

Berthier, Y., M. Bogé, G. Czjzek, D. Givord, C. Jeandey, H. S. Li, and J. L. Oddou, 1986, J. Magn. Magn. Mater. **54-57**, 589.

Berthier, Y., N. Nassar, and T. Vadieu, 1988, J. Phys. (Paris) **49**, C8-585.

Bezinge, A., H. F. Braun, J. Muller, and K. Yvon, 1985, Solid State Commun. **55**, 131.

Bezinge, A., K. Yvon, H. F. Braun, J. Muller, and H.-U. Nissen, 1987, Phys. Rev. B **36**, 1406.

Bhagat, S. M., J. N. Lloyd, and D. K. Paul, 1979, J. Magn. Magn. Mater. **10**, 65.

Blank, R., 1990, J. Magn. Magn. Mater. **83**, 192.

Bocelli, G., G. Calestani, A. Deriu, and F. Leccabue, 1987, Solid State Commun. **61**, 451.

Bogé, M., J. M. D. Coey, G. Czjzek, D. Givord, C. Jeandey, H. S. Li, and J. L. Oddou, 1985, Solid State Commun. **55**, 295.

Bogé, M., G. Czjzek, D. Givord, C. Jeandey, H. S. Li, and J. L. Oddou, 1986, J. Phys. F **16**, L67.

Boller, H., and H. Oesterreicher, 1984, J. Less-Common Met. **103**, L5.

Boltich, E. B., 1988a, J. Appl. Phys. **63**, 3124.

Boltich, E. B., 1988b, J. Appl. Phys. **64**, 4796.

Boltich, E. B., E. Oswald, M. Q. Huang, S. Hirosawa, W. E. Wallace, and E. Burzo, 1985, J. Appl. Phys. **57**, 4106.

Boltich, E. B., A. T. Pedziwiatr, and W. E. Wallace, 1987a, in *High Performance Permanent Magnet Materials,* Materials Research Society Symposia Proceedings Vol. 96, edited by S. G. Sankar, J. F. Herbst, and N. C. Koon (Materials Research Society, Pittsburgh), p. 119.

Boltich, E. B., A. T. Pedziwiatr, and W. E. Wallace, 1987b, J. Magn. Magn. Mater. **66**, 317.

Boltich, E. B., F. Pourarian, R. T. Obermyer, S. G. Sankar, and W. E. Wallace, 1988, J. Appl. Phys. **63**, 3964.

Boltich, E. B., and W. E. Wallace, 1985, Solid State Commun. **55**, 529.

Boltich, E. B., and W. E. Wallace, 1986, J. Less-Common Met. **126**, 35.

Bolzoni, F., J. M. D. Coey, J. Gavigan, D. Givord, O. Moze, L. Pareti, and T. Viadieu, 1987, J. Magn. Magn. Mater. **65**, 123.

Bolzoni, F., A. Deriu, F. Leccabue, L. Pareti, and J. L. Sanchez, 1986, J. Magn. Magn. Mater. **54-57**, 595.

Bolzoni, F., J. P. Gavigan, D. Givord, H. S. Li, O. Moze, and L. Pareti, 1987, J. Magn. Magn. Mater. **66**, 158.

Bolzoni, F., F. Leccabue, O. Moze, L. Pareti, and M. Solzi, 1987a, J. Magn. Magn. Mater. **67**, 373.

Bolzoni, F., F. Leccabue, O. Moze, L. Pareti, M. Solzi, and A. Deriu, 1987b, J. Appl. Phys. **61**, 5369.

Bolzoni, F., F. Leccabue, L. Pareti, and J. L. Sanchez, 1985, J. Phys. (Paris) **46**, C6-305.

Bolzoni, F., O. Moze, and L. Pareti, 1987, J. Appl. Phys. **62**, 615.

Bozorth, Richard M., 1951, *Ferromagnetism* (Van Nostrand, Princeton), p. 568.

Bras, J., J. Degauque, and M. Fagot, 1988, Solid State Commun. **68**, 117.

Bras, J., J. Degauque, M. Fagot, and K. Biyadi, 1990, J. Magn. Magn. Mater. **83**, 203.

Brennan, S., A. Bienenstock, and J. E. Keem, 1989, J. Appl. Phys. **65**, 697.

Brett, R. L., N. Rowlinson, M. M. Ashraf, I. R. Harris, and P. Bowen, 1990, J. Appl. Phys. **67**, 4622.

Brown, W. F., Jr., 1945, Rev. Mod. Phys. **17**, 15.

Burlet, P., J. M. D. Coey, J. P. Gavigan, D. Givord, and C. Meyer, 1986, Solid State Commun. **60**, 723.

Burzo, E., E. B. Boltich, M. Q. Huang, and W. E. Wallace, 1985, in *Proceedings of the Fourth International Symposium on Magnetic Anisotropy and Coercivity in Rare Earth-Transition Metal Alloys,* edited by K. J. Strnat (University of Dayton, Dayton, Ohio), p. 771.

Burzo, E., and H. R. Kirchmayr, 1989, in *Handbook on the Physics and Chemistry of Rare Earths,* edited by K. A. Gschneidner, Jr., and L. Eyring (North-Holland, Amsterdam), Vol. 12, p. 71.

Burzo, E., I. Lupsa, and A. T. Pedziwiatr, 1986, J. Phys. F. **16**, L83.

Burzo, E., M. Morariu, M. Rogalski, and A. T. Pedziwiatr, 1989, Hyp. Interactions **50**, 701.

Burzo, E., E. Oswald, M. Q. Huang, E. Boltich, and W. E. Wallace, 1985, J. Appl. Phys. **57**, 4109.

Burzo, E., A. T. Pedziwiatr, and W. E. Wallace, 1987, Solid State Commun. **61**, 57.

Burzo, E., and N. Plugaru, 1990, J. Magn. Magn. Mater. **86**, 97.

Burzo, E., N. Plugaru, and V. Pop, 1987, J. Magn. Magn. Mater. **70**, 343.

Burzo, E., N. Plugaru, V. Pop, L. Stanciu, and W. E. Wallace, 1986, Solid State Commun. **58**, 803.

Burzo, E., L. Stanciu, and W. E. Wallace, 1985, J. Less-Common Met. **111**, 83.

Buschow, K. H. J., 1971, Phys. Status Solidi A **7**, 199.

Buschow, K. H. J., 1977, Rep. Prog. Phys. **40**, 1179.

Buschow, K. H. J., 1980, in *Ferromagnetic Materials,* edited by E. P. Wohlfarth (North-Holland, Amsterdam), Vol. 1, p. 297.

Buschow, K. H. J., 1984, in *Handbook on the Physics and Chemistry of Rare Earths,* edited by K. A. Gschneidner, Jr. and L. Eyring (North-Holland, Amsterdam), Vol. 6, p. 1.

Buschow, K. H. J., 1986a, Mat. Res. Rep. **1**, 1.

Buschow, K. H. J., 1986b, J. Less-Common Met. **118**, 349.

Buschow, K. H. J., 1987, in *Proceedings of the Ninth International Workshop on Rare-Earth Magnets and Their Applications,* edited by C. Herget and R. Poerschke (Deutsche Physikalische Gesellschaft, Bad Honnef, FRG), p. 453.

Buschow, K. H. J., 1988a, in *Ferromagnetic Materials,* edited by E. P. Wohlfarth and K. H. J. Buschow (North-Holland, Amsterdam), Vol. 4, p. 1.

Buschow, K. H. J., 1988b, J. Less-Common Met. **144**, 65.

Buschow, K. H. J., D. B. de Mooij, M. Brouha, H. H. A. Smit, and R. C. Thiel, 1988, IEEE Trans. Magn. **24**, 1611.

Buschow, K. H. J., D. B. de Mooij, J. L. C. Daams, and H. M. van Noort, 1986, J. Less-Common Met. **115**, 357.

Buschow, K. H. J., D. B. de Mooij, and C. J. M. Denissen, 1988a, J. Less-Common Met. **141**, L15.

Buschow, K. H. J., D. B. de Mooij, and C. J. M. Denissen, 1988b, J. Less-Common Met. **142**, L13.

Buschow, K. H. J., D. B. de Mooij, S. Sinnema, R. J. Radwanski, and J. J. M. Franse, 1985, J. Magn. Magn. Mater. **51**, 211.

Buschow, K. H. J., D. B. de Mooij, and H. M. van Noort, 1985, Philips J. Res. **40**, 227.

Buschow, K. H. J., C. J. M. Denissen, D. B. de Mooij, F. R. de Boer, R. Verhoef, and Z-D. Zhang, 1988, J. Phys. (Paris) **49**, C8-593.

Buschow, K. H. J., J. W. C. de Vries, and R. C. Thiel, 1985a, J. Phys. F **15**, L93.

Buschow, K. H. J., J. W. C. de Vries, and R. C. Thiel, 1985b, Physica **132B**, 13.

Buschow, K. H. J., and R. Grössinger, 1987, J. Less-Common Met. **135**, 39.

Buschow, K. H. J., A. M. van Diepen, and H. W. de Wijn, 1974, Solid State Commun. **15**, 903.

Buschow, K. H. J., H. M. van Noort, and D. B. de Mooij, 1985, J. Less-Common Met. **109**, 79.

Cadieu, F. J., 1987, J. Appl. Phys. **61**, 4105.

Cadieu, F. J., T. D. Cheung, and L. Wickramasekara, 1986a, J. Magn. Magn. Mater. **54-57**, 535.

Cadieu, F. J., T. D. Cheung, L. Wickramasekara, and N. Kamprath, 1986b, IEEE Trans. Magn. **MAG-22**, 752.

Cadieu, F. J., T. D. Cheung, L. Wickramasekara, N. Kamprath, H. Hegde, and N. C. Liu, 1987, J. Appl. Phys. **62**, 3866.

Cadogan, J. M., 1987, J. Less-Common Met. **135**, 269.

Cadogan, J. M., 1988, J. Less-Common Met. **144**, L15.

Cadogan, J. M., and J. M. D. Coey, 1984, Phys. Rev. B **30**, 7326.

Cadogan, J. M., and J. M. D. Coey, 1986, Appl. Phys. Lett. **48**, 442.

Cadogan, J. M., J. M. D. Coey, J. P. Gavigan, D. Givord, and H. S. Li, 1987, J. Appl. Phys. **61**, 3974.

Cadogan, J. M., J. P. Gavigan, D. Givord, and H. S. Li, 1988, J. Phys. F **18**, 779.

Callaway, J., and C. S. Wang, 1977, Phys. Rev. B **16**, 2095.

Callen, E., Y. J. Liu, and J. R. Cullen, 1977, Phys. Rev. B **16**, 263.

Callen, H. B., and E. Callen, 1966, J. Phys. Chem. Solids **27**, 1271.

Campbell, I. A., 1972, J. Phys. F **2**, L47.

Carlisle, B. H., 1985, Machine Design **57**, 73.

Carr, G. E., H. A. Davies, and R. A. Buckley, 1988, Mater. Sci. Eng. **99**, 147.

Chaban, N. F., Yu. B. Kuzma, N. S. Bilonizhko, O. O. Kachmar, and N. V. Petriv, 1979, Dopov. Akad. Nauk Ukr. RSR, Ser. A, No. 10. 873.

Chang, W. C., C. R. Paik, H. Nakamura, N. Takahasi, S. Sugimoto, M. Okada, and M. Homma, 1990, IEEE Trans. Magn. **26**, 2604.

Chang, Y.-J., and X.-R. Qian, 1986, Phys. Status Solidi A **93**, 573.

Chen, J., and H. Kronmüller, 1990, Phys. Status Solidi A **120**, 617.

Chen, J. K., and G. Thomas, 1987, in *High Performance Permanent Magnet Materials,* Materials Reseach Society Symposia Proceedings Vol. 96, edited by S. G. Sankar, J. F. Herbst, and N. C. Koon (Materials Research Society, Pittsburgh), p. 221.

Chen, S. K., J. G. Duh, and H. C. Ku, 1988a, J. Appl. Phys. **63**, 2739.

Chen, S. K., J. G. Duh, and H. C. Ku, 1988b, J. Appl. Phys. **64**, 5546.

Chen, S. K., J. G. Duh, H. C. Ku, and W. C. Chang, 1989, J. Magn. Magn. Mater. **82**, 12.

Chen, Y. L., 1985, IEEE Trans. Magn. **MAG-21**, 1967.

Cheng, B-P., S-C. Fu, Y-C. Yang, and W. J. James, 1988, J. Appl. Phys. **64**, 5543.

Cheng, B-P., Y-C. Yang, S-C. Fu, and W. J. James, 1987, J. Appl. Phys. **61**, 3586.

Cheung, T. D., X. Guo, and F. J. Cadieu, 1987, J. Appl. Phys. **61**, 3979.

Chikazumi, S., 1986, J. Magn. Magn. Mater. **54-57**, 1551.

Chin, G. Y., S. Sibley, J. C. Betts, T. D. Schlabach, F. E. Werner, and D. L. Martin, 1979, IEEE Trans. Magn. **MAG-15**, 1685.

Chin, T. S., Y. Hara, E. J. Lavernia, R. C. O'Handley, and N. J. Grant, 1986, J. Appl. Phys. **59**, 1297.

Ching, W. Y., and Z-Q. Gu, 1987, J. Appl. Phys. **61**, 3718.

Ching, W. Y., and Z-Q. Gu, 1988, J. Appl. Phys. **63**, 3716.

Chourasia, A. R., and D. R. Chopra, 1989, J. Less-Common Met. **148**, 413.

Christodoulou, C. N., E. B. Boltich, and T. B. Massalski, 1989, J. Magn. Magn. Mater. **81**, 209.

Christodoulou, C. N., W. E. Wallace, and T. B. Massalski, 1989, J. Appl. Phys. **66**, 2749.

Chuang, Y. C., C. H. Wu, T. D. Chang, F. H. Wang, and F. R. de Boer, 1988, J. Less-Common Met. **144**, 249.

Chuang, Y. C., C. H. Wu, and J. Q. Xie, 1987, in *Proceedings of the Ninth International Workshop on Rare-Earth Magnets and Their Applications,* edited by C. Herget and R. Poerschke (Deutsche Physikalische Gesellschaft, Bad Honnef, FRG), p. 617.

Chuang, Y. C., C. H. Wu, and J. Q. Xie, 1988, J. Less-Common Met. **144**, 235.

Clark, A. E., 1973, Appl. Phys. Lett. **23**, 642.

Clark, A. E., 1980, in *Ferromagnetic Materials,* edited by E. P. Wohlfarth (North-Holland, Amsterdam), Vol. 1, p. 531.

Clemente, G. B., J. E. Keem, and J. P. Bradley, 1988, J. Appl. Phys. **64**, 5299.

Coehoorn, R., 1991, in *Proceedings of the NATO Advanced Study Institute on Supermagnets, Hard Magnetic Materials,* edited by G. J. Long and F. Grandjean (Kluwer, Dordrecht), p. 133.

Coehoorn, R., and K. H. J. Buschow, 1991, J. Appl. Phys. **69**, 5590.

Coehoorn, R., C. J. M. Denissen, and R. Eppenga, 1991, J. Appl. Phys. **69**, 6222.

Coehoorn, R., and J. Duchateau, 1988, Mater. Sci. Eng. **99**, 131.

Coehoorn, R., J. P. W. B. Duchateau, and C. J. M. Denissen, 1989, J. Appl. Phys. **65**, 704.

Coey, J. M. D., 1986, J. Less-Common Met. **126**, 21.

Coey, J. M. D., 1987, Phys. Scr. **T19**, 426.

Coey, J. M. D., J. M. Cadogan, and D. H. Ryan, 1985, in *Nd-Fe Permanent Magnets: Their Present and Future Applications,* edited by I. V. Mitchell (Elsevier Applied Science, London/New York), p. 143.

Coey, J. M. D., H. S. Li, J. P. Gavigan, J. M. Cadogan, and B. P. Hu, 1989, in *Concerted European Action on Magnets,* edited by I. V. Mitchell, J. M. D. Coey, D. Givord, I. R. Harris, and R. Hanitsch (Elsevier Applied Science, London/New York), p. 76.

Coey, J. M. D., and H. Sun, 1990, J. Magn. Magn. Mater. **87**, L251.

Coey, J. M. D., H. Sun, and Y. Otani, 1990, in *Proceedings of the Sixth International Symposium on Magnetic Anisotropy and Coercivity in Rare Earth-Transition Metal Alloys,* edited by S. G. Sankar (Carnegie Mellon University, Pittsburgh), p. 36.

Coey, J. M. D., A. Yaouanc, and D. Fruchart, 1986, Solid State Commun. **58**, 413.

Coey, J. M. D., A. Yaouanc, D. Fruchart, R. Fruchart, and P. L'Héritier, 1987, J. Less-Common Met. **131**, 419.

Cook, J. S., and P. L. Rossiter, 1989, in *CRC Critical Reviews in Solid State and Materials Sciences* (CRC, Boca Raton, Florida), Vol. 15, p. 509.

Corb, B. W., M. Ringger, H.-J. Güntherodt, and F. E. Pinkerton, 1987, Appl. Phys. Lett. **50**, 353.

Croat, J. J., 1980, Appl. Phys. Lett. **37**, 1096.

Croat, J. J., 1981a, J. Appl. Phys. **52**, 2509.

Croat, J. J., 1981b, J. Magn. Magn. Mater. **24**, 125.

Croat, J. J., 1981c, Appl. Phys. Lett. **39**, 357.

Croat, J. J., 1982, J. Appl. Phys. **53**, 6932.

Croat, J. J., 1982b, IEEE Trans. Magn. **MAG-18**, 1442.

Croat, J. J., 1982c, J. Appl. Phys. **53**, 3161.

Croat, J. J., 1989a, J. Less-Common Met. **148**, 7.

Croat, J. J., 1989b, IEEE Trans. Magn. **25**, 3550.

Croat, J. J., and J. F. Herbst, 1982a, J. Appl. Phys. **53**, 2294.

Croat, J. J., and J. F. Herbst, 1982b, J. Appl. Phys. **53**, 2404.

Croat, J. J., J. F. Herbst, R. W. Lee, and F. E. Pinkerton, 1984a, Appl. Phys. Lett. **44**, 148.

Croat, J. J., J. F. Herbst, R. W. Lee, and F. E. Pinkerton, 1984b, J. Appl. Phys. **55**, 2078.

Czjzek, G., H.-J. Bornemann, and H. S. Li, 1989, J. Magn. Magn. Mater. **80**, 23.

Dadon, D., M. P. Dariel, Y. Gefen, H. Klimker, and M. Rosen, 1986, Appl. Phys. Lett. **48**, 1444.

Dadon, D., Y. Gefen, and M. P. Dariel, 1987, IEEE Trans. Magn. **MAG-23**, 3605.

Dai, S., A. H. Morrish, X. Z. Zhou, B. P. Hu, and S. G. Zhang, 1988, J. Appl. Phys. **63**, 3722.

Das, B. N., and N. C. Koon, 1983, Metall. Trans. **14A**, 953.

Dalmas de Réotier, P., D. Fruchart, L. Pontonnier, F. Vaillant, P. Wolfers, A. Yaouanc, J. M. D. Coey, R. Fruchart, and P. L'Héritier, 1987, J. Less-Common Met. **129**, 133.

Dalmas de Réotier, P., D. Fruchart, P. Wolfers, R. Guillen, P. Vulliet, A. Yaouanc, R. Fruchart, and P. L'Héritier, 1985a, J. Phys. (Paris) **46**, C6-323.

Dalmas de Réotier, P., D. Fruchart, P. Wolfers, P. Vulliet, A. Yaouanc, R. Fruchart, and P. L'Héritier, 1985b, J. Phys. (Paris) **46**, C6-249.

Damento, M. A., and L. J. Demer, 1987, IEEE Trans. Magn. **MAG-23**, 1877.

Davis, R. L., R. K. Day, and J. B. Dunlop, 1985, Solid State Commun. **56**, 181.

De Boer, F. R., Y-K. Huang, D. B. de Mooij, and K. H. J. Buschow, 1987, J. Less-Common Met. **135**, 199.

De Boer, F. R., Y-K. Huang, Z-D. Zhang, D. B. de Mooij, and K. H. J. Buschow, 1988, J. Magn. Magn. Mater. **72**, 167.

De Boer, F. R., R. Verhoef, Z-D. Zhang, D. B. de Mooij, and K. H. J. Buschow, 1988, J. Magn. Magn. Mater. **73**, 263.

Del Moral, A., M. R. Ibarra, C. Marquina, J. I. Arnaudas, and P. A. Algarabel, 1989, Phys. Rev. B **40**, 7192.

Del Moral, A., M. R. Ibarra, C. Marquina, J. I. Arnaudas, and P. A. Algarabel, 1990, J. Magn. Magn. Mater. **83**, 283.

De Mooij, D. B., and K. H. J. Buschow, 1988a, J. Less-Common Met. **136**, 207.

De Mooij, D. B., and K. H. J. Buschow, 1988b, J. Less-Common Met. **142**, 349.

Denissen, C. J. M., D. B. de Mooij, and K. H. J. Buschow, 1988a, J. Less-Common Met. **139**, 291.

Denissen, C. J. M., D. B. de Mooij, and K. H. J. Buschow, 1988b, J. Less-Common Met. **142**, 195.

Deppe, P., M. Rosenberg, S. Hirosawa, and M. Sagawa, 1987, J. Appl. Phys. **61**, 4337.

Deppe, P., M. Rosenberg, and H. H. Stadelmaier, 1988, J. Less-Common Met. **143**, 77.

Deruelle, M. C. D., M. Yamada, H. Yamauchi, and Y. Nakagawa, 1990, Phys. Rev. B **42**, 10291.

Deryagin, A. V., E. N. Tarasov, A. V. Andreev, V. N. Moskalev, and A. I. Kozlov, 1984, JETP Lett. **39**, 629.

Dixon, M., F. E. Hoare, T. M. Holden, and D. E. Moody, 1965, Proc. R. Soc. London, Ser. A **285**, 561.

Durst, K.-D., and H. Kronmüller, 1985, in *Proceedings of the Fourth International Symposium on Magnetic Anisotropy and Coercivity in Rare Earth-Transition Metal Alloys,* edited by K. J. Strnat (University of Dayton, Dayton, Ohio), p. 725.

Durst, K.-D., and H. Kronmüller, 1986, J. Magn. Magn. Mater. **59**, 86.

Durst, K.-D., and H. Kronmüller, 1987, J. Magn. Magn. Mater. **68**, 63.

Durst, K.-D., H. Kronmüller, and G. Schneider, 1987, in *Proceedings of the Fifth International Symposium on Magnetic Anisotropy and Coercivity in Rare-Earth–Transition Metal Alloys,* edited by C. Herget, H. Kronmüller, and R. Poerschke (Deutsche Physikalische Gesellschaft, Bad Honef, FRG), p. 209.

Eckert, D., K.-H. Müller, P. Nothnagel, J. Schneider, and R. Szymczak, 1990, J. Magn. Magn. Mater. **83**, 197.

Elbicki, J. M., W. E. Wallace, and V. Korablev, 1989, IEEE Trans. Magn. **25**, 3567.

Elbicki, J. M., W. E. Wallace, and P. Wynblatt, 1988, J. Magn. Magn. Mater. **74**, 186.

El-Masry, N. A., and H. H. Stadelmaier, 1985, Mater. Lett. **3**, 405.

El-Masry, N. A., and H. H. Stadelmaier, 1989, Z. Metallkde. **80**, 723.

Endoh, M., E. B. Boltich, K. Nakamura, M. Tokunaga, and G. Kido, 1990a, in *Proceedings of the Eleventh International Workshop on Rare-Earth Magnets and Their Applications,* edited by S. G. Sankar (Carnegie Mellon University, Pittsburgh), p. 519.

Endoh, M., E. B. Boltich, Y. Nozawa, and M. Tokunaga, 1990b, in *Proceedings of the Eleventh International Workshop on Rare-Earth Magnets and Their Applications,* edited by S. G. Sankar (Carnegie Mellon University, Pittsburgh), p. 506.

Endoh, M., M. Tokunaga, E. B. Boltich, and W. E. Wallace, 1989, IEEE Trans. Magn. **25**, 4114.

Endoh, M., M. Tokunaga, and H. Harada, 1987, IEEE Trans. Magn. **MAG-23**, 2290.

Enz, U., 1982, in *Ferromagnetic Materials,* edited by E. P. Wohlfarth (North-Holland, Amsterdam), Vol. 3, p. 1.

Erdmann, K., P. Deppe, M. Rosenberg, and K. H. J. Buschow, 1987, J. Appl. Phys. **61**, 4340.

Erdmann, K., and M. Rosenberg, 1989, J. Magn. Magn. Mater. **82**, 273.

Erdmann, K., M. Rosenberg, and K. H. J. Buschow, 1988, J. Appl. Phys. **63**, 4116.

Erdmann, K., T. Sinnemann, M. Rosenberg, and K. H. J. Buschow, 1989, J. Less-Common Met. **146**, 59.

Eshelman, L. J., K. A. Young, V. Panchanathan, and J. J. Croat, 1988, J. Appl. Phys. **64**, 5293.

Ferguson, G. B., K. O'Grady, J. Popplewell, and R. W. Chantrell, 1989, IEEE Trans. Magn. **25**, 3449.

Fernengel, W., 1987, in *Proceedings of the Fifth International Symposium on Magnetic Anisotropy and Coercivity in Rare-Earth–Transition Metal Alloys,* edited by C. Herget, H. Kronmüller, and R. Poerschke (Deutsche Physikalische Gesellschaft, Bad Honnef, FRG), p. 259.

Fernengel, W., 1989, J. Magn. Magn. Mater. **80**, 27.

Fernengel, W., 1990, J. Magn. Magn. Mater. **83**, 201.

Ferreira, L. P., R. Guillen, P. Vulliet, A. Yaouanc, D. Fruchart, P. Wolfers, P. L'Héritier, and R. Fruchart, 1985, J. Magn. Magn. Mater. **53**, 145.

Fidler, J., 1985, IEEE Trans. Magn. **MAG-21**, 1955.

Fidler, J., 1987a, in *Proceedings of the Fifth International Symposium on Magnetic Anisotropy and Coercivity in Rare-Earth–Transition Metal Alloys,* edited by C. Herget, H. Kronmüller, and R. Poerschke (Deutsche Physikalische Gesellschaft, Bad Honnef, FRG), p. 363.

Fidler, J., 1987b, IEEE Trans. Magn. **MAG-23**, 2106.

Fidler, J., and K. G. Knoch, 1989, J. Magn. Magn. Mater. **80**, 48.

Fidler, J., K. G. Knoch, H. Kronmüller, and G. Schneider, 1989, J. Mater. Res. **4**, 806.

Fidler, J., and Y. Tawara, 1988, IEEE Trans. Magn. **24**, 1951.

Fidler, J., and L. Yang, 1985, in *Proceedings of the Fourth International Symposium on Magnetic Anisotropy and Coercivity in Rare Earth-Transition Metal Alloys,* edited by K. J. Strnat (University of Dayton, Dayton, Ohio), p. 647.

Figiel, H., D. Fowler, T. Dumelow, P. C. Riedi, and C. Kapusta, 1987, J. Magn. Magn. Mater. **65**, 83.

Freeman, A. J., and R. E. Watson, 1962, Phys. Rev **127**, 2058.

Friedt, J. M., J. P. Sanchez, P. L'Héritier, and R. Fruchart, 1985, in *Nd-Fe Permanent Magnets: Their Present and Future Applications,* edited by I. V. Mitchell (Elsevier Applied Science, London/New York), p. 179.

Friedt, J. M., A. Vasquez, J. P. Sanchez, P. L'Héritier, and R. Fruchart, 1986, J. Phys. F **16**, 651.

Fruchart, D., S. Miraglia, S. Obbade, P. Ezekwenna, and P. L'Héritier, 1990, J. Magn. Magn. Mater. **83**, 291.

Fruchart, D., L. Pontonnier, F. Vaillant, J. Bartolomé, J. M. Fernandez, J. A. Puertolas, C. Rillo, J. R. Regnard, A. Yaouanc, R. Fruchart, and P. L'Héritier, 1988, IEEE Trans. Magn. **24**, 1641.

Fruchart, D., F. Vaillant, A. Yaouanc, J. M. D. Coey, R. Fruchart, P. L'Héritier, T. Riesterer, J. Osterwalder, and L. Schlapbach, 1987, J. Less-Common Met. **130**, 97.

Fruchart, D., P. Wolfers, P. Vulliet, A. Yaouanc, R. Fruchart, and P. L'Héritier, 1985, in *Nd-Fe Permanent Magnets: Their Present and Future Applications,* edited by I. V. Mitchell (Elsevier Applied Science, London/New York), p. 173.

Fruchart, R., P. L'Héritier, P. Dalmas de Réotier, D. Fruchart, P. Wolfers, J. M. D. Coey, L. P. Ferreira, R. Guillen, P. Vulliet, and A. Yaouanc, 1987, J. Phys. F **17**, 483.

Fuerst, C. D., 1990, J. Appl. Phys. **67**, 4747.

Fuerst, C. D., and E. G. Brewer, 1989, IEEE Trans. Magn. **25**, 4108.

Fuerst, C. D., and E. G. Brewer, 1990, Appl. Phys. Lett. **56**, 2252.

Fuerst, C. D., and E. G. Brewer, 1991, J. Appl. Phys. **69**, 5826.

Fuerst, C. D., and J. F. Herbst, 1988a, J. Appl. Phys. **63**, 3324.

Fuerst, C. D., and J. F. Herbst, 1988b, Appl. Phys. Lett. **52**, 1358.

Fuerst, C. D., and J. F. Herbst, 1988c, J. Appl. Phys. **64**, 1332.

Fuerst, C. D., and J. F. Herbst, 1989a, Appl. Phys. Lett. **54**, 1068.

Fuerst, C. D., and J. F. Herbst, 1989b, J. Appl. Phys. **66**, 1782.

Fuerst, C. D., and J. F. Herbst, 1991, J. Appl. Phys. **69**, 7727.

Fuerst, C. D., J. F. Herbst, and E. A. Alson, 1986, J. Magn. Magn. Mater. **54-57**, 567.

Fuerst, C. D., J. F. Herbst, and F. E. Pinkerton, 1988, J. Appl. Phys. **64**, 5556.

Fuerst, C. D., G. P. Meisner, and F. E. Pinkerton, 1987, J. Appl. Phys. **61**, 2314.

Fuerst, C. D., G. P. Meisner, F. E. Pinkerton, and W. B. Yelon, 1987, J. Less-Common Met. **133**, 255.

Fuerst, C. D., G. P. Meisner, F. E. Pinkerton, and W. B. Yelon, 1988, J. Appl. Phys. **63**, 3119.

Fujii, H., H. Nagata, Y. Uwatoko, T. Okamoto, H. Yamamoto, and M. Sagawa, 1987, J. Magn. Magn. Mater. **70**, 331.

Fujii, H., M. Saga, T. Takeda, S. Komura, T. Okamoto, S. Hirosawa, and M. Sagawa, 1987, IEEE Trans. Magn. **MAG-23**, 3119.

Fujii, H., W. E. Wallace, and E. B. Boltich, 1986, J. Magn. Magn. Mater. **61**, 251.

Fujita, A., H. Onodera, H. Yamauchi, M. Yamada, H. Yamamoto, S. Hirosawa, and M. Sagawa, 1987, J. Magn. Magn. Mater. **69**, 267.

Fukunaga, H., and T. Fukuda, 1990, Jpn. J. Appl. Phys. **29**, 1711.

Fukuno, A., and R. C. O'Handley, 1989, J. Appl. Phys. **65**, 4959.

Gaskell, P. H., 1981, Nature (London) **289**, 474.

Gauder, D. R., M. H. Froning, R. J. White, and A. E. Ray, 1988, J. Appl. Phys. **63**, 3522.

Gaunt, P., 1983, Philos. Mag. B **48**, 261.

Gaunt, P., 1986, J. Appl. Phys. **59**, 4129.

Gaunt, P., 1987, Can. J. Phys. **65**, 1194.

Gaunt, P., G. Hadjipanayis, and D. Ng, 1986, J. Magn. Magn. Mater. **54-57**, 841.

Gavigan, J. P., and D. Givord, 1990, J. Magn. Magn. Mater. **84**, 288.

Gavigan, J. P., D. Givord, H. S. Li, and J. Voiron, 1988, Physica B **149**, 345.

Gavigan, J. P., D. Givord, H. S. Li, O. Yamada, H. Maruyama, M. Sagawa, and S. Hirosawa, 1987, J. Magn. Magn. Mater. **70**, 416.

Gavigan, J. P., H. S. Li, J. M. D. Coey, J. M. Cadogan, and D. Givord, 1988a, J. Phys. (Paris) **49**, C8-557.

Gavigan, J. P., H-S. Li, J. M. D. Coey, T. Viadieu, L. Pareti, O. Moze, and F. Bolzoni, 1988b, J. Phys. (Paris) **49**, C8-577.

Ge, S. H., Y. D. Zhang, F. S. Li, and R. J. Zhou, 1989, Hyp. Interactions **52**, 335.

Girgis, K., M. Kraft, U. Weis, P. Fischer, and M. Sostarich, 1990, J. Less-Common Met. **162**, 335.

Givord, D., C. Heiden, A. Hoëhler, P. Tenaud, T. Viadieu, and K. Zeibig, 1988, IEEE Trans. Magn. **24**, 1918.

Givord, D., and H. S. Li, 1985, in *Nd-Fe Permanent Magnets: Their Present and Future Applications,* edited by I. V. Mitchell (Elsevier Applied Science, London/New York), p. 131.

Givord, D., H. S. Li, J. M. Cadogan, J. M. D. Coey, J. P. Gavigan, O. Yamada, H. Maruyama, M. Sagawa, and S. Hirosawa, 1988, J. Appl. Phys. **63**, 3713.

Givord, D., H. S. Li, and J. M. Moreau, 1984, Solid State Commun. **50**, 497.

Givord, D., H. S. Li, J. M. Moreau, R. Perrier de la Bâthie, and E. Du Trémolet de Lacheisserie, 1985, Physica B **130**, 323.

Givord, D., H. S. Li, J. M. Moreau, and P. Tenaud, 1986, J. Magn. Magn. Mater. **54-57**, 445.

Givord, D., H. S. Li, and R. Perrier de la Bâthie, 1984, Solid State Commun. **51**, 857.

Givord, D., H. S. Li, and F. Tasset, 1985, J. Appl. Phys. **57**, 4100.

Givord, D., A. Lienard, P. Tenaud, and T. Viadieu, 1987, J. Magn. Magn. Mater. **67**, L281.

Givord, D., J. M. Moreau, and P. Tenaud, 1985, Solid State Commun. **55**, 303.

Givord, D., P. Tenaud, and T. Viadieu, 1986, J. Appl. Phys. **60**, 3263.

Givord, D., P. Tenaud, and T. Viadieu, 1988a, IEEE Trans. Magn. **24**, 1921.

Givord, D., P. Tenaud, and T. Viadieu, 1988b, J. Magn. Magn. Mater. **72**, 247.

Givord, D., P. Tenaud, T. Viadieu, and G. Hadjipanayis, 1987, J. Appl. Phys. **61**, 3454.

Goodenough, John B., 1963, *Magnetism and the Chemical Bond* (Interscience, New York/London), pp. 78–80.

Grandjean, F., G. J. Long, O. A. Pringle, and J. Fu, 1990, Hyp. Interactions **62**, 131.

Grandjean, F., G. J. Long, D. E. Tharp, O. A. Pringle, and W. J. James, 1988, J. Phys. (Paris) **49**, C8-581.

Greedan, J. E., and V. U. S. Rao, 1973, J. Solid State Chem. **6**, 387.

Grieb, B., E.-Th. Henig, G. Martinek, H. H. Stadelmaier, and G. Petzow, 1990, IEEE Trans. Magn. **26**, 1367.

Grieb, B., K. G. Knoch, E-Th. Henig, and G. Petzow, 1989, J. Magn. Magn. Mater. **80**, 75.

Grössinger, R., X. C. Chou, R. Krewenka, G. Wiesinger, R. Eibler, X. K. Sun, and Y. C. Chuang, 1988, J. Phys. (Paris) **49**, C8-599.

Grössinger, R., H. Harada, A. Keresztes, H. R. Kirchmayr, and M. Tokunaga, 1987, IEEE Trans. Magn. **MAG-23**, 2117.

Grössinger, R., F. Haslinger, S. Zhang, R. Eibler, Y. Liu, J. Schneider, A. Handstein, and H. R. Kirchmayr, 1988, IEEE Trans. Magn. **24**, 1629.

Grössinger, R., S. Heiss, G. Hilscher, H. R. Kirchmayr, R. Krewenka, and G. Wiesinger, 1989, J. Magn. Magn. Mater. **80**, 61.

Grössinger, R., G. Hilscher, H. Kirchmayr, H. Sassik, R. Strnat, and G. Wiesinger, 1985, Physica **130B**, 307.

Grössinger, R., A. Keresztes, H. Harada, and Z. Shougong, 1987, in *Proceedings of the Ninth International Workshop on Rare-Earth Magnets and Their Applications,* edited by C. Herget and R. Poerschke (Deutsche Physikalische Gesellschaft, Bad Honnef, FRG), p. 593.

Grössinger, R., H. Kirchmayr, and K. H. J. Buschow, 1988, J. Less-Common Met. **136**, 367.

Grössinger, R., R. Krewenka, H. Buchner, and H. Harada, 1988, J. Phys. (Paris) **49**, C8-659.

Grössinger, R., R. Krewenka, H. R. Kirchmayr, P. Naastepad, and K. H. J. Buschow, 1987a, J. Less-Common Met. **134**, L17.

Grössinger, R., R. Krewenka, H. R. Kirchmayr, S. Sinnema, F.-M. Yang, Y.-K. Huang, F. R. de Boer, and K. H. J. Buschow, 1987b, J. Less-Common Met. **132**, 265.

Grössinger, R., R. Krewenka, X. C. Kou, and K. H. J. Buschow, 1990, J. Magn. Magn. Mater. **83**, 130.

Grössinger, R., R. Krewenka, K. S. V. L. Narasimhan, and M. Sagawa, 1985, J. Magn. Magn. Mater. **51**, 160.

Grössinger, R., R. Krewenka, X. K. Sun, R. Eibler, H. R. Kirchmayr, and K. H. J. Buschow, 1986, J. Less-Common Met. **124**, 165.

Grössinger, R., P. Obitsch, X. K. Sun, R. Eibler, H. R. Kirchmayr, F. Rothwarf, and H. Sassik, 1984, Mater. Lett. **2**, 539.

Grössinger, R., X. K. Sun, R. Eibler, K. H. J. Buschow, and H. R. Kirchmayr, 1985, J. Phys. (Paris) **46**, C6-221.

Grössinger, R., X. K. Sun, R. Eibler, K. H. J. Buschow, and H. R. Kirchmayr, 1986, J. Magn. Magn. Mater. **58**, 55.

Gu, Z-Q., and W. Y. Ching, 1986a, J. Magn. Magn. Mater. **54-57**, 525.

Gu, Z-Q., and W. Y. Ching, 1986b, Phys. Rev. B **33**, 2868.

Gu, Z-Q., and W. Y. Ching, 1987a, Phys. Rev. B **36**, 8530.

Gu, Z-Q., and W. Y. Ching, 1987b, J. Appl. Phys. **61**, 3977.

Gubbens, P. C. M., A. M. van der Kraan, and K. H. J. Buschow, 1985, Phys. Status Solidi B **130**, 575.

Gubbens, P. C. M., A. M. van der Kraan, and K. H. J. Buschow, 1986, J. Magn. Magn. Mater. **54-57**, 591.

Gubbens, P. C. M., A. M. van der Kraan, and K. H. J. Buschow, 1988, J. Phys. (Paris) **49**, C8-591.

Gubbens, P. C. M., A. M. van der Kraan, R. P. van Stapele, and K. H. J. Buschow, 1987, J. Magn. Magn. Mater. **68**, 238.

Gueramian, M., A. Bezinge, K. Yvon, and J. Müller, 1987, Solid State Commun. **64**, 639.

Gwan, P. B., J. P. Scully, D. Bingham, J. S. Cook, R. K. Day, J. B. Dunlop, and R. G. Heydon, 1987, in *Proceedings of the Ninth International Workshop on Rare-Earth Magnets and Their Applications,* edited by C. Herget and R. Poerschke (Deutsche Physikalische Gesellschaft, Bad Honnef, FRG), p. 295.

Hadjipanayis, G. C., 1986, in *Rapidly Solidified Alloys and Their Mechanical and Magnetic Properties,* Materials Research Society Symposia Proceedings Vol. 58, edited by B. C. Giessen, D. E. Polk, and A. I. Taub (Materials Research Society, Pittsburgh), p. 187.

Hadjipanayis, G. C., 1989, Mater. Sci. Eng. **B3**, 431.

Hadjipanayis, G. C., R. C. Dickenson, and K. R. Lawless, 1986, J. Magn. Magn. Mater. **54-57**, 557.

Hadjipanayis, G. C., and W. Gong, 1987, J. Magn. Magn. Mater. **66**, 390.

Hadjipanayis, G. C., and W. Gong, 1988, J. Appl. Phys. **64**, 5559.

Hadjipanayis, G. C., R. C. Hazelton, and K. R. Lawless, 1983, Appl. Phys. Lett. **43**, 797.

Hadjipanayis, G. C., R. C. Hazelton, and K. R. Lawless, 1984, J. Appl. Phys. **55**, 2073.

Hadjipanayis, G. C., and A. Kim, 1987, IEEE Trans. Magn. **MAG-23**, 2533.

Hadjipanayis, G. C., and A. Kim, 1988, J. Appl. Phys. **63**, 3310.

Hadjipanayis, G. C., K. R. Lawless, and R. C. Dickerson, 1985, J. Appl. Phys. **57**, 4097.

Hadjipanayis, G. C., and Y. F. Tao, 1985, J. Phys. (Paris) **46**, C6-237.

Hadjipanayis, G. C., Y. F. Tao, and K. R. Lawless, 1985, in *Proceedings of the Fourth International Symposium on Magnetic Anisotropy and Coercivity in Rare Earth-Transition Metal Alloys,* edited by K. J. Strnat (University of Dayton, Dayton, Ohio), p. 657.

Hadjipanayis, G. C., Y. F. Tao, and K. R. Lawless, 1986, IEEE Trans. Magn. **MAG-22**, 1845.

Hadjipanayis, G. C., N. Venkateswaran, and J. Strzeszewski, 1988, J. Phys. (Paris) **49**, C8-639.

Hadjipanayis, G. C., M. Zhang, and C. Gao, 1989, Appl. Phys. Lett. **54**, 1812.

Handstein, A., J. Schneider, U. Heinecke, R. Grössinger, and H. Sassik, 1988, J. Phys. (Paris) **49**, C8-655.

Handstein, A., J. Schneider, U. Heinecke, R. Grössinger, and S. Zhang, 1987, in *Proceedings of the Ninth International Workshop on Rare-Earth Magnets and Their Applications,* edited by C. Herget and R. Poerschke (Deutsche Physikalische Gesellschaft, Bad Honnef, FRG), p. 601.

Handstein, A., J. Schneider, K.-H. Müller, R. Krewenka, R. Grössinger, and H. R. Kirchmayr, 1990, J. Magn. Magn. Mater. **83**, 199.

Handstein, A., J. Schneider, D. Stephan, W. Fischer, U. Heinecke, R. Grössinger, H. Sassik, and H. R. Kirchmayr, 1985, Mater. Lett. **3**, 200.

Harada, T., T. Ando, R. C. O'Handley, and N. J. Grant, 1990a, J. Appl. Phys. **67**, 4233.

Harada, T., T. Ando, R. C. O'Handley, and N. J. Grant, 1990b, J. Appl. Phys. **68**, 4728.

Harris, I. R., 1987, J. Less-Common Met. **131**, 245.

Harris, I. R., and P. J. McGuiness, 1990, in *Proceedings of the Eleventh International Workshop on Rare-Earth Magnets and Their Applications,* edited by S. G. Sankar (Carnegie Mellon University, Pittsburgh), p. 29.

Harris, I. R., P. J. McGuiness, D. G. R. Jones, and J. S. Abell, 1987, Physica Scripta **T19**, 435.

Harris, I. R., C. Noble, and T. Bailey, 1985, J. Less-Common Met. **106**, L1.

Hauet, A., D. Lemarchand, B. Labulle, J. Teillet, and P. Vigier, 1988, J. Phys. (Paris) **49**, C8-607.

Hauet, A., D. Lemarchand, and J. Teillet, 1988, Solid State Commun. **66**, 1191.

Hazelton, R. C., G. C. Hadjipanayis, K. R. Lawless, and D. J. Sellmyer, 1984, J. Magn. Magn. Mater. **40**, 278.

Heinecke, U., A. Handstein, and J. Schneider, 1985, J. Magn. Magn. Mater. **53**, 236.

Heisz, S., and G. Hilscher, 1987, J. Magn. Magn. Mater. **67**, 20.

Heisz, S., G. Hilscher, P. Hundegger, and H. Kirchmayr, 1988, J. Phys. (Paris) **49**, C8-653.

Heisz, S., G. Hilscher, G. Wiesinger, and H. Sassik, 1987, in *Proceedings of the Ninth International Workshop on Rare-Earth Magnets and Their Applications,* edited by C. Herget and R. Poerschke (Deutsche Physikalische Gesellschaft, Bad Honnef, FRG), p. 267.

Heisz, W., and L. Schultz, 1988, Appl. Phys. Lett. **53**, 342.

Hellwig, C., K. Girgis, J. Schefer, K. H. J. Buschow, and P. Fischer, 1990, J. Less-Common Met. **163**, 361.

Helmholdt, R. B., and K. H. J. Buschow, 1988, J. Less-Common Met. **144**, L33.

Henry, N., and K. Lonsdale, 1952, *International Tables for X-ray Crystallography* (Kynoch, Birmingham), Vol. I.

Herbst, J. F., and J. J. Croat, 1982, J. Appl. Phys. **53**, 4304.

Herbst, J. F., and J. J. Croat, 1984, J. Appl. Phys. **55**, 3023.

Herbst, J. F., J. J. Croat, R. W. Lee, and W. B. Yelon, 1982, J. Appl. Phys. **53**, 250.

Herbst, J. F., J. J. Croat, F. E. Pinkerton, and W. B. Yelon, 1984, Phys. Rev. B **29**, 4176.

Herbst, J. F., J. J. Croat, and W. B. Yelon, 1985, J. Appl. Phys. **57**, 4086.

Herbst, J. F., C. D. Fuerst, R. K. Mishra, C. B. Murphy, and D. J. Van Wingerden, 1991, J. Appl. Phys. **69**, 5823.

Herbst, J. F., R. W. Lee, and F. E. Pinkerton, 1986, Annu. Rev. Mater. Sci. **16**, 467.

Herbst, J. F., and J. W. Wilkins, 1979, Phys. Rev. B **20**, 2999.

Herbst, J. F., and J. W. Wilkins, 1987, in *Handbook on the Physics and Chemistry of Rare Earths,* edited by K. A. Gschneidner, Jr., L. Eyring, and S. Hüfner (North-Holland, Amsterdam), Vol. 10, p. 321.

Herbst, J. F., and W. B. Yelon, 1985, J. Appl. Phys. **57**, 2343.

Herbst, J. F., and W. B. Yelon, 1986a, J. Appl. Phys. **60**, 4224.

Herbst, J. F., and W. B. Yelon, 1986b, J. Magn. Magn. Mater. **54-57**, 570.

Herzer, G., W. Fernengel, and E. Adler, 1986, J. Magn. Magn. Mater. **58**, 48.

Hien, T. D., L. T. Tai, R. Grössinger, R. Krewenka, F. R. de Boer, and F. F. Bekker, 1987, J. Less-Common Met. **127**, 111.

Hilscher, G., R. Grössinger, S. Heisz, H. Sassik, and G. Wiesinger, 1986, J. Magn. Magn. Mater. **54-57**, 577.

Hiraga, K., M. Hirabayashi, M. Sagawa, and Y. Matsuura, 1985a, Jpn. J. Appl. Phys. **24**, L30.

Hiraga, K., M. Hirabayashi, M. Sagawa, and Y. Matsuura, 1985b, Jpn. J. Appl. Phys. **24**, 699.

Hiraga, K., M. Hirabayashi, M. Sagawa, and Y. Matsuura, 1985c, Jpn. J. Appl. Phys. **24**, 896.

Hirosawa, S., 1989, IEEE Trans. Magn. **25**, 3437.

Hirosawa, S., A. Hanaki, H. Tomizawa, and A. Hamamura, 1990, Physica B **164**, 117.

Hirosawa, S., Y. Matsuura, H. Yamamoto, S. Fujimura, M. Sagawa, and H. Yamauchi, 1985, Jpn. J. Appl. Phys. **24**, L803.

Hirosawa, S., Y. Matsuura, H. Yamamoto, S. Fujimura, M. Sagawa, and H. Yamauchi, 1986, J. Appl. Phys. **59**, 873.

Hirosawa, S., and M. Sagawa, 1985, Solid State Commun. **54**, 335.

Hirosawa, S., and M. Sagawa, 1987, J. Magn. Magn. Mater. **71**, L1.

Hirosawa, S., and M. Sagawa, 1988, J. Appl. Phys. **64**, 5553.

Hirosawa, S., M. Sagawa, and T. Katayama, 1990, J. Magn. Magn. Mater. **87**, 205.

Hirosawa, S., K. Tokuhara, Y. Matsuura, H. Yamamoto, S. Fujimura, and M. Sagawa, 1986, J. Magn. Magn. Mater. **61**, 363.

Hirosawa, S., K. Tokuhara, and M. Sagawa, 1987, Jpn. J. Appl. Phys. **26**, L1359.

Hirosawa, S., K. Tokuhara, H. Yamamoto, S. Fujimura, M. Sagawa, and H. Yamauchi, 1987, J. Appl. Phys. **61**, 3571.

Hirosawa, S., H. Tomizawa, S. Mino, and A. Hamamura, 1990, IEEE Trans. Magn. **26**, 1960.

Hirosawa, S., and Y. Tsubokawa, 1990, J. Magn. Magn. Mater. **84**, 309.

Hirosawa, S., Y. Yamaguchi, K. Tokuhara, H. Yamamoto, S. Fujimura, and M. Sagawa, 1987, IEEE Trans. Magn. **MAG-23**, 2120.

Hiroyoshi, H., H. Kato, M. Yamada, N. Saito, Y. Nakagawa, S. Hirosawa, and M. Sagawa, 1987, Solid State Commun. **62**, 475.

Hiroyoshi, H., N. Saito, G. Kido, Y. Nakagawa, S. Hirosawa, and M. Sagawa, 1986, J. Magn. Magn. Mater. **54-57**, 583.

Hiroyoshi, H., M. Yamada, N. Saito, H. Kato, Y. Nakagawa, S. Hirosawa, and M. Sagawa, 1987, J. Magn. Magn. Mater. **70**, 337.

Hiroyoshi, H., H. Yamauchi, Y. Yamaguchi, H. Yamamoto, Y. Nakagawa, and M. Sagawa, 1985, Solid State Commun. **54**, 41.

Ho, W.-W., H.-Y. Chen, Y.-C. Yang, J. Wang, B. Liao, C. Lin, F. Xing, Z.-X. Liu, and J. Lan, 1985, in *Proceedings of the Fourth International Symposium on Magnetic Anisotropy and Coercivity in Rare Earth-Transition Metal Alloys,* edited by K. J. Strnat (University of Dayton, Dayton, Ohio), p. 635.

Hock, S., and H. Kronmüller, 1987, in *Proceedings of the Fifth International Symposium on Magnetic Anisotropy and Coercivi-*

ty in Rare-Earth–Transition Metal Alloys, edited by C. Herget, H. Kronmüller, and R. Poerschke (Deutsche Physikalische Gesellschaft, Bad Honnef, FRG), p. 275.

Hoffer, G., and K. Strnat, 1966, IEEE Trans. Magn. **MAG-2**, 487.

Homburg, H., T. Sinnemann, S. Methfessel, M. Rosenberg, and B. X. Gu, 1990, J. Magn. Magn. Mater. **83**, 231.

Hong, N. M., J. J. M. Franse, and N. P. Thuy, 1989, J. Less-Common Met. **155**, 151.

Honma, H., and H. Ino, 1987, IEEE Trans. Magn. **MAG-23**, 3116.

Honma, H., M. Shimotomai, and M. Doyama, 1985, J. Magn. Magn. Mater. **52**, 399.

Hu, J., Y. Wang, M. Feng, D. Dai, Z. Wang, and Y. Cao, 1989, J. Magn. Magn. Mater. **81**, 345.

Hu, J., Y. Wang, X. Li, L. Yin, M. Feng, D. Dai, T. Wang, J. G. Zhao, and Z. Wang, 1988, J. Phys. (Paris) **49**, C8-601.

Huang, G. X., Q. Z. Xu, L. H. Wu, S. Y. Shi, W. M. Gao, S. F. Yu, H. C. Hua, G. A. Wang, and C. H. Zheng, 1990, Phys. Scr. **41**, 372.

Huang, M. Q., E. B. Boltich, W. E. Wallace, and E. Oswald, 1986a, J. Less-Common Met. **124**, 55.

Huang, M. Q., E. B. Boltich, W. E. Wallace, and E. Oswald, 1986b, J. Magn. Magn. Mater. **60**, 270.

Huang, M. Q., E. Oswald, E. Boltich, S. Hirosawa, W. E. Wallace, and E. Schwab, 1985, Physica **130B**, 319.

Huang, Y.-K., C. H. Wu, Y. C. Chuang, F.-M. Yang, and F. R. de Boer, 1987, J. Less-Common Met. **132**, 317.

Hubbard, W. M., E. Adams, and J. V. Gilfrich, 1960, J. Appl. Phys. **31**, 368S.

Hutchings, M. T., 1964, in *Solid State Physics,* edited by F. Seitz and D. Turnbull (Academic Press, New York), Vol. 16, p. 227.

Hütten, A., and P. Haasen, 1987, Scr. Metall. **21**, 407.

Hütten, A., and P. Haasen, 1991, Acta Metall. Mater. **39**, 1.

Ibarra, M. R., P. A. Algarabel, A. Alberdi, J. Bartolomé, and A. del Moral, 1987, J. Appl. Phys. **61**, 3451.

Ibarra, M. R., P. A. Algarabel, C. Marquina, J. I. Arnaudas, A. del Moral, L. Pareti, O. Moze, G. Marusi, and M. Solzi, 1989, Phys. Rev. B **39**, 7081.

Ibarra, M. R., C. Marquina, P. A. Algarabel, J. I. Arnaudas, and A. del Moral, 1988, J. Appl. Phys. **64**, 5537.

Ibarra, M. R., C. Marquina, P. A. Algarabel, J. I. Arnaudas, and A. del Moral, 1989, Solid State Commun. **69**, 131.

Ichinose, K., K. Fujiwara, M. Oyasato, H. Nagai, and A. Tsujimura, 1988, J. Phys. (Paris) **49**, C8-595.

Iida, T., H. Ueki, T. Fukuzawa, T. Saito, K. Shinagawa, and T. Tsushima, 1990, in *Proceedings of the Sixth International Symposium on Magnetic Anisotropy and Coercivity in Rare Earth-Transition Metal Alloys,* edited by S. G. Sankar (Carnegie Mellon University, Pittsburgh), p. 342.

Imry, Y., and S-K. Ma, 1975, Phys. Rev. Lett. **35**, 1399.

Inoue, J., and M. Shimizu, 1985, J. Phys. F **15**, 1511.

Inoue, J., and M. Shimizu, 1986a, J. Phys. F **16**, 1051.

Inoue, J., and M. Shimizu, 1986b, J. Phys. F **16**, L157.

Ishikawa, T., Y. Hamada, and K. Ohmori, 1989, IEEE Trans. Magn. **25**, 3434.

Itoh, T., K. Hikosaka, H. Takahashi, T. Ukai, and N. Mori, 1987, J. Appl. Phys. **61**, 3430.

Jacobs, T. H., K. H. J. Buschow, R. Verhoef, and F. R. de Boer, 1990, J. Less-Common Met. **157**, L11.

Jacobs, T. H., C. J. M. Denissen, and K. H. J. Buschow, 1989, J. Less-Common Met. **153**, L5.

Jang, T. S., and H. H. Stadelmaier, 1990, Mater. Lett. **9**, 483.

Jaswal, S. S., 1990, Phys. Rev. B **41**, 9697.

Jaswal, S. S. , M. A. Langell, Y. G. Ren, M. A. Engelhardt, and D. J. Sellmyer, 1988, J. Appl. Phys. **64**, 5577.

Jedryka, E., M. Wojcik, P. Panissod, and K. H. J. Buschow, 1990, J. Appl. Phys. **67**, 4586.

Jedryka, E., M. Wojcik, P. Panissod, M. Rosenberg, S. Hirosawa, and M. Sagawa, 1988, J. Phys. (Paris) **49**, C8-587.

Jha, A., H. A. Davies, and R. A. Buckley, 1989, J. Magn. Magn. Mater. **80**, 109.

Jiang, S. Y., H. Y. Chen, S. F. Cheng, E. B. Boltich, S. G. Sankar, D. E. Laughlin, and W. E. Wallace, 1988, J. Appl. Phys. **64**, 5510.

Jiang, S. Y., F. Pourarian, E. B. Boltich, and W. E. Wallace, 1987, IEEE Trans. Magn. **MAG-23**, 2720.

Jiang, S. Y., F. Pourarian, J. X. Yan, S. G. Sankar, and W. E. Wallace, 1988, J. Magn. Magn. Mater. **74**, 181.

Jubb, G. A., and R. A. McCurrie, 1987, IEEE Trans. Magn. **MAG-23**, 1801.

Jurczyk, M., 1987a, in *Proceedings of the Fifth International Symposium on Magnetic Anisotropy and Coercivity in Rare-Earth–Transition Metal Alloys,* edited by C. Herget, H. Kronmüller, and R. Poerschke (Deutsche Physikalische Gesellschaft, Bad Honnef, FRG), p. 133.

Jurczyk, M., 1987b, J. Magn. Magn. Mater. **67**, 187.

Jurczyk, M., 1988a, IEEE Trans. Magn. **24**, 1942.

Jurczyk, M., 1988b, J. Magn. Magn. Mater. **73**, 199.

Jurczyk, M., 1988c, J. Magn. Magn. Mater. **73**, 367.

Jurczyk, M., 1990a, J. Less-Common Met. **158**, 117.

Jurczyk, M., 1990b, J. Magn. Magn. Mater. **83**, 237.

Jurczyk, M., G. S. Burchanov, O. D. Chistyakov, 1989, Phys. Status Solidi A **112**, K121.

Jurczyk, M., and O. D. Chistjakov, 1989a, J. Magn. Magn. Mater. **78**, 279.

Jurczyk, M., and O. D. Chistyakov, 1989b, Phys. Status Solidi A **114**, K219.

Jurczyk, M., and O. D. Chistyakov, 1990, Phys. Status Solidi A **117**, 299.

Jurczyk, M., and A. Kowalczyk, 1987, J. Magn. Magn. Mater. **68**, 331.

Jurczyk, M., A. Kowalczyk, and A. Wrzeciono, 1987a, Phys. Status Solidi A **101**, K65.

Jurczyk, M., A. Kowalczyk, and A. Wrzeciono, 1987b, in *Proceedings of the Ninth International Workshop on Rare-Earth Magnets and Their Applications,* edited by C. Herget and R. Poerschke (Deutsche Physikalische Gesellschaft, Bad Honnef, FRG), p. 701.

Jurczyk, M., and W. E. Wallace, 1986a, J. Magn. Magn. Mater. **59**, L182.

Jurczyk, M., and W. E. Wallace, 1986b, J. Less-Common Met. **124**, 149.

Jurczyk, M., and W. E. Wallace, 1986c, IEEE Trans. Magn. **MAG-22**, 755.

Kadin, A. M., R. W. McCallum, G. B. Clemente, and J. E. Keem, 1987, in *Science and Technology of Rapidly Quenched Alloys,* Materials Research Society Symposia Proceedings Vol. 80, edited by M. Tenhover, W. L. Johnson, and L. E. Tanner (Materials Research Society, Pittsburgh), p. 385.

Kajiwara, S., G. Kido, Y. Nakagawa, S. Hirosawa, and M. Sagawa, 1987, J. Phys. Soc. Jpn. **56**, 829.

Kakol, Z., H. Figiel, and C. Kapusta, 1987, in *Proceedings of the Fifth International Symposium on Magnetic Anisotropy and Coercivity in Rare-Earth-Transition Metal Alloys,* edited by C. Herget, H. Kronmüller, and R. Poerschke (Deutsche Physikalische Gesellschaft, Bad Honnef, FRG), p. 125.

Kakol, Z., C. Kapusta, and H. Figiel, 1988, J. Magn. Magn.

Mater. **75**, 141.

Kamal, R., and Y. Andersson, 1985, Phys. Rev. B **32**, 1756.

Kamal, R., and Lovleen, 1989, J. Less-Common Met. **147**, 79.

Kamal, R., M. Rani, and M. S. Saini, 1986, J. Less-Common Met. **125**, L7.

Kamarad, J., Z. Arnold, and J. Schneider, 1987, J. Magn. Magn. Mater. **67**, 29.

Kapusta, C., and H. Figiel, 1988, J. Phys. (Paris) **49**, C8-559.

Kapusta, C., H. Figiel, and Z. Kakol, 1990, J. Magn. Magn. Mater. **83**, 151.

Kapusta, C., Z. Kakol, H. Figiel, and R. Radwański, 1986, J. Magn. Magn. Mater. **59**, 169.

Kato, H., M. Yamada, G. Kido, Y. Nakagawa, S. Hirosawa, and M. Sagawa, 1988, J. Phys. (Paris) **49**, C8-575.

Kawai, T., B. M. Ma, S. G. Sankar, and W. E. Wallace, 1990, J. Appl. Phys. **67**, 4610.

Kido, G., S. Kajiwara, Y. Nakagawa, S. Hirosawa, and M. Sagawa, 1987, IEEE Trans. Magn. **MAG-23**, 3107.

Kim, A. S., 1988a, J. Appl. Phys. **63**, 3519.

Kim, A. S., 1988b, J. Appl. Phys. **63**, 3975.

Kirchmayr, H. R., and C. A. Poldy, 1979, in *Handbook on the Physics and Chemistry of Rare Earths,* edited by K A. Gschneidner, Jr., and L. Eyring (North-Holland, Amsterdam), Vol. 2, p. 55.

Kisker, E., K. Schröder, W. Gudat, and M. Campagna, 1985, Phys. Rev. B **31**, 329.

Kittel, C., and J. K. Galt, 1956, Solid State Phys. **3**, 437.

Knoch, K. G., B. Grieb, E.-Th. Henig, H. Kronmüller, and G. Petzow, 1990, IEEE Trans. Magn. **26**, 1951.

Knoch, K. G., E.-Th. Henig, and J. Fidler, 1990, J. Magn. Magn. Mater. **83**, 209.

Knoch, K. G., G. Schneider, J. Fidler, E.-Th. Henig, and H. Kronmüller, 1989, IEEE Trans. Magn. **25**, 3426.

Kohmoto, O., T. Yoneyama, and K. Yajima, 1987, Jpn. J. Appl. Phys. **26**, 1804.

Kojima, H., 1982, in *Ferromagnetic Materials,* edited by E. P. Wohlfarth (North-Holland, Amsterdam), Vol. 3, p. 305.

Koon, N. C., M. Abe, E. Callen, B. N. Das, S. H. Liou, A. Martinez, and R. Segnan, 1986, J. Magn. Magn. Mater. **54-57**, 593.

Koon, N. C., and B. N. Das, 1981, Appl. Phys. Lett. **39**, 840.

Koon, N. C., and B. N. Das, 1984, J. Appl. Phys. **55**, 2063.

Koon, N. C., B. N. Das, and J. A. Geohegan, 1982, IEEE Trans. Magn. **MAG-18**, 1448.

Koon, N. C., B. N. Das, M. Rubinstein, and J. Tyson, 1985, J. Appl. Phys. **57**, 4091.

Koon, N. C., B. N. Das, and C. M. Williams, 1986, J. Magn. Magn. Mater. **54-57**, 523.

Kostikas, A., V. Papaefthymiou, A. Simopoulos, and G. C. Hadjipanayis, 1985, J. Phys. F **15**, L129.

Kou, X. C., X. K. Sun, Y. C. Chuang, R. Grössinger, and H. R. Kirchmayr, 1989a, J. Magn. Magn. Mater. **80**, 31.

Kou, X. C., X. K. Sun, Y. C. Chuang, T. S. Zhao, R. Grössinger, R. Eibler, and H. R. Kirchmayr, 1989b, Phys. Status Solidi A **112**, 175.

Kou, X. C., X. K. Sun, Y. C. Chuang, T. S. Zhao, R. Grössinger, and H. R. Kirchmayr, 1989c, J. Magn. Magn. Mater. **82**, 327.

Kou, X. C., X. K. Sun, Y. C. Chuang, T. S. Zhao, R. Grössinger, and H. R. Kirchmayr, 1990a, Solid State Commun. **73**, 87.

Kou, X. C., X. K. Sun, Y. C. Chuang, T. S. Zhao, R. Grössinger, and H. R. Kirchmayr, 1990b, J. Less-Common Met. **160**, 109.

Kou, X. C., G. Wiesinger, and R. Grössinger, 1990, in *Proceedings of the Sixth International Symposium on Magnetic Anisotropy and Coercivity in Rare Earth-Transition Metal Alloys,* edited by S. G. Sankar (Carnegie Mellon University, Pittsburgh), p. 262.

Kouvel, J. S., and R. H. Wilson, 1961, J. Appl. Phys. **32**, 435.

Kowalczyk, A., 1989, J. Magn. Magn. Mater. **82**, L1.

Kowalczyk, A., and V. Ivanov, 1990, J. Magn. Magn. Mater. **87**, 330.

Kowalczyk, A., P. Stefanski, A. Szlaferek, and A. Wrzeciono, 1990, J. Magn. Magn. Mater. **83**, 147.

Kowalczyk, A., P. Stefanski, and A. Wrzeciono, 1988, Phys. Status Solidi A **107**, K61.

Kowalczyk, A., P. Stefanski, and A. Wrzeciono, 1989, J. Magn. Magn. Mater. **79**, 109.

Kowalczyk, A., P. Stefanski, and A. Wrzeciono, 1990, J. Magn. Magn. Mater. **84**, L5.

Kowalczyk, A., and A. Wrzeciono, 1988a, Phys. Status Solidi A **110**, 241.

Kowalczyk, A., and A. Wrzeciono, 1988b, J. Magn. Magn. Mater. **74**, 260.

Kowalczyk, A., and A. Wrzeciono, 1988c, J. Phys. (Paris) **49**, C8-605.

Kronmüller, H., 1985, Phys. Status Solidi B **130**, 197.

Kronmüller, H., 1987, Phys. Status Solidi B **144**, 385.

Kronmüller, H., K.-D. Durst, S. Hock, and G. Martinek, 1988, J. Phys. (Paris) **49**, C8-623.

Kronmüller, H., K.-D. Durst, and G. Martinek, 1987, J. Magn. Magn. Mater. **69**, 149.

Kronmüller, H., K.-D. Durst, and M. Sagawa, 1988, J. Magn. Magn. Mater. **74**, 291.

Ku, H. C., J. C. Chen, and L. S. Yen, 1986, J. Magn. Magn. Mater. **54-57**, 533.

Ku, H. C., and L. S. Yen, 1987, J. Less-Common Met. **127**, 43.

Kuji, T., R. C. O'Handley, and N. J. Grant, 1989, Appl. Phys. Lett. **54**, 2487.

Kumar, K., 1988, J. Appl. Phys. **63**, R13.

Kümmerle, W., and U. Gradmann, 1977, Solid State Commun. **24**, 33.

Kuntze, K., D. Kohake, R. Beranek, S. Stieler, and C. Heiden, 1985, J. Phys. (Paris) **46**, C6-253.

Lazaro, F. J., J. Bartolomé, R. Navarro, C. Rillo, F. Lera, L. M. Garcia, J. Chaboy, C. Pique, R. Burriel, D. Fruchart, and S. Miraglia, 1990, J. Magn. Magn. Mater. **83**, 289.

Leccabue, F., F. Bolzoni, G. Bocelli, G. Calestani, A. Deriu, S-Q. Ji, J-G. Zhao, and J. L. Sanchez, 1990, J. Magn. Magn. Mater. **83**, 174.

Leccabue, F., J. L. Sanchez, L. Pareti, F. Bolzoni, and R. Panizzieri, 1985, Phys. Status Solidi A **91**, K63.

Lee, R. W., 1985, Appl. Phys. Lett. **46**, 790.

Lee, R. W., E. G. Brewer, and N. A. Schaffel, 1985, IEEE Trans. Magn. **MAG-21**, 1958.

Lemarchand, D., B. Labulle, and P. Vigier, 1988, J. Phys. (Paris) **49**, C8-637.

Leonowicz, M., 1990a, J. Magn. Magn. Mater. **83**, 211.

Leonowicz, M., 1990b, IEEE Trans. Magn. **26**, 2628.

Leonowicz, M., S. Heisz, and G. Hilscher, 1988, J. Phys. (Paris) **49**, C8-609.

Le Roux, D., H. Vincent, P. L'Héritier, and R. Fruchart, 1985, J. Phys. (Paris) **46**, C6-243.

L'Héritier, P., P. Chaudouet, R. Madar, A. Rouault, J-P. Senateur, and R. Fruchart, 1984, C. R. Acad. Sci. Ser. II **299**, 849.

L'Héritier, P., and R. Fruchart, 1985, J. Phys. (Paris) **46**, C6-319.

Li, D., H. F. Mildrum, and K. J. Strnat, 1985, J. Appl. Phys. **57**, 4140.

Li, D., and K. J. Strnat, 1985, J. Appl. Phys. **57**, 4143.

Li, H. S., J. P. Gavigan, J. M. Cadogan, D. Givord, and J. M. D. Coey, 1988, J. Magn. Magn. Mater. **72**, L241.

Li, H.-S., B.-T. Xie, and M.-Z. Dang, 1990, J. Magn. Magn. Mater. **89**, 355.

Li, H.-S., Z.-W. Zhang, and M.-Z. Dang, 1988, J. Magn. Magn. Mater. **71**, 355.

Li, L., and C. D. Graham, Jr., 1990, J. Appl. Phys. **67**, 4756.

Li, W., L. Jiang, D. Wang, T. Sun, and J. Zhu, 1986, J. Less-Common Met. **126**, 95.

Li, Z. W., Z. Zhou, and A. H. Morrish, 1990, Phys. Rev. B **41**, 8617.

Liebermann, H. H., and C. D. Graham, Jr., 1976, IEEE Trans. Magn. **MAG-21**, 921.

Lin, C., J. Lan, and X.-F. Xu, 1987, J. Appl. Phys. **61**, 3457.

Lin, C., and Z.-X. Liu, 1986, J. Magn. Magn. Mater. **54-57**, 887.

Lin, C., Z.-X. Liu, Y.-X. Sun, C.-X. Bai, and T.-S. Zhao, 1989, Phys. Rev. B **39**, 7273.

Lin, C., Z.-X. Liu, Y.-X. Sun, Z.-H. Lou, and Bayinqilao, 1988, J. Appl. Phys. **63**, 3967.

Lin, C., Z.-X. Liu, and X.-F. Xu, 1987, IEEE Trans. Magn. **MAG-23**, 2296.

Lin, C. H., S. K. Chen, K. D. Lin, W. C. Chang, and T. S. Chin, 1988, J. Appl. Phys. **64**, 5513.

Ling, Q., J. M. Cadogan, and J. M. D. Coey, 1986, Hyp. Interactions **28**, 655.

Liu, J. F., and H. L. Luo, 1989, IEEE Trans. Magn. **25**, 3296.

Liu, N. C., and K. S. Kim, 1990, J. Appl. Phys. **67**, 4629.

Liu, N. C., and H. H. Stadelmaier, 1986, Mater. Lett. **4**, 377.

Liu, N. C., H. H. Stadelmaier, and G. Schneider, 1987, J. Appl. Phys. **61**, 3574.

Livingston, J. D., 1985a, in *Proceedings of the Eighth International Workshop on Rare-Earth Magnets and Their Applications,* edited by K. J. Strnat (University of Dayton, Dayton, Ohio), p. 423.

Livingston, J. D, 1985b, J. Appl. Phys. **57**, 4137.

Livingston, J. D, 1987, IEEE Trans. Magn. **MAG-23**, 2109.

Lloyd, J. N., S. M. Bhagat, A. R. Knudson, and C. R. Gossett, 1979, J. Appl. Phys. **50**, 1614.

Loewenhaupt, M., M. Prager, A. P. Murani, and H. E. Hoenig, 1988, J. Magn. Magn. Mater. **76&77**, 408.

Loewenhaupt, M., I. Sosnowska, and B. Frick, 1990, Phys. Rev. B **42**, 3866.

Long, G. J., and F. Grandjean, 1991, in *Proceedings of the NATO Advanced Study Institute on Supermagnets, Hard Magnetic Materials,* edited by G. J. Long and F. Grandjean (Kluwer, Dordrecht), p. 355.

Lovleen, and R. Kamal, 1988a, J. Magn. Magn. Mater. **73**, 215.

Lovleen, and R. Kamal, 1988b, J. Less-Common Met. **141**, 83.

Lovleen, and R. Kamal, 1988c, J. Less-Common Met. **144**, 227.

Luong, N. H., N. P. Thuy, L. T. Tal, and T. D. Hien, 1989, Phys. Status Solidi A **111**, 591.

Ma, B. M., E. B. Boltich, S. G. Sankar, and W. E. Wallace, 1989, Phys. Rev. B **40**, 7332.

Ma, B. M., V. K. Chandhok, and E. J. Dulis, 1987, IEEE Trans. Magn. **MAG-23**, 2518.

Ma, B. M., and R. F. Krause, 1987, in *Proceedings of the Fifth International Symposium on Magnetic Anisotropy and Coercivity in Rare-Earth-Transition Metal Alloys,* edited by C. Herget, H. Kronmüller, and R. Poerschke (Deutsche Physikalische Gesellschaft, Bad Honnef, FRG), p. 141.

Ma, B.-M., and K. S. V. L. Narasimhan, 1986a, J. Magn. Magn. Mater. **54-57**, 559.

Ma, B.-M., and K. S. V. L. Narasimhan, 1986b, IEEE Trans. Magn. **MAG-22**, 916.

Maki, K., A. Forkl, T. Dragon, and H. Kronmüller, 1989, Phys. Status Solidi A **116**, 803.

Maki, K., and H. Kronmüller, 1990, Phys. Status Solidi A **118**, 253.

Malik, S. K., D. T. Adroja, B. M. Ma, E. B. Boltich, J. G. Sohn, S. G. Sankar, and W. E. Wallace, 1990, J. Appl. Phys. **67**, 4589.

Marquina, C., M. Solzi, P. A. Algarabel, M. R. Ibarra, and L. Pareti, 1989, Solid State Commun. **72**, 1167.

Martinek, G., and H. Kronmüller, 1990, J. Magn. Magn. Mater. **86**, 177.

Martinek, G., H. Kronmüller, and S. Hirosawa, 1990, J. Magn. Magn. Mater. **89**, 369.

Marusi, G., L. Pareti, M. Solzi, O. Moze, A. Paoluzi, M. R. Ibarra, J. I. Arnaudas, C. Marquina, P. A. Algarabel, and A. del Moral, 1990, J. Magn. Magn. Mater. **83**, 133.

Marusin, E. P., O. I. Bodak, A. O. Tsokol', and V. S. Fundamenskii, 1985, Sov. Phys. Crystallogr. **30**, 338.

Maruyama, H., H. Yamazaki, D. Givord, J. Gavigan, H.-S. Li, M. Sagawa, and S. Hirosawa, 1988, J. Phys. (Paris) **49**, C8-563.

Matsui, M., M. Doi, and T. Shimizu, 1987, IEEE Trans. Magn. **MAG-23**, 3113.

Matsumoto, F., H. Sakamoto, M. Komiya, and M. Fujikura, 1988, J. Appl. Phys. **63**, 3507.

Matsuura, Y., S. Hirosawa, H. Yamamoto, S. Fujimura, and M. Sagawa, 1985a, Appl. Phys. Lett. **46**, 308.

Matsuura, Y., S. Hirosawa, H. Yamamoto, S. Fujimura, M. Sagawa, and K. Osamura, 1985b, Jpn. J. Appl. Phys. **24**, L635.

McCallum, R. W., A. M. Kadin, G. B. Clemente, and J. E. Keem, 1987, J. Appl. Phys. **61**, 3577.

McCurrie, R. A., 1982, in *Ferromagnetic Materials,* edited by E. P. Wohlfarth (North-Holland, Amsterdam), Vol. 3, p. 107.

McCurrie, R. A., and P. Gaunt, 1964, in *Proceedings of the International Conference on Magnetism* (Institute of Physics and the Physical Society, London), p. 780.

McGuiness, P. J., A. Ahmed, D. G. R. Jones, I. R. Harris, S. Burns, and E. Rozendaal, 1990, J. Appl. Phys. **67**, 4626.

McGuiness, P. J., E. Devlin, I. R. Harris, E. Rozendaal, and J. Ormerod, 1989, J. Mater. Sci. **24**, 2541.

McGuiness, P. J., and I. R. Harris, 1988, J. Appl. Phys. **64**, 5308.

McGuiness, P. J., I. R. Harris, E. Rozendaal, J. Ormerod, and M. Ward, 1986, J. Mater. Sci. **21**, 4107.

McGuiness, P. J., X. J. Zhang, H. Forsyth, and I. R. Harris, 1990, J. Less-Common Met. **162**, 379.

McGuiness, P. J., X. J. Zhang, X. J. Yin, and I. R. Harris, 1990, J. Less-Common Met. **158**, 359.

Meisner, G. P., 1987, Appl. Phys. Lett. **50**, 116.

Meisner, G. P., and C. D. Fuerst, 1986, IEEE Trans. Magn. **MAG-22**, 744.

Melamud, M., L. H. Bennett, and R. E. Watson, 1987, Scr. Metall. **21**, 573.

Menth, A., H. Nagel, and R. S. Perkins, 1978, Annu. Rev. Mater. Sci. **8**, 21.

Meyer, C., J. P. Gavigan, G. Czjzek, and H.-J. Bornemann, 1989, Solid State Commun. **69**, 83.

Mayer, C., F. Hartmann-Boutron, Y. Gros, and J. J. Capponi, 1980, J. Phys. (Paris) **41**, C1-191.

Mishima, T., 1932, Iron Age **130**, 346.

Mishra, R. K., 1986, J. Magn. Magn. Mater. **54-57**, 450.

Mishra, R. K., 1987a, in *High Performance Permanent Magnet Materials,* Materials Research Society Symposia Proceedings

Vol. 96, edited by S. G. Sankar, J. F. Herbst, and N. C. Koon (Materials Research Society, Pittsburgh), p. 83.

Mishra, R. K., 1987b, J. Appl. Phys. **62**, 967.

Mishra, R. K., E. G. Brewer, and R. W. Lee, 1988, J. Appl. Phys. **63**, 3528.

Mishra, R. K., J. K. Chen, and G. Thomas, 1986, J. Appl. Phys. **59**, 2244.

Mishra, R. K., T-Y. Chu, and L. K. Rabenberg, 1990, J. Magn. Magn. Mater. **84**, 88.

Mishra, R. K., and R. W. Lee, 1986, Appl. Phys. Lett. **48**, 733.

Mishra, R. K., G. Thomas, T. Yoneyama, A. Fukuno, and T. Ojima, 1981, J. Appl. Phys. **52**, 2517.

Mizoguchi, T., I. Sakai, and K. Inomata, 1986a, Appl. Phys. Lett. **48**, 1309.

Mizoguchi, T., I. Sakai, H. Niu, and K. Inomata, 1986b, IEEE Trans. Magn. **MAG-22**, 919.

Mizoguchi, T., I. Sakai, H. Niu, and K. Inomata, 1987, IEEE Trans. Magn. **MAG-23**, 2281.

Mohn, P., and E. P. Wohlfarth, 1987, J. Phys. F **17**, 2421.

Moosa, I. S., G. W. Johnson, and J. Nutting, 1990a, J. Less-Common Met. **158**, 51.

Moosa, I. S., G. W. Johnson, and J. Nutting, 1990b, J. Less-Common Met. **167**, 153.

Moosa, I. S., and J. Nutting, 1988, J. Less-Common Met. **144**, 221.

Morelli, D. T., J. P. Heremans, and G. M. Umana, 1990, in *Thermal Conductivity 21*, edited by C. J. Cremers and H. A. Fine (Plenum, New York), p. 621.

Moze, O., L. Pareti, G. Marusi, M. Solzi, and W. I. F. David, 1989, Physica B **156&157**, 747.

Moze, O., L. Pareti, M. Solzi, F. Bolzoni, W. I. F. David, W. T. A. Harrison, and A. W. Hewat, 1988, J. Less-Common Met. **136**, 375.

Muir, W. B., Z. Altounian, G-H. Tu, and W-R. Chen, 1989, J. Magn. Magn. Mater. **81**, 168.

Mukai, T., Y. Okazaki, H. Sakamoto, M. Fujikura, and T. Inaguma, 1990, in *Proceedings of the Eleventh International Workshop on Rare-Earth Magnets and Their Applications,* edited by S. G. Sankar (Carnegie Mellon University, Pittsburgh), p. 72.

Mukai, T., and H. Sakamoto, 1989, Appl. Phys. Lett. **54**, 1597.

Müller, K.-H., A. Handstein, D. Eckert, and J. Schneider, 1987, Phys. Status Solidi A **99**, K61.

Mulyukov, K. Y., R. Z. Valiev, G. F. Korznikova, and V. V. Stolyarov, 1989, Phys. Status Solidi A **112**, 137.

Nadolski, S., E. Machowska, and E. Burzo, 1989, Solid State Commun. **71**, 97.

Nagata, H., S. Hirosawa, M. Sagawa, A. Ishibashi, and S. Endo, 1987, J. Magn. Magn. Mater. **70**, 334.

Nakagawa, Y., H. Hiroyoshi, M. Sagawa, S. Hirosawa, and K. Tokuhara, 1987, IEEE Trans. Magn. **MAG-23**, 2530.

Nakagawa, Y., H. Kato, D. W. Lim, G. Kido, and M. Yamada, 1990, in *Proceedings of the Sixth International Symposium on Magnetic Anisotropy and Coercivity in Rare Earth-Transition Metal Alloys,* edited by S. G. Sankar (Carnegie Mellon University, Pittsburgh), p. 12.

Nakagawa, Y., G. Kido, H. Hiroyoshi, H. Kato, M.Yamada, S. Hirosawa, and M. Sagawa, 1987, in *Proceedings of the Fifth International Symposium on Magnetic Anisotropy and Coercivity in Rare-Earth–Transition Metal Alloys,* edited by C. Herget, H. Kronmüller, and R. Poerschke (Deutsche Physikalische Gesellschaft, Bad Honnef, FRG), p. 87.

Nakagawa, Y., G. Kido, M. Yamada, H. Kato, H. Hiroyoshi, N. Saito, D. W. Lim, S. Hirosawa, and M. Sagawa, 1989, Physica B **155**, 279.

Nakayama, R., T. Takeshita, M. Itakura, N. Kuwano, and K. Oki, 1990, J. Appl. Phys. **67**, 4665.

Narasimhan, K. S. V. L., 1985, J. Appl. Phys. **57**, 4081.

Néel, L., 1936, Ann. Phys. (Paris) **5**, 232.

Nesbitt, E. A., J. H. Wernick, and E. Corenzwit, 1959, J. Appl. Phys. **30**, 365.

Nesbitt, E. A., H. J. Williams, J. H. Wernick, and R. C. Sherwood, 1961, J. Appl. Phys. **32**, 342S.

Nesbitt, E. A., H. J. Williams, J. H. Wernick, and R. C. Sherwood, 1962, J. Appl. Phys. **33**, 1674.

Niarchos, D., and A. Simopoulos, 1986, Solid State Commun. **59**, 669.

Nowik, I., K. Muraleedharan, G. Wortmann, B. Perscheid, G. Kaindl, and N. C. Koon, 1990, Solid State Commun. **76**, 967.

Nozawa, Y., K. Iwasaki, S. Tanigawa, M. Tokunaga, and H. Harada, 1988, J. Appl. Phys. **64**, 5285.

Nozières, J. P., and R. Perrier de la Bathie, 1989, IEEE Trans. Magn. **25**, 4117.

Nozières, J. P., R. Perrier de la Bathie, and J. Gavinet, 1988, J. Phys. (Paris) **49**, C8-667.

Nozières, J. P., R. Perrier de la Bathie, and D. W. Taylor, 1989, J. Magn. Magn. Mater. **80**, 88.

Oesterreicher, H., 1985a, Phys. Status Solidi B **131**, K123.

Oesterreicher, H., 1985b, in *Proceedings of the Fourth International Symposium on Magnetic Anisotropy and Coercivity in Rare Earth-Transition Metal Alloys,* edited by K. J. Strnat (University of Dayton, Dayton, Ohio), p. 705.

Oesterreicher, H., and C. Abache, 1985, J. Phys. (Paris) **46**, C6-45.

Oesterreicher, H., F. Spada, and C. Abache, 1984, Mater. Res. Bull. **19**, 1069.

Oesterreicher, K., and H. Oesterreicher, 1984, Phys. Status Solidi A **85**, K61.

Ogilvy, A. J. W., G. P. Gregan, and H. A. Davies, 1985, in *Nd-Fe Permanent Magnets: Their Present and Future Applications,* edited by I. V. Mitchell (Elsevier Applied Science, London/New York), p. 93.

Ohki, T., T. Yuri, M. Miyagawa, Y. Takahashi, C. Yoshida, S. Kambe, M. Higashi, and K. Itayama, 1989, in *Proceedings of the Tenth International Workshop on Rare-Earth Magnets and Their Applications* (Society of Non-Traditional Technology, Tokyo), p. 399.

Okada, M., and M. Homma, 1985, in *Proceedings of the Eighth International Workshop on Rare-Earth Magnets and Their Applications,* edited by K. J. Strnat (University of Dayton, Dayton, Ohio), p. 507.

Okada, M., S. Sugimoto, C. Ishikaza, T. Tanaka, and M. Homma, 1985, J. Appl. Phys. **57**, 4146.

Ono, F., Y. Ohtsu, and O. Yamada, 1986, J. Phys. Soc. Jpn. **55**, 4014.

Ono, F., Y. Ohtsu, and O. Yamada, 1987, J. Magn. Magn. Mater. **70**, 319.

Onodera, H., A. Fujita, H. Yamamoto, M. Sagawa, and S. Hirosawa, 1987, J. Magn. Magn. Mater. **68**, 6.

Onodera, H., Y. Yamaguchi, H. Yamamoto, M. Sagawa, Y. Matsuura, and H. Yamamoto, 1984, J. Magn. Magn. Mater. **46**, 151.

Onodera, H., H. Yamauchi, M. Yamada, H. Yamamoto, M. Sagawa, and S. Hirosawa, 1987, J. Magn. Magn. Mater. **68**, 15.

Ormerod, J., 1985, J. Less-Common Met. **111**, 49.

Ostertag, W., and K. J. Strnat, 1966, Acta Crystallogr. **21**, 560.

Otani, Y., J. M. D. Coey, B. Barbara, H. Miyajima, S. Chikazumi, and M. Uehara, 1990, J. Appl Phys. **67**, 4619.

Otani, Y., H. Miyajima, and S. Chikazumi, 1987, IEEE Trans. Magn. **MAG-23**, 2527.

Otani, Y., H. Miyajima, and S. Chikazumi, 1989, IEEE Trans. Magn. **25**, 3431.

Otani, Y., H. Miyajima, S. Chikazumi, S. Hirosawa, and M. Sagawa, 1986, J. Magn. Magn. Mater. **60**, 168.

Otani, Y., H. Miyajima, T. Kubodera, and S. Chikazumi, 1990, IEEE Trans. Magn. **26**, 1742.

Otani, Y., H. Sun, J. M. D. Coey, H. A. Davis, A. Manaf, and R. A. Buckley, 1990, J. Appl. Phys. **67**, 4616.

Overfelt, R. A., and J. J. Becker, 1984, Appl. Phys. Lett. **44**, 925.

Paik, C. R., H. Miho, M. Okada, and M. Homma, 1987, IEEE Trans. Magn. **MAG-23**, 2512.

Paik, C. R., M. Okada, and M. Homma, 1990, IEEE Trans. Magn. **26**, 1730.

Pan, S., J. Liu, D. Li, and R. Ma, 1990, in *Proceedings of the Eleventh International Workshop on Rare-Earth Magnets and Their Applications,* edited by S. G. Sankar (Carnegie Mellon University, Pittsburgh), p. 571.

Panchanathan, V., and J. J. Croat, 1989, IEEE Trans. Magn. **25**, 4111.

Panissod, P., E. Jedryka, M. Wojcik, and J. I. Budnick, 1989, Phys. Rev. B **40**, 2606.

Pareti, L., F. Bolzoni, and O. Moze, 1985, Phys. Rev. B **32**, 7604.

Pareti, L., F. Bolzoni, M. Solzi, and K. H. J. Buschow, 1987, J. Less-Common Met. **132**, L5.

Pareti, L., O. Moze, D. Fruchart, P. L'Héritier, and A. Yaouanc, 1988, J. Less-Common Met. **142**, 187.

Pareti, L., M. Solzi, F. Bolzoni, O. Moze, and R. Panizzieri, 1987, Solid State Commun. **61**, 761.

Pareti, L., H. Szymczak, and H. K. Lachowicz, 1985, Phys. Status Solidi A **92**, K65.

Parker, F. T., 1987, J. Appl. Phys. **61**, 2606.

Parker, S. F. H., P. J. Grundy, and J. Fidler, 1987, J. Magn. Magn. Mater. **66**, 74.

Parker, S. F. H., R. J. Pollard, D. G. Lord, and P. J. Grundy, 1987, IEEE Trans. Magn. **MAG-23**, 2103.

Parthé, E., B. Chabot, and E. Hovestreydt, 1983, Acta Crystallogr. B **39**, 596.

Pastushenkov, J., K.-D. Durst, and H. Kronmüller, 1987, Phys. Status Solidi A **104**, 487.

Pearson, W. B., 1972, *The Crystal Chemistry and Physics of Metals and Alloys* (Wiley-Interscience, New York), p. 643.

Pedziwiatr, A. T., 1988, Solid State Commun. **65**, 519.

Pedziwiatr, A. T., H. Y. Chen, and W. E. Wallace, 1987, J. Magn. Magn. Mater. **67**, 311.

Pedziwiatr, A. T., H. Y. Chen, W. E. Wallace, and S. K. Malik, 1987, IEEE Trans. Magn. **MAG-23**, 2717.

Pedziwiatr, A. T., S. Y. Jiang, and, W. E. Wallace, 1986, J. Magn. Magn. Mater. **62**, 29.

Pedziwiatr, A. T., S. G. Sankar, and W. E. Wallace, 1988, J. Appl. Phys. **63**, 3710.

Pedziwiatr, A. T., and W. E. Wallace, 1986a, J. Less-Common Met. **126**, 41.

Pedziwiatr, A. T., and W. E. Wallace, 1986b, Solid State Commun. **60**, 653.

Pedziwiatr, A. T., and W. E. Wallace, 1987a, J. Magn. Magn. Mater. **65**, 139.

Pedziwiatr, A. T., and W. E. Wallace, 1987b, J. Magn. Magn. Mater. **66**, 63.

Pedziwiatr, A. T., and W. E. Wallace, 1987c, Solid State Commun. **64**, 1017.

Pedziwiatr, A. T., and W. E. Wallace, 1987d, J. Appl. Phys. **61**, 3439.

Pedziwiatr, A. T., W. E. Wallace, and E. Burzo, 1986a, J. Magn. Magn. Mater. **59**, L179.

Pedziwiatr, A. T., W. E. Wallace, and E. Burzo, 1986b, J. Magn. Magn. Mater. **61**, 173.

Pedziwiatr, A. T., W. E. Wallace, and E. Burzo, 1986c, J. Magn. Magn. Mater. **61**, 177.

Pedziwiatr, A. T., W. E. Wallace, and E. Burzo, 1987, IEEE Trans. Magn. **MAG-23**, 1795.

Pedziwiatr, A. T., W. E. Wallace, E. Burzo, and V. Pop, 1987, Solid State Commun. **61**, 61.

Pelcovits, R. A., E. Pytte, and J. Rudnick, 1978, Phys. Rev. Lett. **40**, 476.

Perkins, R. S., and H. Nagel, 1975, Physica B **80**, 143.

Perkins, R. S., and S. Strässler, 1977a, Phys. Rev. B **15**, 477.

Perkins, R. S., and S. Strässler, 1977b, Phys. Rev. B **15**, 490.

Pinkerton, F. E., 1986a, J. Magn. Magn. Mater. **54-57**, 579.

Pinkerton, F. E., 1986b, IEEE Trans. Magn. **MAG-22**, 922.

Pinkerton, F. E., 1987, in *High Performance Permanent Magnet Materials,* Materials Research Society Symposia Proceedings Vol. 96, edited by S. G. Sankar, J. F. Herbst, and N. C. Koon (Materials Research Society, Pittsburgh), p. 65.

Pinkerton, F. E., 1988a, J. Appl. Phys. **63**, 5427.

Pinkerton, F. E., 1988b, J. Appl. Phys. **64**, 5565.

Pinkerton, F. E., and W. R. Dunham, 1984, Appl. Phys. Lett. **45**, 1248.

Pinkerton, F. E., and W. R. Dunham, 1985, J. Appl. Phys. **57**, 4121.

Pinkerton, F. E., and C. D. Fuerst, 1990a, J. Appl. Phys. **67**, 4753.

Pinkerton, F. E., and C. D. Fuerst, 1990b, J. Magn. Magn. Mater. **89**, 139.

Pinkerton, F. E., and C. D. Fuerst, 1991, J. Appl. Phys. **69**, 5817.

Pinkerton, F. E., C. D. Fuerst, and G. P. Meisner, 1987, J. Appl. Phys. **61**, 3562.

Pinkerton, F. E., C. D. Fuerst, and G. P. Meisner, 1988a, Appl. Phys. Lett. **52**, 2188.

Pinkerton, F. E., C. D. Fuerst, and G. P. Meisner, 1988b, J. Appl. Phys. **64**, 2783.

Pinkerton, F. E., and D. J. Van Wingerden, 1986, J. Appl. Phys. **60**, 3685.

Plusa, D., J. J. Wyslocki, B. Wyslocki, and R. Pfranger, 1986, Appl. Phys. A **40**, 167.

Plusa, D., J. J. Wyslocki, B. Wyslocki, and R. Pfranger, 1987, J. Less-Common Met. **133**, 231.

Pollard, R. J., S. F. H. Parker, and P. J. Grundy, 1988, J. Magn. Magn. Mater. **75**, 239.

Potenziani, E., II, 1985, J. Appl. Phys. **58**, 2764.

Potenziani, E., II, H. A. Leupold, J. P. Clarke, and A. Tauber, 1985, J. Appl. Phys. **57**, 4152.

Pourarian, F., 1990, in *Proceedings of the Sixth International Symposium on Magnetic Anisotropy and Coercivity in Rare Earth-Transition Metal Alloys,* edited by S. G. Sankar (Carnegie Mellon University, Pittsburgh), p. 381.

Pourarian, F., M. Q. Huang, and W. E. Wallace, 1986, J. Less-Common Met. **120**, 63.

Pourarian, F., S. Y. Jiang, S. G. Sankar, and W. E. Wallace, 1987, Solid State Commun. **63**, 1119.

Pourarian, F., S. Y. Jiang, S. G. Sankar, and W. E. Wallace, 1988, J. Appl. Phys. **63**, 3972.

Pourarian, F., S. Y. Jiang, and W. E. Wallace, 1987, in *High Peformance Permanent Magnet Materials,* Materials Research

Society Symposia Proceedings Vol. 96, edited by S. G. Sankar, J. F. Herbst, and N. C. Koon (Materials Research Society, Pittsburgh), p. 231.

Pourarian, F., S. Y. Jiang, L. Y. Zhang, E. B. Boltich, S. G. Sankar, and W. E. Wallace, 1988, J. Appl. Phys. **64**, 5540.

Pourarian, F., S. G. Sankar, A. T. Pedziwiatr, E. B. Boltich, and W. E. Wallace, 1987, in *High Performance Permanent Magnet Materials,* Materials Research Society Symposia Proceedings Vol. 96, edited by S. G. Sankar, J. F. Herbst, and N. C. Koon (Materials Research Society, Pittsburgh), p. 103.

Pourarian, F., S. G. Sankar, and W. E. Wallace, 1988, J. Magn. Magn. Mater. **74**, 177.

Price, D. C., R. K. Day, and J. B. Dunlop, 1986, J. Appl. Phys. **59**, 3585.

Pringle, O. A., J. Fu, G. J. Long, W. J. James, D. Xie, W. B. Yelon, and F. Grandjean, 1990, J. Appl. Phys. **67**, 4762.

Pringle, O. A., G. J. Long, G. K. Marasinghe, W. J. James, A. T. Pedzwiatr, W. E. Wallace, and F. Grandjean, 1989, IEEE Trans. Magn. **25**, 3440.

Pringle, O. A., G. J. Long, D. E. Tharp, W. J. James, and Y.-C. Yang, 1988, Hyp. Interactions **40**, 437.

Pringle, O. A., G. K. Marasinghe, G. J. Long, W. J. James, D. Xie, J. Li, and W. B. Yelon, 1991, "'Preferential silicon site occupation in $Nd_2Fe_{14-x}Si_xB$ and $Y_2Fe_{14-x}Si_xB$," University of Missouri-Rolla preprint.

Pringle, O. A., G. K. Marasinghe, G. J. Long, W. J. James, W. B. Yelon, D. Xie, and F. Grandjean, 1988, J. Appl. Phys. **64**, 5580.

Quan, C., Y. Wang, L. Yin, and J. Zhao, 1989, Solid State Commun. **72**, 955.

Quan, C. R., J. G. Zhao, Y. Z. Wang, L. Yin, B. G. Shen, Z. X. Cheng, Y. F. Cheng, and S. W. Niu, 1990, Phys. Rev. B **42**, 6697.

Quang, P. H., T. H. Anh, N. H. Luong, L. T. Tai, T. D. Hien, and J. J. M. Franse, 1987, in *Proceedings of the Fifth International Symposium on Magnetic Anisotropy and Coercivity in Rare-Earth–Transition Metal Alloys,* edited by C. Herget, H. Kronmüller, and R. Poerschke (Deutsche Physikalische Gesellschaft, Bad Honnef, FRG), p. 205.

Radwański, R. J., 1986a, Z. Phys. B **65**, 65.

Radwański, R. J., 1986b, J. Magn. Magn. Mater. **62**, 120.

Radwański, R. J., F. R. de Boer, J. J. M. Franse, and K. H. J. Buschow, 1989, Physica B **159**, 311.

Radwański, R. J., and J. J. M. Franse, 1987, Phys. Rev. B **36**, 8616.

Radwański, R. J., and J. J. M Franse, 1988, J. Magn. Magn. Mater. **74**, 43.

Radwański, R. J., and J. J. M. Franse, 1989, J. Magn. Magn. Mater. **80**, 14.

Radwański, R. J., J. J. M. Franse, and S. Sinnema, 1987, J. Magn. Magn. Mater. **70**, 313.

Radwański, R. J., J. J. M. Franse, and R. Verhoef, 1990a, J. Magn. Magn. Mater. **83**, 127.

Radwański, R. J., R. Verhoef, and J. J. M. Franse, 1990b, J. Magn. Magn. Mater. **83**, 141.

Ramesh, R., 1990, J. Appl. Phys. **68**, 5767 (Part I); **68**, 5772 (Part II).

Ramesh, R., J. K. Chen, and G. Thomas, 1987, J. Appl. Phys. **61**, 2993.

Ramesh, R., and K. Srikrishna, 1988, J. Appl. Phys. **64**, 6406.

Ramesh, R., G. Thomas, and B. M. Ma, 1987, in *High Performance Permanent Magnet Materials,* Materials Research Society Symposia Proceedings Vol. 96, edited by S. G. Sankar, J. F. Herbst, and N. C. Koon (Materials Research Society, Pittsburgh), p. 203.

Ramesh, R., G. Thomas, and B. M. Ma, 1988, J. Appl. Phys. **64**, 6416.

Rani, M., and R. Kamal, 1986, J. Less-Common Met. **125**, 97.

Rani, M., and R. Kamal, 1987a, J. Less-Common Met. **128**, 343.

Rani, M., and R. Kamal, 1987b, J. Magn. Magn. Mater. **66**, 379.

Rani, M., M. S. Saini, and R. Kamal, 1986, Phys. Lett. A **118**, 103.

Rechenberg, H. R., J. P. Sanchez, P. L'Héritier, and R. Fruchart, 1987, Phys. Rev. B **36**, 1865.

Reck, R. A., and D. L. Fry, 1969, Phys. Rev. **184**, 492.

Regnard, J.-R., A. Yaouanc, D. Fruchart, D. Le Roux, P. L'Héritier, J. M. D. Coey, and J. P. Gavigan, 1987, J. Appl. Phys. **61**, 3565.

Richter, H. J., K. A. Hempel, and R. Verhoef, 1989, J. Magn. Magn. Mater. **79**, 113.

Rillo, C., J. Chaboy, R. Navarro, J. Bartolomé, D. Fruchart, B. Chenevier, A. Yaouanc, M. Sagawa, and S. Hirosawa, 1988, J. Appl. Phys. **64**, 5534.

Rodewald, W., 1985, in *Proceedings of the Fourth International Symposium on Magnetic Anisotropy and Coercivity in Rare Earth-Transition Metal Alloys,* edited by K. J. Strnat (University of Dayton, Dayton, Ohio), p. 737.

Rodewald, W., 1987, in *Proceedings of the Ninth International Workshop on Rare-Earth Magnets and Their Applications,* edited by C. Herget and R. Poerschke (Deutsche Physikalische Gesellschaft, Bad Honef, FRG), p. 609.

Rodewald, W., and W. Fernengel, 1988, IEEE Trans. Magn. **24**, 1638.

Rodewald, W., and P. Schrey, 1989, IEEE Trans. Magn. **25**, 3770.

Rodewald, W., and P. Schrey, 1990, J. Magn. Magn. Mater. **83**, 206.

Rodewald, W., and B. Wall, 1989, J. Magn. Magn. Mater. **80**, 57.

Rosenberg, M., P. Deppe, K. Erdmann, M. Sostarich, and H. Stadelmeier, 1986, J. Magn. Magn. Mater. **54-57**, 599.

Rosenberg, M., P. Deppe, and H. Stadelmaier, 1986, Hyp. Interactions **28**, 503.

Rosenberg, M., P. Deppe, M. Wójcik, and H. Stadelmeier, 1985, J. Appl. Phys. **57**, 4124.

Rotenberg, L. R. K., R. F. Oliveira, H. R. Rechenberg, and F. P. Missell, 1985, J. Appl. Phys. **57**, 4127.

Rowlinson, N., M. M. Ashraf, and I. R. Harris, 1989, J. Magn. Magn. Mater. **80**, 93.

Rowlinson, N., M. M. Ashraf, and I. R. Harris, 1990, J. Magn. Magn. Mater. **87**, 93.

Ruhl, R. C., 1967, Mater. Sci. Eng. **1**, 313.

Ryan, D. H., Z. Altounian, L. X. Liao, J. O. Strom-Olsen, and W. B. Muir, 1990, J. Appl. Phys. **67**, 4742.

Ryan, D. H., Z. Altounian, J. O. Strom-Olsen, and W. B. Muir, 1989, Phys. Rev. B **39**, 4730.

Sagawa, M., S. Fujimura, N. Togawa, H. Yamamoto, and Y. Matsuura, 1984a, J. Appl. Phys. **55**, 2083.

Sagawa, M., S. Fujimura, H. Yamamoto, Y. Matsuura, and K. Hiraga, 1984b, IEEE Trans. Magn. **MAG-20**, 1584.

Sagawa, M., S. Fujimura, H. Yamamoto, Y. Matsuura, and S. Hirosawa, 1985a, J. Appl. Phys. **57**, 4094.

Sagawa, M., S. Fujimura, H. Yamamoto, Y. Matsuura, S. Hirosawa, and K. Hiraga, 1985b, in *Proceedings of the Fourth International Symposium on Magnetic Anisotropy and Coercivity in Rare Earth-Transition Metal Alloys,* edited by K. J. Strnat (University of Dayton, Dayton, Ohio), p. 587.

Sagawa, M., and S. Hirosawa, 1987, in *High Performance Permanent Magnet Materials,* Materials Research Society Symposia Proceedings, Vol. 96, edited by S. G. Sankar, J. F. Herbst, and N. C. Koon (Materials Research Society, Pittsburgh), p. 161.

Sagawa, M., and S. Hirosawa, 1988a, J. Phys. (Paris) **49**, C8-617.

Sagawa, M., and S. Hirosawa, 1988b, J. Mater. Res. **3**, 45.

Sagawa, M., S. Hirosawa, Y. Otani, H. Miyajima, and S. Chikazumi, 1987a, J. Magn. Magn. Mater. **70**, 316.

Sagawa, M., S. Hirosawa, K. Tokuhara, H. Yamamoto, S. Fujimura, Y. Tsubokawa, and R. Shimizu, 1987b, J. Appl. Phys. **61**, 3559.

Sagawa, M., S. Hirosawa, Y. Tsubokawa, and R. Shimizu, 1987c, in *Proceedings of the Fifth International Symposium on Magnetic Anisotropy and Coercivity in Rare-Earth–Transition Metal Alloys,* edited by C. Herget, H. Kronmüller, and R. Poerschke (Deutsche Physikalische Gesellschaft, Bad Honnef, FRG), p. 229.

Sagawa, M., S. Hirosawa, H. Yamamoto, S. Fujimura, and Y. Matsuura, 1987d, Jpn. J. Appl. Phys. **26**, 785.

Sagawa, M., S. Hirosawa, H. Yamamoto, Y. Matsuura, S. Fujimura, H. Tokuhara, and K. Hiraga, 1986, IEEE Trans. Magn. **MAG-22**, 910.

Sagawa, M., P. Tenaud, F. Vial, and K. Hiraga, 1990, IEEE Trans. Magn. **26**, 1957.

Sakuma, A., and S. Takeda, 1990, IEEE Trans. Magn. **26**, 1745.

Sakuma, A., S. Tanigawa, and M. Tokunaga, 1990, J. Magn. Magn. Mater. **84**, 52.

Sanchez, J. L., S. Diaz, N. Suarez, F. Leccabue, and R. Panizzieri, 1989a, Solid State Commun. **71**, 229.

Sanchez, J. L., S. Garcia, N. Suarez, S. Diaz, F. Leccabue, R. Panizzieri, G. Bocelli, and G. Calestani, 1989b, J. Magn. Magn. Mater. **79**, 249.

Sanchez, J. P., J. M. Friedt, A. Vasquez, P. L'Héritier, and R. Fruchart, 1986, Solid State Commun. **57**, 309.

Sankar, S. G., and K. S. V. L. Narasimhan, 1986, J. Magn. Magn. Mater. **54-57**, 530.

Sankar, S. G., V. U. S. Rao, E. Segal, W. E. Wallace, W. G. D. Frederick, and H. J. Garrett, 1975, Phys. Rev. B **11**, 435.

Sano, Y., H. Onodera, H. Yamauchi, and H. Yamamoto, 1989, J. Magn. Magn. Mater. **79**, 67.

Schmitt, D., 1979a, J. Phys. F **9**, 1745.

Schmitt, D., 1979b, J. Phys. F **9**, 1759.

Schneider, G., E.-T. Henig, F. P. Missell, and G. Petzow, 1990, Z. Metallkd. **81**, 322.

Schneider, G., E.-T. Henig, G. Petzow, and H. H. Stadelmaier, 1986, Z. Metallkd. **77**, 755.

Schneider, G., E.-T. Henig, H. H. Stadelmaier, and G. Petzow, 1987, in *Proceedings of the Fifth International Symposium on Magnetic Anisotropy and Coercivity in Rare-Earth–Transition Metal Alloys,* edited by C. Herget, H. Kronmüller, and R. Poerschke (Deutsche Physikalische Gesellschaft, Bad Honnef, FRG), p. 347.

Schrey, P., 1986, IEEE Trans. Magn. **MAG-22**, 913.

Schrey, P., 1988, J. Magn. Magn. Mater. **73**, 260.

Schultz, L., K. Schnitzke, and J. Wecker, 1988, J. Appl. Phys. **64**, 5302.

Schultz, L., K. Schnitzke, and J. Wecker, 1989, J. Magn. Magn. Mater. **80**, 115.

Schultz, L., and J. Wecker, 1987, in *Proceedings of the Ninth International Workshop on Rare-Earth Magnets and Their Applications,* edited by C. Herget and R. Poerschke (Deutsche Physikalische Gesellschaft, Bad Honnef, FRG), p. 301.

Schultz, L., and J. Wecker, 1988, Mater. Sci. Eng. **99**, 127.

Schultz, L., J. Wecker, and E. Hellstern, 1987, J. Appl. Phys. **61**, 3583.

Sellmyer, D. J., A. Ahmed, G. Muench, and G. Hadjipanayis, 1984, J. Appl. Phys. **55**, 2088.

Sellmyer, D. J., M. A. Engelhardt, S. S. Jaswal, and A. J. Arko, 1988, Phys. Rev. Lett. **60**, 2077.

Shah, N. J., J. W. Ross, and H. Yamamoto, 1987, J. Phys. F **17**, L19.

Shen, X., Y. Wang, Z. Diao, and X. Liu, 1987, J. Appl. Phys. **61**, 3433.

Shi, Y., H. Jin, and M. Jin, 1989, Phys. Status Solidi B **151**, 249.

Shimao, M., H. Ido, G. Kido, and K. Ohashi, 1987, IEEE Trans. Magn. **MAG-23**, 2722.

Shimoda, T., K. Akioka, O. Kobayashi, and T. Yamagami, 1988a, J. Appl. Phys. **64**, 5290.

Shimoda, T., K. Akioka, O. Kobayashi, and T. Yamagami, 1988b, J. Phys. (Paris) **49**, C8-631.

Shimoda, T., K. Akioka, O. Kobayashi, T. Yamagami, and A. Arai, 1990, in *Proceedings of the Eleventh International Workshop on Rare-Earth Magnets and Their Applications,* edited by S. G. Sankar (Carnegie Mellon University, Pittsburgh), p. 17.

Shimoda, T., K. Akioka, O. Kobayashi, T. Yamagami, T. Ohki, M. Miyagawa, and T. Yuri, 1989, IEEE Trans. Magn. **25**, 4099.

Shimotomai, M., H. Miyake, and M. Doyama, 1980, J. Phys. F **10**, 707.

Shoemaker, C. B., D. P. Shoemaker, and R. Fruchart, 1984, Acta Crystallogr. C **40**, 1665.

Sievers, J., 1982, Z. Phys. B **45**, 289.

Singleton, E. W., and G. C. Hadjipanayis, 1990, J. Appl. Phys. **67**, 4759.

Sinnema, S., J. J. M. Franse, R. J. Radwański, K. H. J. Buschow, and D. B. de Mooij, 1985, J. Phys. (Paris) **46**, C6-301.

Sinnema, S., R. J. Radwański, J. J. M. Franse, D. B. de Mooij, and K. H. J. Buschow, 1984, J. Magn. Magn. Mater. **44**, 333.

Slater, J. C., 1930, Phys. Rev. **36**, 57.

Smit, H. H. A., R. C. Thiel, and K.H. J. Buschow, 1987, Physica **145B**, 329.

Sommerfeld, A., and H. Bethe, 1933, in *Handbuch der Physik,* edited by A. Smekal (Springer, Berlin), Vol. 24, Part 2, p. 597.

Sousa, J. B., M. M. Amado, R. P. Pinto, V. S. Amaral, and M. E. Braga, 1990, J. Phys.: Condens. Matter **2**, 7543.

Spada, F., C. Abache, and H. Oesterreicher, 1984, J. Less-Common Met. **99**, L21.

Stadelmaier, H. H., and N. A. El-Masry, 1985, in *Proceedings of the Fourth International Symposium on Magnetic Anisotropy and Coercivity in Rare Earth-Transition Metal Alloys,* edited by K. J. Strnat (University of Dayton, Dayton, Ohio), p. 613.

Stadelmaier, H. H., N. A. El-Masry, and S. Cheng, 1983, Mater. Lett. **2**, 169.

Stadelmaier, H. H., N. A. El-Masry, and N. C. Liu, 1987, in *Proceedings of the Fifth International Symposium on Magnetic Anisotropy and Coercivity in Rare-Earth–Transition Metal Alloys,* edited by C. Herget, H. Kronmüller, and R. Poerschke (Deutsche Physikalische Gesellschaft, Bad Honnef, FRG), p. 389.

Stadelmaier, H. H., N. A. El-Masry, and S. R. Stallard, 1985, J. Appl. Phys. **57**, 4149.

Stadelmaier, H. H., and T. S. Jang, 1989, IEEE Trans. Magn. **25**, 3423.

Stadelmaier, H. H., and N. C. Liu, 1986, Mater. Lett. **4**, 304.

Stadelmaier, H. H., N. C. Liu, and N. A. El-Masry, 1985, Mater. Lett. **3**, 130.

Stadelmaier, H. H., and H. K. Park, 1981, Z. Metallkde. **72**, 417.

Stäblein, H., 1982, in *Ferromagnetic Materials,* edited by E. P. Wohlfarth (North-Holland, Amsterdam), Vol. 3, p. 441.

Stancil, D. D., 1987, J. Appl. Phys. **61**, 4111.

Stevens, K. W. H., 1952, Proc. Phys. Soc. London, Sec. A **65**, 209.

Stoner, E. C., and E. P. Wohlfarth, 1948, Philos. Trans. R. Soc. London, Ser. A **240**, 599.

Street, R., D. Bingham, R. K. Day, and J. B. Dunlop, 1988, J. Phys. (Paris) **49**, C8-629.

Street, R., L. Folks, and S. Hirosawa, 1990, in *Proceedings of the Sixth International Symposium on Magnetic Anisotropy and Coercivity in Rare Earth-Transition Metal Alloys,* edited by S. G. Sankar (Carnegie Mellon University, Pittsburgh), p. 1.

Streever, R. L., 1979, Phys. Rev. B **19**, 2704.

Strnat, K. J., 1987, IEEE Trans. Magn. **MAG-23**, 2094.

Strnat, K. J., 1988, in *Ferromagnetic Materials,* edited by E. P. Wohlfarth and K. H. J. Buschow (North-Holland, Amsterdam), Vol. 4, p. 131.

Strnat, K., G. Hoffer, J. Olson, W. Ostertag, and J. J. Becker, 1967, J. Appl. Phys. **38**, 1001.

Strnat, K. J., D. Li, and H. Mildrum, 1985, in *Proceedings of the Eighth International Workshop on Rare-Earth Magnets and Their Applications,* edited by K. J. Strnat (University of Dayton, Dayton, Ohio), p. 575.

Strnat, K. J., H. F. Mildrum, M. Tokunaga, and H. Harada, 1988, J. Appl. Phys. **63**, 3321.

Strzeszewski, J., G. C. Hadjipanayis, and A. S. Kim, 1988, J. Appl. Phys. **64**, 5568.

Strzeszewski, J., A. Nazareth, G. C. Hadjipanayis, K. Aylesworth, Z. R. Zhao, and D. J. Sellmyer, 1988, Mater. Sci. Eng. **99**, 153.

Sugimoto, M., 1982, in *Ferromagnetic Materials,* edited by E. P. Wohlfarth (North-Holland, Amsterdam), Vol. 3, p. 393.

Sun, H., J. M. D. Coey, Y. Otani, and D. P. F. Hurley, 1990, J. Phys.: Condens. Matter **2**, 6465.

Sun, X. K., X. C. Kou, Y. C. Chuang, R. Grössinger, and H. R. Kirchmayr, 1989a, IEEE Trans. Magn. **25**, 3298.

Sun, X. K., X. C. Kou, Y. C. Chuang, R. W. Zhao, J. Y. Li, F. M. Yang, R. Grössinger, and H. R. Kirchmayr, 1989b, Phys. Status Solidi A **115**, K219.

Sun, X. K., Z-G. Zhao, W. Liu, and Y. C. Chuang, 1990, Phys. Status Solidi A **122**, K69.

Suzuki, T., and K. Hiraga, 1986, J. Magn. Magn. Mater. **54-57**, 527.

Suzuki, T., K. Hiraga, and M. Sagawa, 1984, Jpn. J. Appl. Phys. **23**, L421.

Szpunar, B., 1986, Phys. Lett. A **115**, 157.

Szpunar, B., 1987, J. Less-Common Met. **127**, 55.

Szpunar, B., and B. Kozarzewski, 1977, Phys. Status Solidi B **82**, 205.

Szpunar, B., and P. A. Lindgård, 1979, J. Phys. F **9**, L55.

Szpunar, B., and J. A. Szpunar, 1985, J. Appl. Phys. **57**, 4130.

Szpunar, B., W. E. Wallace, and J. Szpunar, 1987, Phys. Rev. B **36**, 3782.

Szymczak, H., 1985, J. Phys. (Paris) **46**, C6-225.

Szymczak, R., E. Burzo, and W. E. Wallace, 1985, J. Phys. (Paris) **46**, C6-309.

Szymczak, R., H. Szymczak, and E. Burzo, 1987, IEEE Trans. Magn. **MAG-23**, 2536.

Takeshita, T., and R. Nakayama, 1989, in *Proceedings of the Tenth International Workshop on Rare-Earth Magnets and Their Applications* (Society of Non-Traditional Technology, Tokyo), p. 551.

Takeshita, T., and R. Nakayama, 1990, in *Proceedings of the Eleventh International Workshop on Rare-Earth Magnets and Their Applications,* edited by S. G. Sankar (Carnegie Mellon University, Pittsburgh), p. 49.

Takano, Y., Y. Satoh, and K. Sekizawa, 1988, J. Phys. (Paris) **49**, C8-561.

Tang, W., S. Zhou, and R. Wang, 1988, J. Magn. Magn. Mater. **75**, 416.

Tanigawa, S., Y. Hara, E. J. Lavernia, T. S. Chin, R. C. O'Handley, and N. J. Grant, 1986, IEEE Trans. Magn. **MAG-22**, 746.

Tao, Y. F., and G. C. Hadjipanayis, 1985, J. Appl. Phys. **57**, 4103.

Tenaud, P., A. Chamberod, and F. Vanoni, 1987, Solid State Commun. **63**, 303.

Tharp, D. E., G. J. Long, O. A. Pringle, G. K. Marasinghe, W. J. James, and F. Grandjean, 1988, J. Appl. Phys. **64**, 5583.

Tharp, D. E., Y-C. Yang, O. A. Pringle, G. J. Long, and W. J. James, 1987, J. Appl. Phys. **61**, 4334.

Thuy, N. P., T. D. Hien, N. M. Hong, and J. J. M. Franse, 1988, J. Phys. (Paris) **49**, C8-579.

Tokuhara, K., Y. Ohtsu, F. Ono, O. Yamada, M. Sagawa, and Y. Matsuura, 1985, Solid State Commun. **56**, 333.

Tokunaga, M., M. Endoh, and H. Harada, 1987, in *Proceedings of the Ninth International Workshop on Rare-Earth Magnets and Their Applications,* edited by C. Herget and R. Poerschke (Deutsche Physikalische Gesellschaft, Bad Honnef, FRG), p. 477.

Tokunaga, M., H. Harada, and S. R. Trout, 1987, IEEE Trans. Magn. **MAG-23**, 2284.

Tokunaga, M., H. Kogure, M. Endoh, and H. Harada, 1987, IEEE Trans. Magn. **MAG-23**, 2287.

Tokunaga, M., N. Meguro, M. Endoh, S. Tanigawa, and H. Harada, 1985, IEEE Trans. Magn. **MAG-21**, 1964.

Tokunaga, M., Y. Nozawa, K. Iwasaki, M. Endoh, S. Tanigawa, and H. Harada, 1989a, IEEE Trans. Magn. **25**, 3561.

Tokunaga, M., Y. Nozawa, K. Iwasaki, S. Tanigawa, and H. Harada, 1989b, J. Magn. Magn. Mater. **80**, 80.

Tokunaga, M., M. Tobise, N. Meguro, and H. Harada, 1986, IEEE Trans. Magn. **MAG-22**, 904.

Tsubokawa, Y., R. Shimizu, S. Hirosawa, and M. Sagawa, 1988, J. Appl. Phys. **63**, 3319.

Tsutai, A., I. Sakai, T. Mizoguchi, and K. Inomata, 1987, Appl. Phys. Lett. **51**, 1043.

Tu, G-H., Z. Altounian, D. H. Ryan, and J. O. Ström-Olsen, 1988, J. Appl. Phys. **63**, 3330.

Van Diepen, A. M., H. W. de Wijn, and K. H. J. Buschow, 1973, Phys. Rev. B **8**, 1125.

Van Engelen, P. P. J., and K. H. J. Buschow, 1987, J. Magn. Magn. Mater. **66**, 291.

Van Mens, R., 1986, J. Magn. Magn. Mater. **61**, 24.

Van Mens, R., D. B. de Mooij, and K. H. J. Buschow, 1988, J. Appl. Phys. **64**, 5708.

Van Noort, H. M., and K. H. J. Buschow, 1985, J. Less-Common Met. **113**, L9.

Van Noort, H. M., D. B. de Mooij, and K. H. J. Buschow, 1985, J. Appl. Phys. **57**, 5414.

Van Noort, H. M., D. B. de Mooij, and K. H. J. Buschow, 1986, J. Less-Common Met. **115**, 155.

Vasquez, A., J. M. Friedt, J P. Sanchez, P. L'Héritier, and R. Fruchart, 1985, Solid State Commun. **55**, 783.

Vasquez, A., and J. P. Sanchez, 1987, J. Less-Common Met.

127, 71.

Verhoef, R., F. R. de Boer, J. J. M. Franse, C. J. M. Denissen, T. H. Jacobs, and K. H. J. Buschow, 1989a, J. Magn. Magn. Mater. **80**, 41.

Verhoef, R., F. R. de Boer, T. H. Jacobs, and K. H. J. Buschow, 1990, J. Appl. Phys. **67**, 4774.

Verhoef, R., F. R. de Boer, F-M. Yang, Z-D. Zhang, D. B. de Mooij, and K. H. J. Buschow, 1989b, J. Magn. Magn. Mater. **80**, 37.

Verhoef, R., J. J. M. Franse, A. A. Menovsky, R. J. Radwański, S-Q. Ji, F-M. Yang, H. S. Li, and J. P. Gavigan, 1988, J. Phys. (Paris) **49**, C8-565.

Verhoef, R., P. H. Quang, J. J. M. Franse, and R. J. Radwański, 1990a, J. Appl. Phys. **67**, 4771.

Verhoef, R., P. H. Quang, J. J. M. Franse, and R. J. Radwański, 1990b, J. Magn. Magn. Mater. **83**, 139.

Verhoef, R., R. J. Radwański, and J. J. M Franse, 1990, J. Magn. Magn. Mater. **89**, 176.

Villas-Boas, V., F. P. Missell, and S. F. da Cunha, 1988, J. Appl. Phys. **64**, 5549.

Wada, M., and F. Yamashita, 1990, IEEE Trans. Magn. **26**, 2601.

Wallace, W. E., 1968, Prog. Rare Earth Sci. and Tech., Vol. III, p. 1.

Wallace, W. E., 1985, Prog. Solid State Chem. **16**, 127.

Wallace, W. E., and A. T. Pedziwiatr, 1987, in *Proceedings of the Fifth International Symposium on Magnetic Anisotropy and Coercivity in Rare-Earth–Transition Metal Alloys,* edited by C. Herget, H. Kronmüller, and R. Poerschke (Deutsche Physikalische Gesellschaft, Bad Honnef, FRG), p. 31.

Wallace, W. E., A. T. Pedziwiatr, E. B. Boltich, H. K. Smith, S. Y. Jiang, S. G. Sankar, and E. Oswald, 1987, in *High Performance Permanent Magnetic Materials,* Materials Research Society Symposia Proceedings Vol. 96, edited by S. G. Sankar, J. F. Herbst, and N. C. Koon (Materials Research Society, Pittsburgh), p. 17.

Wallace, W. E., F. Pourarian, A. T. Pedziwiatr, and E. B. Boltich, 1987, J. Less-Common Met. **130**, 33.

Wallace, W. E., S. G. Sankar, J. M. Elbicki, and S. F. Cheng, 1989, Mater. Sci. Eng. **B3**, 351.

Watson, R. E., L. H. Bennett, and M. Melamud, 1988, J. Appl. Phys **63**, 3136.

Watson, R. E., M. Melamud, and L. H. Bennett, 1987, J. Appl. Phys. **61**, 3580.

Wecker, J., and L. Schultz, 1987a, J. Appl. Phys. **62**, 990.

Wecker, J., and L. Schultz, 1987b, Appl. Phys. Lett. **51**, 697.

Wecker, J., and L. Schultz, 1989, Appl. Phys. Lett. **54**, 393.

Wecker, J., and L. Schultz, 1990, J. Magn. Magn. Mater. **83**, 189.

Wernick, J. H., and S. Geller, 1959, Acta Crystallogr. **12**, 662.

White, R. M., 1985, J. Appl. Phys. **57**, 2996.

Wiesinger, G., R. Grössinger, R. Krewenka, X. C. Chou, X. K. Sun, and Y. C. Chuang, 1989, Hyp. Interactions **50**, 693.

Wiesinger, G., G. Hilscher, and R. Grössinger, 1987, J. Less-Common Met. **131**, 409.

Wlliams, C. M., N. C. Koon, and B. N. Das, 1987, in *High Performance Permanent Magnet Materials,* Materials Research Society Symposia Proceedings Vol. 96, edited by S. G. Sankar, J. F. Herbst, and N. C. Koon (Materials Research Society, Pittsburgh), p. 111.

Williams, C. M., N. C. Koon, and B. N. Das, 1988, J. Phys. (Paris) **49**, C8-567.

Wohlfarth, E. P., 1958, J. Appl. Phys. **29**, 595.

Wohlfarth, E. P., 1980, in *Ferromagnetic Materials,* edited by E. P. Wohlfarth (North-Holland, Amsterdam), Vol. 1, p. 1.

Wojcik, M., E. Jedryka, G. Jasiolek, W. Paszkowicz, and M. Slepowronski, 1988, J. Magn. Magn. Mater. **72**, 330.

Wojcik, M., E. Jedryka, P. Panissod, S. Hirosawa, and M. Sagawa, 1989, J. Magn. Magn. Mater. **80**, 19.

Wojcik, W., E. Jedryka, P. Panissod, and K. H. J. Buschow, 1990, J. Magn. Magn. Mater. **83**, 243.

Wolfers, P., S. Miraglia, D. Fruchart, S. Hirosawa, M. Sagawa, J. Bartolome, and J. Pannetier, 1990, J. Less-Common Met. **162**, 237.

Wu, C. H., X. P. Zhong, Z. D. Zhang, Y. C. Chuang, and F. R. de Boer, 1990, J. Less-Common Met. **159**, 91.

Wyslocki, J. J., and F. Bolzoni, 1990, J. Magn. Magn. Mater. **83**, 239.

Xiao, Y., K. J. Strnat, H. F. Mildrum, and A. E. Ray, 1987, in *Proceedings of the Ninth International Workshop on Rare-Earth Magnets and Their Applications,* edited by C. Herget and R. Poerschke (Deutsche Physikalische Gesellschaft, Bad Honnef, FRG), p. 467.

Xie, J. Q., and C. D. Graham, Jr., 1990, in *Proceedings of the Sixth International Symposium on Magnetic Anisotropy and Coercivity in Rare Earth-Transition Metal Alloys,* edited by S. G. Sankar (Carnegie Mellon University, Pittsburgh), p. 308.

Xie, J. Q., C. H. Wu, Y. C. Chuang, and F. M. Yang, 1988a, J. Magn. Magn. Mater. **75**, 361.

Xie, J. Q., C. H. Wu, Y. C. Chuang, and F. M. Yang, 1989, Solid State Commun. **71**, 329.

Xie, J. Q., C. H. Wu, Y. C. Chuang, and F. M. Yang, 1990a, Phys. Rev. B **41**, 7162.

Xie, J. Q., C. H. Wu, Y. C. Chuang, and F. M. Yang, 1990b, J. Appl. Phys. **68**, 4208.

Xie, J. Q., C. H. Wu, Y. C. Chuang, and F. M. Yang, 1990c, in *Proceedings of the Sixth International Symposium on Magnetic Anisotropy and Coercivity in Rare Earth-Transition Metal Alloys,* edited by S. G. Sankar (Carnegie Mellon University, Pittsburgh), p. 300.

Xie, J. Q., C. H. Wu, Y. C. Chuang, Z. D. Zhang, and F. R. de Boer, 1988b, J. Phys. (Paris) **49**, C8-603.

Xing, F., and W. W. Ho, 1987, in *Proceedings of the Fifth International Symposium on Magnetic Anisotropy and Coercivity in Rare-Earth-Transition Metal Alloys,* edited by C. Herget, H. Kronmüller, and R. Poerschke (Deutsche Physikalische Gesellschaft, Bad Honnef, FRG), p. 47.

Xing, F., and W.-W. Ho, 1988, J. Magn. Magn. Mater. **74**, 271.

Xing, F., and W-W. Ho, 1990, J. Appl. Phys. **67**, 4604.

Xu, Y., W. B. Muir, and Z. Altounian, 1989, J. Magn. Magn. Mater. **82**, 43.

Yajima, K., H. Nakamura, O. Kohmoto, and T. Yoneyama, 1988, J. Appl. Phys. **64**, 5528.

Yamada, M., H. Kato, H. Hiroyoshi, H. Yamamoto, and Y. Nakagawa, 1987, J. Magn. Magn. Mater. **70**, 328.

Yamada, M., H. Kato, H. Yamamoto, and Y. Nakagawa, 1988, Phys. Rev. B **38**, 620.

Yamada, M., Y. Yamaguchi, H. Kato, H. Yamamoto, Y. Nakagawa, S. Hirosawa, and M. Sagawa, 1985, Solid State Commun. **56**, 663.

Yamada, O., Y. Ohtsu, F. Ono, M. Sagawa, and S. Hirosawa, 1987, J. Magn. Magn. Mater. **70**, 322.

Yamada, O., H. Tokuhara, F. Ono, M. Sagawa, and Y. Matsuura, 1986, J. Magn. Magn. Mater. **54-57**, 585 (1986).

Yamamoto, H., S. Hirosawa, S. Fujimura, K. Tokuhara, H. Nagata, and M. Sagawa, 1987, IEEE Trans. Magn. **MAG-23**, 2100.

Yamamoto, H., Y. Matsuura, S. Fujimura, and M. Sagawa, 1984, Appl. Phys. Lett. **45**, 1141.

Yamamoto, H., M. Nagakura, T. Katsuno, and T. Yamamoto, 1990, IEEE Trans. Magn. **26**, 2595.

Yamamoto, H., M. Nagakura, Y. Ozawa, and T. Katsuno, 1989, IEEE Trans. Magn. **25**, 4123.

Yamasaki, J., A. Furuta, and Y. Hirokado, 1989, IEEE Trans. Magn. **25**, 4120.

Yamasaki, J., H. Soeda, M. Yanagida, K. Mohri, N. Teshima, O. Kohmoto, T. Yoneyama, and N. Yamaguchi, 1986, IEEE Trans. Magn. **MAG-22**, 763.

Yamauchi, H., M. Yamada, Y. Yamaguchi, H. Yamamoto, S. Hirosawa, and M. Sagawa, 1986, J. Magn. Magn. Mater. **54-57**, 575.

Yamauchi, H., H. Yamamoto, H. Hirosawa, and M. Sagawa, 1987, J. Magn. Magn. Mater. **70**, 340.

Yang, C. J., and R. Ray, 1988, J. Appl. Phys. **63**, 3525.

Yang, C. J., R. Ray, and R. C. O'Handley, 1988, Mater. Sci. Eng. **99**, 137.

Yang, F-M., X-W. Li, R-W. Zhao, Y. Zhu, T-S. Zhao, Y-K. Huang, and F. R. de Boer, 1988, J. Phys. (Paris) **49**, C8-571.

Yang, F-M., R-W. Zhao, X-W. Li, Y-K. Huang, F. R. de Boer, and R. Radwanski, 1988, IEEE Trans. Magn. **24**, 1945.

Yang, Y-C., W. J. James, H-Y. Chen, and H. Sun, 1986a, J. Magn. Magn. Mater. **54-57**, 895.

Yang, Y-C., W. J. James, X-D. Li, H-Y. Chen, and L-G. Xu, 1986b, IEEE Trans. Magn. **MAG-22**, 757.

Yang, Y-C., D. E. Tharp, G. J. Long, O. A. Pringle, and W. J. James, 1987, J. Appl. Phys. **61**, 4343.

Yang, Y-C., F. Xing, L-S. Kong, J-L. Yang, Y-F. Ding, B-S. Zhang, C-T. Ye, L. Jin, and H-M. Zhou, 1988, J. Phys. (Paris) **49**, C8-597.

Yang, Y-C., and X-D. Zhang, 1990, J. Appl. Phys. **67**, 4765.

Yaouanc, A. J., J. Budnick, E. Albert, M. Hamma, A. Weidinger, R. Fruchart, P. L'Héritier, D. Fruchart, and P. Wolfers, 1987, J. Magn. Magn. Mater. **67**, L286.

Yelon, W. B., 1988, Mater. Sci. Forum **27/28**, 371.

Yelon, W. B., 1989, Physica B **156&157**, 744.

Yelon, W. B., B. Foley, C. Abache, and H. Oesterreicher, 1986, J. Appl. Phys. **60**, 2982.

Yelon, W. B., and J. F. Herbst, 1986, J. Appl. Phys. **59**, 93.

Yelon, W. B., D. Xie, C. M. Hsueh, C. D. Fuerst, and G. P. Meisner, 1989, Phys. Rev. B **39**, 9389.

Yen, L. S., J. C. Chen, and H. C. Ku, 1987, J. Appl. Phys. **61**, 1990.

Yethiraj, M., W. B. Yelon, and K. H. J. Buschow, 1991, J. Magn. Magn. Mater. **97**, 45.

Yoneyama, T., O. Kohmoto, and K. Yajima, 1987, in *Proceedings of the Ninth International Workshop on Rare-Earth Magnets and Their Applications,* edited by C. Herget and R. Poerschke (Deutsche Physikalische Gesellschaft, Bad Honnef, FRG), p. 495.

Yoneyama, T., H. Nakamura, K. Anan, A. Nishiuchi, and A. Fukuno, 1990, IEEE Trans. Magn. **26**, 1963.

Zasadzinski, J. F., C. U. Segre, and E. D. Rippert, 1987a, J. Appl. Phys. **61**, 4278.

Zasadzinski, J. F., C. U. Segre, E. D. Rippert, J. Chrzas, and P. Radusewicz, 1987b, in *High Performance Permanent Magnet Materials,* Materials Research Society Symposia Proceedings Vol. 96, edited by S. G. Sankar, J. F. Herbst, and N. C. Koon (Materials Research Society, Pittsburgh), p. 55.

Zeng, X.-Y., and X.-Y. Yu, 1987, Solid State Commun. **64**, 635.

Zhang, L. Y., F. Pourarian, and W. E. Wallace, 1988a, J. Magn. Magn. Mater. **71**, 203.

Zhang, L. Y., F. Pourarian, and W. E. Wallace, 1988b, J. Magn. Magn. Mater. **74**, 101.

Zhang, M., D. Ma, X. Jiang, and S. Liu, 1985, in *Proceedings of the Eighth International Workshop on Rare-Earth Magnets and Their Applications,* edited by K. J. Strnat (University of Dayton, Dayton, Ohio), p. 541.

Zhang, Y. D., J. I. Budnick, E. Potenziani II, A. T. Pedziwiatr, W. E. Wallace, and P. Panissod, 1988, J. Appl. Phys. **63**, 3719.

Zhang, Y. D., J. I. Budnick, M. Wojcik, E. Potenziani II, A. T. Pedziwiatr, and W. E. Wallace, 1987, Phys. Rev. B **36**, 8213.

Zhang, Z-D., Y-K. Huang, X. K. Sun, Y. C. Chuang, F-M. Yang, F. R. de Boer, and R. J. Radwański, 1989a, Physica B **155**, 269.

Zhang, Z-D., Y-K. Huang, X. K. Sun, Y. C. Chuang, F-M. Yang, F. R. de Boer, and R. J. Radwański, 1989b, J. Less-Common Met. **152**, 67.

Zhang, Z-D., X. K. Sun, Y. C. Chuang, F. R. de Boer, and R. J. Radwański, 1988, J. Phys. (Paris) **49**, C8-569.

Zhang, Z-D., X. K. Sun, Y. C. Chuang, F. R. de Boer, and R. J. Radwański, 1990a, J. Magn. Magn. Mater. **89**, 304.

Zhang, Z-D., X. K. Sun, Y. C. Chuang, F. R. de Boer, and R. J. Radwański, 1990b, Phys. Status Solidi A **121**, 617.

Zhang, Z-D., X. K. Sun, F. R. de Boer, Y. C. Chuang, and R. J. Radwański, 1991, Phys. Rev. B **43**, 555.

Zhang, Z-D., X. K. Sun, Z-W. Zhang, Y. C. Chuang, and F. R. de Boer, 1990c, Phys. Status Solidi A **121**, 241.

Zhang, Z-D., X. K. Sun, Z-G. Zhao, and Y. C. Chuang, 1990d, J. Magn. Magn. Mater. **92**, 191.

Zhang, Z.-W., M. Z. Dang, and H. S. Li, 1989, J. Magn. Magn. Mater. **81**, 361.

Zhang, Z.-W., R.-W. Huang, M.-Z. Dang, and L.-K. Zhang, 1990, J. Magn. Magn. Mater. **92**, 196.

Zhao, T., Z. Fan, and H. Jin, 1990, Phys. Status Solidi B **157**, 677.

Zhao, T., and H. Jin, 1987, Solid State Commun. **64**, 103.

Zhao, T., H. Jin, J. Deng, F. Wu, J. Song, and Y. Shi, 1986, J. Magn. Magn. Mater. **54-57**, 573.

Zhao, T., H. Jin, and Y. Zhu, 1989, J. Magn. Magn. Mater. **79**, 159.

Zhao, T., Y. Zhu, and H. Jin, 1988, Phys. Status Solidi B **145**, 679.

Zhong, X.-F., and W. Y. Ching, 1988, J. Appl. Phys. **64**, 5574.

Zhong, X.-F., and W. Y. Ching, 1989, Phys. Rev. B **39**, 12018.

Zhong, X.-F., and W. Y. Ching, 1990, J. Appl. Phys. **67**, 4768.

Zhou, G. F., Y. C. Chuang, X. K. Sun, R. Grössinger, and H. R. Kirchmayr, 1990, J. Less-Common Met. **158**, 41.

Zhou, G. F., S. Y. Fu, X. K. Sun, and Y. C. Chuang, 1990, Phys. Status Solidi A **121**, 257.

Zhou, G. F., X. K. Sun, Y. C. Chuang, L. Gao, Z. Yu, C. L. Xiao, and W. Liu, 1988, J. Phys. (Paris) **49**, C8-573.

Zhou, G. F., X. K. Sun, S. Y. Fu, Y. C. Chuang, R. Grössinger, and H. R. Kirchmayr, 1990, Phys. Status Solidi A **120**, 627.

Zhou, G. F., Z. C. Zhong, X. K. Sun, and Y. C. Chuang, 1990, J. Less-Common Met. **166**, 253.

Zhou, S.-X., P. Johansson, S. J. Savage, and L.-Y. Cui, 1990, IEEE Trans. Magn. **26**, 1739.

Zhu, Y., T. Zhao, H. Jin, F. Yang, J. Xie, X. Li, and R. Zhao, 1989, IEEE Trans. Magn. **25**, 3443.

Zijlstra, H., 1982, in *Ferromagnetic Materials,* edited by E. P. Wohlfarth (North-Holland, Amsterdam), Vol. 3, p. 37.

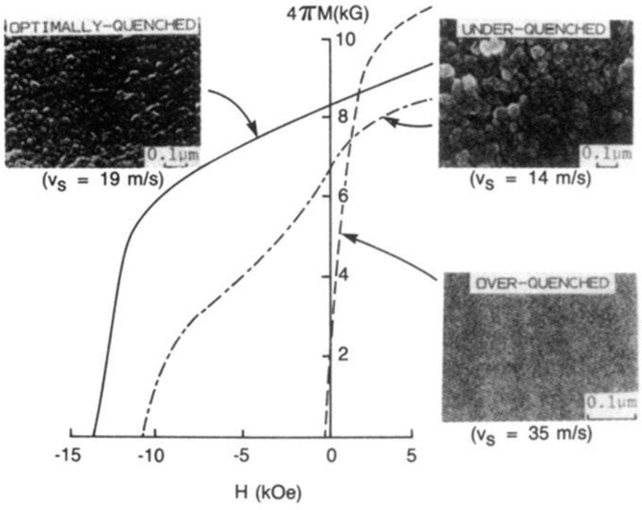

FIG. 21. Room-temperature demagnetization curves and corresponding scanning electron micrographs of melt-spun $Nd_{0.135}Fe_{0.817}B_{0.048}$ ribbon fracture surfaces.

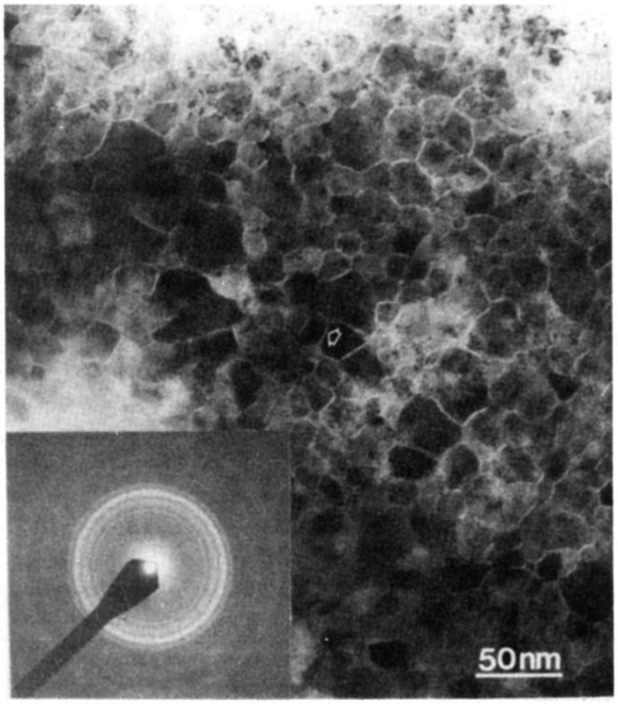

FIG. 22. Bright-field transmission electron micrograph of optimally quenched Nd-Fe-B ribbon (Mishra, 1986). The inset is a selected area diffraction pattern whose rings indicate random distribution of $Nd_2Fe_{14}B$ grains. Note the very thin intergranular phase indicated by the arrow.

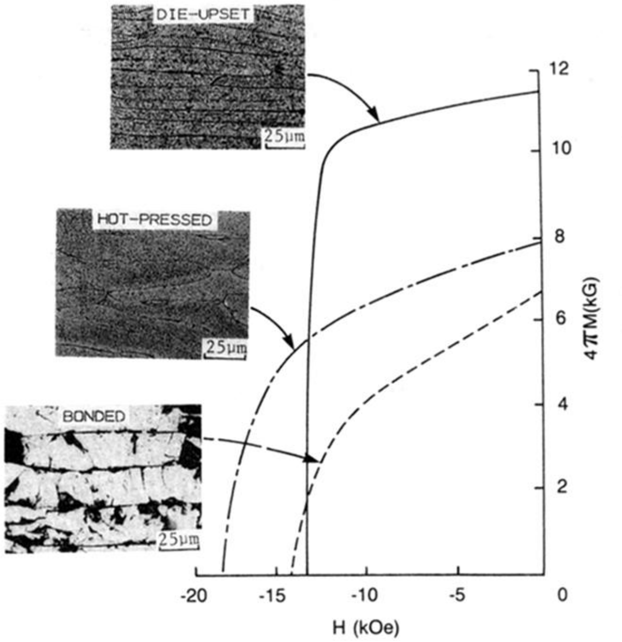

FIG. 23. Room-temperature demagnetization curves and optical micrographs of bonded, hot-pressed, and die-upset Nd-Fe-B magnets prepared from melt-spun ribbons.

FIG. 24. Transmission electron micrograph of a die-upset Nd-Fe-B magnet (courtesy R. K. Mishra).

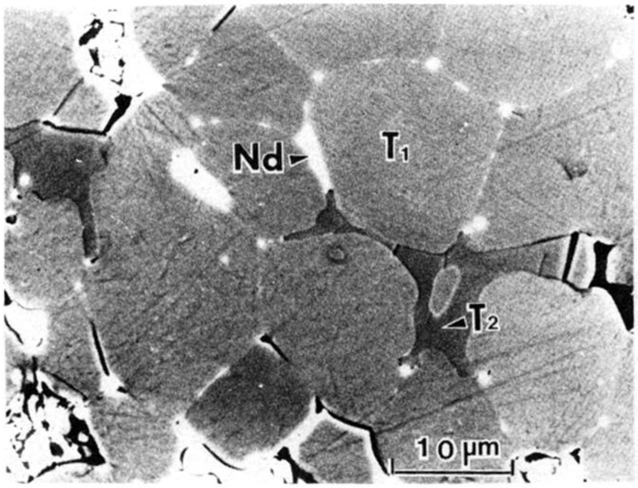

FIG. 27. X-ray composition micrograph of a sintered $Nd_{0.15}Fe_{0.77}B_{0.08}$ magnet; T_1, T_2, and Nd denote $Nd_2Fe_{14}B$, $Nd_{1+\epsilon}Fe_4B_4$, and a Nd-rich phase, respectively (Sagawa, Hirosawa, *et al.*, 1987d).